INTERMEDIATE LOW VOLTAGE DIRECT CURRENT (ILVDC) INTERCONNECTION SYSTEMS FOR SPARSE ELECTRIFIED AREAS

by

MARTIAL GIRANEZA

Thesis submitted in fulfilment of the requirements for the degree

Doctor of Engineering: Electrical Engineering

in the Faculty of Engineering

at the Cape Peninsula University of Technology

Supervisor: Prof M.T.E Kahn

Bellville December 2018

DECLARATION

I, **Martial Giraneza**, declare that the contents of this dissertation/thesis represent my own unaided work, and that the dissertation/thesis has not previously been submitted for academic examination towards any qualification. Furthermore, it represents my own opinions and not necessarily those of the Cape Peninsula University of Technology.

Signed	**Date**

ABSTRACT

Electricity access is seen as an economic growth enabler and a commodity to improve people's welfare. Hence, electrification is one of the aspects highly regarded by governments worldwide. In Africa, electricity access is still a challenge, this is well illustrated by the low electrification rate of 41%, which is more significant in sub-Saharan region with an electrification rate of 35%. In this part of the continent, on one hand, the reliability of the power supply in electrified areas is still an issue and on the other hand, in areas far from the grid, there are less perspective for grid extension if considered the financial situation and top down model of grid extension used by the utilities. This leads to the extensive use of diesel generators in urban and rural areas. The traditional top down model for grid extension requires huge capitals that are mainly provided by the utility. The return on investment on extended grid determines the approval for extension or not. It is difficult for remote rural areas with no major economic activities like mining to cross the threshold of return on investment acceptable by the utility. Hence new approaches are sought to increase the electrification rate in Africa while maintaining the cost as minimum as possible. Bottom up grid extension using swarm electrification and off-grid solutions such as microgrids are gaining interest of researchers as alternative to the traditional method. It is in this line that this thesis entitled "Intermediate Low Voltage Direct Current (ILVDC) interconnection systems for sparse electrified areas" is looking into combining both approaches by building up a network from the bottom considering the locally available off-grid solutions such as nanogrid diesel generators for microgrids formation. "Olympic rings" microgrids approach is used to extend the electrified areas and anticipate an eventual interconnection with the grid. For this end, nanogrid and microgrid networks are developed, designed and tested. Bi-directional Nanogrid converter are designed with modularized topology to allow easy and economic repair as only affected module should be replaced if needed. Proposed bidirectional converters for nanogrid, microgrid and minigrid are modelled and simulated in PSIM environment. Simulation results show that the design criteria set are met by the converters. Control strategies for power exchange within nanogrids and microgrids, as well as the overall control are proposed. Communication based control strategy algorithms for nanogrids and microgrids are developed. Power line communication (PLC) technique is adopted as a communication system while a DC opto-capacitive coupler for PLC communication system is developed to enhance the safety of the equipment and users. Interconnection of microgrids through ILVDC network is performed with respect to IEC60038 and IEEE 1547. Load flow analysis using DigSilent PowerFactory is performed on individual and interconnected microgrids, with contingency scenario in the latter case. The simulation results proved a successful interaction and improved loading on the machine during the contingency as opposite to results in the Islanded mode.

ACKNOWLEDGEMENTS

I wish to thank:

DEDICATION

To my family, may they see in this work the fruit of their love and support.

TABLE OF CONTENTS

LIST OF FIGURES

LIST OF TABLES

GLOSSARY

Terms/Abbreviations	Definition/Explanation
3G	Third Generation of wireless mobile telecommunication
4G	Fourth Generation of wireless mobile telecommunication
AAAC	All Aluminium Alloy Conductor)
AAC	All Aluminium Conductor
ABC lines	Aerial bundled conductors
AC	Alternative Current
ACSR	Aluminium Conductor Steel Reinforced
ANSI	American National Standards Institute
CT	Current Transformer
DC	Direct Current
DigSilent	Power system modelling, analysis and simulation software for applications in generation, transmission, distribution and industrial systems.
GIL	Gas Insulated Lines
HTS	High Temperature Superconductor lines/cables
HVAC	High Voltage Alternative Current
HVDC	High Voltage Direct Current
IEA	International Energy Agency

IEC	International Electrotechnical Commission
IEEE	Institute of Electrical and Electronics Engineers
IGBT	Insulated-Gate Bipolar Transistor
ILVDC	Intermediate Low Voltage Direct Current
IP	Internet protocol
IRENA	International Renewable Energy Agency
LTS	Low Temperature Superconductor lines/cables
LVAC	Low Voltage Alternative Current
LVDC	Low Voltage Direct Current
MVAC	Medium Voltage Alternative Current
MVDC	Medium Voltage Direct Current
OSI	open source interconnection layered model protocols
PI	Proportional Integral controller
PID	Proportional Integral–derivative controller
PLC	Power Line Communication
PSIM	Power electronic modelling analysis and simulation for electronics and power electronics circuits
PWM	Pulse Width Modulation
REA	Rural Electrification Agency
REF	Rural Electrification Fund

Simulink,   Software for modelling, simulation and analysis for dynamic systems

TCP   Transmission Control Protocols

VSC   Voltage Source Converter

VT   Voltage Transformer

XLPE   Cross-linked polyethylene insulation.

CHAPTER ONE

INTRODUCTION

1.1 Introduction

The last century has demonstrated that every facet of human development is woven around a sound and stable energy supply regime. As such, electrification is among governments' priorities. The electrification rate in Africa compared to the rate on other continents, is still low. In addition, reliability of supply in electrified areas is a challenge and power blackouts are still common in many African urban and rural areas.

On the African continent, the sub-Saharan region is the greatly affected by not having access to electricity, with 633 million being affected(Avila et al., 2017). By contrast only 1 million people in northern Africa are without electricity (IEA, 2017). New methods are needed to correct the situation and improve the electrification rate.

1.2 Background

The electrification rate is very low in Africa (41%) compared to developing countries in South Asia, which is at 68,5%, and Latin American, which has a 93, 2% electrification rate. In Africa, specifically in sub-Saharan countries, the rate is 35%(Tagliapietra, 2017; IEA, 2017) .

According to the International Energy Agency (IEA) (2017), besides South Africa, the main economic countries in the sub-Saharan region have a shortage of electricity. This is in contrast with the general rule that suggests that the growth of the electricity generation capacity should increase at about the same rate as the economy. For instance, the urban electrification in Nigeria, the biggest oil producing country in Africa with an annual GDP per capita of $2,758 in 2017, has its urban electrification at around 58%; while for Angola, also electrification rate is 32%(Tagliapietra, 2017). The worse picture is expected in weak economy in sub-Saharan countries.

Various reasons are behind the actual status of electrification in the sub-Saharan region, from the disruption, damage or destruction of power plants and distributions lines due to wars, to various other political reasons, including cartels that benefit from generators fuel selling (Leba, 2011). As result, diesel power generator for many users is the only affordable off-grid option or in case of power shortage. Moreover, daily power outages are frequent in 30 sub-Saharan countries to such an extent that diesel generators are the main source of power (IRENA, 2012). In countries like the Democratic Republic of Congo and Equatorial Guinea, diesel generators are used to produce at least 50% of the power consumed, while in West Africa, 17% of the power generated is diesel-based (IEA, 2017; IRENA, 2012). In Nigeria only, around 15 million diesel generators are in use for electricity generation(Research and Markets, 2017; Awofeso,

2011). Similar situations can be observed in many sub-Saharan countries, mostly in cities where urbanisation is constantly taking place (World Bank, 2013).

The power sector structure of many sub-Saharan countries is changing to conform to the global electricity market restructuration. The structure that used to be the monopoly of utilities, mostly government-owned, is changed to allow for private companies to enter the electricity market. Although reforms were meant for the introduction of the competition to the whole level of the electricity market, from generation to distribution, in many sub-Saharan countries the competition is only at generation level. Utilities, mostly government-owned, are still the only responsible means of transmission and distribution of electricity to customers (Bacon & Besant, 2001). Being responsible for the transmission and distribution grid, sub-Saharan African utilities are in charge of operation, maintenance and the extension of the grid.

The actual grid extension model is a top-down model with utilities at the top initiating and financing the process. In sub-Saharan countries, the same model with variation in management has been used for rural and urban electrification or grid extension to those areas. On a macro level in the case of rural electrification, institutional approaches such as the creation of a separate division within the utility, creation of a Rural Electrification Agency (REA)/Rural Electrification Fund (REF), or the creation of private companies as well as small and medium-sized businesses are used to manage grid extension; while on the micro level are the rural cooperative approaches, where the targeted users through a cooperative manage the extension.

The common point for all those approaches is the preponderant role of utilities from the initiation of the process till its accomplishment. Top-down grid extension faces various challenges in its implementation due to the weak financial situation many utilities are facing that may prevent them financing the extension of their distribution grid. New approaches for grid extension that may avoid all those challenges as well as take into account off-grid generation are required.

1.3 Significance of the research

The extension of the grid is one of the solutions for increasing the low electrification rate of the sub-Saharan countries. With the current approaches that are used for grid extension by utilities, it has been observed that there are challenges likely to slow if not completely inhibit the process. Finding a new approach that overcomes the shortage of the current ones is important for both utilities and users. This research focuses on developing from a technical perspective a new grid extension strategy, which starts from the users' side through interconnection of sparse generating point. The strategy is a bottom-up grid extension based on the DC network: nano and microgrid.

There is a gap in bottom-up grid extension implementation strategy from a techno-economic aspect. This research provides guidelines for this gap.

1.4 Research question

The electrification rate of sub-Saharan countries is still low, and the majority of the population is relying extensively on off-grid generation, which happens to be expensive. Grid extension is one of the ways to increase the number of grid connected electricity users.

This research investigates how to expand the grid to the dispersed off-grid areas with respect to the local generating sources using Intermediate and Low Voltage Direct Current system.

1.5 Aim and objectives of the study

The study aims for the implementation of interconnection systems of sparse electrified areas based on intermediate low voltage direct current.

Specific objectives include:

a) To review existing theories and the practice of power system distribution network, operation and extension for both DC and AC systems.

b) To develop strategies for the interconnection of off-grid generation sources based on DC network with eventual utility grid connection.

c) To design converters and control strategies for nanogrid, microgrid and minigrid formation as well as the interconnection of the minigrid with utility grid

d) To design an intermediate low voltage direct current distribution grid, simulation and perform power flow analysis.

e) To design a communication system for the intermediate low voltage direct current (ILVDC) network.

f) To Propose a ILVDC implementation strategy.

1.6 Research Design and Methodology

This thesis focuses on bottom-up grid extension based on the interconnection of distributed generation, using the intermediate low voltage direct current network as a back bone. To achieve those goals, the following methods were used:

- To define, contextualise, and gain knowledge about the research area as well as onto the topic, an extensive literature review was performed. From the literature review the state of art and future trends of electrical power distribution system as well as of Low Voltage Direct Current distribution networks were identified.

- From literature, knowledge gained and gaps in research identified; improvement and solution strategies were proposed. In this regard, lack of access to electricity, challenges for grid expansion and disparity of generating source in rural areas were identified. Intermediate Low Voltage DC network interconnection of distributed generation source was proposed as solution for grid extension.

- Modelling, designing, and simulations of proposed strategies. ILVDC network system component such as generator, converter and communication system were modelled and simulated using Simulink, PSIM and DIgSILENT software for load flow analysis.

- Analysis of results and reflection on improvement onto the proposed solution. From the simulation results, an analysis is performed for design criteria fulfilment and the effectiveness of the proposed solutions.

1.7 Research contributions

This thesis, through the objectives, results and recommendation, has made the following research contributions:

1. It presents state of arts and practice for electrical power distribution systems. The structure, control, operation, network extension and related challenges were identified. LVDC networks concept and perspectives on application for bottom-up grid extension in Africa.
Part of the contribution is published in: M. Giraneza and M. T. E. Kahn, "Intermediate low voltage direct current based decentralized grid extension," 2015 International Conference on the Industrial and Commercial Use of Energy (ICUE), Cape Town, 2015, pp. 272-276. doi: 10.1109/ICUE.2015.7280278

2. Intermediate low voltage direct current concept network is presented, and component designed for bottom-up grid extension. The interconnection of different source in swarm electrification concept as presented, requires a communication system. Low cost communication system and a novel coupler for power line communication are presented.

3. Part of this contribution is published in: M. Giraneza and M. T. E. Kahn, Broad band opto-capacitive power line communication coupler for DC nanogrids, Journal of King Saud University Engineering Sciences. https://doi.org/10.1016/j.jksues.2019.02.001.It aims, among other objectives, for the implementation of grid extension from the bottom-up using sparse electrified areas. In this regard, energy management systems algorithms for nanogrid, microgrids and for grid interaction are developed in this work. Modularised converters are designed with the intention to facilitate the repair or maintenance.

4. The implementation of ILVDC network for grid extension part of the bottom-up strategy in terms of financing and metering is laid out. Opinions from the thesis are presented in:" M. Giraneza and M.T.E Kahn, DC nanogrid-based energy bank for rural community" published in Energize, Nov-Dec 2018, pp32-33.

1.8 Thesis outline

This thesis titled 'Intermediate Low Voltage Direct Current (ILVDC) interconnection systems for sparse electrified areas' focuses on the interconnection of distributed generation and integration of non-electrified entities by using DC networks in the framework of swarm electrification. Related concepts, design, simulations results and analysis are presented throughout this thesis. The rest of this thesis is organised into seven chapters, structured as follows:

Chapter 1: Lays out the introduction of the research question, its background, objectives and methodology used to reach the main objectives. It also discusses the outcomes of the research and the outline of the thesis with a glance on each chapter.

Chapter 2: Introduces theory and practice of the electrical power system, with emphasis on distribution network, topology, components, operation, planning and extension. It also highlights the challenges related to distribution network extension.

Chapter 3: Discusses low voltage direct current in the distribution network, its components, standards, voltage, topology, protection, control, application, and perspectives of LVDC distribution systems in Africa.

Chapter 4: Introduces the intermediate voltage direct current network for sparse electrified areas as a concept; modelling, design and simulations of the all components of the system. Converters, communication system design and simulations as well as protection systems are discussed. Algorithms for energy sharing management systems at all level of the ILVDC network are developed in this chapter.

Chapter 5: In this chapter, load flow analysis, short circuit, protection coordination and an analysis of the proposed network system are discussed.

Chapter 6: Provides a summary of the relevant results, draws conclusion, and offers suggestions for further studies.

1.9 Conclusion

This chapter discusses the problem statement of the research and its background. Research significance, objectives and aims of this study as well as the methodology used are discussed. It also includes the contribution of this research and the structure of this report.

For solution to be developed, a good understanding of the problem is essential. This is achieved through an extensive literature review focusing on operation, challenges, actual and future solutions.

1.10   Publications Emanating from this Thesis

[1.] M. Giraneza and M. E. Kahn, "Intermediate low voltage direct current based decentralized grid extension," 2015 International Conference on the Industrial and Commercial Use of Energy (ICUE), Cape Town, 2015, pp. 272-276.
doi: 10.1109/ICUE.2015.7280278

[2.] M. Giraneza and M.T.E Kahn, "DC nanogrid-based energy bank for rural community".

Energize, Nov/Dec 2018, ISSN 1818-2127.

[3.] M. Giraneza and M.T.E Kahn, "Broad band Opto-capacitive power line communication coupler for DC nanogrids" Journal of King Saud University - Engineering Sciences ,2019 Elsevier, DOI: 10.1016/j.jksues.2019.02.001

CHAPTER TWO
ELECTRICAL POWER DISTRIBUTION NETWORK EXTENSION

2.1   Introduction on power system network

The invention of the electric incandescent bulb by Edison in the 1870s opened doors for the first electric power system, the Pearl street system in 1882 in New York. Since then the power system has not ceased to evolve, from initial DC system to AC system, from solely underground cable systems to the actual overhead lines, and from short range networks to continental interconnected systems. The AC system imposed itself in 1893 due to the impracticability of the DC system associated with high losses for long transmission (Zhang, 2010).

However, the battle of currents seems resumed with DC systems coming back into perspective, thanks to new power electronics technologies. In fact, in application for long transmission, High Voltage Direct Current (HVDC) systems demonstrate better features in terms of transmission losses, stability, control, and power quality (Rudervall et al., 2000). Application of the DC system is currently expanding throughout all levels in the power system structure (Bathurst et al., 2015; Hakala et al., 2015b).

The traditional power system structure shown in Figure 2.1 is undergoing changes due to the introduction of distributed generation (DG) at all levels of the electrical power system (Georgilakis et al., 2013). The modern power system, shown in Figure 2.2, is characterised by the introduction of distributed generation units. Most of the DGs are renewable energy based and are usually situated closer to the load centres, which is in contrast with the traditional power system where the generation stations are situated far from load centres. The modern power structure differs from the traditional structure which is centrally managed and largely passive, it is highly distributed and more complex (Xiao-Ping Zhang, 2010).
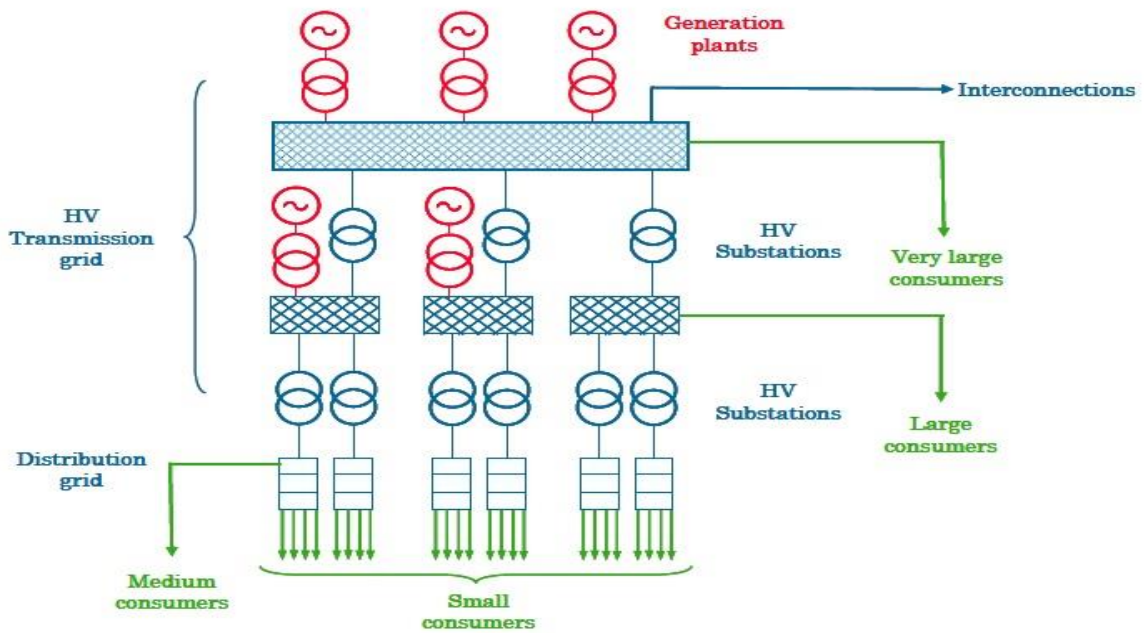
Figure 2. 1: Traditional power system structure
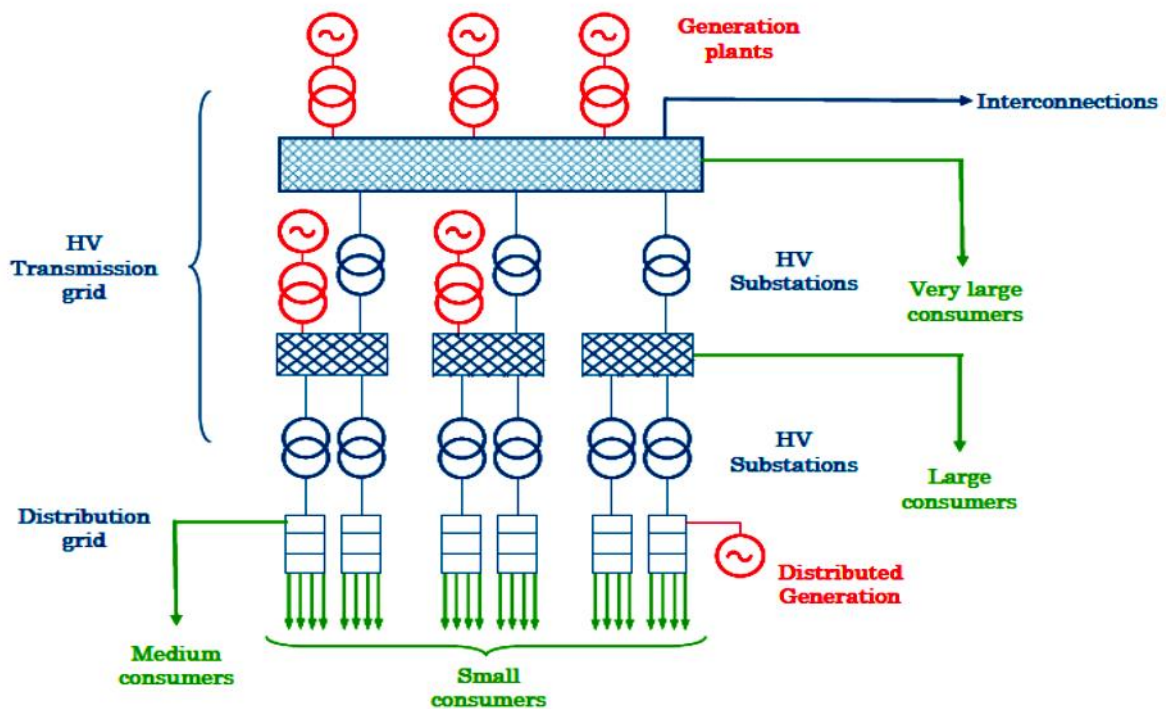
Figure 2. 2: Modern power system structure.

2.2 Transmission network

The purpose of the electric transmission system is to interconnect electrical energy generation stations or power plants with main load centres. High Voltage AC (HVAC) systems are used for most transmissions as well as High Voltage DC (HVDC) systems. Overhead transmission

lines are also used to interconnect neighbouring utilities for regional economic power dispatch purposes during normal operating conditions and for power transfer during emergencies. Operational transmission voltages range up to 765 kV for ANSI standards and up to 1200 kV for IEC standards. Transmission lines carry the power to substations where the voltage is stepped down to suitable levels for distribution and switching in and out are performed. Those substations are also known as high voltage substations or switching substations respectively. The portion of transmission network between substations and the distribution network is called a sub-transmission network. Voltage levels at this stage of the power system structure generally range from 69 to 138 kV (El-Hawary, 2002). Large industrial loads are connected on sub-transmission networks. Capacitor and reactor banks for transmission network voltage stability are housed in substations.

2.3 Distribution network

The distribution network serves as the last link of the supply chain between the generation station and the customers. It ensures safe and reliable transportation of electricity to various customers across the entire geographical service. Distribution systems voltage ranges from 11 to 60kV for primary distribution mainly for huge load customers and less than 1kV for secondary distribution that terminates at customers' meter. Three-phase connections are used for primary distribution while for secondary distribution both three and single-phase connections are used depending on utility regulations.

Early electricity distribution was done through underground DC system networks and then evolved to AC system networks. Due to economic reasons, overhead distribution lines are preferred over underground systems. The installation cost is hiked due to the civil works involved such as duct and manhole construction and need of conductors with special insulations. However, underground power distribution systems have advantages in visual pollution restricted areas. The overhead distribution systems are economical with regards to installation and maintenance. On the other hand, they are not practical in densely populated areas and they are subject to fault due to lightning strikes and storms, therefore they are preferred in rural areas (Patrick & Fardo, 2009). Between the two systems, the deciding factor is economic, while sometimes, non-economic factors like public safety might also be considered in system selection.

Main network topologies used in the distribution system are radial, ring, and interconnected systems(V.K. Mehta and R. Mehta, 2011). The radial system shown in Figure 2.3 is the simplest and most economic topology in terms of initial cost. However, it is disadvantaged by the fact that the distributor side near the feeder is more loaded than the distributor end-side where the voltage fluctuations are observed, as well as reliability issues as the costumers

depend on a single distributor. The radial system is mainly used in rural electrification. The ring distribution system in Figure 2.4 addresses reliability issues and voltage fluctuation inherent to the radial system; while the interconnected system in Figure 2.5 increases reliability and reduces the reserve power capacity therefore improving the efficiency of the system.

Electrical energy is currently viewed more as a product than a service, therefore quality criteria are applied to the power distribution system, which is thus required to continuously supply proper voltage, power on demand, and to be reliable all the time (Bollen, 2000). Therefore, in the design and operation of a distribution system voltage stability is an important aspect, as modern loads are very sensitive to voltage fluctuation. The latter results from load variation on the system and consequences are the burning out of motors and inefficient lighting for low voltage, while the burn out of lighting and malfunction of some appliances would result in case of higher than rated voltage at terminals of the customers. Beside voltage stability, continuous supply of energy, reliability, and minimal outages are expected from the power distribution system (Bíscaro et al., 2016).
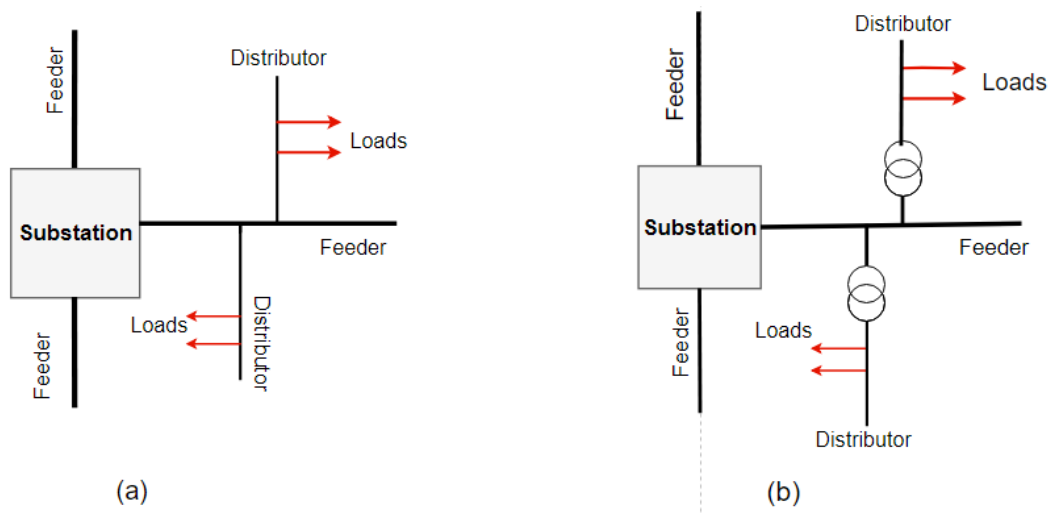
Figure 2. 3: Radial distribution systems: a) DC and b) AC.
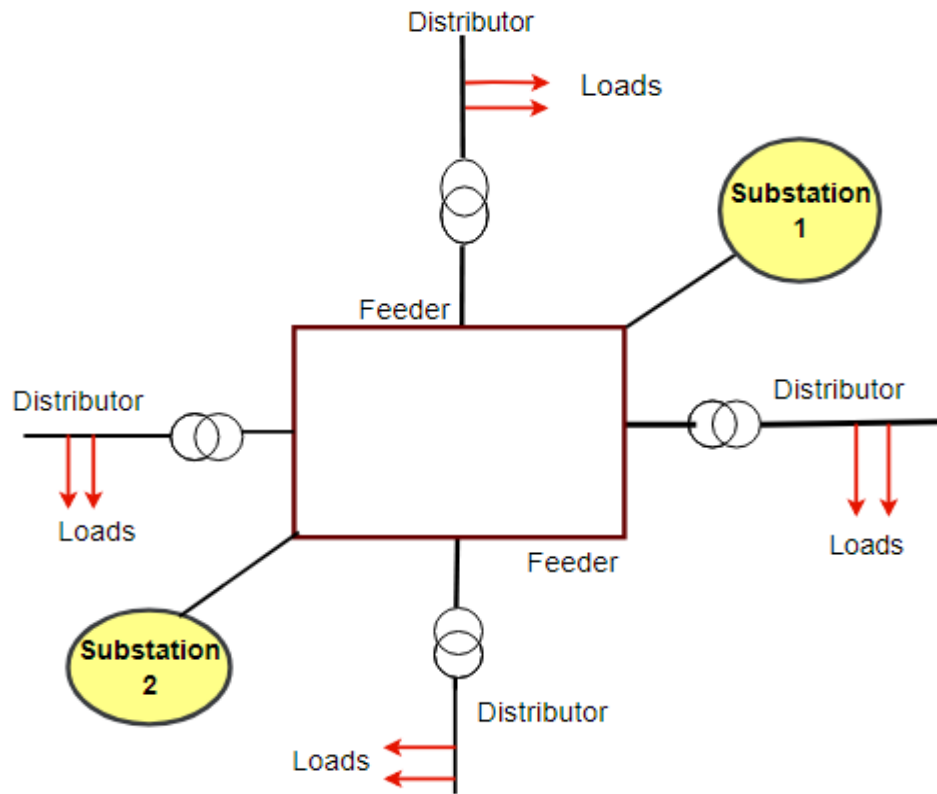
Figure 2.4: Ring main distribution system.
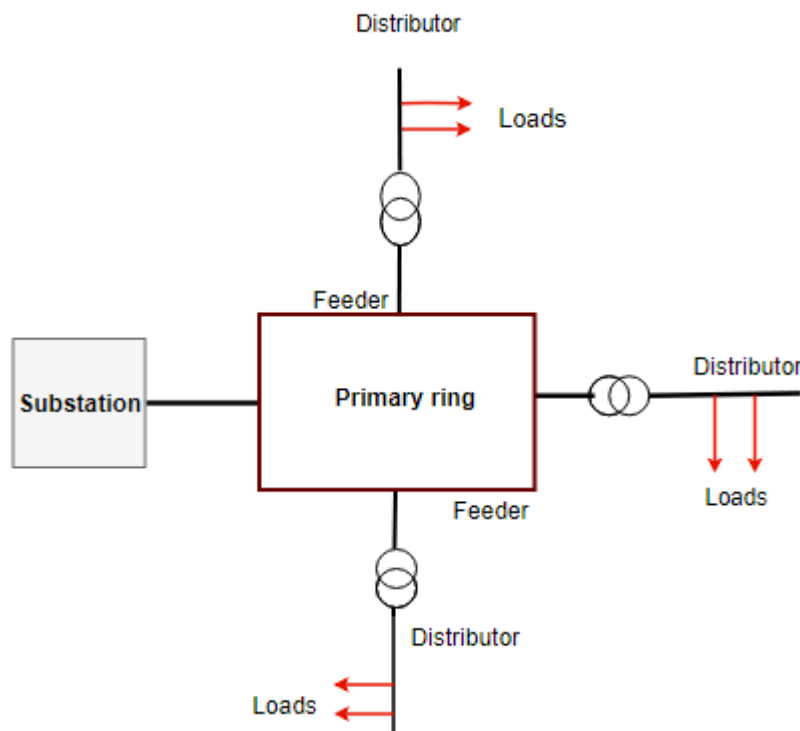
Figure 2.5: Interconnected/meshed system.

2.4   Distribution network components

The role of the electricity distribution network is to provide a path for electrical energy to flow from the transmission substation or distributed generation to each customer at a suitable rated voltage. Electrical energy has become the backbone of modern society, therefore the need for a reliable, good quality, and safe supply. To achieve this, a combination of various equipment and components is arranged in a systematic way. Different components are used depending on the network topology, but the main components are cables or lines, poles, transformers, protection systems, and substations.

2.4.1   Cables and lines

Depending on the design and considering economic and legal constraints, the distribution of electrical energy to the customers might be performed using overhead lines or underground cables. Overheard lines are economical compared to cables. Specific characteristics such as high electric conductivity, high tensile strength, least weight and least cost, are sought for a good overhead conductor. Other factors like safety might be taken into consideration over the previously mentioned characteristics. In distribution networks, mainly two types of overhead lines are used: insulated and uninsulated conductors.

Uninsulated conductors are bare conductors previously made from copper but currently in aluminium alloys. Though copper has a higher conductivity compared to aluminium, it is heavier and more expensive than aluminium, hence the general use of aluminium conductors for overhead lines. Traditional power delivery systems use three types of aluminium conductors: aluminium conductor steel reinforced (ACSR), all aluminium alloy conductor (AAAC), all aluminium conductor (AAC). Due to the high-power demand and convergence of the population in the cities, it might be impossible to build new transmission and distribution system from environment point of view. Therefore, emphasis is put on developing new conductors with high efficiency, less environmental impact and public acceptance. Hence the development of superconducting cables and lines (Thomas et al., 2016). They are classified into: High Temperature Superconductor lines/cables (HTS) and Low Temperature Superconductor lines/cables (LTS) (Geun-Joon, 2011). Among the modern power delivery systems are also the Gas Insulated Lines (GIL) largely discussed in Magier, Tenzer, & Koch (2018) they are also used in transmission of bulk power.

The *aluminium conductor steel reinforced* shown in Figure 2.6 is a bimetallic conductor consisting of two stranded layers. The inner layers are steel wires while the external layers are hard drawn aluminium, which increase the conductor's mechanical strength. This kind of conductors find applications in high voltage and medium voltage overhead transmission lines. They are stranded in order to prevent breakage and minimize skin effects. Having an improved mechanical strength allows for long span use.

Figure 2.6: Aluminium conductor steel reinforced (electrical4u, 2017).

All Aluminium Alloy Conductor (AAAC) shown in Figure 2.7 differs from the ACSR conductor as there is no steel and is therefore lighter. The alloy compensates in terms of strength, but also makes it more expensive. Its application can be found in transmission and sub-transmission networks where the environments, like mountains and swamps, impose limitations on support structures. AAAC are more resistant to corrosion and have low losses compared to ACSR conductors.

Figure 2. 7: All aluminium alloy conductor (HBE Centrado, 2017).

All Aluminium Conductor (AAC), shown in Figure 2.8, is widely used in primary and secondary distribution networks. It consists of aluminium wires stranded in single or multiple concentric layers. All aluminium conductors have a better conductivity at a low voltage level and less strength compared to the ACSR, hence its use in distribution where a shorter span is required. They are also corrosion resistant, which makes them preferred for coastal areas (Ridley, 2017).

Figure 2. 8: All aluminium conductor (Hebei Huatong Wires & Cables Group Co., Ltd., 2017).

The other type of overhead lines used in a distribution network is with insulated conductors. The idea behind the use of insulated conductors for overhead lines comes from the utility's need to improve reliability, quality service, electromagnetic concerns, the right of way deliverance issue, and safety as the clearance in congested areas is difficult to maintain (Clapp et al., 1997; Newswire, 2014).

Three types of insulated conductors are categorised as unshielded: weatherproof wire, tree-wire, and spacer cable. Weather-proof wires were used to reduce outages caused by the weather as the insulation serves to protect overhead conductors against weather conditions by preventing accidental contact between lines or other objects due to wind and storms. Initially made from asphalt-saturated cotton braids and natural rubber compounds, this insulation suffered from cracking after a short time (Landinger et al., 1997). Similarly, gravy polyethylene and cross-linked polyethylene were used, but they cracked due to extensive sunlight exposure. Modern line wires use non-cracking insulators made of a thin layer of thermoplastic or cross-linked polyethylene and they are governed by ANSI/ICEA S-70-547. For an aerial space cable, a dual layer of insulation in polyethylene with abrasion resistance properties for the external layer is used (Bouford, 2008). This provides a protection against any pinholes by trees through the insulator layers that might cause accidental contact between lines. Tree wire are all insulated wires with properties between weatherproof and spacer aerial ones. They are available with single or double layer insulation.

Shielded cables differ from the unshielded due to the fact that for the former, the insulation is rated for continuous operation voltage of the line and they have a shielding that provides a path for leakage current in the event of an insulation failure.

Aerial bundled conductors shown on Figure 2.9 are composed of insulated conductors bundled together. Two systems of aerial bundled conductors are in use: a self-supporting system which consists of four carbon loaded XLPE insulated aluminium wires of the same cross section and supporting-core system which consists of three carbon loaded XLPE insulated aluminium wires of the same size wrapped around a supporting insulated aluminium alloy conductor. An optional sub-conductor can be added depending on whether it is applied as a messenger or lightning rod. The use of aerial bundled conductors owes its roll out in the distribution network to the issues faced by bare overhead lines in urban and forested areas. In urban areas, the increased risk of faults due to proximity with buildings and trees favours the use of ABC lines; while in forested areas the risk of wild fire caused by the arc from lines faults due to wind motivates the current trend in the use of aerial bundled over headlines (Celina & George, 1995; C. Bayliss & Hardy, 2007). Moreover , a loss reduction method and new antitheft techniques are being developed through the use of aerial bundled conductors (La Salvia, 2006; Sahito et al., 2015).

Figure 2. 9: Aerial bundled conductors.

Three aerial bundled conductor systems are widely used: 1) Finnish system, which consists of three insulated aluminium conductors and a non-insulated messenger wire in the aluminium alloy which is used as neutral; 2) French system, which also consists of three insulated aluminium conductors, but unlike the Finnish system the messenger is also insulated; 3) Germany system that consist of four aluminium alloy conductors of the same size, three phases and 1 neutral (Agarwal & Barua, 2010). All these systems can accommodate additional conductors for street light.

Figure 2.10 shows different components of an aerial bundled line system in distribution with street lights service. One of the features of the system is the insulation piercing connector that eases the connection between the main and derived cable, reducing installation and maintenance cost.
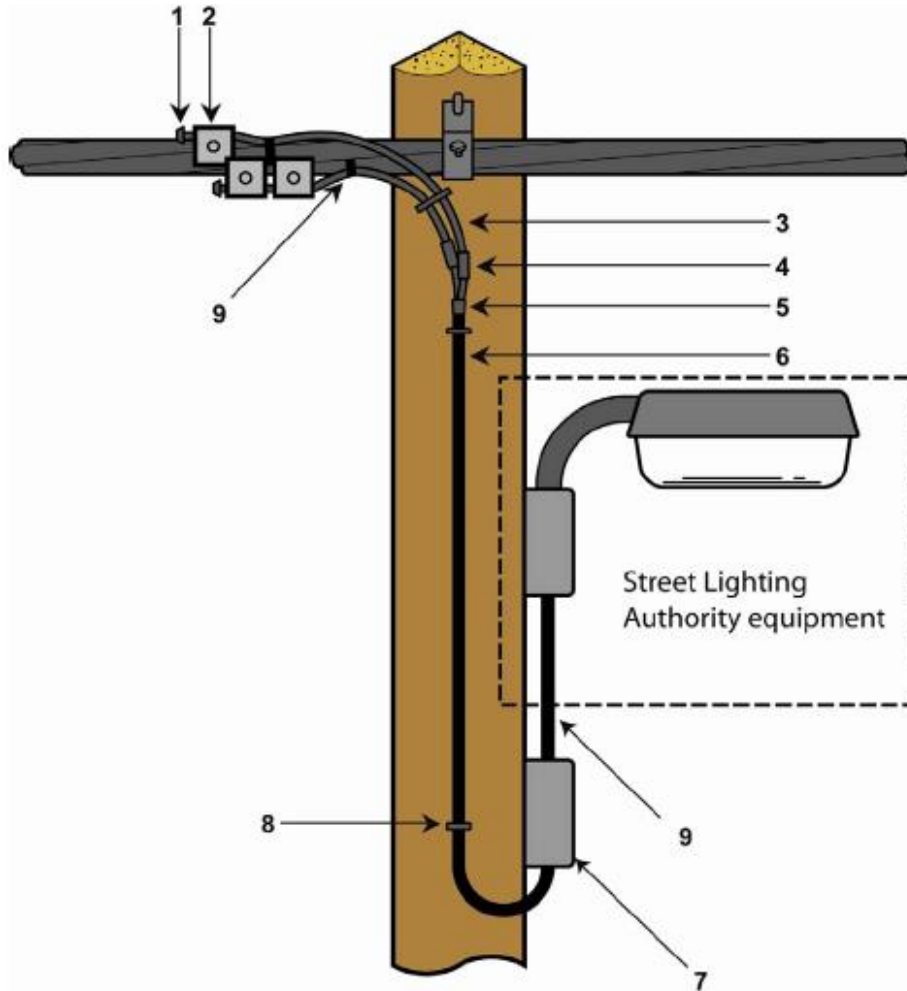
Figure 2. 10: Aerial bundled conductor with street light connection(ukpowernetworks, 2012).

1. Conductor fitting cap-end
2. Conductor fitting insulator piercing connector
3. Conductor
4. Conductor compression non-tension
5. Cable termination break out kit
6. Cable
7. Service box
8. Cleat
9. Local Authority Street Light Tails

2.4.2   Over headlines support

Lines support, known also as poles or towers, are one of the expensive parts of an overhead lines distribution network. They are expected to be mechanically strong to support conductors and insulators weight and withstand weather conditions, while at the same time being light in

weight and affordable to install and maintain. They should also have a long life span (V.K. Mehta and R. Mehta, 2011).

In distribution networks, wooden poles, steel poles, reinforced concrete, and lattice steel towers are the main lines support in use up to date. The selection of any the above-mentioned poles depends on the size of the lines, voltage, environment, and the cost associated. Of course, with reference to the characteristics of an ideal pole.

Poles in wood are commonly used in the distribution network in rural areas, as they are economically viable, available, and have sufficient insulation properties. Wooden poles, however, have shorter life spans and one of the major drawbacks is that they suffer from rot. The latter is prevented by the impregnation of the pole with Creosote. For the impregnation to take, wood moisture should be less than 30% to avoid later cracks that might occur due to the poles shrinking as they dry up (Sayer, 1986; Li et al., 2006; Lehtinen, 2016). Figure 2.11 shows different types of wooden poles. It is worth mentioning the fact that wooden poles cannot be used for voltage over 20 kV (Wahlberg & Rönnberg, 2011; V.K. Mehta and R. Mehta, 2011).
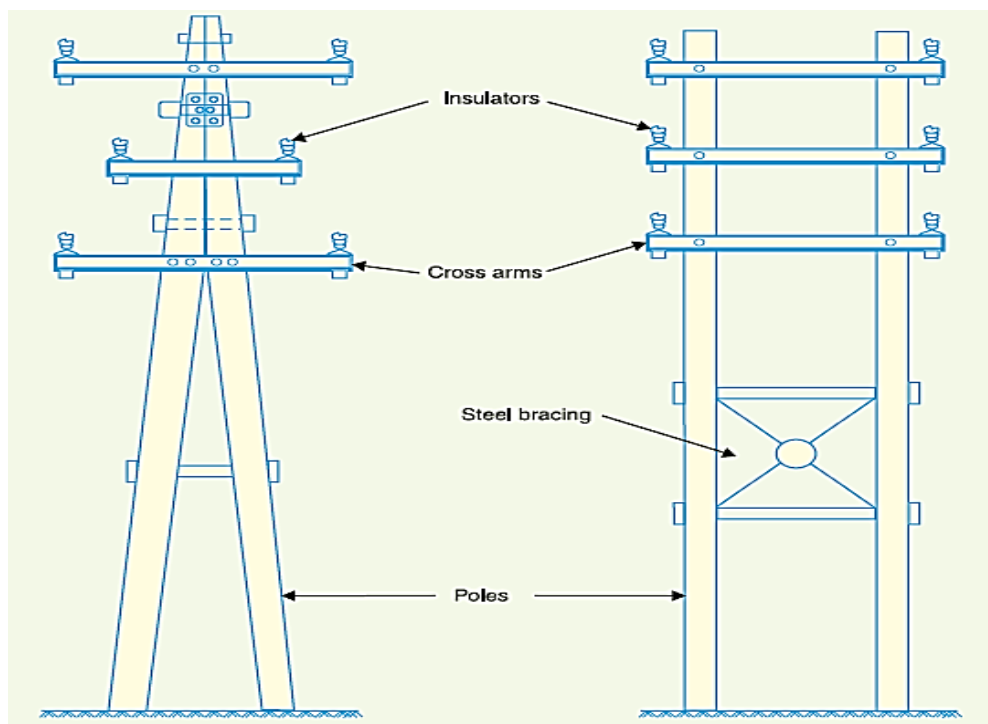
Figure 2. 11: Wooden poles (V.K. Mehta and R. Mehta, 2011).

Steel poles are used as a substitute to wooden poles due to their strength, lightness, resistance to animal damage, long life, and not needing chemical preservatives (Salman & Li, 2015). However, steel poles rise electrocution concerns, hence the use of alternative material such as fiberglass cross arms to minimize the risk (Harness, 1998; Deegan, 2008). Steel poles suffer from corrosion due to the salt and moisture in the air, so they are being replaced by composite poles that are safe and environmental friendly (Sarmento & Lacoursiere, 2006;

Thimons, 2014). Steel poles are used in distribution networks in cities and three types of them, shown in Figure 2.12 are on the market: rails poles, rolled steel joint, and tubular poles (V.K. Mehta and R. Mehta, 2011).

Figure 2. 12:Steel pole (pinterest.com, 2015).

Reinforced concrete poles have improved mechanical characteristics compared to wood and steel poles. In addition to looking good and having good insulation, its mechanical strength allows for longer spans and an extended service life of the poles which saves on operational and maintenance costs (V.K. Mehta and R. Mehta, 2011). However, the weight of reinforced concrete poles makes the installation a bit difficult as heavy lifting equipment is needed. The breaking of the pole due to seismic activities is also a concern (Rahnavard et al., 2013). Negative impacts of reinforced concrete on the environment have been reported in Harness, Gombobaatar & Yosef, (2008) and in Prather & Messmer (2010). Corrosion inside reinforced concrete poles might raise due to AC currents interference (Brenna et al., 2017; Aghajani et al., 2013), which might affect lightning grounding design as well as the protective design of the network (Miyazaki et al., 2006; Shen et al., 2014; Sekioka, 2008). Figure 2.13 shows reinforced concrete poles for single and double circuit. The holes on the poles are for easy climbing during the installation and maintenance; they are also made in order to reduce the mass of the pole (V.K. Mehta and R. Mehta, 2011; Fouad & Detwiler, 2012).
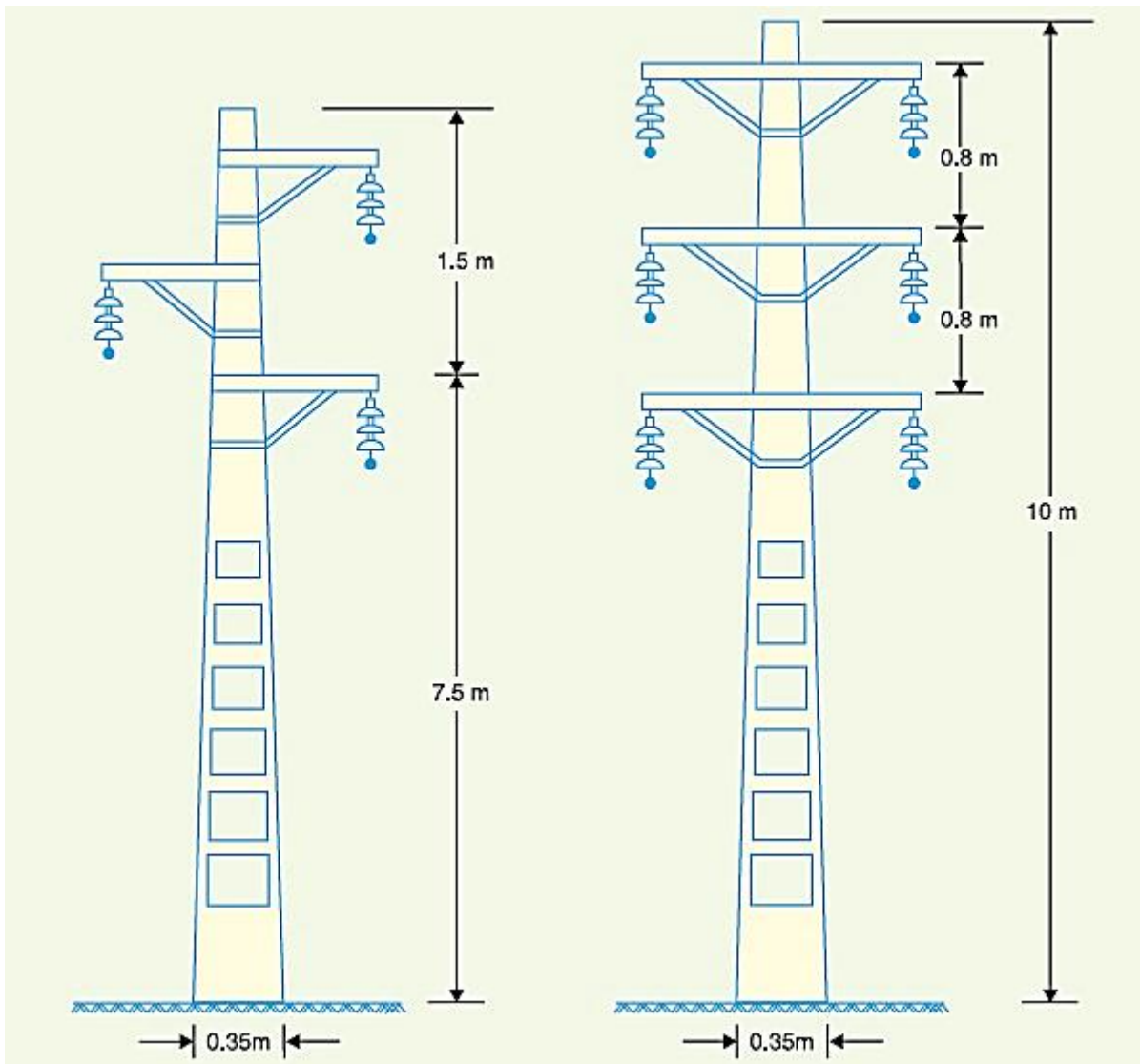
Figure 2. 13: Reinforced concrete poles for single and double circuit (V.K. Mehta and R. Mehta, 2011).

2.4.1 Transformers

Transformers are the main components of a distribution network technically and economically-wise. They are used for voltage levels transition between primary distribution and consumers (Huang, 2003). They are operated as step down three phases transformers or single phase depend on application. Furthermore, their construction depends on their application which goes in line with the intended cooling system. Thus, for an indoor application, a dry type transformer is used while for outdoor applications it is immersed in liquid (C. R. Bayliss & Hardy, 2007).

Distribution transformers consists of a core and windings. The role of the core is to provide a route to the magnetic field lines generated from the windings through electromagnetic induction. The core is made of a lamination of steel sheet insulated from each other by a thin insulation coating. However, the core generates heat that must be dissipated. Despite the fact

that laminated steel coating might sustain high temperatures, being in contact with winding's insulation it might damage the winding's insulation (Coltman, 2002). Studies indicate the replacement of the steel sheet by new soft magnetic materials, mainly amorphous alloys, as transformer cores will have economic and ecological advantages (Najgebauer et al., 2011; Kefalas & Kladas, 2012).

Distribution transformer windings are current carrying conductors made of copper or aluminium, depending on the intended application of the transformer as aluminium is lighter and economic but a large amount of it is required to match the copper performance. On the other hand, copper with its high mechanical strength can withstand the force resulting from high short circuit current, and is therefore used for high rating transformer (Olivares-Galván et al., 2010). Different ways of windings arrangements are used such as pancake windings, layer, and helical winding (Heathcote, 2007).

The electromagnetic thermal effect transformers windings need to control to avoid its negative impact on the efficient and safety usage of transformers (Arifianto & Cahyono, 2009; Amoiralis et al., 2012). Hence the use of different cooling methods like air, water and oil-immersed, which are used individually or combined as a coolant. For dry type transformers, air natural and air forced cooling systems are used, while for oil immersed, the following systems are used: oil natural cooling, oil natural air forced (ONAF) cooling, oil natural water forced (ONWF) cooling, oil forced air natural (OFAN) cooling, oil forced air forced (OFAF) cooling and oil forced water forced (OFWF) cooling (Blair, 2016). With oil immersed transformers, through condition monitoring test transformers the oil helps in determining its status, which allows preventive maintenance (Haema & Phadungthin, 2013).

Three-phase transformer windings can be connected in star (Y), delta (D), and inter-star also known as zig-zag (Z), depending on requirements. In distribution, usually the high voltage side is connected in delta for the sake of saving conductors from primary distribution, and often low voltage windings connections are in zig zag (Xiaodong et al., 2007). Ideally, the secondary would be connected in star but to prevent phase loading imbalance, the zig-zag connection is preferred. These connection arrangements create phase difference between primary and secondary windings which has an effect on the voltage sag propagation in the network (Mendes et al., 2008; Geno, 2011). These differences in phase angle are also known as vector groups. It is worth mentioning that the phase difference serves when there is a need to remove specific harmonics. These characteristics are useful for distributed generation integration as many of them use converters as an interface to the distribution network (Wen et al., 2012; Awadallah et al., 2015). DYn11 connection is often used in the distribution network for voltage step-down and is applied in industrial, commercial and residential areas (Aung & Milanović,

2006). The advantage with this arrangement is that the delta on the primary side blocks the third harmonics while the star on the secondary winding gives the neutral connection.

The location of distribution transformers depends on the environment and the load centre, and can be overhead, underground, and pad-mounted. Overhead, also known as pole mounted transformers are usually used in rural areas for economic reasons though it is susceptible to be subjected to various weather conditions. Pad-mounted or ground-mounted transformers are mounted on an open space on ground in urban areas and for industrial applications. Underground or buried transformers are used where there is a desire for protection against damage from weather conditions, vehicles, and trucks (Dudley & Mulkey, 2004).

In distribution networks, transformers are key components, hence the need to protect them against internal and external faults that might affect them and by occasion the entire service. There are 6 categories of transformer faults (IEEE, 2000; Jan et al., 2015):

1. Winding and terminal faults
2. Core faults
3. Tank and transformer accessories faults
4. On load tap change faults
5. Abnormal operating conditions
6. Sustained or uncleared external faults

Transformer protection against winding faults is usually achieved using a differential protection scheme complimented with restricted earth fault (REF) protection to provide good sensitivity for near earth ground faults detection (Kasztenny et al., 2010; Faiz & Heydarabadi, 2014; Etumi & Anayi, 2016). Part of the internal faults is core faults, which are characterised by the overheating of the transformer. A buchholz relay for oil cooled transformer, thermocouple, temperature sensors, and various monitoring systems are used for fault detection as well as protection (Rusov & Zhivodernikov, 2007; Kang et al., 2007; Prudhvi Raj, 2013; Thangavelan et al., 2016). In the same line, overvoltage and overcurrent relays running circuit breakers are used in addition to fuse for transformer protection against abnormal conditions and sustained or uncleared faults (Grabovickic et al., 2012; Mozina, 2006).

2.5 Distribution network protection

2.5.1 Introduction

Electrical power distribution networks are the last mile between power generation and customers. From the latter perspective, the distribution network or system is required to deliver a reliable, quality, and safe electrical energy at an economic price. Therefore, distribution should be properly designed and maintained to prevent the faults that might occur.

To ensure the safety, reliability, and quality of the power supply in distribution networks, various auxiliary equipment are coordinated to detect and isolate faults that might rise. The combination and coordination of monitoring, detecting and isolating devices constitute what is called a protection system as shown in Figure 2.14.
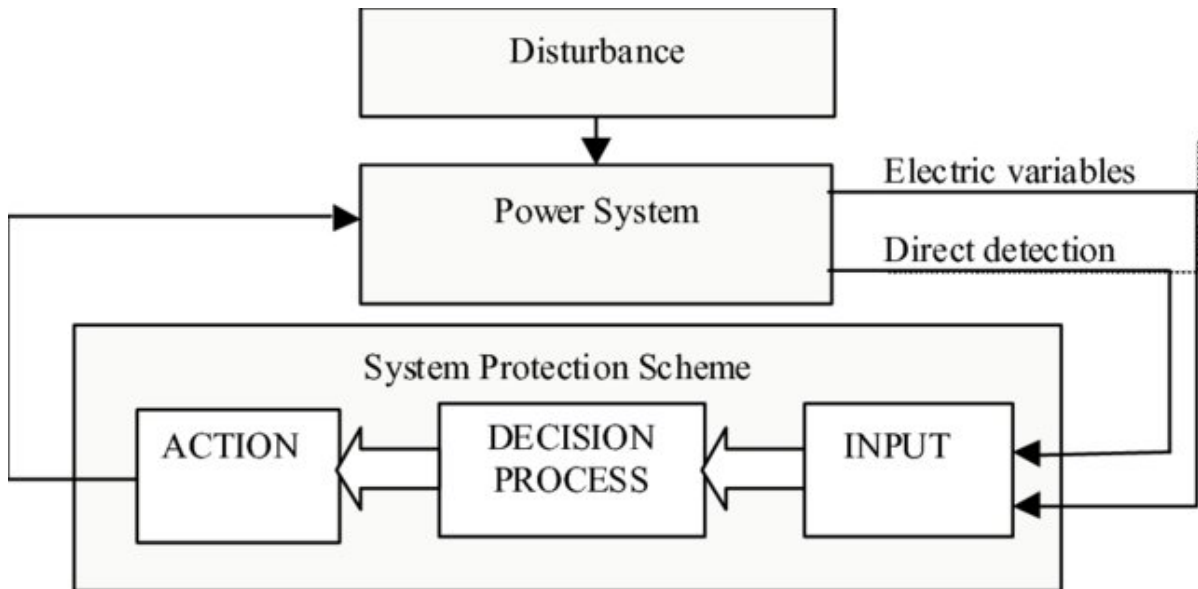
Figure 2. 14: General structure of a system protection scheme
(Mccalley et al., 2015).

2.5.2 Monitoring

In the protection system, current and voltage are the parameters which are monitored for detecting abnormalities. Current and voltage transformers are used as measurement tools which will feed information to the detecting devices. Also known as measurement transformers, CT and VT operate as step-down transformers by bringing down the current or voltage to be measured to the level that can be handled by the measuring instrument. Usually a measurement range of 5 A or 1 A for current and 110 V or 100 V for voltage is used to feed the detecting equipment (Laslo, 2012). Regulated by IEC 60044, CT and VT, either used for measurement, control or protection, their main role is to transform high voltage or current values to a manageable value for the mentioned application (Bayliss & Hardy, 2012).

Depending on the application, current transformers should be correctly sized to meet burden requirements. Protection CT are mostly accurate for running a batch of indication instruments, but it cannot be sustained by the low burden from metering instruments. Connecting low burden metering instruments to protection class CT would let high currents run into the instruments, and consequently the high thermal stress might damage the instrument. To avoid

the situation, an interposing auxiliary transformer is used and arranged such that its saturation point is beyond few 10s Amps. Hence for the purpose of protection, the CT appropriate look is required for certain characteristics such as, transformer ratio, polarity, frequency, class, voltage ratings, current ratings, thermal ratings, and saturation voltage, etc (Ganesan, 2006; Fernandes & Santos Mota, 2007; Ferreira& Filho, 2016).

The role of the voltage transformer (VT) is for the transformer signal to be measured from a high value to the value that can be handled by measuring instrument or relays thus isolating the metering equipment from high voltage. Two types of VT are in use, the inductive voltage transformer and a capacitor voltage transformer. Inductive VT being nonlinear in nature suffers from inaccuracy in measurement when subjected to a sudden increase of frequency or fast impulse (Lamedica et al., 2016). A capacitive voltage transformer has higher accuracy and find application for high voltage classes. It has a simple structure and low cost compared to inductive VT (Zhang et al., 2016).

2.5.3 Faults detection

The occurrence of a fault in the network is characterised by a substantial change in current, voltage and frequency values or magnitudes from the rated or pre-set values. Therefore, it is important to detect those changes that might cause damages to the equipment and users. Detection is made from measurement taken by monitoring equipment, such as CT and VTs. The analysis and decision making out of the information provided by the monitoring system is performed by protective relays. The latter can pick between tolerable and intolerable conditions for the system. Though a common indicator of fault is the sudden increase in current, other parameters can also indicate a fault condition. Parameters such as temperature, impedance, phase angle, power and current direction, indicate the health of the network.

Protective relays are detectors and a decision maker in terms of the protection scheme. They have been in use in the power system since the 18th century and have evolved with technology (Rebizant et al., 2013; Singh, 2007). As shown in Figure 2.15, early relays were of the electromechanical type that evolved to solid-state type, and actual trends is digital or microprocessor-based relays (Abdelmoumene & Bentarzi, 2014). Electromechanical relays have good precision and high sensitivity; however, the moving part requires time which impacts on the fault clearance overall time. The solid-state relays relieved that challenge of operation speed and have an additional advantage of reduced reset time compared to electromechanical relays. Digital or microprocessor-based relays built on progress made by solid-state relays and in additional to their multifunctional nature, reduced installation cost and communication capability are aspects that made them popular and powerful tools in the modern power system (Aibangbee & Onohaebi, 2015). The capability of digital or microprocessor relays finds application in smart grid and renewable energy integration.

Table 2.1 shows the feature comparison of protective relays technologies.
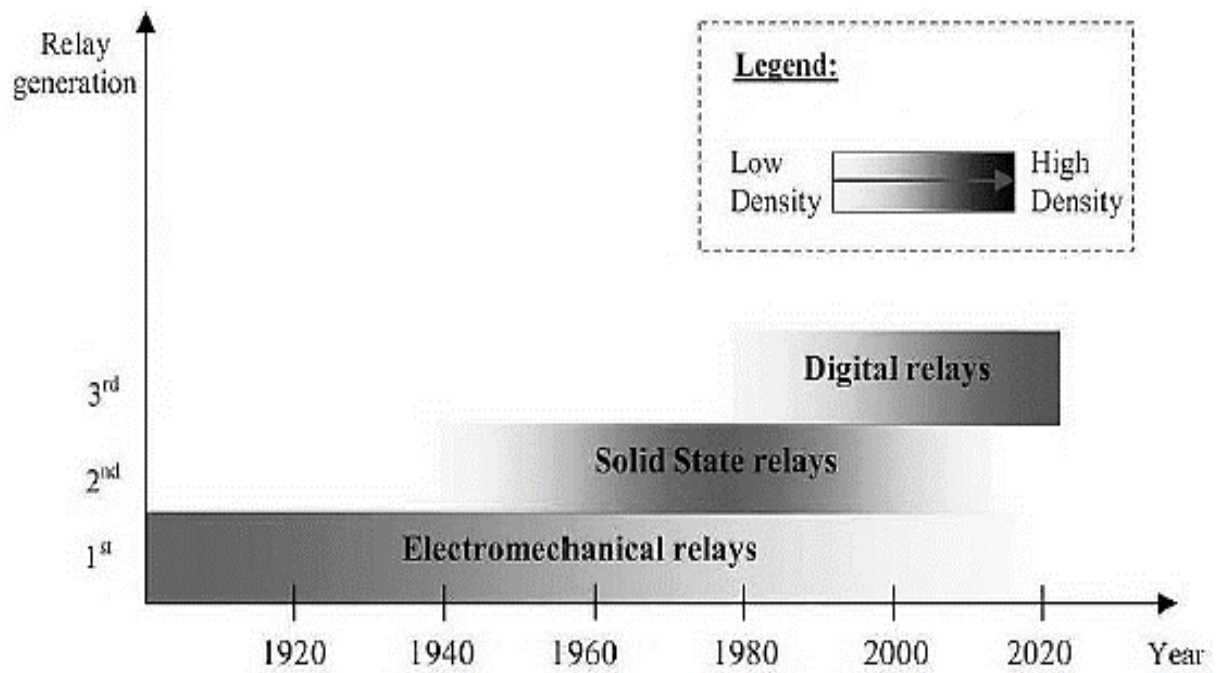
Figure 2. 15: Evolution eras of protective relays (Abdelmoumene & Bentarzi, 2014).

Table 2. 1: Protective relay technology characteristics comparison.

Characteristics	Relay type		
	Electromechanical	Solid state	Digital
Accuracy and sensitivity	Good	Very good	Excellent
Reliability	High	Good	Moderate
Discrimination	Low level	Good	Excellent
Multifunction	No		Yes
Range of settings	Limited	Wide	Vey Wide
Self- monitoring	No	No	Yes
Speed of response	Slow	Fast	Very fast
Metering	No	No	Yes
Disturbance immunity	High	Low	Very low
Lifetime	Long	Short	Short
Parameter settings	Difficult	Easy	Very easy
Remote operation	No	No	Yes
Visual indication	Targets, Flags	LED	LCD
Event log	No	No	Yes
Relay Size	Bulky	Small	Compact
Scada capability	No	No	Yes
Maintenance	Frequent	Low	Low

Various types of relays are used for detection and control in a protection system. Based on their performance, protective relays can be classified as (Walter, 2003):

- Overcurrent relays
- Overvoltage relays
- Undervoltage
- Distance relay
- Differential relay
- Inverse time relay

- Definite time relay
- Phase relay

A. Overcurrent relays

Overcurrent demand in the network is one of the indicators of a fault occurrence in the network. Therefore, there is a need for the protective system to pick and act upon the development of such a condition. To achieve this, overcurrent relays are used. They are protective relays set to operate when the current exceeds a specific magnitude. Measurements taken by the current transformer are feed to the overcurrent relay which then compares them to pre-defined values and a tripping action will be initiated in case of excess current.

Three types of operating overcurrent relays are used, namely, the instantaneous or definite current, the definite time overcurrent relay (DT), and the inverse time definite overcurrent relay (IDTM). Identified as device number 50 by ANSI/IEEE C37.2 standard device numbers, the instantaneous overcurrent relay operates as soon as the current crosses the defined value. Although referred to as instantaneous, it has an inherited time delay for operation in range of milliseconds. Figure 2.16 shows the characteristics of an instantaneous overcurrent relay.
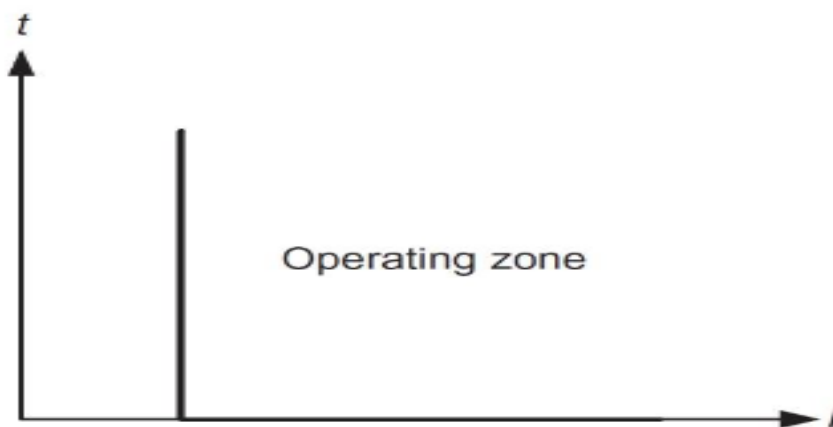
Figure 2. 16: Definite (instantaneous) overcurrent relay operating characteristic.

The definite time overcurrent relay, as indicated by the name, operates when the current exceeds a certain level for a continuous pre-set time. As the fault occurs the relay will check the level of the fault current and how long it stays there, and if both values exceed pre-set values the relay will operate to open the circuit breaker. This type of overcurrent relay overcomes the discrimination and selectivity short fall of instantaneous relay when used in a feeder with small impedance. Definite time overcurrent relays have adjustable pick up current and time. Modern relays can combine multiple stages, each one with independent current and time settings. They require coordination when used, such that the circuit breaker closest to the

27

fault is operated in the shortest time and the following circuit breaker towards upstream will follow in case the first one failed and so on. A definite time overcurrent operates slowly for faults closer to the source, which led to the development of the inverse time definite relay. Figure 2.17 shows the operating characteristic of a definite time overcurrent relay. It is applied as the main protection for outgoing feeders and as a backup protection with time delay for transformer differential relay and transmission lines (Baruti, 2017).
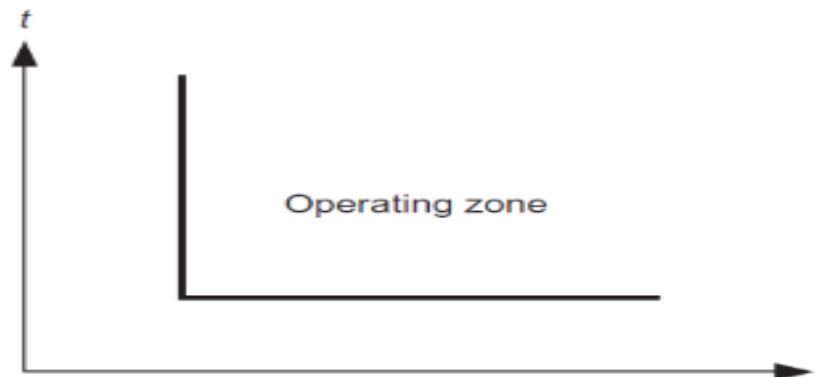
Figure 2. 17: Operating characteristic of a definite time overcurrent relay.

Inverse time definite overcurrent relay (IDTM) overcomes the slow operation speed issue that definite time overcurrent relays face when a fault occurs closer to the source. With this type of relay, the speed of operation is inversely proportional to the fault current magnitude. The higher the fault current, the shorter the relay operation time. Three characteristic types of this relay are available on the market: standard inverse, very inverse, and extremely inverse characteristics. Table 2.2 shows the equation of inverse time definite overcurrent relay according to the IEC 60255 standards, and on Figure 2.18 characteristics of different types are shown. Pick up settings are calculated using $I_r = (I/Is)$ where I_s is a setting, I_r fault current and the time multiply settings TMS.

Table 2. 2: Inverse time definite overcurrent relay IEC 60255 characteristics equations.

Relay Characteristic	Equation (IEC 60255)
Standard Inverse (SI)	$t = TMS \times \dfrac{0.14}{I_r^{0.02} - 1}$
Very Inverse (VI)	$t = TMS \times \dfrac{13.5}{I_r - 1}$
Extremely Inverse (EI)	$t = TMS \times \dfrac{80}{I_r^2 - 1}$
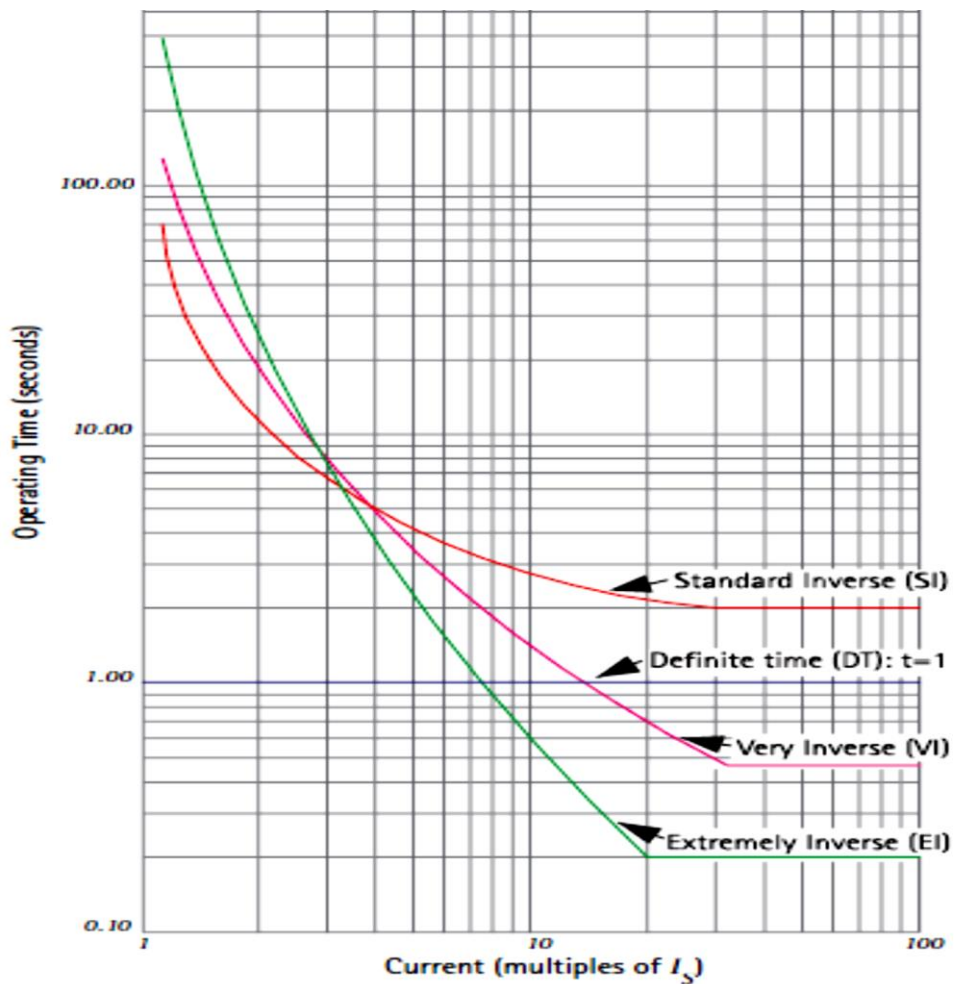
Figure 2. 18: inverse time definite overcurrent relay characteristics.

B. Overvoltage relay

Overvoltage phenemenon might rise in the power system due to various reasons such as the grounding of the cnductor, the circuit breaker opening, and lighting etc. The overvoltage might affect equipment connected and depending on the overvoltage magnitude, their breaker insulation can be damaged and the overall performace of the protective devices might be affected (V.K. Mehta and R. Mehta, 2008; Surajit et al., 2011). Thus, the protection against overvoltage is important. To achieve this, overvoltage relays are used to detect excess voltage value to the pre-set settings and operate the circuit breaker to isolate the affected zone. Identified as device number 59 by the ANSI/IEC standard, overvoltage relays are fed by voltage transformers. They can operate instantaneously or timely-delayed. For the setting up of an instantaneous overvoltage relay, the pick up voltage and voltage transformer ratio should be specified. For time setting, in case of definite time relay, time dial, inverseness characteristics, system and relay voltage are essential. Figure 2.19 shows the characteristics of an instantenous overvoltage relay (Sleva, 2009).
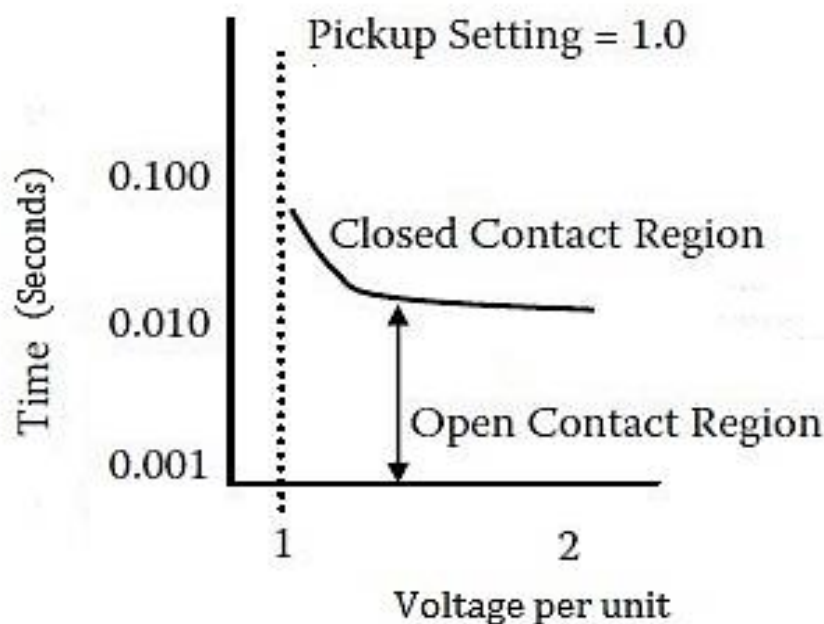
Figure 2. 19: Instantaneous overvoltage relay characteristic.

C. Undervoltage relay

Identified as device 27 by ANSI/IEC standards, the under voltage relay operates when voltage falls below the pre-set value. It is usually instantaneous but can be used with timers activated by instantaneous relay to achieve a time delay. The delay serves to allow the system to ride through momentary sags and therefore avoiding unnecessary tripping. For an undervoltage

relay set up, the set point or the minimum voltage value for it to trip should be specified as well as the ratio of the voltage transformer that is feeding it. Figure 2.20 shows the characteristic of an instantaneous undervoltage relay (Hewitson et al., 2015). Undervoltage relay applications extend to load shielding scheme, permissible function and timing applications (Kolluri et al., 2015; Gabba & Hill, 2001).
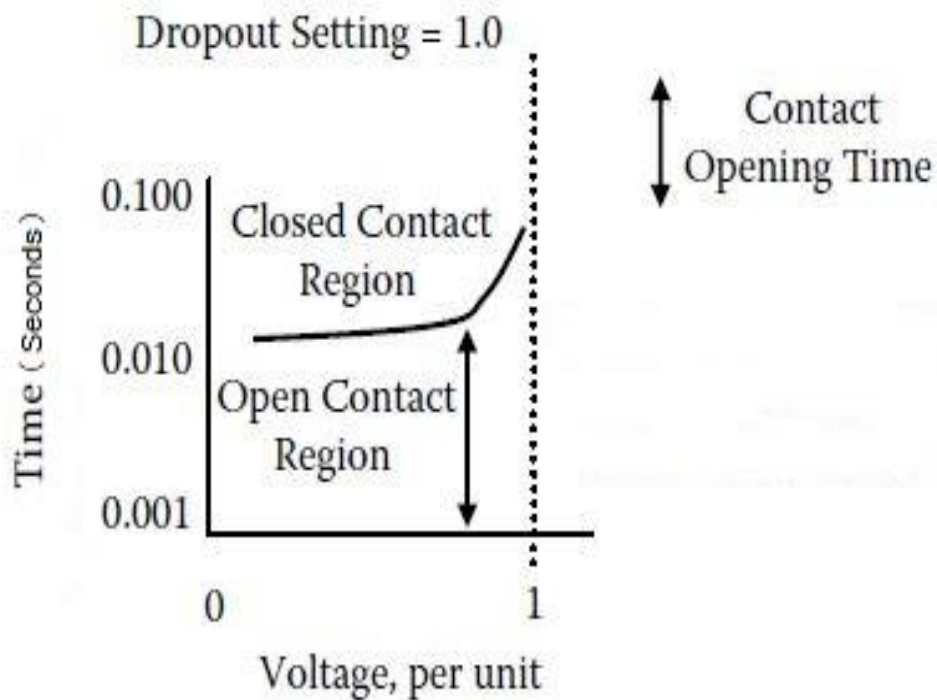
Figure 2. 20:Instantaneous undervoltage relay characteristic(Sleva, 2009).

D. Differential relay

The ANSI/IEEE Standard C37.2 Standard for Electrical Power System Device Function Numbers, Acronyms, and Contact Designations identifies the differential protective relay as device number 87. Differential relays operate when there is a phase difference between two measured identical quantities exceeding a pre-set value. As shown in Figure 2.21, the measured quantities by the current transformers are picked from both sides of the protected zone or unit. A difference between those quantities indicates a fault, hence the instantaneous operation of the relay. It is used as the primary protection for generators, bus bars, and transformers.
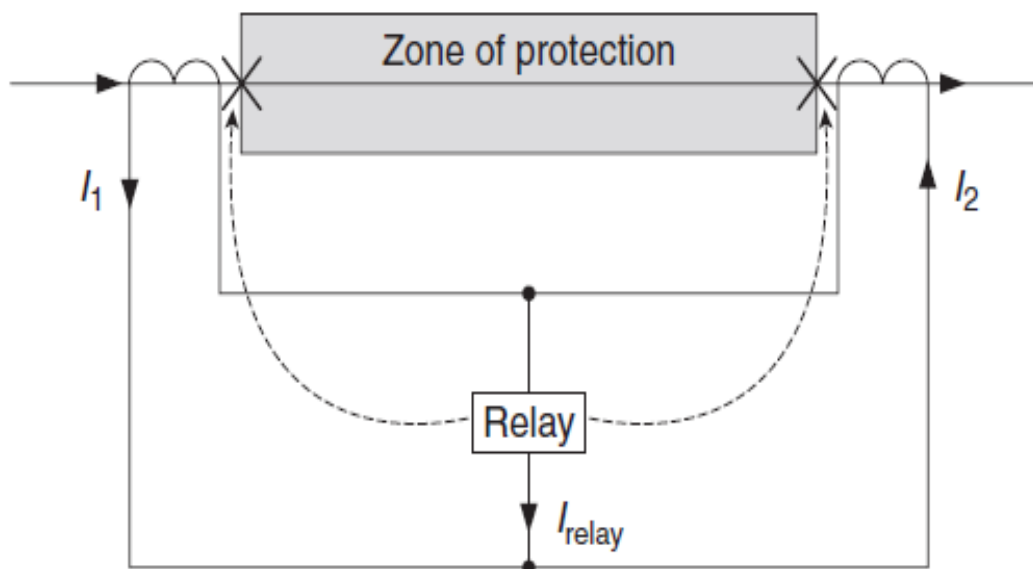
Figure 2. 21:Current differential relay protection(BOOTH & BELL, 2013).

E. Distance relay

Distance relay is a protective relay identified as device number 21 by ANSI/IEC standards. It is an instantaneous relay that operates when the impedance of the protect zone (pre-set distance along the transmission line) drops below a pre-set value. The protect zone ranging from the relay point location to the predetermined point is called reach point. The working principle of distance relay consist in calculating the impedance at the reach point using the voltage and current measured at that point, the ratio results are compared to the that point impedance. In case the measured impedance is less than the pre-defined reach point impedance value, a fault presence within the protection zone is assumed and the relay operates.

2.5.4 Switchgear equipment

The detection of faults and decision of tripping or isolating is done by the protective relays, but the isolation action is performed by isolating or switchgear equipment such as isolator switches, fuses, and circuit breakers. Moreover, switchgears allow for the isolation and interconnection of different part of the network, safe access for maintenance, and service of equipment in the network (Pryor, 2003).

A. Isolator switches

They are used to open or close circuits in the appropriate way. Isolator switches are referred to as device number 89 by ANSI/IEC and IEEE standards. They are meant to open or close the circuit under load or no load, however they do not have fault current interruption capability. Current interruption by switches is accompanied by an arc between the contact, and the

quenching of that arc depends on type of switch in use. Three types of switches are available on the market: air-break switch, isolator or disconnecting switch, and oil switch.

Mostly used for outdoor application air-break switches, Figure 2.22, have underload interruption capabilities and are equipped with arc quenching horns. The quenching is achieved through lengthening, cooling, and interruption of the developed arc during the switching operation Air-breaker switches are utilised for outdoor installation for an industrial area substation (Jonsson et al., 2014). Similarly, oil switches have underload switching capacity and uses oil as an arc quenching medium. On the other hand, the isolators or disconnecting switches operate under no load to isolate a portion of the circuit for safety purposes when the circuit breaker repair or maintenance is occurring. They are usually used on both sides of the circuit breaker and they are the first to close before the circuit breaker (V.K. Mehta and R. Mehta, 2011).

a) Center   b) Vertical

Figure 2. 22: Air-break switches : (a) Centre V break and (b) Vertical break(SEECO, 2016).

Figure 2. 23: Isolator or disconnecting switch (LUNO, 2017).

B. Circuit breaker

The circuit breaker is equipment that serves as a switch for a circuit under all conditions without causing injury to itself. It has the capability of closing or opening a circuit under no load, at full load, and during fault conditions. Controlled by a relay, it can be operated manually or by remote control and automatically on the occurrence of a fault. Circuit breakers are the links between the supply and customers, hence, they are required to carry the full load current under normal conditions without overheating and can safely interrupt normal condition current as well as fault current with minimum delay (Bakshi & Bakshi.M.V, 2009).

Circuit breakers are classified according to various aspects such as breaking medium, service, way of operation, action, control method, mounting method, construction, and contacts. Figure 2.24 shows circuit breakers classification according to breaking medium and voltage.
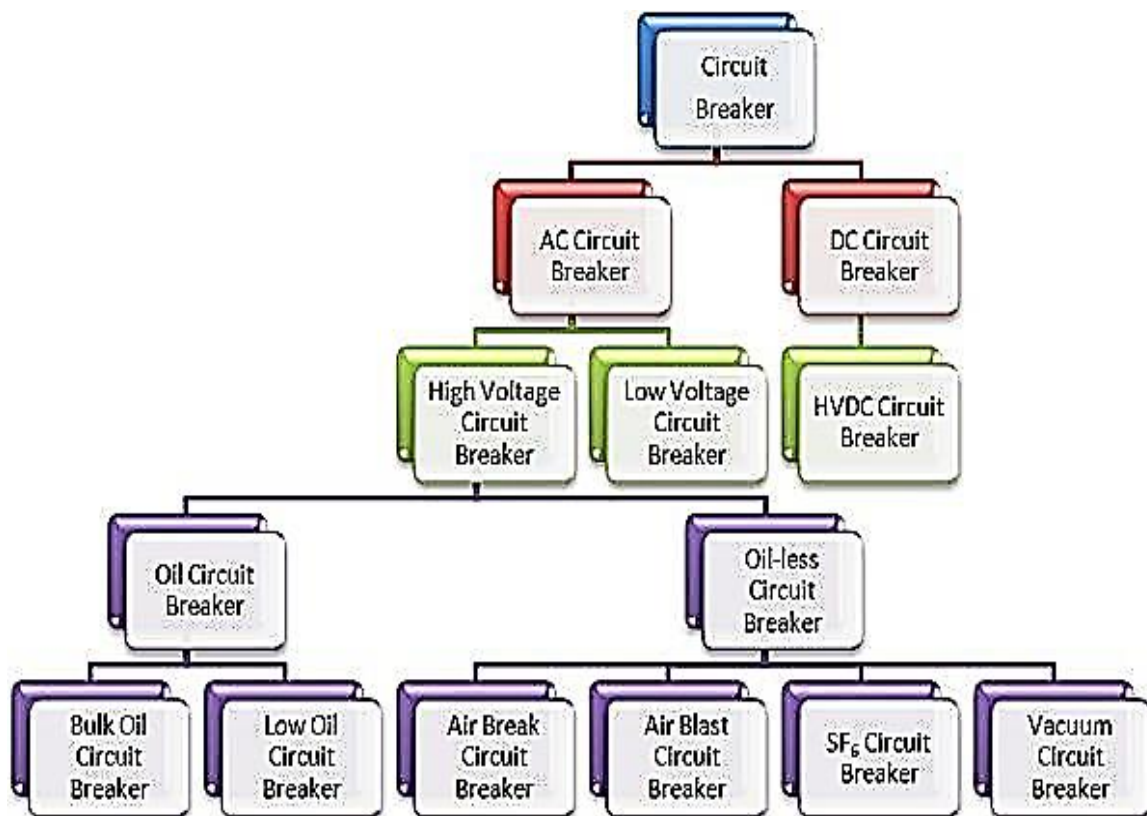
Figure 2. 24: Circuit breaker classification according to voltage and medium.

C. Fuse

Differently from the circuit breaker, the fuse combines detection and interruption functions. Based on electrical thermal effect, the fuse is a short piece of a conductor or strip that melts when excess electric current flows through it for a sufficient time. It is in series with the equipment or circuit to be protected. For rated current, the wire temperature stays below the

melting point. Short circuit current or prolonged overloading will rise the heating of the wire causing it to melt and break the protected circuit (Alexander et al., 2006; V.K. Mehta and R. Mehta, 2011)

2.5.5 Protection coordination

A distribution network consists of various equipment interconnected from the substation transformers to customers. Thus, in the event of a fault all the equipment connected will be affected and each equipment unit protection will try to isolate itself from the fault. Therefore, an uncoordinated isolation of all equipment, also known as sympathetic tripping, will raise and will lead to a complete black out of the system. Hence, the need for the coordination of protective devices.

Protection coordination consists of a combination use of protective relays with an appropriate selection of time delays and set points, while also taking into consideration reasonable expected errors or inaccuracies. The settings serve as a control mechanism for a circuit breaker to operate. The goal of protection coordination is the sequencing of relays communication and operation for the fault isolation only in the affected zone. For instance, in a distribution network, protection coordination means that the relay closest to the fault point will be the one to operate before upstream ones goes into action should the latter fail. Hence, containing the outage in the network to the smallest portion as possible. Protection coordination is not an easy task, rather is considered as an art that is time consuming and difficult (Gers & Holmes, 2004).

A. Radial network protection coordination

Radial distribution networks are popular due to their low cost, easy operation, and they require a simple protection scheme coordination. Moreover, with this type of network voltage compensation techniques can be easily implemented and is easy to analyse. Hence, it is adapted for low voltage generation at the load centre (Hossain et al., 2014; Rajaram et al., 2015).

For radial distribution networks using overhead lines, like the one shown in Figure 2.25, they are subdivided into several protection zones. The substation gateway is considered as the first zone and is protected by relayed circuit breakers or reclosers. The latter are also deployed all along downstream zones. Single-phases connect from three-phase lines and are protected using single-phase reclosers while gang operated-recloser devices are for three-phase lines protection. Moreover, time and instantaneous overcurrent relays are used as well as ground overcurrent instantaneous and time relays. The overall coordination is achieved through two objectives, which is, the setting of protection relays for low pick up of faults at the end of the line and setting protection time relay as short as possible to minimize the arc flash. The relay

time should be set to be short enough for a fast reaction and long enough for downstream to react (Saboori et al., 2015; Fox, 2010; Sleva, 2009).
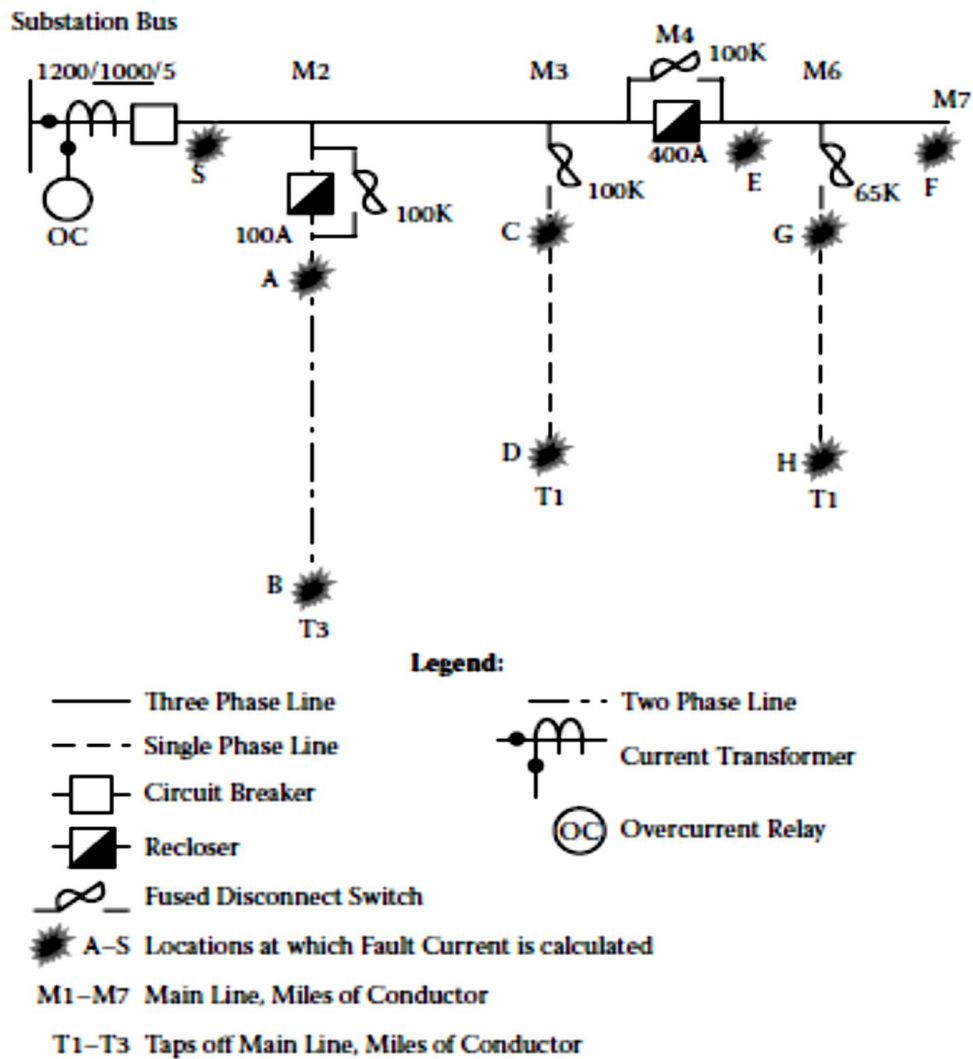
Figure 2. 25: Simplified one-line diagram radial overhead distribution line (Sleva, 2009).

The purpose of the protection coordination in radial newtorks is to ensure that permanent fault that might arise on one of the lateral feeders only affects that feeder as shown on Figure 2.26. Moreover, the use of fuse and midline reclosers in protection coordination is extensive for long feeders.
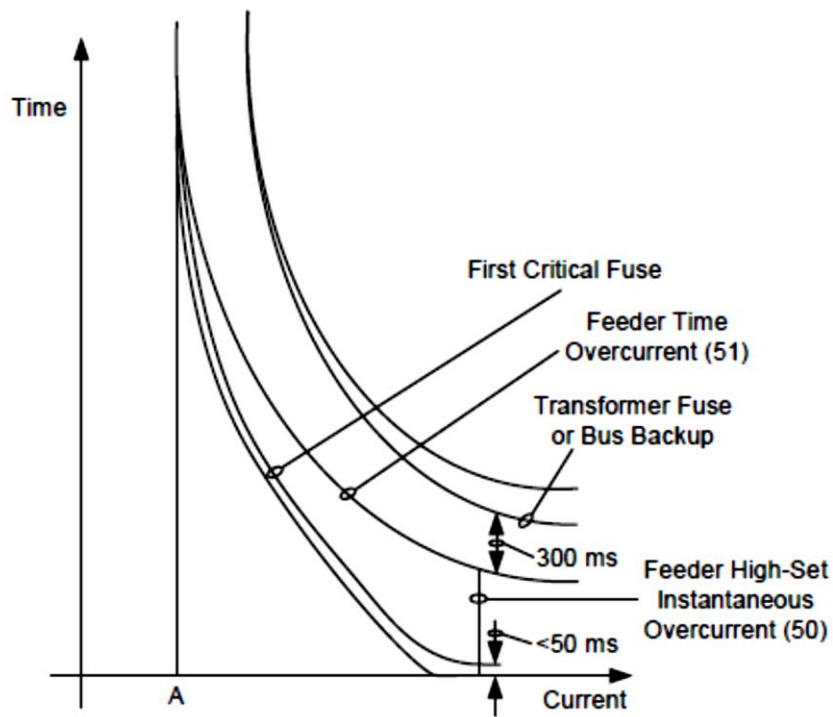
Figure 2.26: Typical coordination of distribution feeder (Sinclair et al., 2014).

B. **Network Lines protection coordination**

A networked distribution system, as shown in Figure 2.27, offers redundancy in power delivery to the customers. Unlike radial networks, the loss of a feeder or a transformer does not cut service to customers. The latter can still be served by another network feeder. The network design is made such that they can withstand the loss of one or more feeders as well as one or more transformers without overloading the rest of the network. The protection of networked distribution system is achieved through the use of a high current circuit breaker associated with overcurrent relays and reverse power relays. Substations, on the other hand, are protected by instantaneous overcurrent relays, timed and instantaneous overcurrent relays, definite time or instantaneous ground relays, directional overcurrent relays, and phase relays (Haron et al., 2012; Sharaf et al., 2015; Sleva, 2009).
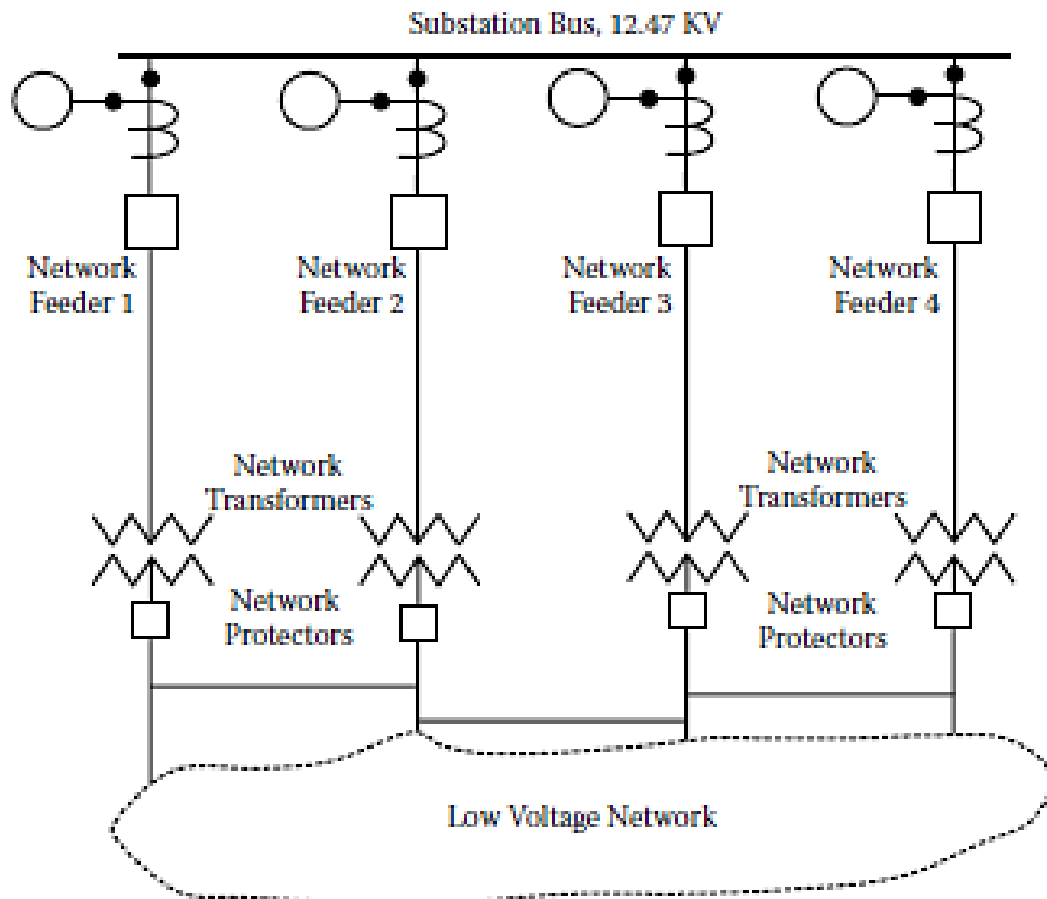
Figure 2. 27: One-line diagram of a networked distribution system (Sleva, 2009).

2.6 Power system communication

2.6.1 Introduction

Power system networks covers a wide area for daily operation communication systems are required. It is used for the control, monitoring, and protection of networks through monitoring and communication between field devices on the substation or along the network and control centre. They are responsible for data transmission from one source to one or many destinations, the data generation source ranging from the protection or monitoring device to the customer meter. Beside real-time operation of the network, communication systems are also used for administrative service by the network operator. Figure 2.28 shows the application of communication systems for supervisory control and data acquisition (SCADA) in the power system.
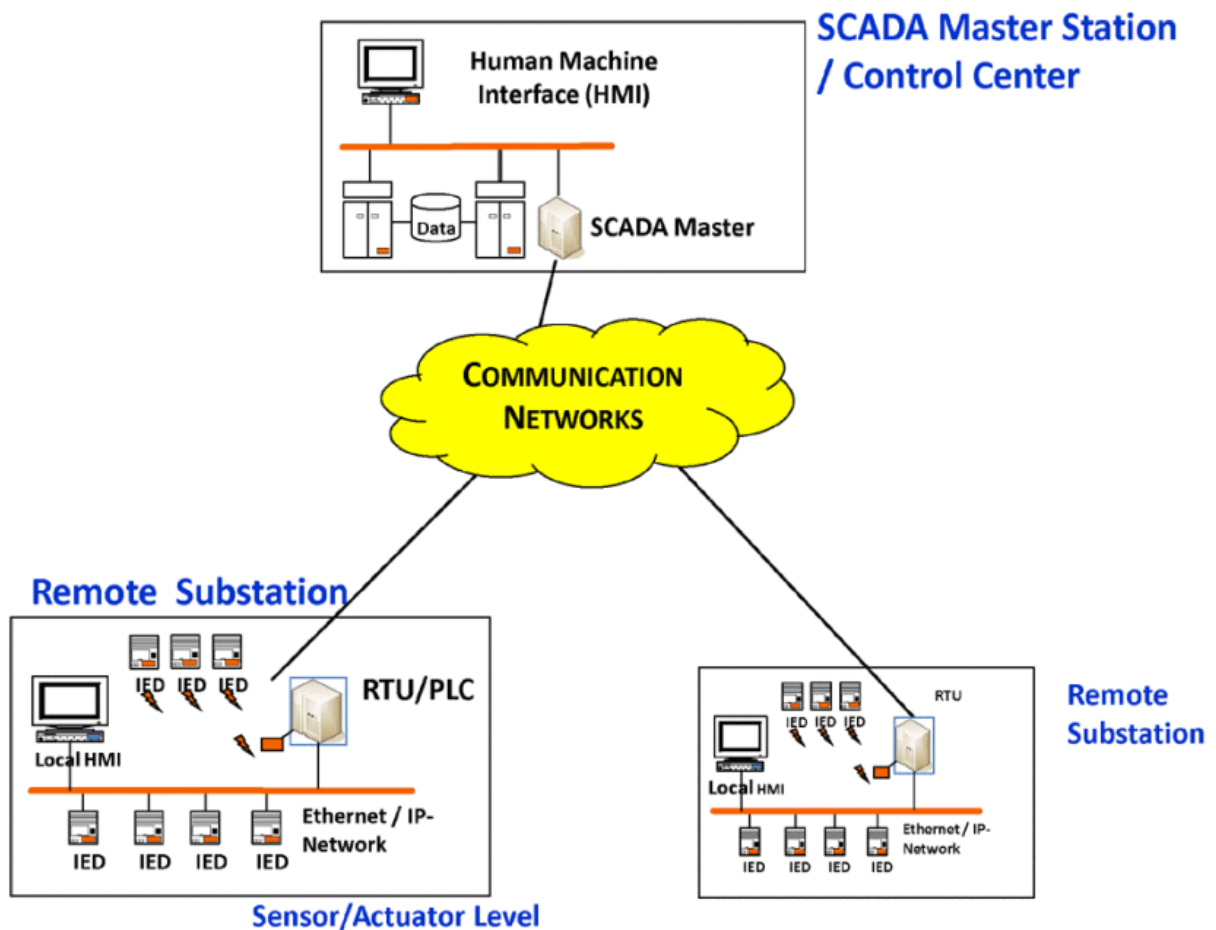
**Figure 2. 28: SCADA system in application for power grid
(Galli et al., 2011).**

Power system automation, restructuring of the power system, and the introduction of distribution generation, coupled to today's trends for smart grid require communication systems that meets certain criteria as shown in Table 2.3. Current and future power systems rely heavily on communication systems than it has before, therefore, a clear understanding of those systems is essential.

There are different communication systems in use:

- Cellular radio communication
- Power line communication systems
- Packet switched network
- Optical fibre
- Satellite communication systems

Table 2.3: Basic requirement for communication system in application for power system (Wang et al., 2011).

Requirements	Description
Network latency	Defines data speed within network. Critical parameter especially for event driven communication such as protection and control. It dictates time taken by the system to pick up and respond to the event.
Data delivery criticality	System should provide means for checking successful delivery of data or messages. Depending on application this requirement might be evaluated high, medium, and lower. With high level, data delivery confirmation is a must otherwise data is resent again till successful delivery confirmed. If not at a critical level, there is no need for confirmation rather repetitive transmissions are done to ensure delivery to receiving end.
Reliability	System immunity to failure such as time-out, network, and resources failures. As communication systems are at the heart of the power system operations such as protection, control and metering, any failure would result in damage of equipment and personnel, having a huge economic impact.
Security	System ability to remain hermetic to intruders. As power communication systems share the medium with system outsiders. With global issue of cyber criminality and power system geographic expansion, the communication system should be able to secure information exchange by preventing, detecting and isolating any intrusion within the system. Among security measures are access control to real time data and control functions as well as encryption of data exchanged.
Time synchronization	Depending on applications, various equipment and devices require a continuous synchronization. Especially measuring devices such as phasor measurement units, control devices such as Intelligent Electronic Devices (IED) which have strict tolerance and resolution as they deal will with real time data processing. IEEE 1588 defines synchronization time protocol for Ethernet networks with Nanosecond accuracy. Time synchronization reference can also be gotten from Global Positioning System (GPS) or from Simple Time Network Protocol.
Multicast support	The system should be able to communicate with many devices simultaneously using a single message. This is important in terms of protection coordination where field devices have to talk to each other.

2.6.2   Cellular radio communication

For data transmission, using radio frequency signals, cellular or radio signals technologies are used for power system communication. It is based on electromagnetic waves propagation that are created by the transmitter at the source and transmitted through the air to the receiver area. Radio communication system relies on line of sight and antenna placed at an elevated point for transmitter-receiver link establishment (Freeman, 2006; Kalivas, 2009). While radio system use a certain frequency for data transmission, cellular technology that is usually 3G and 4G use a frequency bandwidth between 824-894/1900MHz with re-use possibility (Gungor et al., 2013; Güngör et al., 2011; Grami, 2016).

2.6.3   Satellite communication systems

Satellite communication system overcomes the issue of remoteness and absence of line of sight that cellular radio communication systems suffer from. It accommodates a wide coverage of remote areas such as rural and inaccessible urban areas. It might be an effective solution to place a remote station in areas without any other communication infrastructure (De Sanctis et al., 2016). Moreover, in terms of installation, they are quick to set up compared to wired communication systems. For cost-efficient purposes in case of remote substation monitoring, very small aperture terminal satellites services are used (Anthony, 2004). Satellite communications systems are also used for global positioning system time synchronisation as they can provide better accuracy in range of microseconds as well as be an alternative route in events of congestion or interruption in other communication systems at the substation (Ziegler, 2004; Usman & Shami, 2013). However, satellite communication systems might be subject to long delays in signal transmission and are weather sensible which impact on the overall performance of the system (Hu & Li, 2001; Sun, 2006; De Sanctis et al., 2016) On the other hand, delay issues are addressed by the use of low earth orbit satellites (Qu et al., 2017).

2.6.4   Optical fibre

In use since the 1960s, optical fibre communication systems have better performance compared to communication systems using copper (Huurdeman, 2003). Its advantages range from high data rate to radio frequency as well as the immunity to electromagnetic, which makes it preferable for communication systems in high voltage substations (Awad, 2006). Moreover, optic fibre develops less losses over distance compared to wired communications such as copper. Thus, it is used for long distance data transmission as it becomes cost-effective in terms of the number of signal repeaters required along the line (Essiambre & Tkach, 2012; Temprana et al., 2015).

Although efficient, the installation cost of optical fibre communication systems is still expensive. Despite that, it has large bandwidth capacity which allows high rates of data transmission that

can go up to 10Gbps if single wavelength, and up to 160Gbps if wavelength division multiplexing is used (Richardson, 2016; Jia et al., 2017; Daleep, Singh Sekhon ; Harmandar & Malhotra, 2016).

2.6.5 Packet switched network

Modern power systems use packet switched communications for monitoring, measurement, and control purposes (Chuang et al., 2010). They are computer-based communication systems that consists of grouping data into small packets at the source and sending them to the destination over computer networks. In this type of communication, both the sending and receiving computers are interconnected through the mentioned network and are IP identified. For interoperability and data exchange within the network, open source interconnection layered model protocols (OSI) are used (Ibe, 2018). The latter can be referred to as computer communication language based. Among those protocols, Internet Protocol (IP) and Transmission Control Protocols (TCP) are very important on the network layer level (Mehta et al., 2016). The former is responsible for data addressing, which defines the sequences and destination of data. On the other hand, Transmission Control Protocols (TCP) deal with data delivery and accuracy to the destination which might be within or outside the local network.

These days, packet-switched communication systems are bases for smart grids and automated substation implementation in line with the IEEE 61850 (Harvey, 2016). The latter provides to the substation an integration platform for monitoring, protection, measurement, and control functions. Moreover, through high speed Ethernet, fast protection applications, inter tripping, and interlocking operations within the substation are possible. It is worth noting that IEC61850 has extended beyond substation to substation communication, to control, assets condition monitoring, operational communication, and synchro phasor measurement transmission (Cigre, 2017).

2.6.6 Power line communication systems

The concept of using power line as a transmission medium for communication signals materialised in the 1910s by George Squier's demonstration of multichannel analogue voice signals through a single power line. Also known as wired wireless communication, it uses a carrier frequency transmission technique and its development for telephony services was started in 1914 by AT&T in USA with its commercial inauguration in 1918. In the same year, in Japan, the first test and commercial operation took place and was referred to as wave telephony (Schwartz, 2009; Ferreira et al., 2010).
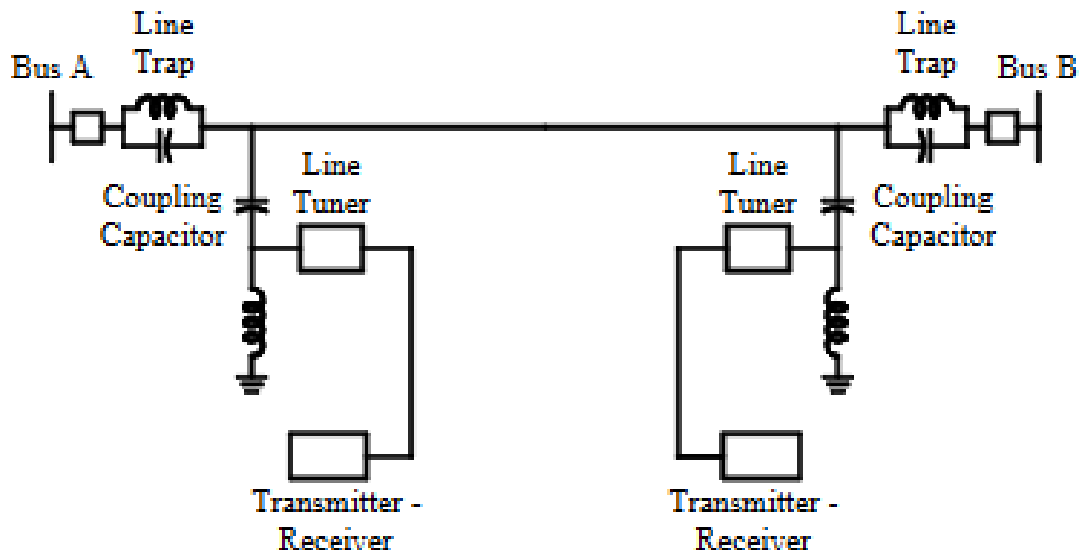
Figure 2. 29:Power line carrier communication system(Mork et al., 2005).

The power line communication system shown in Figure 2.29 consists of transmission and receiving end line buses, communication signal transmitter and receiver as well as coupling systems. Power lines could be alternating current or direct current and signals of PLC are injected to the line through the coupling circuit. For an alternating current power line, the coupling circuit is responsible for filtering out the main AC voltage signal. A similar process happens with the DC power lines carrying communication signals. The DC main voltage signal is blocked to only let in the communication signal.

Initially in 1970 and in the early 1980s, power line communication initially operated in a frequency range between 5 and 500 kHz. Later, it evolved to a range from 9 kHz to 30 MHz due to some constraints such as power transmitted and distance. Ongoing research is looking to expand the frequency up to 500 MHz (Meng et al., 2004; Ferreira et al., 2010; Kale & Patra, 2015). Based on operational frequencies band power line communication systems can be classified as narrowband or broadband. The latter applies to data communication within the frequency band from 1.7 to 500 MHz, while the former refers to operational frequency band ranging from 0 to 500 kHz (Pinomaa et al., 2015b). Broadband power line communication systems are associated with high speed data.

Power line communication systems are appreciated for providing communication signal path without the need to install new wire and cable dedicated to it. This reduces the cost and time for implementation of this system. PLC are used for monitoring, control and metering. Moreover, banking on the omnipresence of electrical power system infrastructure, PLC can be extended for communication services for customers.

Among different parts of a power line communication (PLC) system, coupling is essential. PLC couplers are devices that inject and extract communication signals into and from electric power lines. There are various type of couplers and their classification is usually based on different factors such as physical connection, operational voltage level and type, propagation mode, frequency as well as the number of connections (Luis Guilherme et al., 2017).Figure 2.30 below shows a classification of power line communication couplings.
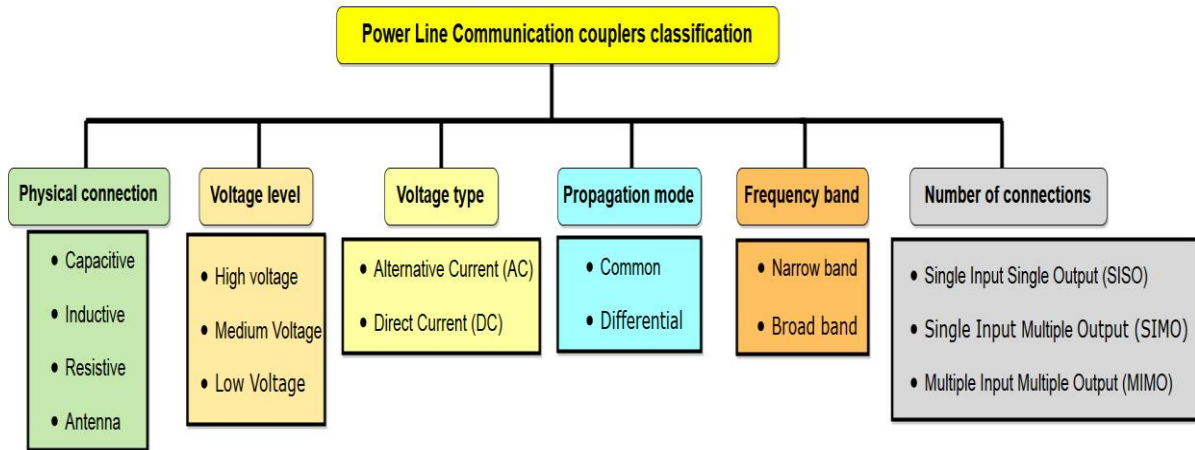
Figure 2. 30: Power line communication coupling classification.

Capacitive coupling consists of a single or series of capacitors in contact with the power line. However, these capacitors can be connected through a transformer or not. A transformer provides galvanic isolation to the rest of the circuit act as a limiter to transients. It is recommended for AC network for high rating voltage networks. It can also be used on direct current (DC) network buses (Grassi & Pignari, 2012) and for low voltage direct current (ILVDC) as suggested by (Pinomaa et al., 2015a). Transformerless PLC capacitive coupling, on the other hand, despite the lack of galvanic isolation, is economic. Both types are shown in Figure 2.31. A capacitive coupling method for the PLC has the highest power transfer compared to other methods (Costa et al., 2015).
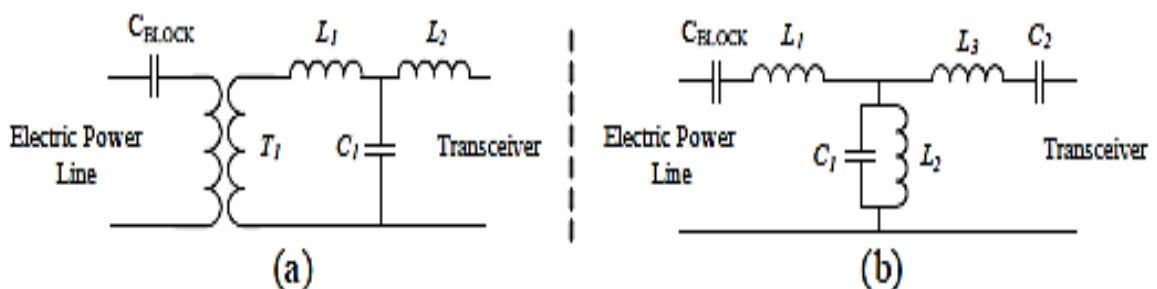
Figure 2. 31: PLC capacitive couple circuit a) with transformer b) without transformer.

Inductive power line communication couplers consist of series or parallel inductor providing galvanic isolation between the line and communication equipment. As shown in Figure 2.32a, current flows through the inductor which creates an electromagnetic field which in turn is induced into the line by Faraday Law. The advantage with this coupling method is that there is no need for lockout of the power line during the installation as there is not a direct connection between the power line and the communication couples and it has low insertion losses. Serial inductive couplers inject communication signals through transformer T1 as shown in Figure 2.32b, while for parallel or shunt inductive couplers the communication signal current flows through toroidal transformer T2 clamped over the power lines (Binkofski, 2005). The core material of the toroidal transformer determines its linearity, maximum primary current, phase error and amplitude (Kikkert, 2011).
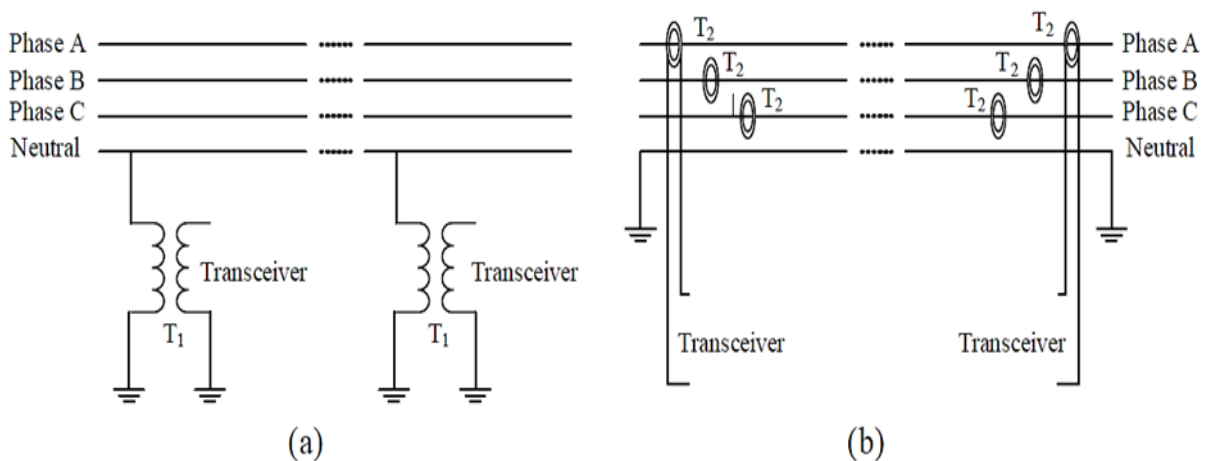
Figure 2. 32: AC lines PLC couplers (a) serial inductive coupler and (b) shunt inductive coupler.

Resistive power line coupler is shown in Figure 2.33. The main part is the voltage divider that brings down the power line voltage to the band pass level voltage for communication signal extraction. Thereafter, the pass band signal is amplified for further signal processing. The application of this kind of configuration seem to be logical for communication signal extraction than injection and fits for narrow band power line communication coupling for low voltage networks. However, according to (Swana et al., 2015) though promising, the method has some drawback such as earth leakage protection, linearity of resistors at the PLC frequencies, and its non-application for transmission.
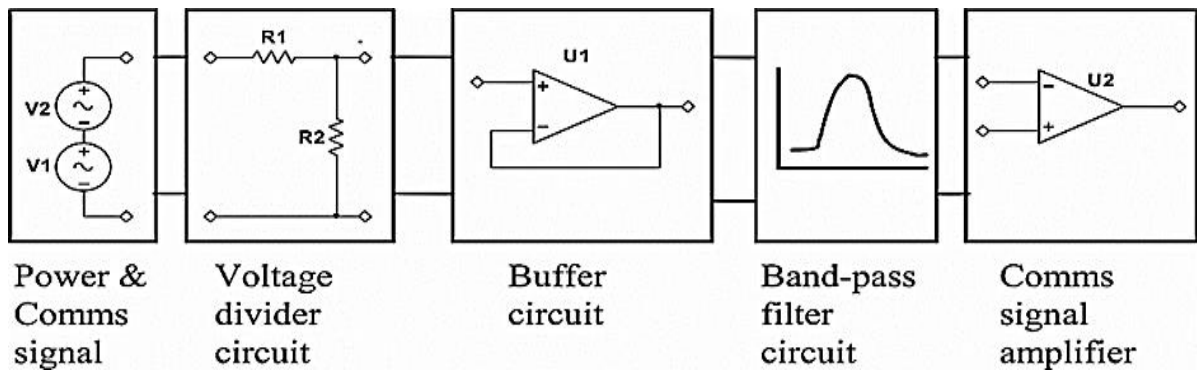
Figure 2. 33: Resistive power line communication coupler block diagram (Swana et al., 2015).

Antenna power line communication coupler was the first coupler to be implemented for the communications circuit connection to power lines (Schwartz, 2009). It is simple to install and operate and has a low cost. As shown on Figure 2.34, antenna couplers are mounted on the tower structure under the power lines, and through antenna communication signals are induced into the power lines (Boddie, 1927). Antenna coupling are challenged by their inefficiency due to communication signal power leakage during coupling to power line, however ongoing research investigate the application of antenna coupling for broadband power line communication (PLC)(Oliveira; et al., 2013; Oliveira et al., 2016). The antenna coupling can be looked at from a different perspective where power lines themselves are considered as antenna for radio frequency broadcasting (Emleh et al., 2013; Jordaan et al., 2013). The advantages are reduced cost in terms of repeaters and cabling. Furthermore, Jordaan et al. (2015) demonstrated the use of low voltage power lines as antenna in Ultra High Frequency range 1- 3 GHz.
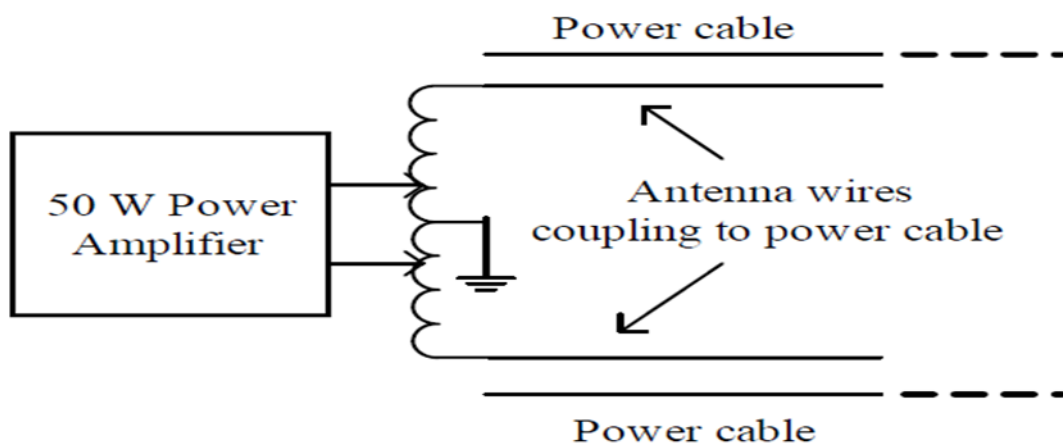
Figure 2. 34: PLC antenna coupling circuit.

Power line communications couplers are used at all levels of the power system structure from high voltage to low voltage levels (Nguyen et al., 2013). Usually for high voltage applications, capacitive coupling is used. They are required to conform to ANSI C93.1 standards of high voltage capacitive coupling (ANSI, 1999). Inductive couplers are also used, however, unlike capacitive couplings, they are more sensitive to line voltage fluctuations, corona, noise and voltage arcing as they lead to core saturation and higher insertion loss (Pighi & Raheli, 2005).

Standardized in ANSI C93.1, medium voltage power line communication couplers are used in a distribution network for data communication for protection, metering, control, distribution and interconnecting substations (Papadopoulos et al., 2013). They are subject to high differentials voltages between lines and ground. They are required to withstand surge currents without mechanical damage that might occur due to short circuit or switching. This leads to the requirement for special equipment which makes the coupling more complex and expensive to realise (Issa et al., 2004; Cataliotti et al., 2012).

For low voltage, two lines are used for power line communication, usually a phase and ground or neutral. Though safer in terms of voltage rating for the PLC implementation compared to high and medium voltage network, PLC coupling in low voltage face challenges due to dynamic loads that create emissions in addition to interference from equipment, motors, and other inductive loads (Picorone et al., 2010; Andrade et al., 2013). This makes the application of power line communication in low voltage network more difficult than in high voltage networks. However, low voltage couplers are cheaper and some of their drawbacks such as impedance matching can be improved by coupling through the radio frequency transformer. Various studies on the application of PLC in motor cables and for low voltage DC networks have been conducted in (Kosonen et al., 2010) and (Pinomaa et al., 2015b).

Power line communication systems for AC networks is a mature subject much like couplers. However, with the new trend towards the DC network the application of power line communication on them is gaining the interest of researchers (Pinomaa et al., 2014). DC PLC couplers are based on the philosophy of AC PLC couplers and have the same physical types for connecting to the power line (Wade & Asada, 2006; Grassi et al., 2011; Lobato et al., 2015).

Power line couplers can be classified according to its operational frequency, low or high frequency band. The latter ranges in between 1.7MHz and 500MHz, while the former is situated in range from 0 kHz and 500 kHz

2.7   Distribution network extension planning

Since electrical energy has become the backbone of modern society, as the world population grows so does the electrical energy demand, leading to the continuous extension and the interconnection of electrical power system networks. Besides the social factors associated with being connected to the grid, economic and technical factors are also drivers of network expansion (Mahmoud 1983; Cossi et al. 2012). The restructure of the electricity market opened doors for electricity sales opportunities between regions from the economic perspective, while in regard to the technical aspect, interconnections and expansions improved the load factor as well as networks reliability by exchanging reserves.

The network extension goes hand in hand with the geographic extension of cities and load centres. Therefore, proper planning to match the continuously increasing demand in cities and rural areas is needed. Planning in network extensions provides methods and models for less operation investment costs as well as minimal system's reliability costs in the contingency events (Lotero & Contreras, 2011; Ault & McDonald, 2000; Fu-min et al., 2012).

2.8   Distribution network extension models and methodology used

To meet the increasing demand, the power system should be modified and expended in adequate technical and financial range. Thus there is the need for fast and efficient economical and technical tools for planning the network expansion and modification (Mahmoud & Systems, 1983; Temraz & Quintana, 1993; Ganguly et al., 2013). The planning looks at various parameters such as substation location and size, feeder's numbers and route, switches locations and number, network topology, etc. In doing so, without compromising network constraint such as voltage deviation and substation capacity among others, the planner's main objectives are to:

-   Minimize as much as possible the set-up costs of new facilities
-   Minimize the upgrading capacity of the existing facilities
-   Minimize operations cost, like maintenance and losses
-   Maximize the reliability of the system

These objectives can be expanded on different hierarchies as shown in Figure 2.35. They are the mostly adopted by many utilities and they are being upgraded to include sustainable development aspect. Before the planning process takes place, an assessment against technical criterions such as voltage level, thermal capacity, losses, short circuit capacity, service reliability, coordinated protection, harmonics, voltage fluctuation, insulation and physical limitations is performed (You et al., 2014).

Various planning models and approaches are used to help planners to achieve the above-mentioned target, while planning for distribution network extension or upgrade. They can be classified into 4 groups from a time and structure perspective, namely:

- static load subsystem planning model
- static load total system planning model
- dynamic load subsystem planning model
- dynamic load total system planning model
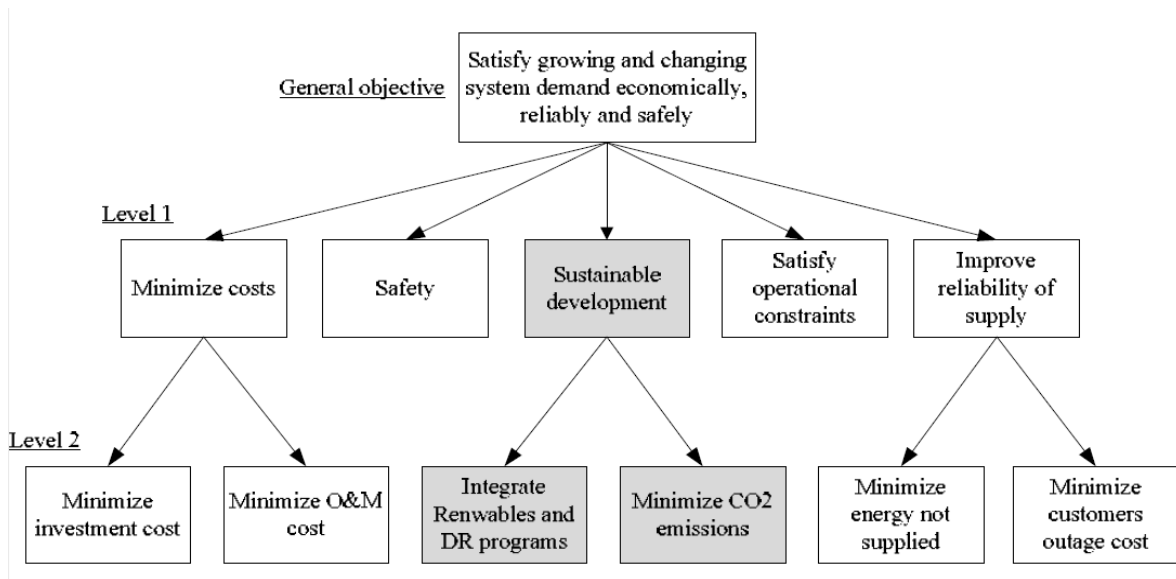
Figure 2. 35: Hierarchy of distribution network planning objectives(You et al., 2014).

However in (Das et al., 2013) the classification is done based on either the models taking into account reliability factor or not. Planning that excludes the reliability factor have two approaches; planning with or without uncertainty of future load. Similar scenarios for planning models considering the reliability factor takes place, where future load uncertainty is considered or not, in both case of modelling under normal or contingency conditions.

The reforms in the electricity market and the introduction of distributed generations have an impact on the power system in general and on the distribution network particularly. The classic top-down model of the power system is currently evolving to the bottom-up model, with the distribution network system becoming more active due to the integration of distributed generations (DG). Therefore, planning methods and techniques for network expansion are adapting to new realities (Bak et al., 2012; Ault & McDonald, 2000; Grond et al., 2013).

Among the advantages of distribution generations, from the planning perspective, is the reduced cost of feeders, energy loss cost, DG investment and additional operational costs

(Ouyang et al., 2010; Wang et al., 2008). However, the Integration of distributed generation can have some disadvantages such as increased short circuit levels, load losses, voltage transients, probability of congestion in the branches and change in voltage profiles as well as the malfunctioning of the protection system (Dulău et al., 2014).The literature provides different methods of planning under various conditions. In Hemmati et al.(2015) the methodology considers several practical aspects in distribution network expansion such as distributed generation, uncertainty, load growth, the electricity market. The dynamic expansion is presented and the proposed plan reduces investment as well as the operational costs. Martins & Borges (2011) present a model for active distribution systems planning taking into consideration alternatives to expansion such as network reconfiguration, new protection devices installation, as well as distributed generation. Two methodologies for uncertainty incorporation are developed. Sultana et al.(2016) reviewed different approaches for optimum location and size of the distributed generation for their efficient utilization.

The introduction of distribution generation and advancement in information technologies opened doors for the smart grid concept (Cecati et al., 2010; Hamidi et al., 2010). The modern power systems are equipped with information exchange devices and rely on them for operations and planning. Therefore, various research have been conducted to understand and find optimum solutions for distribution networks planning in a new environment involving information and communication technologies (Mohtashami et al., 2016). Information and communication technologies are of great importance in the power system in general and distribution network expansion planning, as it contributes to load data gathering which is the starting point for any planning activity.

2.9 Challenges to distribution network extension

Distribution networks being part of the power system network have same challenges as the latter in terms of planning. Although there have been successful research on various network expansion techniques and models, power system expansion still experiences challenging issues inherent to its large scale and complexity (Grond et al., 2012; Lumbreras & Ramos, 2016).

The restructuring of the electricity market increased the challenges that network planners face when it comes to network expansion (Fox-Rogers & Murphy, 2014). Liberalization of the electricity sector from monopoly and vertically integrated public companies, development and integration of renewable energies brought in many stakeholders and various factors that should be taken into consideration by planners for the expansion. Besides the fact that planners rely on existing conditions in the network, especially for distribution networks expansion, they are forced to accommodate distributed generations injected in the distribution

network which sometimes are not even designed to be active. That is the result of multiple divergent interests of involved stakeholders. Therefore there is a need for a comprehensive multiple objective planning approach that can accommodate all stakeholders interests (Lai et al., 2011; Piccolo & Siano, 2009).

Apart from technical and policy challenges, the expansion of distribution networks also suffers due to the high financial investment required. In a deregulated market driven by the profit making the question will be, who will pay or what will be the price of electricity for new customers in order recover the investment (Lassila et al., 2007). At the end, the decision for network expansion towards new customers depends on the ability for the distribution network operators to get the necessary financials for it and on the customers' ability to afford electricity price that will make enough return on investment.

2.10   Distribution network extension in Africa

Electrification rate is proportional to economic development, therefore the access to electricity in sub-Saharan Africa is still low. Governments on the continent are striving for the increase of electricity access to people (Winkler et al., 2011; Wolde-Rufael, 2006). Access to electricity changes lives in the places connected, by opening the door for various business opportunities, improving their daily life, and saving the environment (Panos et al., 2016; Grimm et al., 2013). For this reason, the electrification rollout observed across the continent aims for millennium sustainability goals achievement.

The current status of the electricity market in Africa vis a vis to the electricity market deregulation models is still a single buyer model (Eberhard, 2000; Gentzoglanis, 2013). As the utility is mostly state owned, it is common that there is a monopoly on the transmission and distribution network. The liberalization and competition is only on the generation level, where independent power producers have a single buyer which is the utility (Jamasb, 2006; Trotter et al., 2017).

Therefore, since the transmission and distribution is utility owned, the utility oversees operation, maintenance and expansion of the grid. A closer look on the distribution network coverage shows that urban and peri-urban areas are the most connected to the grid compared to rural areas. However, even connected areas suffer from poor reliability service due to the aging of equipment and ongoing demand growth (Onyeji et al., 2012; IEA, 2016). The utility is expected to handle maintenance and address system inefficiency all at once.

Poor performance affects utilities financial revenues, which in turn weakens its ability to maintain, reinforce, upgrade and expand the network. Hence, the low rate of electrification, as the cost of the distribution network expansion would be too high for the utility to raise enough

capital and for the customers to afford the effective price for an acceptable return on investment.

Moreover, as mentioned in (Othieno & Awange, 2016), settlements structure in rural Africa are scattered over vast areas, which makes the expansion of the distribution network to individual settlements or households too expensive for the utility to invest in. Additionally, the tariff or price of the electricity would be high to be afforded by customers there. However, as developed in(Parshall et al., 2009), a case study in Kenya, which can be related to majority of sub-Saharan countries, attempted to determine the least costly electrification approach and technology showed that grid expansion is more economical than off-grid solutions.

In terms of a network expansion approach applicable to Africa, especially rural areas, Blyden suggests a bottom-up approach "Olympic ring" in which grid connection is anticipated through the interconnection of microgrids. However, no technical research on the latter approach within the African context has not yet been done.

2.11   Conclusion

This chapter reviewed the electrical power system structure and operation. It focused on distribution network operation and protection. Equipment involved and the actual principles and new trends in terms of protection, different communication systems used in daily operation of distribution network and power system in large are also presented.

The network extension planning and challenges associated with it, have been also reviewed. Technical challenges such as the incorporation of distributed generation into the networks that were initially designed to be passive and its effect on protection system are reviewed. Furthermore, distribution network extension in Africa have been discussed, and it was found that the financing is the main challenge on the network extension for both the utility and the consumers. Idea of grid extension based on bottom up approach using "Olympic ring" microgrid interconnection in anticipation of grid connection is in line with this study intermediate low voltage direct current systems interconnection system for sparse electrified areas.

.

CHAPTER THREE
LOW VOLTAGE DC IN DISTRIBUTION NETWORK

3.1   Introduction

The DC systems were used in the beginning of the power industry before being overtaken by the AC systems due to the lack of mature technology of DC at the time. Currently, with the development of advanced technologies in power electronics, DC systems are back again with a lot of advantages exploitable in transmission and distribution networks. Specialized applications such as telecommunication systems (Gruzs & Hall, 2000), electric vehicles (Tabari & Yazdani, 2014; Kumar & Revankar, 2017), shipboard systems(Shen et al., 2012; Maqsood & Corzine, 2017) and traction use DC systems.

In a transmission network for extensive and bulk power, high voltage direct current is preferred over high voltage alternative current as it is more economical and efficient. High voltage direct current is also used for the interconnection of asynchronous networks and the integration of renewable energy into the grid (Kalair et al., 2016; Khazaei et al., 2018).

Direct current systems are used in wind farms for the interconnection of different turbines spread on site. As the turbines all over the farm are not turning at the same speed depending on their location on the site, different voltages are generated, which requires a collection system that considers these variations in voltage. On the other hand, DC systems are used in commercial and residential housing. The concept, enabling technologies and motivations are presented in Rodriguez-Diaz et al., (2016) .The feasibility analysis of low voltage distribution system and issues regarding the design of the system as well as the economical comparison discussed in (Fregosi et al., 2015; Sannino et al., 2003) which concluded DC supply being an advantage in terms of safety, reduction of electromagnetic fields and improvement of power quality if a proper voltage level is chosen. Table 3.1 shows the DC system characteristics in terms of power, voltage and applicable distance.

Table 3. 1: DC systems characteristics (Mesas et al., 2015).

	LVDC	MVDC	HVDC
Power (MW)	< 0.1	0.1 - 250	>250
Voltage (kV)	0.12 – 1.5	1.5 - 30	30 - 600
Cable length (km)	< 10	10 – 100	>100
Note: The cable lengths are reference values			

3.2   DC systems categories

3.2.1 High Voltage DC systems

High voltage direct current systems operate in a range of 30 kV to 1100 kV (Rongsheng, 2017). They are mostly used in transmissions of bulk power over long distances to the load center, where the HVAC transmission systems would be economically inefficient due to the losses in the lines and consequently the required high amount of the lines needed to overcome that issue. The previous high voltage DC systems are thyristor based (Owen, 2009).

HVDC systems can also be found in applications in which connects two HVAC networks. In this case, the HVDC network is called the back-to-back station and is used for the coupling of the AC networks with different frequencies and/or different phase numbers (Bahrman & Brian, 2007). Different configurations and operation modes of HVDC that are in use today are shown in Figure 3.1.
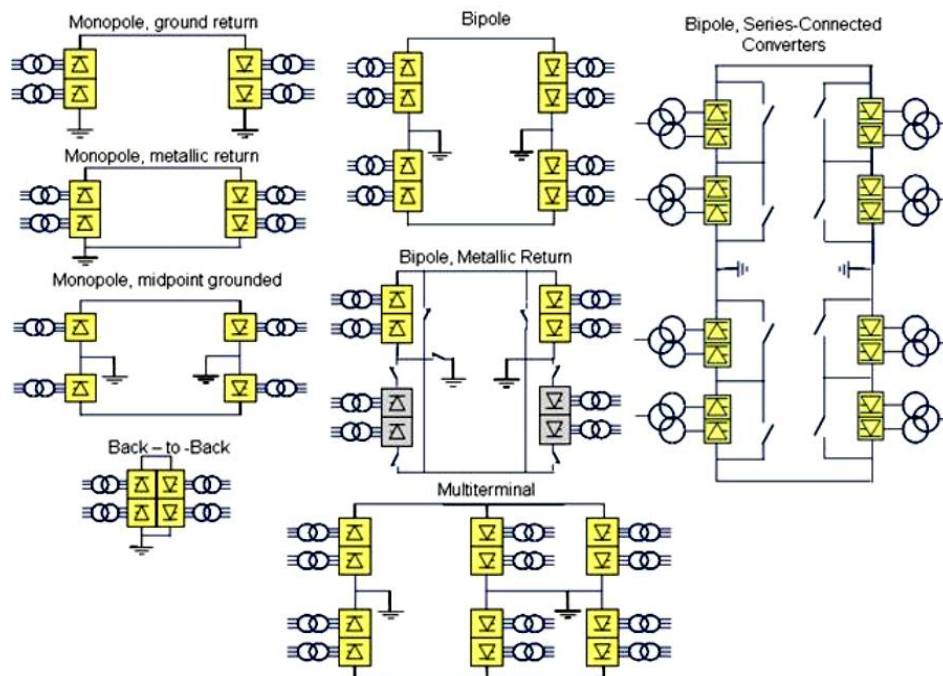
Figure 3. 1: HVDC configuration modes (Bahrman & Johnson, 2007).

The most used configuration for modern overhead HVDC transmission lines is bipolar with a single pole at each terminal. A bipolar is a combination of two poles which shares a common return or ground. This configuration is also preferred in case of failure of one pole, as half of the power may still be available through monopole operations. For a normal balanced operation, there is no earth current.

Emergency ground or earth return operation can be minimized during monopole outages by using the opposite pole line for metallic return via pole and converter bypass switches at each end. This is valid during converter outages as well as during line insulation failures where the

remaining insulation has strength to withstand the low resistive voltage drop in the metallic return path. In a power pool with bulk power HVDC transmission above ± 500kV, variations of bipolar operation, like series connected converters, are performed in order to avoid the energy unavailability for individual converter outages or partial line insulation failure (Oni et al., 2016; Sood, 2011)

3.2.2 Medium Voltage DC systems

a. Introduction

Medium voltage direct current systems operate in a range of 1.5 kV to 30 kV(IEEE, 2010; Qawasmi et al., 2017). Medium Voltage Direct Current (MVDC) stands as an interface between the transmission and distribution networks, the direct supply of power needed in industrial areas or to different plants (Gecan, Chindris, & Pop, 2009).

MVDC were also designed for the integration of renewable energies, energy storage system into transmission and the distribution grid (Gregory, Brandon, & Zhi-Hong, 2012). Figure 3.2 shows a MVDC system with different applications in networks, from the interaction between transmission and distribution, the distributed units' integration, to industrial and residential networks. As can be noted, converters are the heart of the system and therefore must withstand disturbances that may occur in the network.
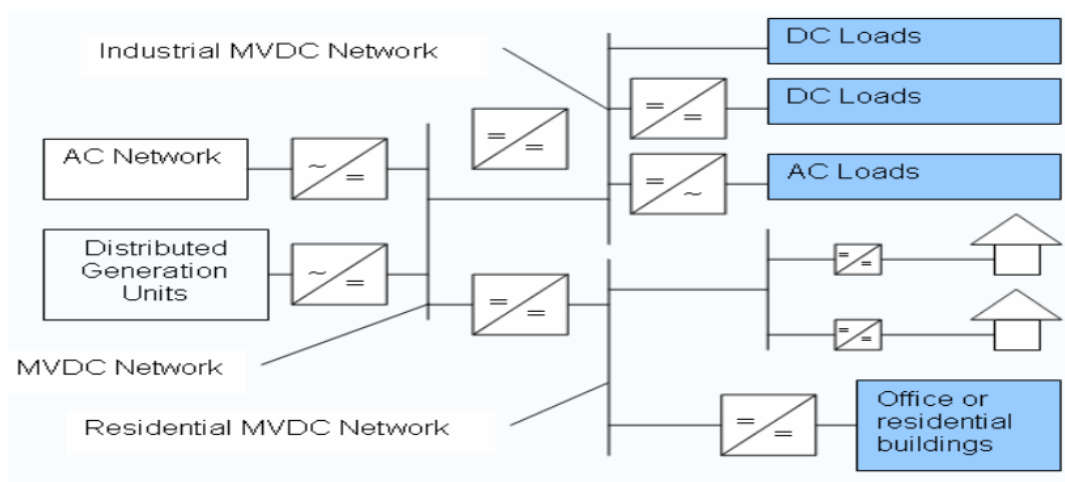
Figure 3. 2: MVDC system for industrial and residential areas (Gecan, Chindris & Pop, 2009).

b. Opportunities and challenges

Various authors have researched the sustainability of using Direct Current (DC) for power delivery in low and medium voltage distribution networks. In (Nilsson & Sannino, 2004) a comparison of a DC and a mixed AC-DC network system efficiency is performed. Results show that the DC network system has less losses compared to a mixed AC-DC network system. The

DC system is more efficient than the AC-DC system, under provision of using low losses semiconductors and less conversion stage(Shivakumar et al., 2015). The implications are that with few losses within the system, less electrical energy that matches the demand is produced as the compensations for losses are minimized.

Medium voltage DC systems will be needed for future distribution networks as the grid is in transition from what it used be to the current integration of renewable energies generation. Furthermore, the AC network systems have limited energy storage capabilities, no quick response, and little automation (Stagge, 2014).

The use of the medium voltage DC network system in urban areas is sought due to various technical and performance such as the ability to integrate distributed generation and energy storage system that it inherits. As majority of household loads are power electronics-based, for example TVs, LED lights, computers, communication equipment, and security equipment, the idea of the DC home was developed to reduce the conversion step involved within loads (Iyer et al., 2015; Stieneker, 2016). On the other hand, a medium voltage DC distribution system can improve the overall efficiency in supplying DC homes by reducing the conversion steps involved, full utilisation of conductors, and increased transfer capacity of the network (Bathurst et al., 2015).

Furthermore, the MVDC network system can be used in enhancing the distribution network by increasing its transfer capability and improving the power quality. Moreover, the fact that the system has fully controlled converters, unlike the medium voltage AC system (MVAC), it can thus be used for network stability and for distributed generation integration. The interconnection of two feeders with different load factors, increasing the network capacity while maintaining the fault voltage level and deferred reinforcement of the networks are amongst the opportunities that the medium voltage direct current systems offer.

MVDC can also be used for substation reinforcement in case increased power transfer is needed, on the one hand, but on the other hand, the up rating of cables and transformers is challenged by the cost. In that case, the MVDC can be used as "Soft Open Point" configuration as shown on Figure 3.3, which is basically a back-to-back converter configuration.
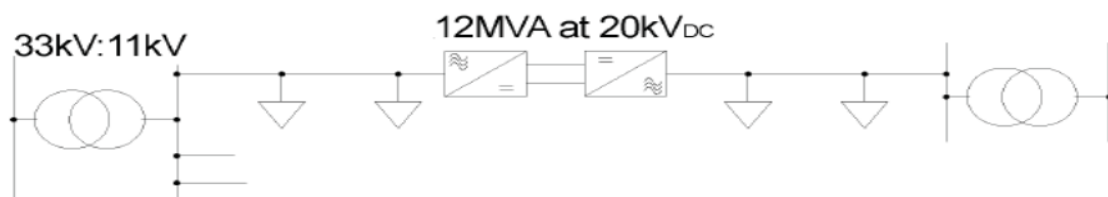
Figure 3. 3: 12 MVA/11kV Soft Open Point formed with back-to-back converters (Bathurst et al., 2015).

This configuration improves power balancing and reliability at the heavily-loaded substation while keeping fault voltage levels in the detection range of protection devices. It also helps the overall system or network to overcome potentials differences in phase-angle for multi feed medium voltage substations. In addition, with converters controllability, Power control of each phase flow is possible, thus phase loading balance can be achieved and in turn a better usage of network capacity (Bathurst et al., 2015; Chiandone et al., 2014; Long et al., 2016).

The MVDC system application for distribution electrical energy in urban areas, as well as its efficiency and investment cost vs a medium voltage AC system for the same application have been analysed in (Stieneker, 2016) and a comparative evaluation between conventional medium voltage AC distribution network and MVDC implementation approaches is made. It is found that DC distribution has several advantages in terms of less losses and less conduction materials. On 6,6kV AC and ± 5kV DC medium voltage grids used for example for investment cost and aluminium and copper as conducting materials, the author results in Figure 3.4 which shows that, using low voltage AC (LVAC) networks as a basis, total the MVDC costs is cheaper than LVAC at a range of 43% despite a minor high investment of 6,6% vis a vis of LVAC investment cost. Therefore, the MVDC distribution network for urban areas is more economically viable than the other system.
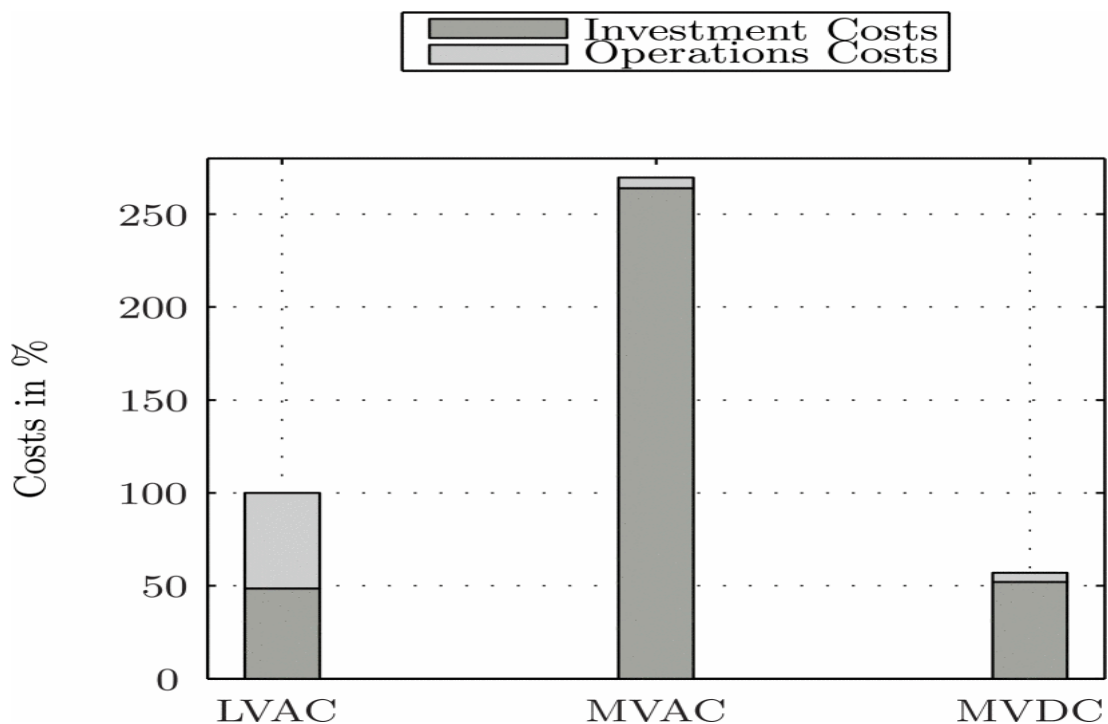
Figure 3. 4: Comparison of the investment and operation costs (Stieneker, 2016).

c. Faults and protection aspect

The main challenge that faces MVDC network systems, which is also similar for all DC networks system, is the protection issue (Ouroua et al., 2009). The arc quenching issue resulting from current breaking by the circuit breaker is more challenging for the DC system than an AC system, since unlike the nature of AC which has inherent zero crossing, DC provides a constant current. Hence, AC sophisticated protection equipment cannot be applied in DC networks. Moreover, the nature of the DC fault current rise-time is very short to be detected by AC protection equipment currently on the market. This fast rise of fault currents results from the fact that in the instant of fault occurrence, capacitors in the circuit immediately discharge and feed the fault point.

The fast rise of a fault current at the beginning of the fault can be illustrated with the circuit on Figure 3.5. The occurrence of a fault, F1, on the DC network corresponds to a sudden discharge of the capacitor C into the network, thus contributing to the fault. The discharge current is governed by the Equation 3.1 with the initial rate of change depending on the capacitor voltage prior to the fault occurrence and on the inductance of the fault path. The network has been developed and characteristics analysed in (Fletcher et al., 2011), with F1 and F2 faults located 5 meters and 30 meters respectively from the grid converter and with fault impedance values of 1 mΩ for short circuit and 500 mΩ for arc fault respectively. Results from the simulations are shown on Figure 3.6. The current rate of change $(\frac{di}{dt})$ decays fast for high impedance faults and the initial rate of change $(\frac{di}{dt})$ depends also on fault location and is the same for both resistances.
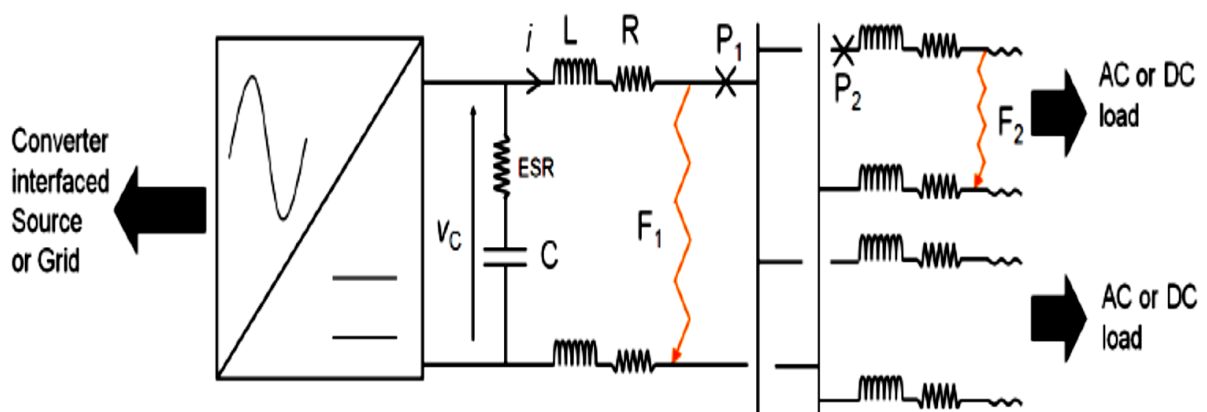
**Figure 3. 5: Equivalent circuit for the faulted network
(Fletcher et al., 2011).**

Equation 3.1

$$\frac{di(t \to 0)}{dt} \to \frac{v_{C_F}(0) - i_L(0)R}{L}$$
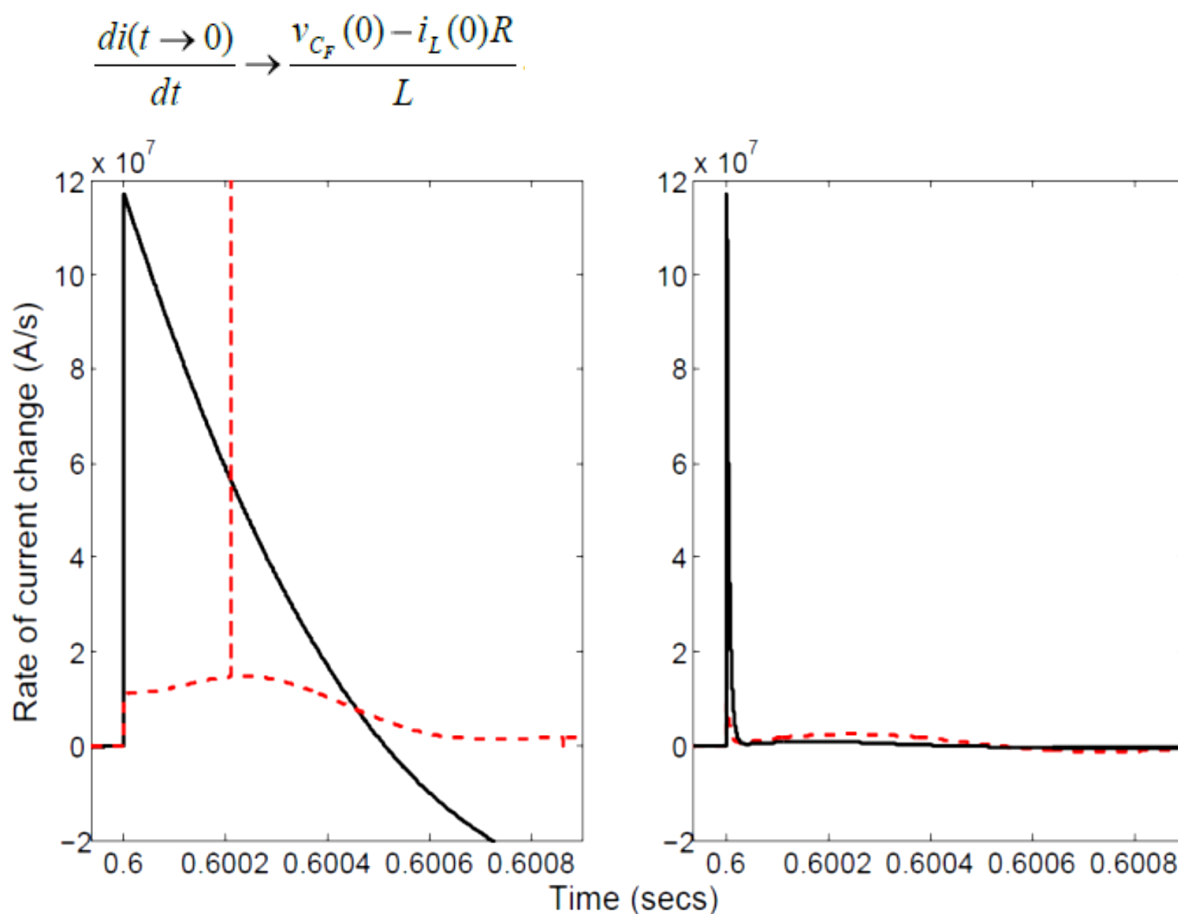
Figure 3. 6: MVDC Network di/dt fault response: for 1mΩ (left) and 500mΩ (right) faults at F₁ (solid) and F₂ (dotted) (Fletcher et al., 2011).

In the DC system, there exists mainly two types of faults: line-to-line faults and line-to-ground faults. Converters internal switch faults might cause line-to-line faults; however, they can be cleared, and the unit must be replaced. To protect the converter from that terminal faults fuses are used.

Various techniques are used for faults detection such as current differential detection method, rate of change of the voltage detection method, directional change of current with a comparison method, grounded point current detection method, line charging current detection, and the measurement of DC line resistance (Hamilton & Schulz, 2007). As mentioned, the quick rise of fault current rate of change makes the use of AC equipment already on market inappropriate for DC protection. Hence, the development of appropriate DC equipment such as ultra-fast hybrid DC circuit breakers and protection scheme to associate with AC equipment for improved protection (Elsayed et al., 2015; Monadi et al., 2015).

Medium voltage DC circuit breakers are a key part in the implementation of the MVDC network system (Barnes & Beddard, 2012), hence, the continuous research for improved and cost-effective circuit breakers. Three categories of the MVDC circuit breaker are available on the market: mechanical circuit breakers, solid-state breakers, and conventional hybrid circuit breakers. Mechanical circuit breakers use moving contact to interrupt the current flow, which causes the arc formation that needs to be quenched. Various arc quenching techniques are used such as air arc chute, vacuum, Sulfur hexafluoride (SF6) for low voltage DC currents and passive and active resonance circuits. Mechanical MVDC circuit breakers suffers from the low operation speed between 10-100msecs. On the other hand, solid-state circuit breakers are the quickest as they are able to interrupt the DC flow within 100µsec, but they have high on-states losses. Hence, the development of the conventional hybrid circuit breaker as they combine characteristics of both mechanical and solid-state breakers, fast and low on-state losses. Research is still ongoing and new technologies start emerging, amongst them are the general hybrid DC circuit breakers, proactive DC circuit breakers, hybrid circuit breaker with commutation booster, DC circuit breaker using a superconductor for current limiting, and the superconducting hybrid circuit breaker(Pei et al., 2016). The idea is to improve the operation time while keeping on-state losses as low as possible. A comparative analysis of the available technologies is shown in Table 3.2.

Table 3.2: DC circuit breaker technologies comparison(Pei et al., 2016).

Type	Advantages	Disadvantages
Mechanical circuit breaker	- Low contact resistance	- Slow operating speed
Solid state circuit breaker	- Ultra-fast operation	- High on-state losses
Conventional hybrid circuit breaker	- Low losses - Reasonable operation speed	- Current commutation relies on the arc voltage
Proactive hybrid circuit breaker	- Fast operation - Reasonable efficiency	- On-state losses in load commutation switch
Hybrid circuit breaker with commutation booster	- Faster operation with high rate of rise of the fault current	- Losses in the coupled inductor
DC circuit breaker using superconductor for current limiting	- Low losses - Inherent fault current limiting	- Self-oscillation circuit needed for the mechanical switch. - Cryogenic system required.
Superconducting hybrid circuit breaker	- Low losses - Fast operation	- Cryogenic system required

d. MVDC converters

Converters are important components of the MVDC distribution network. The difference between them and those used in low voltage can be seen in the voltage ratings they can handle. Different conversions are done depending on the types of converters involved: AC-DC, DC-AC, AC-AC, DC-DC converters. They are also classified according to their topology, operation, power flow direction, and voltage levels. Figure 3.7 shows a classification of DC-DC Voltage Source Converters per configuration; VSC are used in a MVDC system due to their controllability. For high and medium voltage, multilevel converters are used. Converters are essential components in MVDC networks hosting distributed generation and energy storage units; DC-DC buck boost converters, in this case, are operated in bidirectional mode.
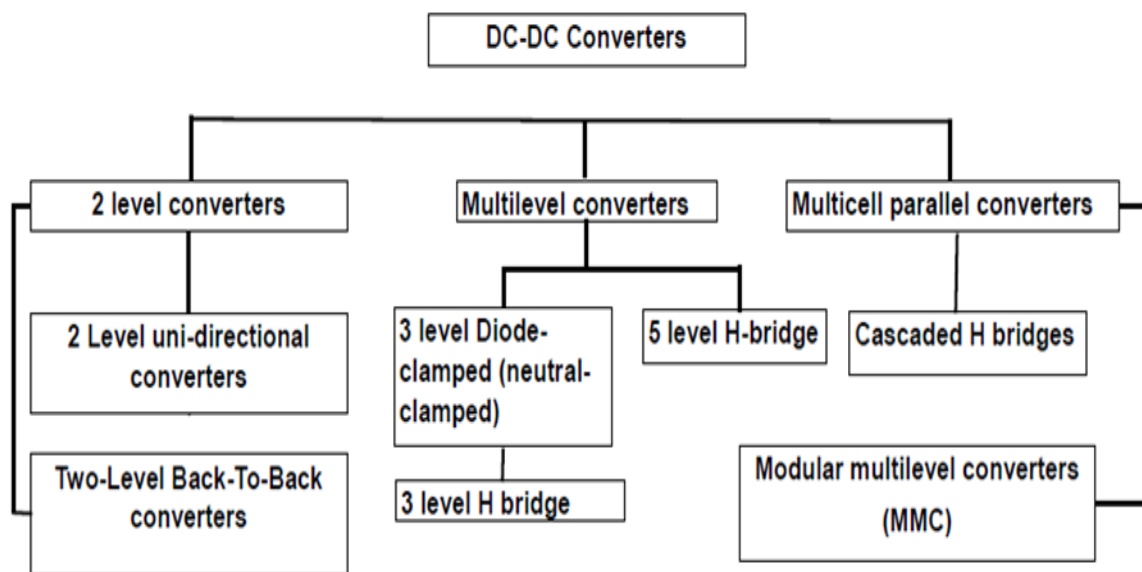
Figure 3. 7: Classification of Voltage Source Converters per configuration(Shri et al., 2012).

1. Two-level converters

Based on two levels half-bridge circuits as shown in Figure 3.8, a three-phase half-bridge with six valves, each switch is a combination of an IGBT and an antiparallel diode. The converter is named as two-level since it provides voltage levels as positive and negative $V/_2$ to the AC side depending on which switches group is on. Moreover, a parallel connection of two half bridge on DC side will make a two-level full bridge converter, known also as H-bridge converter. The advantage with this connection is that the output voltage on AC side will be twice of a half bridge. Pulse Width Modulation (PWM) method is used for switches control.
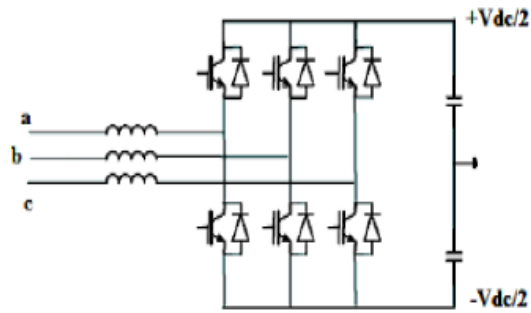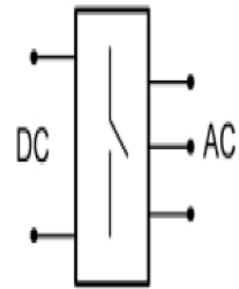
Three-phase two level VSC **Three-phase two level VSC symbolic**

Figure 3. 8: Two level three phase VSC.

2. Multilevel converters

Multilevel inverter technology has emerged recently as a very important alternative in high-power medium-voltage energy control. Multilevel converters consist of semi-conductor arrays and DC source voltages combined to fulfil voltage and current requirements that cannot be achieved by a two-level converter. Coordinated commutation of semiconductors allows for the addition of DC source voltages, which in turn generates different high voltage levels on AC side without damaging semiconductors which are rated for less voltages. Multilevel converters have a better performance in comparison to two-level converters and have a more complex control which makes them expensive (Bose, 2009; Khomfoi & Tolbert, 2011b).

There are three topologies used in multilevel converters (Rodríguez et al., 2002; Peng et al., 2010):

- The H-bridge-based multilevel
- The diode-clamped multilevel
- The capacitor-clamped multilevel

H-bridge-based multilevel converters

The H-bridge multilevel, Figure 3.9 also known as cascaded H-bridge multilevel, consists of multiple converter modules connected in series with several DC sources isolated from each other. Each level can supply three different DC voltage levels output: +V/2,0 and -V/2. The number *m* of voltage levels output per phase depends on the number *n* of DC sources connected: *m=2n+1*. Hence, the more DC sources or modules the converters have, the higher the number of voltage levels it can generate at the outputs. In this way high voltages can be achieved (Nami et al., 2015)

63
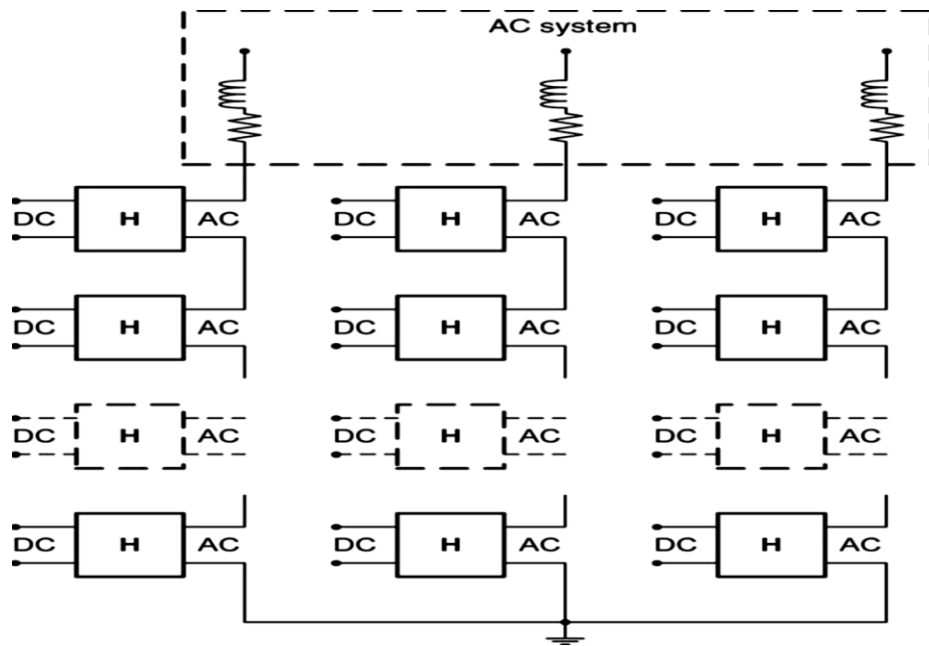
Figure 3. 9 : H-bridge based multilevel converter diagram (Amirnaser & Iravani, 2010).

Diode-clamped multilevel converters

Diode-clamped also known as Neutral Point Clamped (NPC) multilevel configuration is a modification of a two-level converter with an addition of diodes to maintain the DC source voltages, which allows for it to have different steps in out voltage. Diodes balance out voltage stress between switches (Rodríguez et al., 2002). It is associated in series to achieve more voltage steps which, in turn, results in a sinusoidal output voltage. This configuration was introduced in 1981 by Nabae, Takashi and Akagi. On Figure 3.10 (a) and (b) are respectively shown topology diagrams of a three and five-level diode-clamped converter. Currently, six and above level diode-clamped converters are available on the market (Colak et al., 2011; Gayathri Devi et al., 2014). The fact that the mid-point voltage is taken as a neutral point is the reason behind the name Neutral Point Connected (NPC) converter.
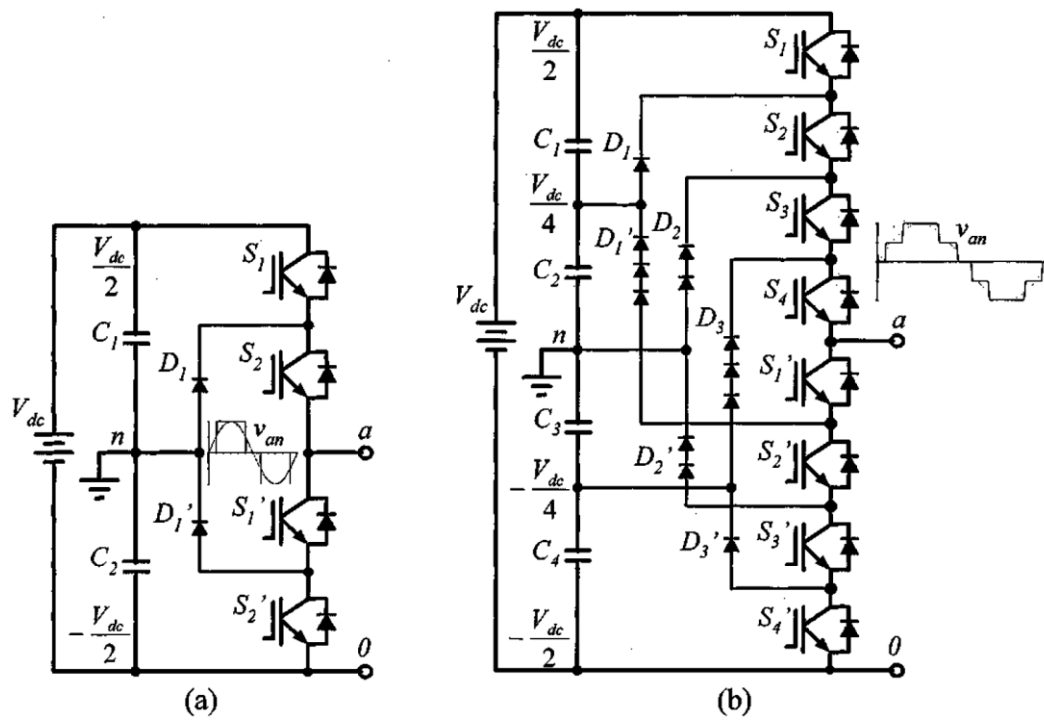
Figure 3. 10: Diode-clamped multilevel converter schematic diagram (Bindeshwar et al., 2012).

The challenge with diode-clamped converters rises from control circuit complexity and cost, as the requirement for a high-quality output voltage closer to sinusoidal waveform requires more levels and therefore more devices. As for a certain number of level N, (n-1) voltage sources or capacitors, 2(n-1) switching devices and (n-1) (n-2) diodes are required (Gupta et al., 2016)

Capacitor-clamped multilevel converter

Capacitor-clamped converters shown in Figure 3.11 are another topology of multilevel converters which is also known as flying capacitor converters, with independent capacitors clamping the device voltage to one capacitor voltage. This kind of circuit involves capacitors of a large size, which reduces the size of filters. For an *m* level converter, *(m-1) (m-2)/2* clamping capacitors are required per phase in addition to *(m-1)* main capacitors (G. P. Adam et al., 2011; Barghi Latran & Teke, 2015). This is valid on the condition that each capacitor has the same voltage rating as the main capacitor at the DC-bus. Capacitor-clamped multilevel converters are suitable for high power and voltage applications to replace the cascaded multilevel converter in order to reduce the number of separate DC sources (Khomfoi & Tolbert, 2011a; Mittal et al., 2012).
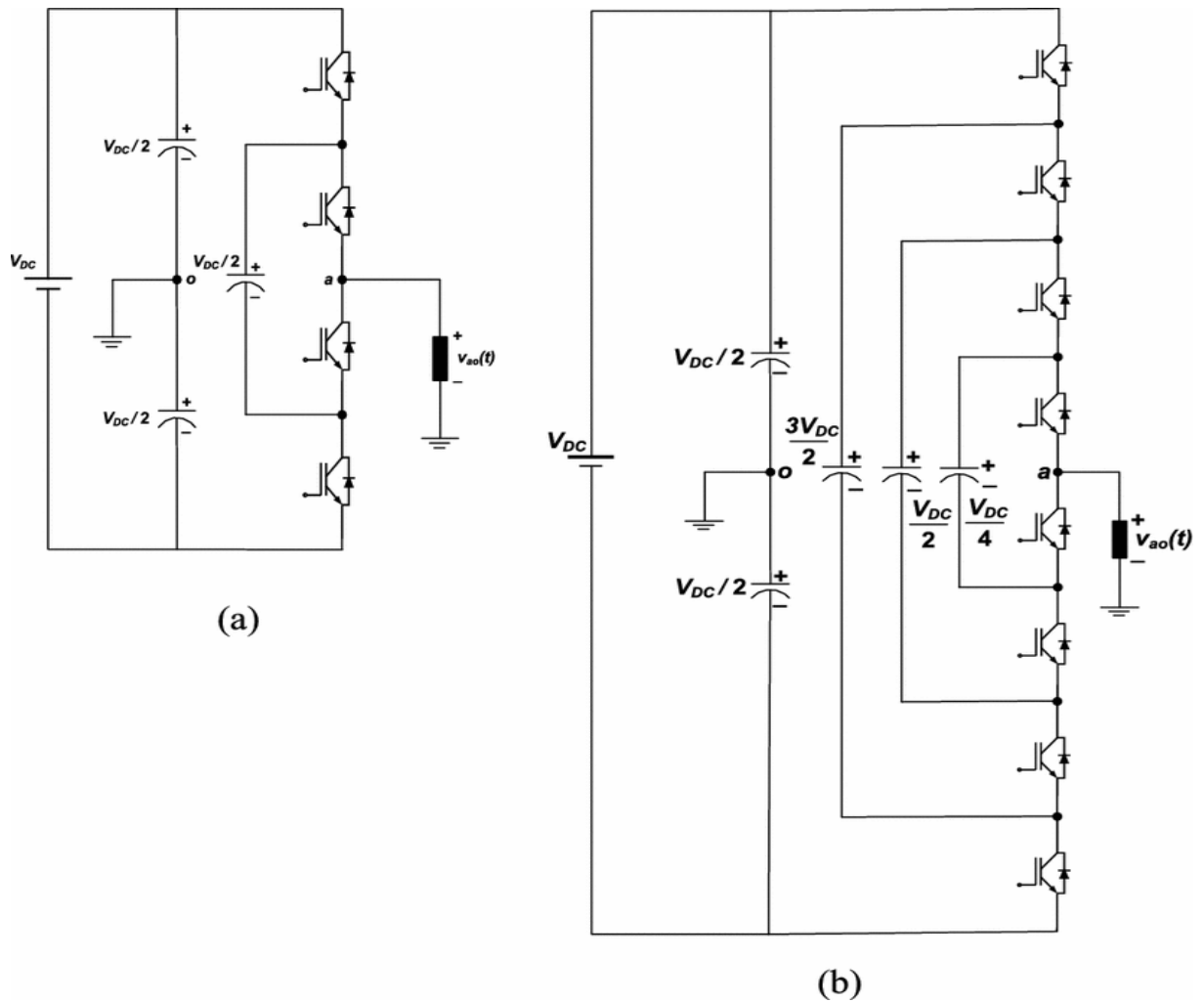
Figure 3. 11: Capacitor-clamped multilevel inverter circuit topologies (a) Three-level (b) Five-level
(Gupta et al., 2016).

3. Multimode converters

The main challenge in applying converters to medium and high voltages is the power handling limitation and on-state losses of switches used. Therefore, combinations of switches in series and parallel are used to overcome voltage/current requirement. However, even those combination, called valves, have limitations such as form factor, unequal-off state voltage distribution, and simultaneous gate requirements. To overcome this challenge, individual small power converters are added up in series and parallel combination to achieve the required power. Figure 3.12 shows a combination of *N* identical converter modules connected in series and parallel respectively to their AC and DC busses. A variant connection can be seen in Figure 3.13 with series connection on both the AC and DC side. To achieve the desired output voltage on the AC side, voltage transform are added up. For both configurations in Figure 3.12 and Figure 3.13, modularity is evident. Identical modules and transformers are combined, which makes it easy for maintenance, repairs, and also reduces the cost of spare parts.
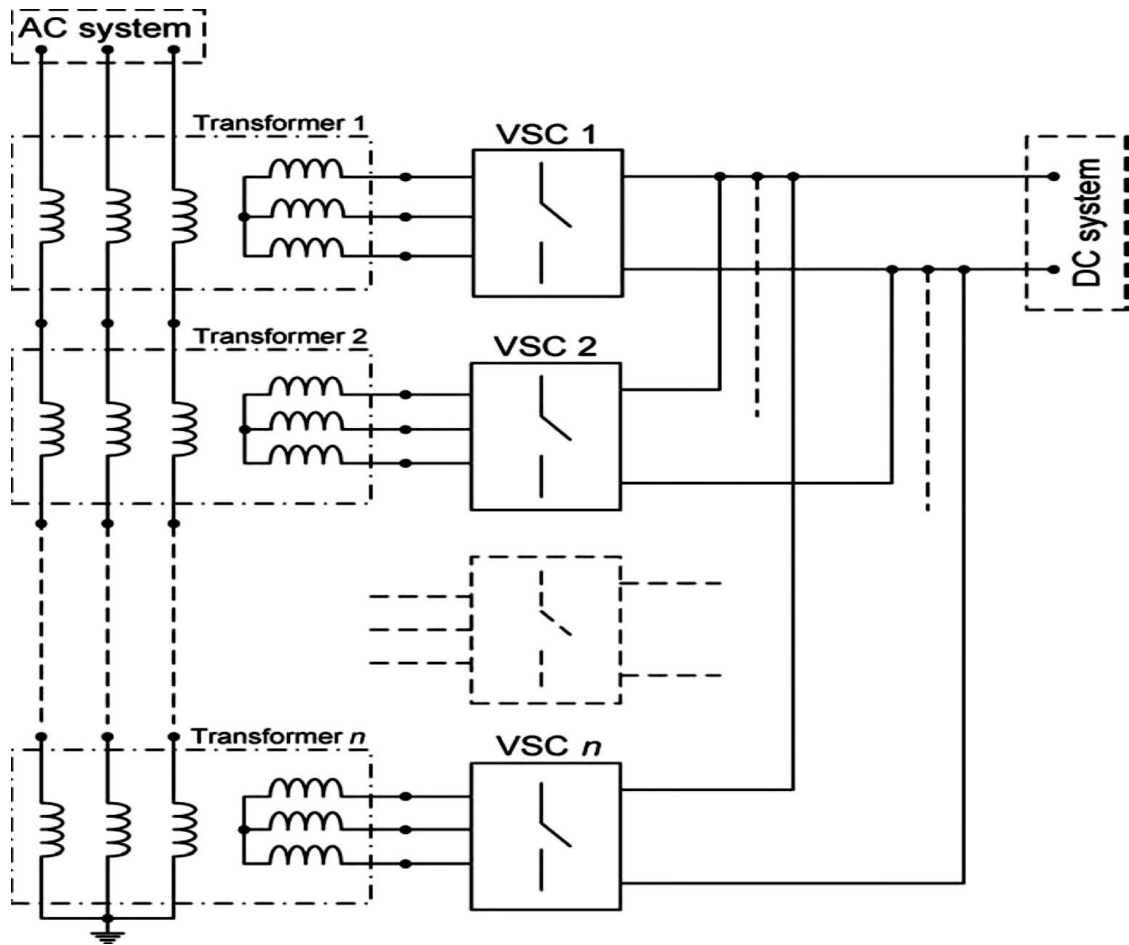
Figure 3. 12: Multimodal VSC diagram with parallel N two-level modules (Amirnaser & Reza Iravani, 2010).
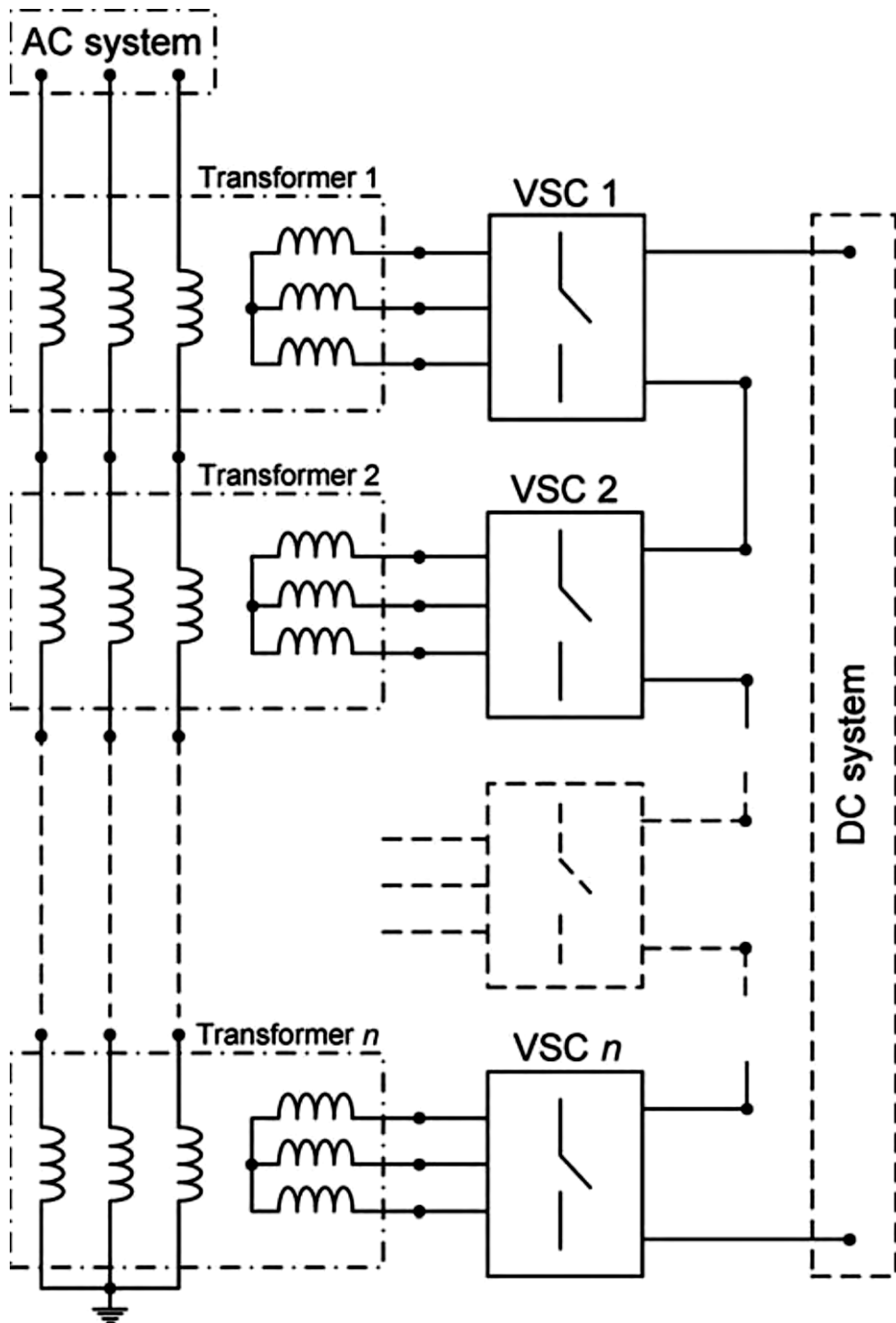
Figure 3. 13: Multimodule VSC composed of N two-level VSC modules in series.

Multimodule configuration offers the possibilities of harmonic reduction through phase shift switching of modules and open transformers. The harmonics reduction allows converters to operate at low switching frequency, which in turn contributes to low switching losses and decreased the need for low frequency harmonics filters (Ilves et al., 2012; Grain P. Adam et al., 2011; Gawande et al., 2017)

3.3 Low Voltage DC systems

The idea of low voltage DC systems in the distribution of electrical power is not new, as in the beginning of the electricity era, in 1880s the power was distributed using DC voltage systems(Kalair et al., 2016). At the time the electricity was generated and transmitted in low voltage DC current form, which required the generating units to be closer to the load centre in order to cut down the high dissipative power losses in lines. This system invented by Thomas Edison had to concede to the Nikolas Tesla's alternative current system for power transmission and distribution. The AC system with its ability to transmit high voltage had overcome the transmission distance limit faced by DC system at that time. However, with the technological evolution and precisely the invention of grid-controlled mercury arc valve in the 1912; The DC transmission system idea was resuscitated. In 1954, Moscow–Kashira HVDC transmission system was put in service. Later inventions in semiconductors such as thyristor, transistor and others switch used in converters, contributed to the maturity of DC systems as know nowadays(Peake, 2009; Tiku, 2014). The basic of a low voltage direct current distribution, as presented in Figure 3.14, consists of transmitting power to the end-user using the DC voltage instead of the AC voltage as usual. The power from transmission lines is transformed before the conversion from AC to DC voltage. The distribution of power to end-users is using low voltage DC which is converted back to AC by the end-user's individual converter(Peltoniemi & Partanen, 2015) (Salonen, Kaipia, Nuutinen, Peltoniemi, & Partanen, 2008). LVDC based distribution systems has advantages such as a high transmission capacity compared to the AC(Kaipia et al., 2017; Yong et al., 2013). The high transmission capacity depends on the voltage level used as well as the LVDC configuration used. In Salonen et al. (2008) the main configurations of LVDC systems into distribution are presented as unipolar and bipolar configurations. The latter seems to be the most advantageous, as with it more power can be transmitted and in terms of redundancy with the loss of one pole the power would still be available through the remaining pole.
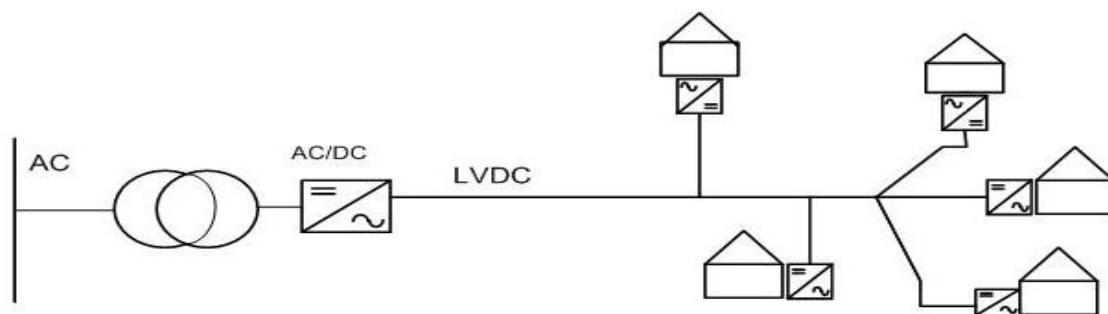
Figure 3. 14: Basic low voltage direct distribution system configuration.

3.4   LVDC voltage standards

The boundaries for low voltage and high voltage levels are well defined by engineers, therefore the standards and products. On the other hand, the medium voltage demarcation seems to be difficult in comparison as various electrical environments and applications are considered. For the IEEE 1585-2002 for medium voltage for electronic devices in application for voltage fluctuation compensation, the medium voltage ranges from 1 kV to 35 kV in AC; while NECA standards 600-2003 for medium voltage cable installation and maintenance defines the medium voltage range as 600 V to 69 kV. IEEE standard 1709-2010 defines recommended practice for ship MVDC power system in range from 1 kV to 35 kV DC (Reed et al., 2012).E.U directive, LVDC 72/23/EEC, on low voltage (E.U, 1973) defines the operation range of low voltage DC systems as below 1500 V.

Previously used in telecommunications systems on ships and electrical vehicles(Elsayed et al., 2015); low voltage DC systems show a great potential for application in power distribution in near future(Kaipia et al., 2016). This is due to the development in power electronics that resulted in an exponential increase of electronic equipment in households and offices. Many equipment works on different parameter levels compared to that supplied from the grid, either in frequency or voltage and current magnitude. Hence, the need for voltage level change. However, the conversion process has a huge impact on the quality of the supplied power after those changes and is a challenge. To overcome this, the use of DC voltage instead of AC voltage as a supply source is seen as one of the ways to reduce the cost and losses involved in the transformation process (Mackay et al., 2017).

3.5   Converters

They are the main components of the system as they interface AC to DC on the supply side and vice versa on the end-user side. They are required to regulate the voltage on the DC side, provide high power quality with low losses, as well as have bidirectional flow capability in case of an active distribution network, and serve as protection in fault and disturbance conditions etc.

Different types of converters that might be used, depending on the nature of the distribution network, are: Diode Rectifier based converters, Voltage Source Converter (VSC), Three-Level Voltage Source Converter, and Voltage Source Converter with DC/DC Buck Converter (Nilsson, 2005). For sufficient quality output voltage at the end-user side, the converter filtering techniques used are LC and LCL (Nuutinen, 2007).

a) Diode Rectifier based converters

These are simple diode rectifier bridges with one functionality, rectification from AC/DC. They can be designed for single and three phase connections.

Figure 3.15 shows a three-phase diode rectifier topology, as can be noted, the output DC voltage is not controlled and an increase on load side results in a voltage decrease and therefore, a poor power factor on the load side. The converter generates high quantities of harmonics. An addition of controllable devices can give the converter the additional characteristic like buck or boost converters, shown on Figure 3.16, with voltage control and power factor correction (PFC) capability.
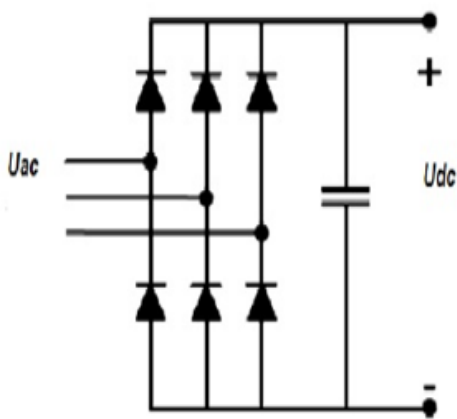
Figure 3. 15: Three-phase diode rectifier.   **Figure 3.16: Three-phase diode rectifier with PFC.**
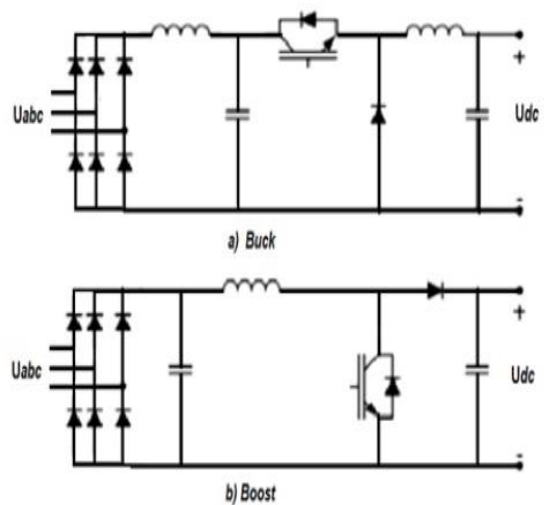
b) Voltage Source Converter (VSC)

With the voltage source converter, power can flow in both directions from or towards the networks and the power factor is controlled. This bidirectional power flow ability is sought specially for active distribution networks. Based on high switching devices, the VSC generates harmonics thus the need for filters to be installed between the converter and the AC network. Figure 3.17 shows a two level VSC with a transformer. The transformer steps down the AC voltage to the converter voltage level and serves as isolation between AC and DC sides; and finally acts also as a filter.
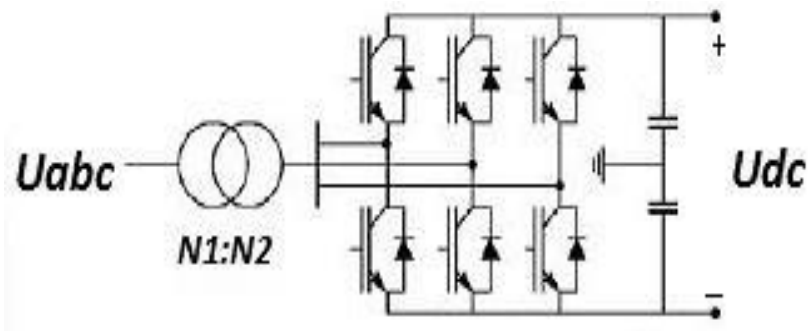
Figure 3. 17: Two-level Voltage Source Converter.

Various types of VSCs are in use today alongside two-level VSCs, namely three-level and five-level converters. The three-level VSC on Figure 3.18 provides two controlled DC links, positive and negative, rather than one as in the case for a two-level VSC. With the three-level VSC converters it is possible to maintain a balanced DC voltage and improve overall harmonic performance. In order to optimize the DC output voltage controllability, converters can be connected in series. Figure 3.19 shows a series connection of a two-level VSC with a DC/DC buck converter, where the output voltage is controlled by the buck converter and can vary on a large range. Bidirectional power flow is also possible with this configuration.
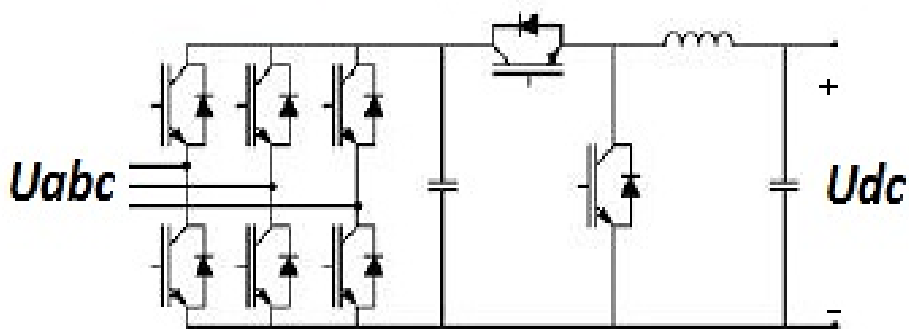
Figure 3. 18: Three-level Voltage Source Converter.
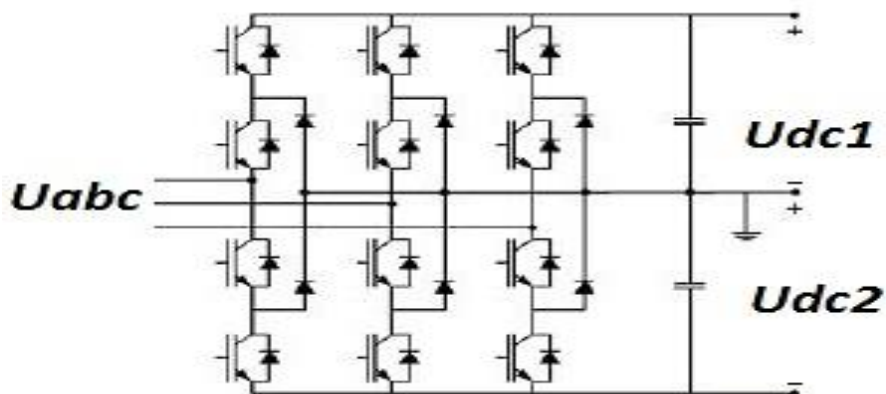
Figure 3. 19: Voltage Source Converter coupled with DC/DC Buck converter.

3.6 Control and protection for LVDC distribution systems

a. Introduction

The control of power flow and protection are crucial for LVDC distributions as it is for any power system network. DC networks introduces new kind of faults as well as other challenges in comparison to AC networks. The lack of natural current zero is the most challenging issue for the protection of LVDC distribution systems and of DC systems in general. The requirements for any DC protection system are high speed, good performance, and to be economical and simple (Cuzner & Venkataramanan, 2008).

Two types of faults mainly encountered in the DC system are:

- Short circuit between positive pole and negative pole also known as line-to-line fault.

- Short circuit between positive pole or negative pole to ground also known as line-to ground fault.

Line-to-ground fault are the main kind of faults usually found in distribution systems and their damaging effect is high compared to the line-to-line faults. In addition to the above-mentioned faults, there are also power converter internal switch faults which might result as line-to-line faults. These types of faults are clearable as they are on terminals, hence the use of the DC fuse to prevent the AC side circuit breaker to trip (Jahromi et al., 2015) The switch should be replaced afterwards.

b. Fault analysis in LVDC system

DC networks require a high filtering capacity to attenuate the DC voltage harmonics generated by converters. On the other hand, converter capacitors contribute to the fault current, in case of a short circuit onto the DC bus; hence creating overheating and malfunctioning of switches and circuit breakers (Baran & Mahajan, 2006).

In general, LVDC networks integrate the AC network through the converter, mainly by fully controlled converters such as IGBT based VSC converters for its ability in terms of active and reactive power flow control. In the occurrence of a fault on feeders, converters switches are blocked in a self-protection attempt. At the same time, the filter smoothing capacitor reacts as a DC voltage source. As shown in Figure 3.20, it will feed high transient current exponentially decaying at a rate given by Equation 3.2, till complete discharge of the capacitor initially charge according to Equation 3.3 (Yang et al., 2010).
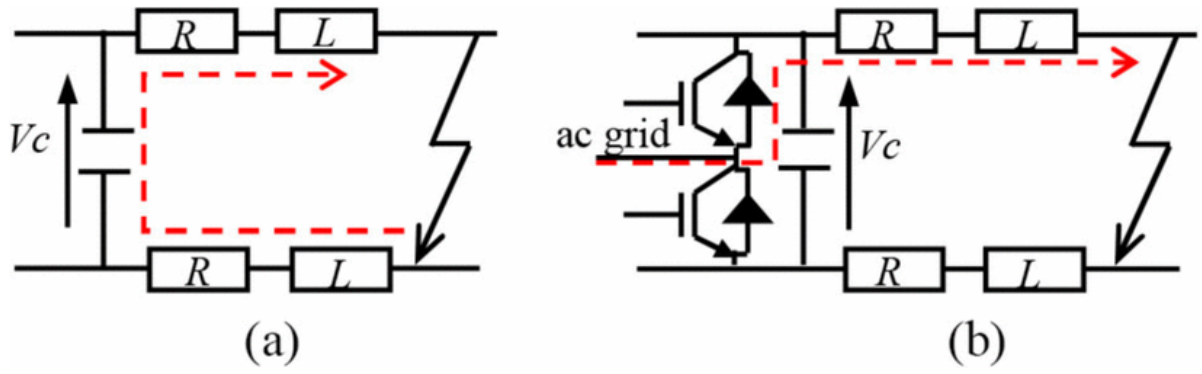
Figure 3. 20: Equivalent circuit of faulted DC feeder: (a) Capacitor discharge current contribution (b) Anti-parallel diodes fault current contribution (Emhemed & Burt, 2014).

$$i_C = c\frac{dV_C}{dt} = -\frac{I_0\omega_0}{\omega}e^{-\delta t}\sin(\omega t - \beta) + \frac{V_0}{\omega L}e^{-\delta t}\sin\omega t \qquad\qquad \text{Equation 3. 2}$$

$$V_C = -\frac{V_0\omega_0}{\omega}e^{-\delta t}\sin(\omega t + \beta) + \frac{I_0}{\omega C}e^{-\delta t}\sin\omega t \qquad\qquad \text{Equation 3. 3}$$

Where V_C and i_C are the capacitor voltage and discharge current, respectively. V_o and I_o are pre-fault voltage and current for smoothing capacitor, while the C is the capacitance, $\delta = R\,/\,2L$ and initial angular frequency $\omega_0 = \sqrt{\delta^2 + \omega^2}$. R and L are resistance and inductance of line from fault to DC source. Furthermore,

$$\omega = \sqrt{\left(\frac{1}{LC}\right) - \left(\frac{R}{2L}\right)^2} \qquad\qquad \text{Equation 3.4}$$

$$\beta = \arctan\left(\frac{\omega}{\delta}\right) \qquad\qquad \text{Equation 3.5}$$

The complete discharge time of the capacitor is given by:

$$t_1 = t_0 + (\pi - \gamma)/\omega \qquad\qquad \text{Equation 3.6}$$

where,

t_0: the initial time when the fault occurs and Y given by $\qquad\qquad$ Equation 3.7

$$\gamma = \arctan\left[\frac{\sin\beta}{\cos\beta - \left(\frac{I_O}{V_O\omega_O C}\right)}\right]$$ Equation 3.7

The converter contribution to fault continues even after the complete discharge of the capacitor as shown in Figure 3.21. Though the switches turn off, the anti-parallel diode will continue to supply the fault current to the feeder. Equation 3.8 gives this.
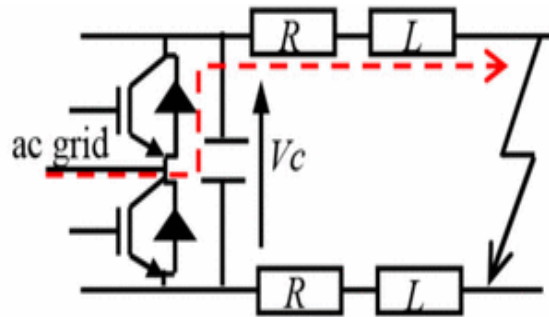
Figure 3. 21: Anti-parallel diodes fault current contribution.

$$i_L = I'_O e^{-\left(\frac{R}{L}\right)t}$$ Equation 3. 8

where,

I_o is the inductor pre-fault current, L is the inductor, and R is the resistance. Therefore, a steady-state fault current will continue to flow from the grid to the feeder through antiparallel diodes. Equation 3.9 gives the phase current and the total contribution is the sum of the three individual grid phase currents i_{ga}, i_{gb} and i_{gc}.

$$i_{ga} = I_m \sin(\omega_s t + \alpha - \varphi) + (i_{mo} \sin(\alpha - \varphi_0) - I_m\sin(\alpha - \varphi)e^{-t/\tau}$$ Equation 3. 9

where,

ω_s = the synchronous angular frequency

α = phase voltage angle

φ = power factor angle, given by:

$$\varphi = \tan^{-1}\left(\frac{\omega_s(L_g + L)}{R}\right) \qquad\qquad \text{Equation 3. 10}$$

I_m = grid current magnitude

I_{mo} = pre-fault grid current

φ_o = pre-fault grid phase angle

Time constant T is given by:

$$\text{T} = \frac{L_g + L}{R} \qquad\qquad \text{Equation 3. 11}$$

where,

L_g= grid inductance.

From the above equations, it can be seen that it is difficult to clear the high transient current, with no zero crossing, that rises from the fault. Therefore, there is a need for extra requirements compared to the AC system for faults isolation in terms of operation speed, fault detection, and protection against voltage disturbances.

The need for high speed operation results comes from the power electronics inability to handle high fault current found in DC systems. This leads to the requirement for a quick fault isolation to avoid the damage to the components that would result from high transient and steady-state fault currents. Moreover, high speed operations in fault isolation prevents control loss by the main converter as well as unnecessary tripping off. Thus, preventing cascaded tripping due to stability and power quality issues in the DC network. Fast isolation of the transient fault current is important, as according to Emhemed and Burt (2013) transients can be higher as 35 times the steady ones in as short a period of time as 4 ms.

Fast detection and location of the fault is required for the clearance before the transient current reaches significant values. On the other hand, the fault locating in DC systems is complex due to the small impedance of DC lines. This results in a fast rise of fault currents. Moreover, for predominant resistive faults, there is difficulty using impedance-based relay protection and overcurrent relays coordination will be affected by error in impedance estimation and therefore the selectivity (Chaudhuri et al., 2014).

As mentioned above, DC fault currents are difficult to interrupt due to their no-zero characteristics when compared to AC with natural zero crossing. There is no low point for current interruption without an arc. Hence, the need to use large circuit breakers compared to AC systems and the use of various arc quenching techniques such as arch splitter, as well as arc lengthening. Though the interruption of a direct current fault current using a mechanical

76

circuit breaker in high voltage DC is impractical, they can be achieved in low and intermediate DC voltage range (Callavik et al., 2013; Emhemed et al., 2017).

Depending on the type of fault occurring in DC systems, two types of voltage disturbance are usually observed: a fast voltage drop and overvoltage on the DC side. A short circuit on the DC feeder causes a fast drop in voltage. Voltage disturbance propagates quickly due to the low impedance of DC cables. This will result in converter control loss, unless a rapid protection system is activated. Overvoltage occurs from a line-to-ground fault on the AC side or the loss of ground in a DC bipolar system. The fault needs to be cleared quickly to avoid a post-fault voltage spike from the released energy within inductors. The use of voltage surge protection might be one of the solutions to reduce fault magnitude and time (Salomonsson, Soder & Sannino, 2009).

The no zero crossing nature of the DC current not only makes the fault current interruption difficult, but its aggressive arc also increases fire risks and equipment degradation. Furthermore, regarding the safety with LVDC installations, the protection against indirect contacts is an issue as no commercial DC residual current devices are available nor the standards (IET standard, 2015).

c. LVDC system grounding

Electrical system grounding or earthing consists of connecting parts of the installation or parts of the equipment with earth conductive point for safety or functional end. Grounding for functionality serves to connect the equipment to the ground for its normal operation. An example would be the traction system in railways and in distribution systems with a single wire earth return. In this case, one conductor is used for the circuit and sustains the full load current.

Protective grounding or earthing aims for the safety of the equipment and users. As LVDC distribution systems are being mainly used for the public, safety is a key consideration. In the LVDC system according to Zadeh and Manjrekar (2012) and the IEC 60364-1 (2005), the usual AC grounding scheme can be adopted. There are three categories of grounding systems:

- TT (Terra Terra) system
- IT system
- TN system

TT (Terra Terra) earthing system as shown in Figure 3.22 is a protective system for consumers that consists of a local earth electrode and all equipment is directly connected on it through the protective earthing conductor (PE). The advantage with the TT system is that it provides a shield against interferences. In distribution systems, there is no risk of the ground to be in contact with overhead lines. However, the system needs a residual current device (RCD) to

provide an automatic disconnection in case of a short circuit with the protective earth (PE) by tripping the circuit as fast as possible.
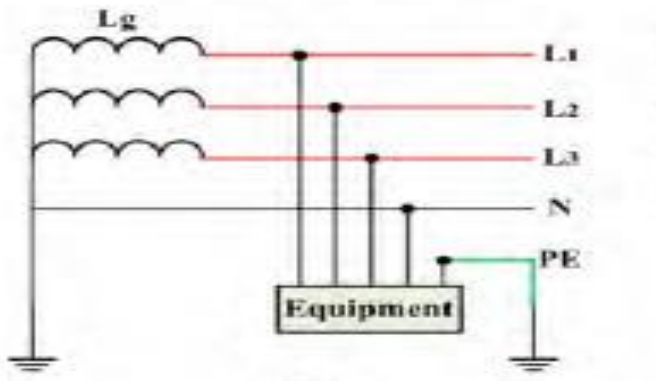
Figure 3. 22: TT (Terra Terra) earthing system.

With IT earthing for the DC system as illustrated in Figure 3.24, the connection to earth is done through high impedance. Compared to an IT earthing system for AC, in Figure 3.23, the same low touch current would result in the case of a ground fault. Hence, there is no need for residual current devices to be incorporated in the circuit. However, Almaguer et al. (2013) and (Li et al,(2013) suggest that due to second ground faults that might be formed in the same circuit, touch voltage might rise between the half-full voltage and full voltage. Therefore, a residual current device is required, despite its sensitivity. The use of other detection methods can be explored.
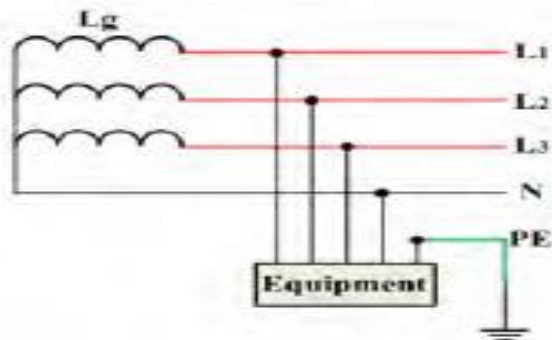
Figure 3. 23: IT earthing system for AC
(Kumar et al., 2017).
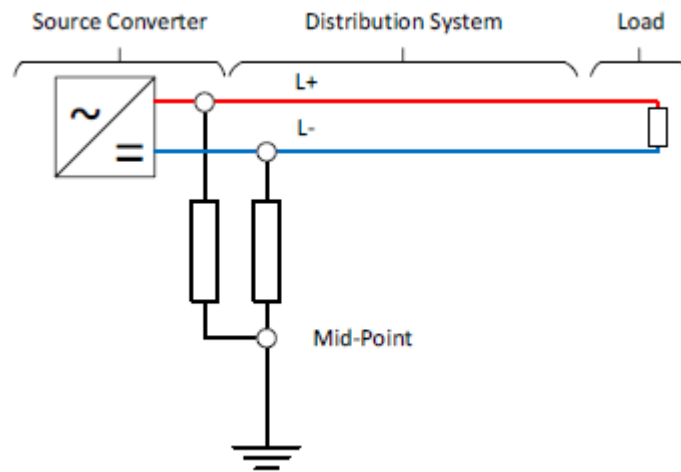
Figure 3. 24: IT earthing system for DC
(Whaite et al., 2015).

TN AC grounding systems, shown in Figure 3.25 and Figure 3.26, consist of a combination of the protective earth conductor and the neutral line. This combination is done at the distribution substation or at the converter, and the separation of both is done at consumer premises. TN can be categorized into three types (Kumar et al., 2017):

- TN-S
- TN-C
- TN-C-S

With TN-C-S, the neutral conductor and protective earthing conductor are only connected near the power source. While in the case of TN-C, a single conductor is used for protective earthing and neutral function from the substation to consumers. Due to safety concerns this type is not recommended for LVDC applications in the distribution system, particularly in residential or commercial areas. In a TN-S configuration, the protective earth conductor and the neutral are separate from the substation or supply to the load/consumers. According to the investigation done by Li et al. (2013), TT and TN-S negative pole grounding in a LVDC system are safer and are the best choice for future low voltage direct current distribution systems. However, for a DC distribution system of a higher voltage 380V - 400V; IT grounding through high resistance midpoint offers more safety compared to the TN-S concept shown in Figure 3.26 (Whaite et al., 2015).
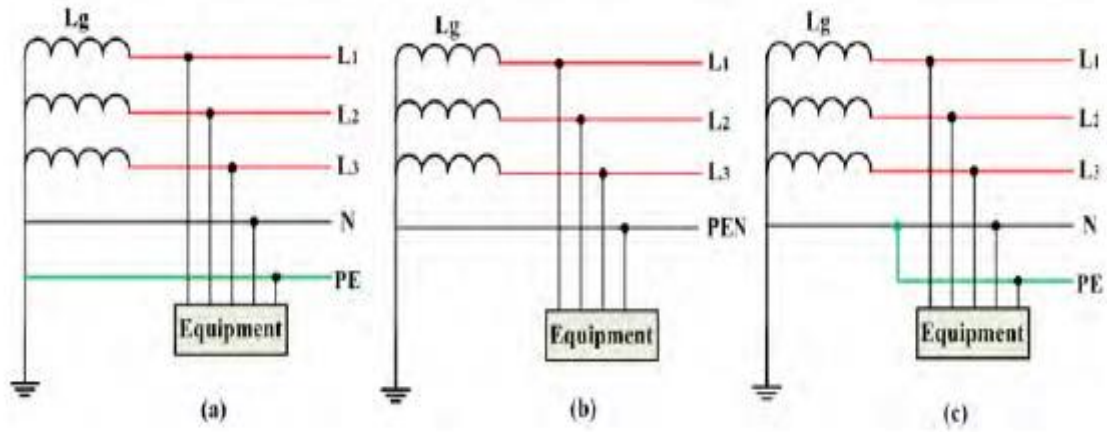
Figure 3. 25: TN AC grounding systems (a) TN-S, (b) TN-C,, and (c) TN-S-C (Kumar et al., 2017).
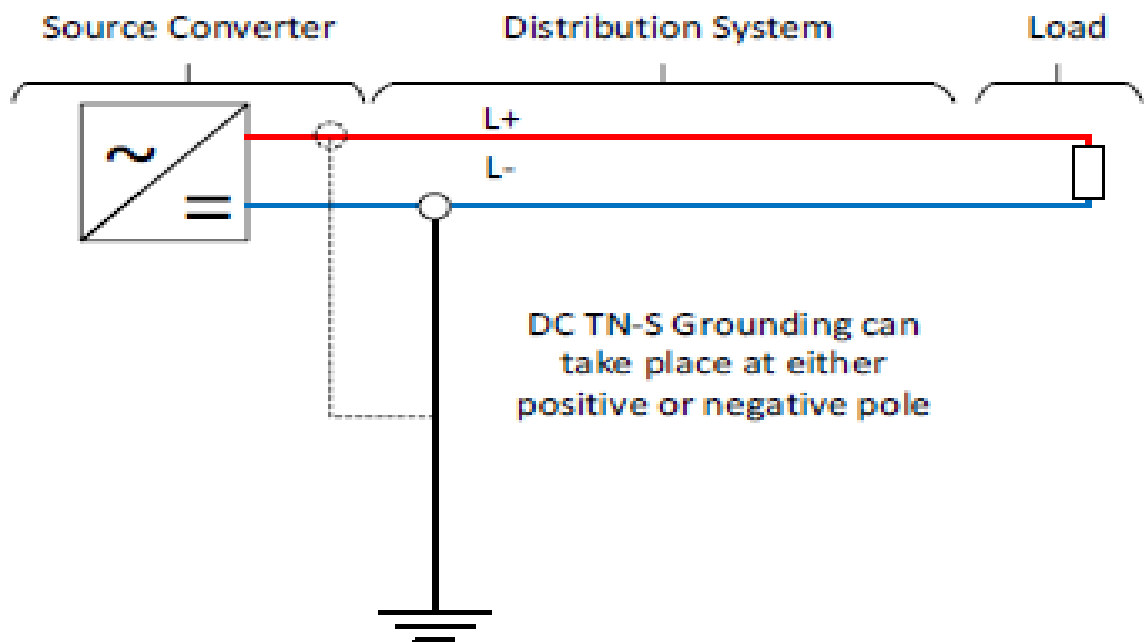
Figure 3. 26: TN-S DC grounding system (Whaite et al., 2015).

3.7 Cables

In low voltage direct current distribution systems, underground cables and overhead cables are used as a power distribution medium. A low voltage AC cable can be used in DC distribution systems as suggested by HD603 and HD626. However, a clear differentiation

between the cables that are used for AC and DC is required to avoid the accidental mixing of both systems conductors (Nuutinen et al., 2017).

AC cables with 4 or 5 wires can be adopted for the DC system in any configuration, bipolar or unipolar, by making parallel connection of different conductors as shown in Figure 3.27.

(a)   (b)
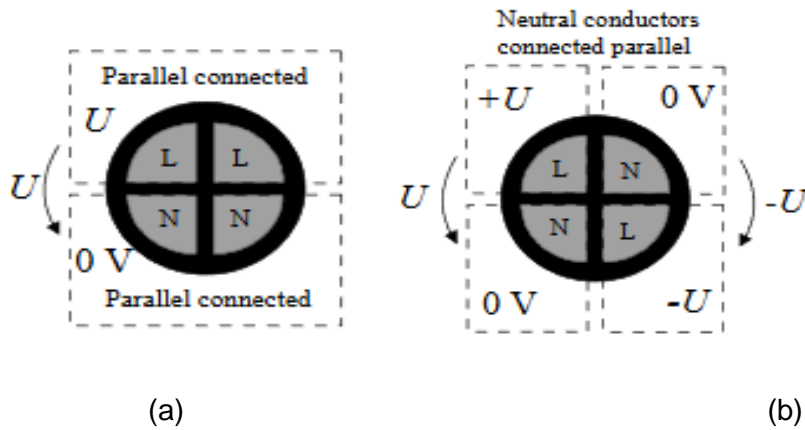
Figure 3. 27: Possible cable connections for DC distribution system using 4-wire AXMK cable for various configurations a) unipolar or b) bipolar system (Salonen et al., 2008).

Besides underground cables, aerial bundled cable (ABC) are also used in low voltage direct current and distinct labels are used to identify DC cables onto the pole in case the latter is supporting various lines with different voltages. Labelling stripes are used as shown in Figure 3.28. Moreover, IEC 60446 colour coding is also used to identify different conductor and polarities for underground and aerial cables in AC and DC. These codes are shown in Table 3.3

Figure 3. 28: Aerial bundled cable with notification stripe between lines connected to different voltage levels(Kaipia et al., 2017).

Table 3. 3: Colours and coding of underground cables and ABCs (Nuutinen et al., 2017).

Underground cable color (A.C)	D.C
Brown (L1)	Positive pole (+DC)
Black (L2)	Middle pole (M)
Gray (L3)	Negative pole (-DC)
Blue (N) , if available	Not used
Yellow - green (PE), if available	Protective Earth (PE)
Sheath (N or PE or PEN) , if available	Protective Earth (PE)
ABC coding (A.C)	DC
Two - ridge (L1)	Positive pole (+DC)
Three - ridge (L2)	Middle pole (M)
Four – ridge (L3)	Negative pole (-DC)
Suspension wire (PEN or PE)	Protective Earth (PE)

3.8 LVDC applications

Lower voltage direct current distribution systems are viewed as the replacement for medium voltage AC networks in the near future due to their high power transmission capability (Kaipia et al., 2006; Afamefuna et al., 2014; Hakala et al., 2015a). They can be used for the integration of renewable energies by considering the fact that renewable energies such as solar, PV, fuel cells, and energy storage systems are DC-based like most of the loads in households (Meier, 2006; E.C.W. de Jong & P.T.M Vaessen, 2007; Moreno & Mojica-Nava, 2014).

LVDC systems are in use in aerospace, marine, automotive, and in the telecommunication industry as power supply distribution system for data centres(Elsayed et al., 2015; Becker & Sonnenberg, 2011). The latter require huge and reliable power supply, thus the integration of uninterrupted power supply combined with energy storage systems (Pratt et al., 2007; Lana et al., 2015). The use of LVDC in those system proved to be more efficient than when traditional AC system were used (Tschudi et al., 2008; Manandhar et al., 2016).

The LVDC system finds its place in combined effort for clean and sustainable transport, especially in electrical cars charging station. According to Smith et al. (2016) , the LVDC system integrated with the DC street lightning network can efficiently and quickly charge electrical cars compared to AC charging systems.

3.9 Perspectives of LVDC distribution systems in Africa

The electrification rate in Africa is still very low, especially in rural and sub-urban areas. Hence, the continent embarked on finding solutions to the current situation where the electrification based on centralized and state-supported top-down model extension grid is no longer cost-efficient in many cases (Bhattacharyya & Palit, 2016; Gironaa et al., 2018). This is especially true for remote rural areas, sparse communities with low loads in the range between 1-10MW, where grid connection with high voltage AC systems would be required for efficient power transfer over distances (Nutkani et al., 2014). Considering the capacity of those systems in comparison to the load demand of remote areas in Africa, they will be underused and totally cost-inefficient. On the other hand, low voltage DC proved to be cost efficient for interconnection.

Various approaches are being applied to tackle energy poverty which is in line with sustainable development goals, by increasing the electricity access for African rural and peri-urban areas. Beside the traditional approaches which tend to be expensive, other approaches include individual solutions, microgrid and swarm electrification. Individual solutions are PV solar home system and fuels generators. This approach is limited by the fact that those solutions are prone to the mismatch of household power demand, which would lead to an inefficient use of energy with unused power capacity or the shading of some loads (Okoye & Oranekwu-Okoye, 2018). In the same line, microgrids, though usually sized to meet the local demand, require subsequent investment (Bhattacharyya, 2014). However, they are still comparatively less expensive than a grid extension (Das & Balakrishnan, 2012; Azimoh et al., 2017).

A combination of advantages of both abovementioned approaches can be obtained through swarm networks or swarm electrification. The latter approach provides the benefit of grid extension while maintaining the low initial investment characteristics of the microgrid and is flexible for renewable energies solution integration (Hollberg, 2015; Kirchhoff et al., 2016). In this line, the DC based swarm electrification approach is getting attention and some projects are being implemented in East Africa (Pepukaye & Shepherd, 2016). Part of the bottom-up solution, DC swarm electrification essentially based on PV has been a success in Kenya, Tanzania, Bangladesh, and India. Therefore, a roll out in the rest of sub-Saharan Africa is seen as the next step in which low voltage DC systems will play a huge role interconnecting sparse microgrids and users.

3.10 Conclusion

This chapter discussed the low voltage direct current in distribution network, however a general overview of DC systems categories and their applications in power system is given for a better understanding of the subject. The focus is put on low and medium voltage DC, components, applications, challenges and new trends. In terms equipment, different types of converters used in both low and medium voltage operation are presented. On the other hand, in terms of operation of DC distribution network, voltage standards, cable, protection and control are discussed as well.

DC systems protection challenges such as the need for high speed isolation devices for fault clearance are highlighted along with actual and new trends in research on DC system protection especially in distribution network.

From the literature reviewed it is understood that the DC systems in medium and low voltage investment and operation costs are less compared to AC system costs. The perspective of success of DC systems in microgrid development in Africa are promising. Hence an interconnection of microgrids using DC voltage systems is feasible.

CHAPTER FOUR
DESIGN OF ILVDC DISTRIBUTION NETWORK FOR SPARSE ELECTRIFIED AREAS INTERCONNECTION

4.1 Introduction

Rural electrification in many African countries is still an issue and more than 88% of the people in sub-Saharan Africa without access to electricity are found in rural areas (IEA & World Bank, 2015). Among the characteristics of African rural areas are the remoteness and sparse density of the population, which makes it technically and economically difficult for grid extension. This contributes to the extensive use of diesel generators.

In this chapter, a bottom-up grid extension Intermediate Low Voltage Direct Current based on the swarm electrification concept with an ILVDC network as a backbone is presented. The aim is to build a network extension from sparse electrified areas up to the main grid. This network should be self-sustained, reliable, safe, and able to meet grid requirements.

4.2 Proposed system for interconnection

To achieve a bottom-up extension, the concept of swarm electrification taking into account demographic and geographic common realities found in African rural and suburban areas is used.

The choice of swarm as electrification which itself derive from swarm intelligence concept are the similarities between them and the realities in sparse electrified areas. Where standalone generating units, mostly diesel generators, are used for individual household power supply. Table 4.1 shows analogy between swarm intelligence characteristics and sparsed-electrified on ground realities.

Table 4. 1: Swarm intelligence concept vs sparsed electrified areas characteristics.

Swarm intelligence system characteristics	Sparsed electrified realities/possibilities
Individuals homogenous elements or identical systems	Stand-alone household electric power generators
Interactions between individual systems	Possible parallel connection of stand-alone household electric power generators
Overall improved system resulting from elements interactions with each other.	Increased electric power generation capacity that would result from the interconnection

The evolution approach will be used for the implementation of the proposed model, building on the single element, nanogrid, as shown on Figure 4.1. The individual household power generator and local load conditions, such as an untapped household that can be connected

on the local network is shown. This could eventually connect to the utility grid through interconnection of individual household elements. Four steps are involved in the process which starts from the individual households' power generation, also known as prosumer according to some of the literature. The four steps to be covered for the total implementation of the ILVDC networks are:

1. Pre–electrification
2. Microgrid development
3. Minigrid development
4. Minigrid Integration to the main grid
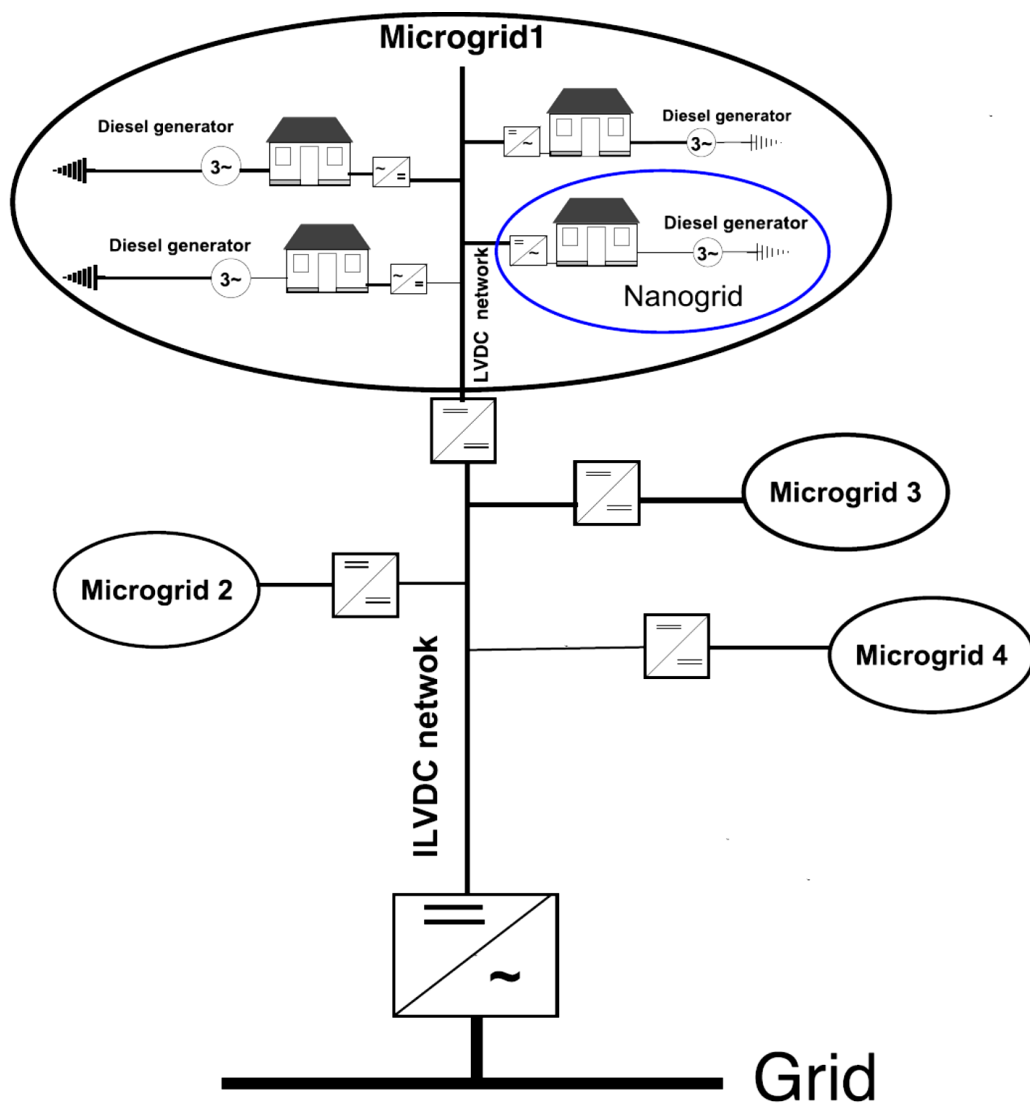
Figure 4. 1: ILVDC network layout.

4.2.1 Pre-electrification (Nanogrid)

Nanogrids usually have power generation capacity more than required for household consumption. In this study, the nanogrids are considered to be in same neighbourhood but not interconnected as shown in Figure 4.2. In step two, nanogrids are interconnected through the DC microgrid on to which are connected households without generators. Nanogrid generators being the AC type, they are interfaced to the DC microgrid through a bi-directional converter. The idea behind the choice of a bi-directional converter is to allow the nanogrids to benefit power from the microgrid should their generators fail.

The main part at this stage are the diesel generator and household loads. Daily power consumption in our case is less than 3 kW. Bearing in mind the eventuality of power exportation to the microgrid, the generator is set to have 10 kVA.
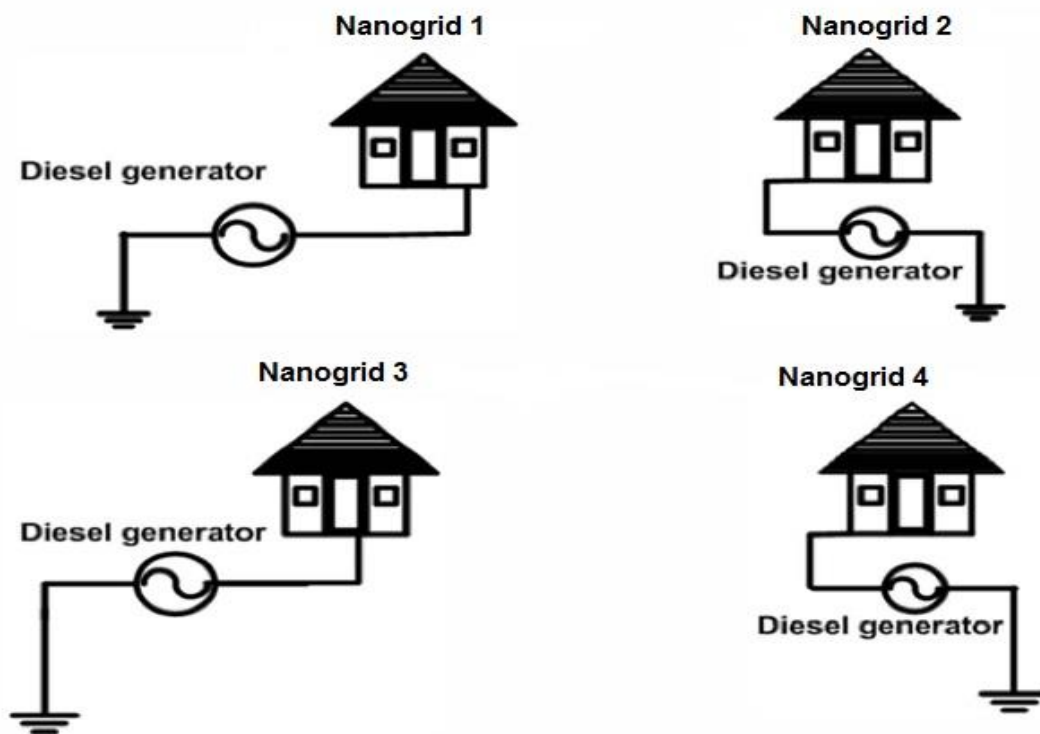
Figure 4. 2: Standalone nanogrids.

A. Diesel generator

It consists of a set of a diesel engine and a governor that converts diesel energy into mechanical energy which will be converted into electrical energy by a synchronous generator mechanically coupled to the diesel engine. Figure 4.3 depicts different functional blocks of a generator set and their interconnection.

The engine speed control or governor regulates the speed of the engine to match the speed required to maintain the set frequency of 50HZ. This is achieved by regulating the amount of fuel entering the engine. On the other hand, the voltage regulates the output power and voltage from the synchronous generator driven by the diesel engine, by regulating the excitation or the field current.
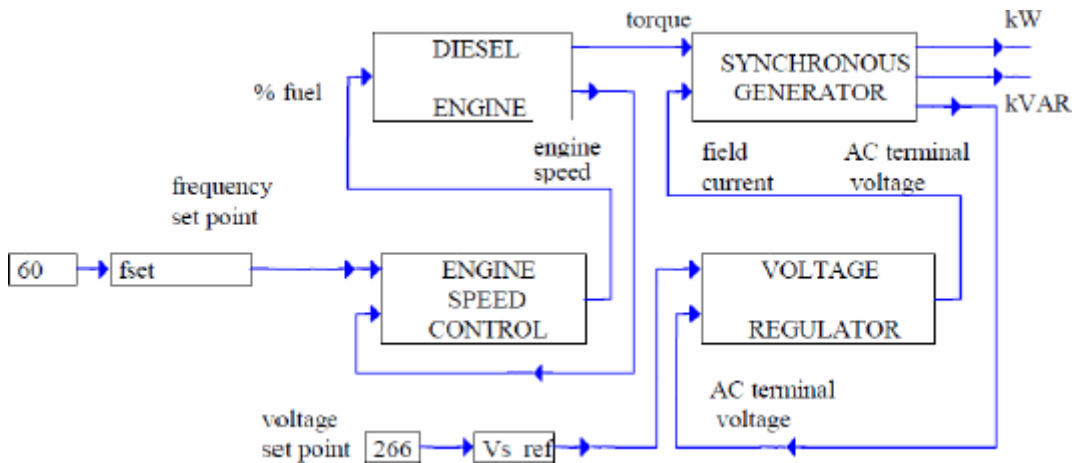
Figure 4. 3: Diesel generator module blocks diagram.

The diesel generator is modelled, as in Figure 4.4, for a dynamic study in Simulink. The model represents mathematical and physical characteristics. With this model, electrical stability, transient voltage and currents as well the performance can be evaluated. Moreover, it allows for the analysis of mechanical interactions independently from the electrical conversion system configuration.

As it is shown the diesel engine mechanical output depends on three parameters: the amount of fuel injected, rotor speed ω_r, and the atmospheric pressure P_{atm}. Fuel injection is controlled by a PID controller with reference to rotor speed ω_r for required frequency and the actual rotor speed as input.
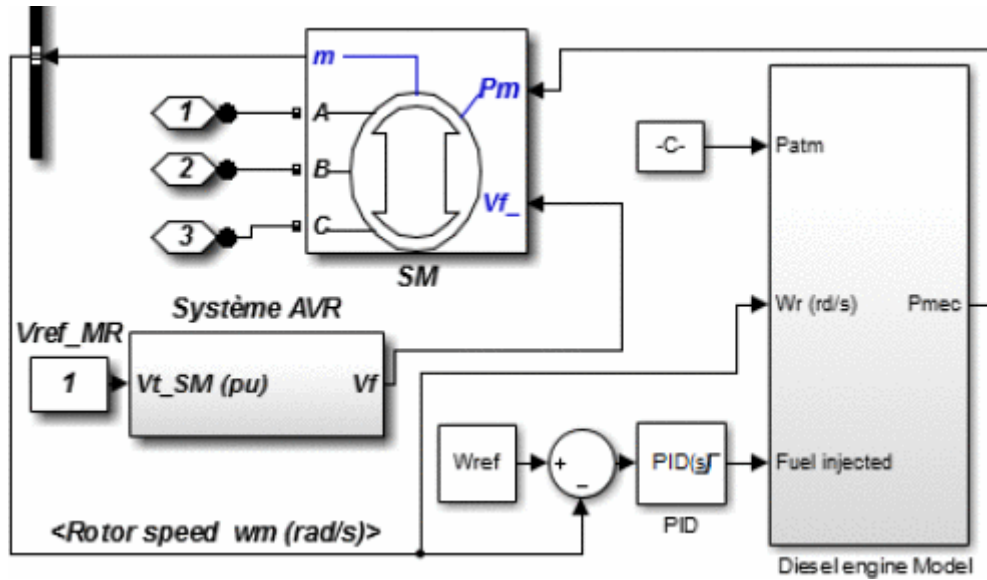
Figure 4. 4: Diesel generator with automatic voltage regulator (AVR) model.

A synchronous machine (SM) electrical model is shown in Figure 4.5. Stator, rotor and damper winding dynamics are considered by the model. Dq frame state space equations are used to represent the model. Note that the stator was taken as a reference for all electrical quantities and parameters.
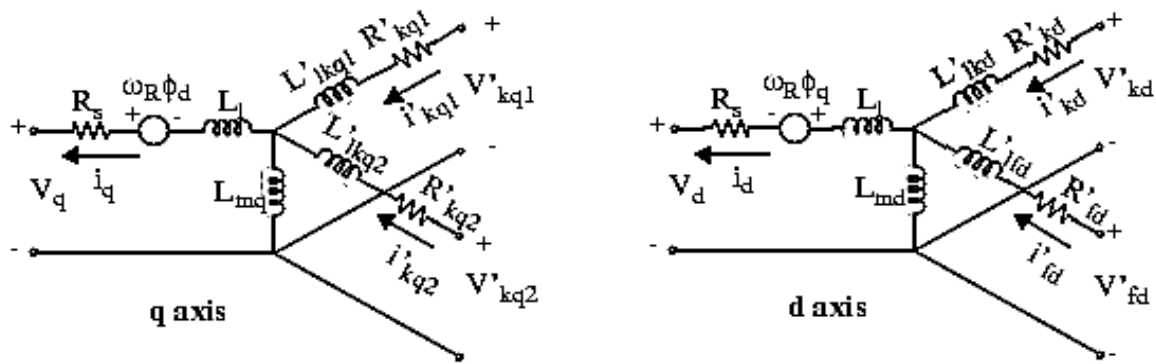
Figure 4. 5: Synchronous machine electrical model in dq frame.

Electrical state equations are derived with the assumption of three phase balanced windings (Chen et al., 2005):

$$V_d = R_s i_d + \frac{d}{dt}\varphi_d - \omega_R \varphi_q \varphi_d = L_d i_d + L_{md}(i'_{fd} + i'_{kd}) \qquad \text{Equation 4.1}$$

$$V_q = R_s i_q + \frac{d}{dt}\varphi_q - \omega_R \varphi_d \varphi_q = L_q i_q + L_{mq}(i'_{fd} + i'_{kq})$$

Equation 4.2

$$V'_{fd} = R'_{fd} i'_{fd} + \frac{d}{dt}\varphi'_{fd}\varphi'_{fd} = L'_{fd} i'_{fd} + L_{md}(i_d + i'_{kd})$$

Equation 4.3

$$V'_{kd} = R'_{kd} i'_{kd} + \frac{d}{dt}\varphi'_{kd}\varphi'_{fd} = L'_{kd} i'_{kd} + L_{md}(i_d + i'_{fd})$$

Equation 4.4

$$V'_{kq1} = R'_{kq1} i'_{kq1} + \frac{d}{dt}\varphi'_{kq1}\varphi'_{kq1} = L'_{kq1} i'_{kq1} + L_{mq} i_q$$

Equation 4.5

$$V'_{kq2} = R'_{kq2} i'_{kq2} + \frac{d}{dt}\varphi'_{kq2}\varphi'_{kq2} = L'_{kq2} i'_{kq2} + L_{mq} i_q$$

Equation 4.6

Where:

V_d = d-axis terminal voltage   ; i_d = d-axis stator current

V_q = q-axis terminal voltage   ; i_q = q-axis stator current

V'_{fd} = field voltage   ; i'_{fd} = field current

V'_{kd} = d- axis damper voltage   ; i'_{kd} = d-axis damper winding current

V'_{kq1}, V'_{kq2} = q- axis damper voltages   ; i'_{kq1} , i'_{kq2} = q-axis damper windings currents

L_{md} = d-axis magnetizing inductance   ; L'_{fd}= d-axis field inductance

L'_{kq1} , L'_{kq2} = q-axis dampers inductances referred to stator

L_{mq}= q-axis magnetizing inductances

R'_{kd} = d-axis dampers resistance referred to stator

R'_{fd} = field winding resistance

R'_{kq1}, R'_{kq2} = q-axis dampers inductances referred to the stator

φ_d= d-axis stator winding flux linkage

φ_q= q-axis stator winding flux linkage

φ'_{fd} = d-axis field winding flux referred to the stator

φ'_{kd}= d-axis dampers flux referred to the stator

φ'_{kq1} , φ'_{kq2}= q-axis dampers flux referred to the stator

For household load power supply, a 8 kVA generator should sustain urban or peri urban house consumption which usually ranges between 1.5 kVA and 2.5 kVA. Therefore, the surplus power can be injected into the local microgrid network where neighbouring households can connect. Figure 4.6 shows an 8.1 kVA diesel generator modelling in Simulink, with a total load of 2.5 kW divided into two of loads of 0.5 and 2 kW. The first load, 0.5 kW, emulates the household continuous loading while the second load emulates the additional loading from the neighbours who will eventually be connected through the microgrid. Figure 4.7 shows the results of the model simulations over a period of 20 seconds, with load 1 connected all along the period while load 2 is connected from t = 5 seconds to t=12 seconds. From the results, it shows that the diesel engine provides a slightly constant mechanical output irrespective of the demand. Therefore, it would be more economical to integrate additional load from neighbours for fuel cost sharing.
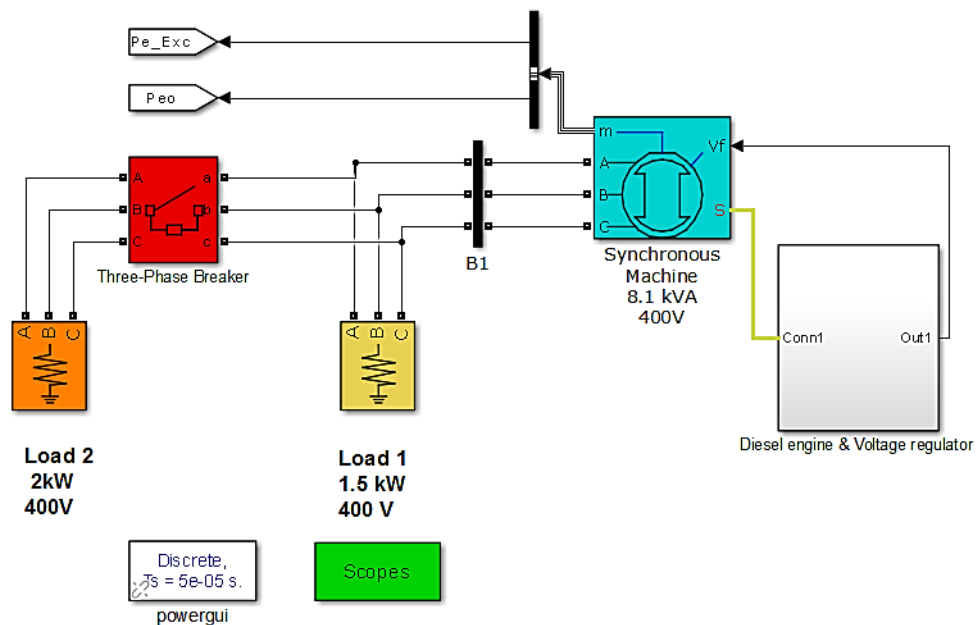
Figure 4. 6: Diesel power generator with loads.
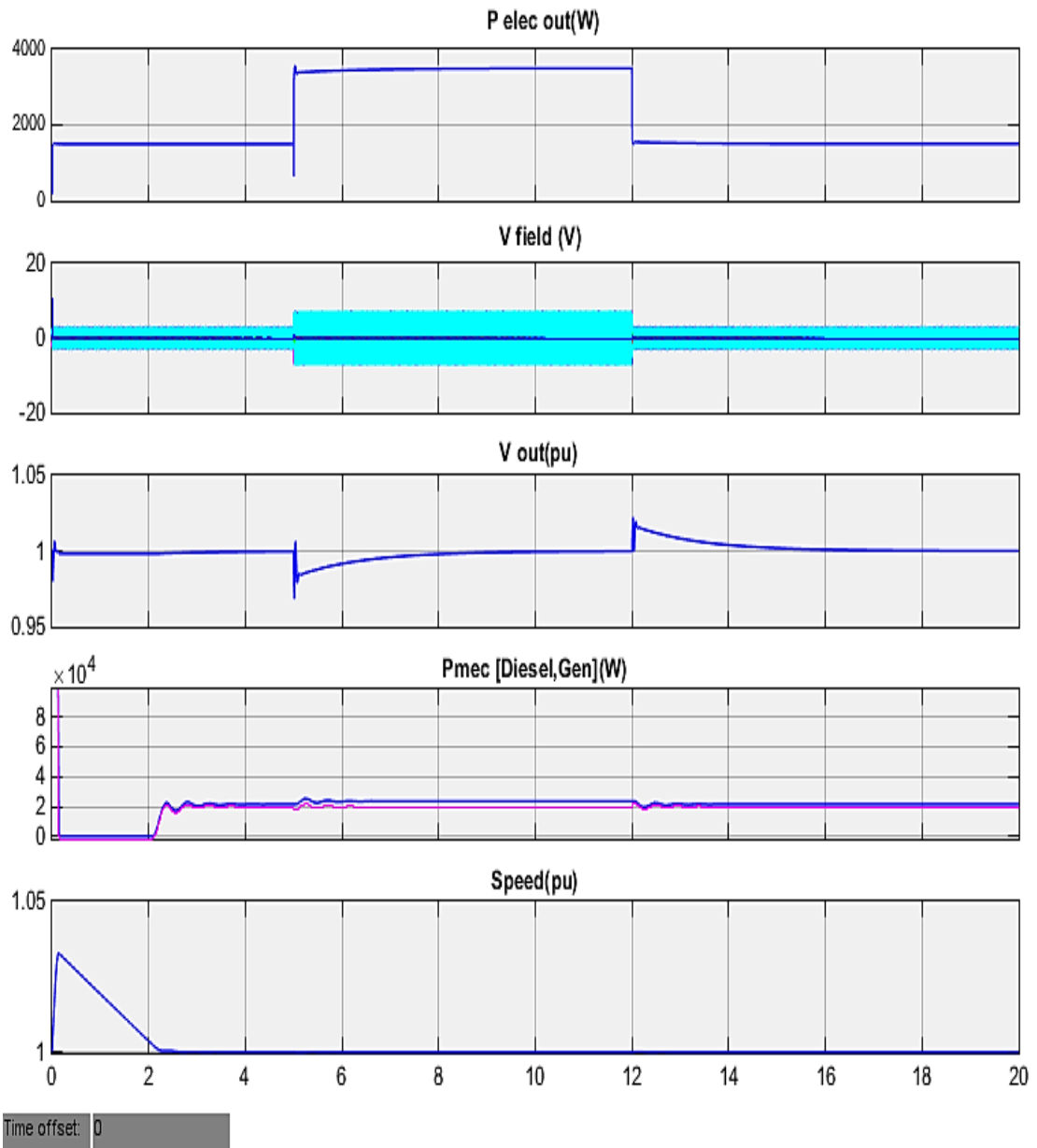
Figure 4. 7: Simulation results of an 8kVA diesel power generator with 2,5kW total load.

B. Generator protection

A protection system is essential for the safety of both users and equipment. Hence, the need for a protective device to be well-sized to be able to effectively interrupt a fault current that might occur. Generator parameters necessary for fault current calculations are shown in Table 4.2

Table 4. 2: Diesel generator parameters.

Power nominal, (Pn)	8100 VA
Voltage nominal, (Vn)	400 V
Frequency	50 HZ
Stator	
Resistance	1.62 Ω
Leakage inductance (Ll)	0.004527 H
Magnetizing inductance d-axis (L$_{md}$)	0.1086 H
Magnetizing inductance q-axis (L$_{mq}$)	0.05175 H
Field	
Resistance	1.208 Ω
Leakage inductor	0.01132 H
Dampers	
Dampers resistance referred - d-axis (R$_{kd'}$)	3.142 Ω
d- axis dampers inductances ($Ll_{kd}{}'$)	0.007334 H
q- axis dampers inductances, ($Ll_{kq1}{}'$)	0.01015 H
Dampers resistance referred - q-axis (R$_{kq1}$')	4.772 Ω
Pole pairs	2
Inertia	0.2252 J (Kg.m^2)
Friction factor	0.009 F (Nm/s)

One of the characteristics of a diesel generator, which is referred to as a standby alternator, is the limited fault current. On the other hand, its magnitude changes considerably during the sub-transient period of the fault, 10 ms to 20 ms from the fault starting. As shown on Figure 4.8 at the occurrence of symmetrical faults at generator terminals, fault currents rise to a value between 3 to 5 times the full load current.

Fault current starts dropping rapidly from the maximum over transient period, which lasts between 80ms to 280ms depending on generator characteristics such as size and type. Fault currents stabilise around 0.5 second or beyond depending on the generator excitation type,

such as a manual or automatic voltage regulator. With the latter, the steady-state fault current during the transient period rises the fault current in the range of 2.5 In to 4 In. In our case, a diesel generator with automatic voltage regulator is chosen as they are the ones currently on market (Htay & Win, 2008; ESKOM, 2015).
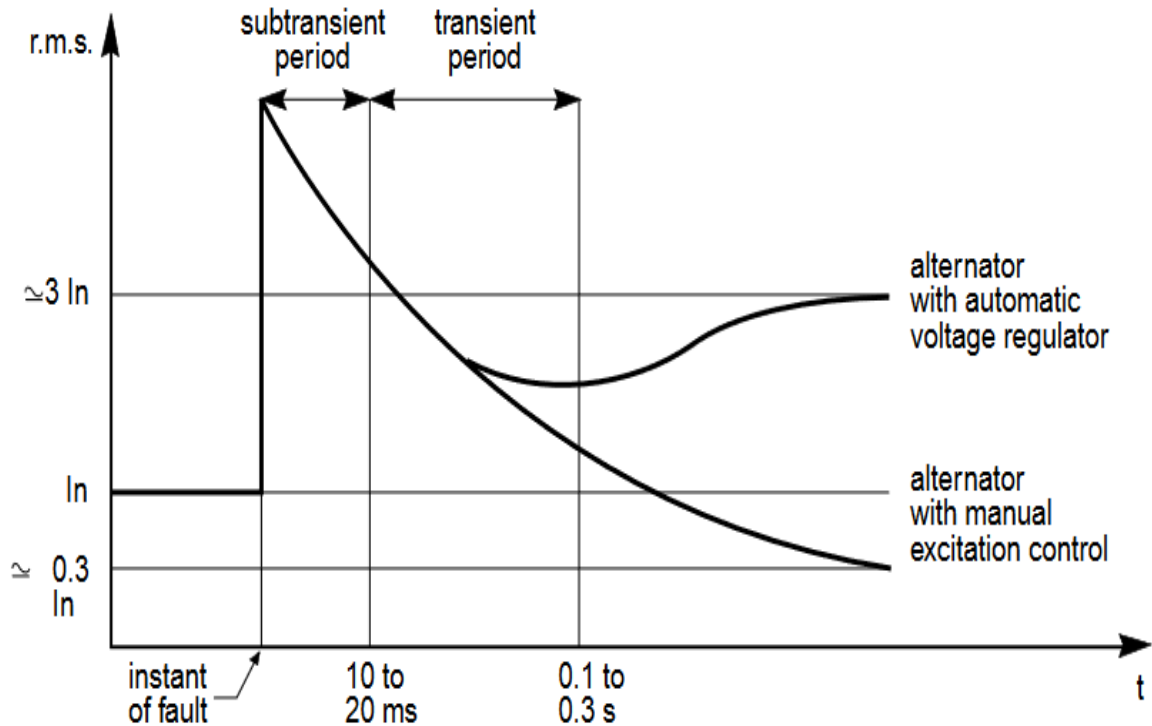
Figure 4. 8: Establishment of short circuit current for a three-phase short circuit at the terminals of an alternator.

From the specifications, the fault current is calculated as follows:

Full load current (In) $= \dfrac{Nominal\ power}{nominal\ voltage}$ Equation 4.7

$= \dfrac{81000\ VA}{400\ V}$

$= 25$ kA

$\therefore$ Full load current (I_n) $= 25$ kA

Short Circuit Current (I_{sc}) = 5 x Full load current (I_n)

= 5 x 25 kA

= 125 kA

94

$\therefore$ Short Circuit Current (I_{SC}) = 125 kA

Hence, the generator will be protected by a circuit breaker with interrupting capacity greater than 125kA and tripping current set at 25 kA.

4.2.2 Microgrid development

The second step in the bottom-up grid extension evolution approach is as explained in section 4.2. Power excess from each nanogrid (prosumer) will be transferred to nearby loads, households without a generator or with one that is not running. These will be achieved through the interconnection of neighbouring prosumers through an overhead line low voltage DC network with a bidirectional AC/DC power flow converter as interface.

Figure 4.9 shows a conceptual interconnection for microgrid development. Estate or village dwelling types are considered as the model, so the microgrid will cover 1Km radius. Radial and ring network configurations will be considered. However, emphasis will be on the radial network configuration due its low initial cost and maintenance as described in Chapter 2, section 2.3.
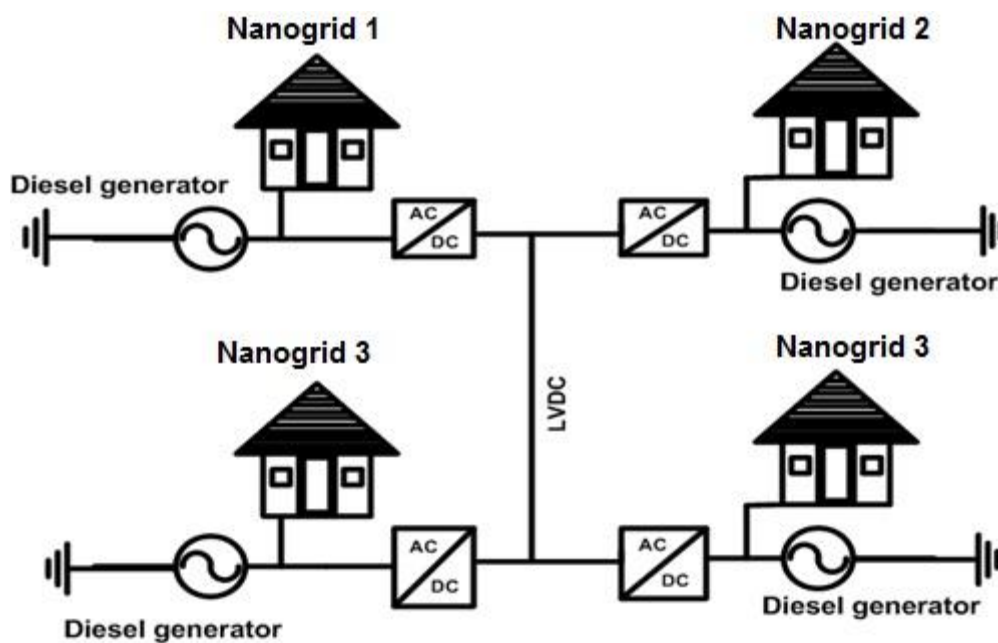
Figure 4. 9: LVDC microgrid.

A. Nanogrid AC/DC converter design

The AC/DC converter serves as interfaces for the nanogrid to integrate with the microgrid. The converter should be a bi-directional type, acting as a rectifier during the power transfer to the microgrid on one hand; and on the other hand, acts as an inverter during power import to the nanogrid in case the diesel generator is not operational.

Figure 4.10 shows the nanogrid bi-directional converter configuration. A 10kW, 400V operating in two modes, namely rectification and inverter mode. Rectifier mode is active whenever the diesel generator is running and producing more power than required by the local load. Hence, power excess is injected to the LVDC microgrid through the converter operating as a rectifier. A reverse process is activated during the inverter mode, where now power is imported from the LVDC microgrid to local loads. During inverter mode, the diesel generator is not running and for safety purposes should be disconnected from the load.
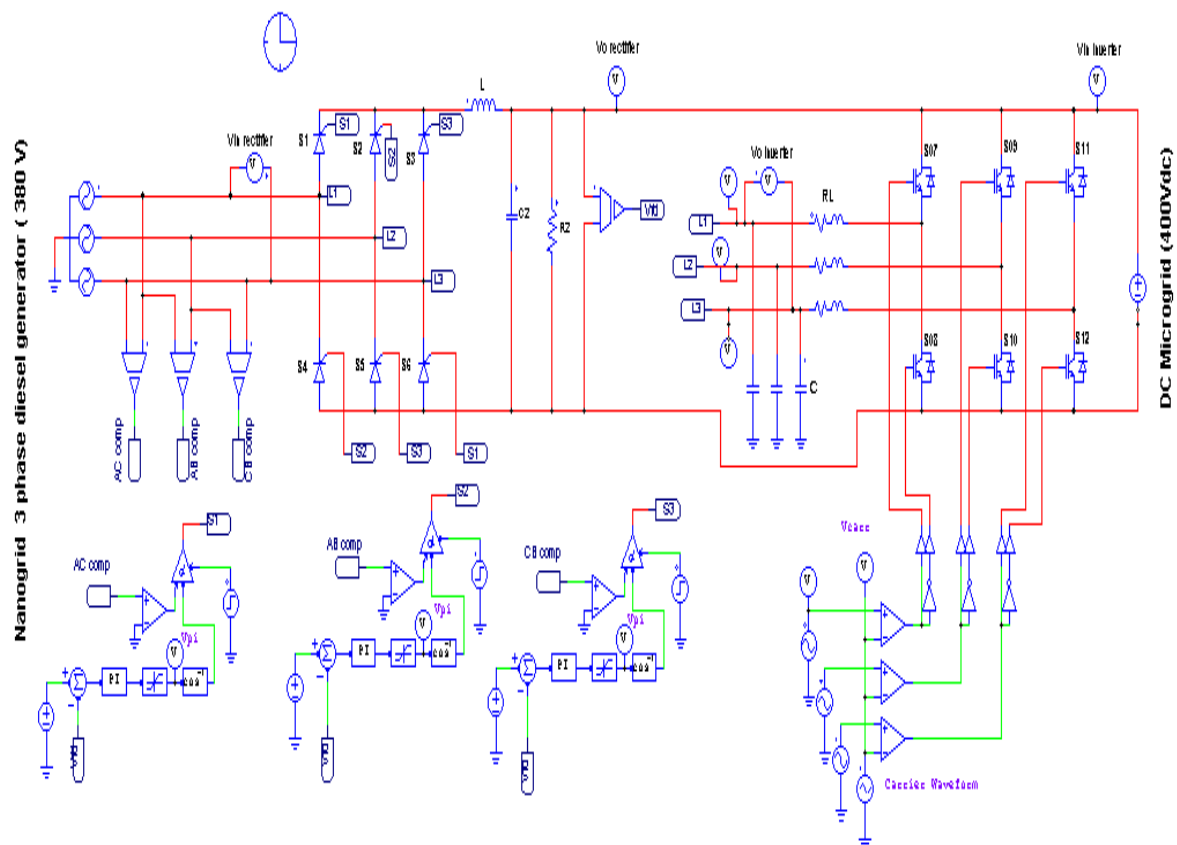
Figure 4. 10: Nanogrid AC/DC bi-direction converter.

Modular design was chosen to facilitate the maintenance and repair. Instead of replacing the whole converter in case of a faulty component as commonly done with compact ones on the market; with a modular topology, only a defective module would be replaced. The motives of such an approach are at the same time environmental and economical.

Environmental: as technology is evolving and society relies more and more on electronic equipment. Thus, electronics equipment are being produced in large quantity. On the other hand, there are no relevant or appropriate systems for disposal of discarded appliances which are also known as e-waste (Gaidajis et al., 2010). Moreover, as the grid nature is changing towards smart grids and intermittent resources integration which mainly rely on electronic

equipment, namely converters, for grid integration. With the proposed grid extension in this work, converters will be extensively used and in practical at a certain moment they might be faulty. Instead of replacing the entire converter, only the defective module should be replaced. Thus, the reason for modular topology is to allow for quick and easy fault location and mitigation. This approach reduces the amount of waste which is in line with the four strategies for e-waste management as portrayed in Lotlikar (2017).

Economical: beside concerns for the environment, there are economic benefits in modular topology equipment. If supported by legislation, it will lead to job creation for repairers, as modular equipment would be easy to fix. With legislation that not only enforces the right to repair but also module inter-operability of different brands, this would help small firms to fit into the market by focusing on modules instead of the entire converter.

- **Rectifier mode:**

During rectifier mode, power transfer is from an AC nanogrid to the DC microgrid. Figure 4.11 shows the circuit topology of a 6-pulse thyristor-based rectifier, modelled in PSIM, that operate during the rectification. Thyristors gate are driven by alpha controller with a close loop control using the PI controller.

The switching sequence is given in Table 4.3, where thyristors are fired according to the sequence and firing angle that is controlled by the PI controller. The latter improves the output voltage by adjusting thyristor start time to meet the expected output voltage.
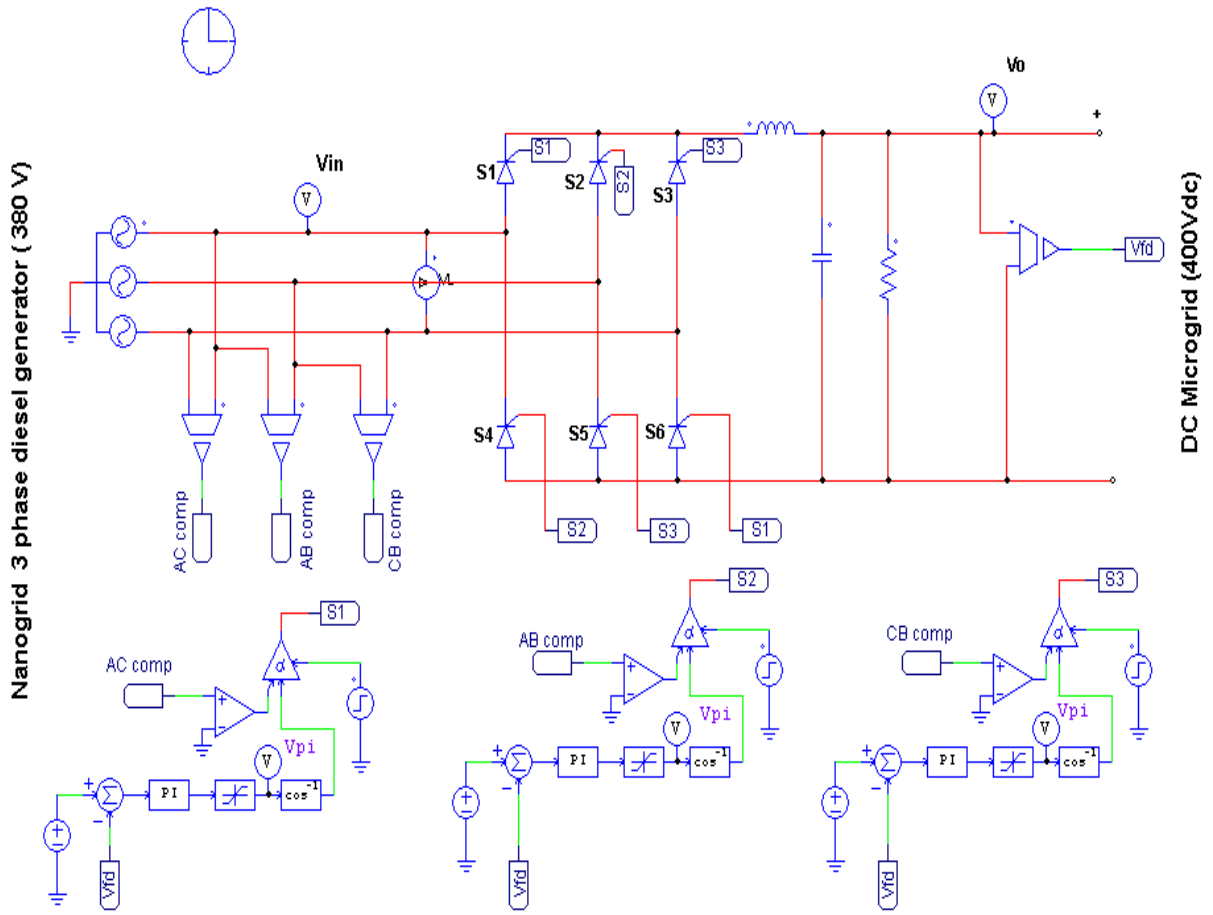
Figure 4. 11: Rectifier operation model in PSIM.

Table 4. 3: Rectifier mode switching sequence.

	S1	S2	S3	S4	S5	S6
V_A	**On**	Off	Off	Off	Off	**On**
V_B	Off	**On**	Off	**On**	Off	Off
V_C	Off	Off	**On**	Off	**On**	Off

The above three-phase six-pulse rectifier average DC output voltage is calculated based on an "m" number pulse fully controlled rectifier which results in "m" number of peaks within a cycle of input AC supply and they are symmetrical over the period of the cycle.

Hence, the duration of each peak would be equal to $\frac{2\pi}{m}$ radians and taking into account the delay angle α, output voltage waveform looks as shown on Figure 4.12.
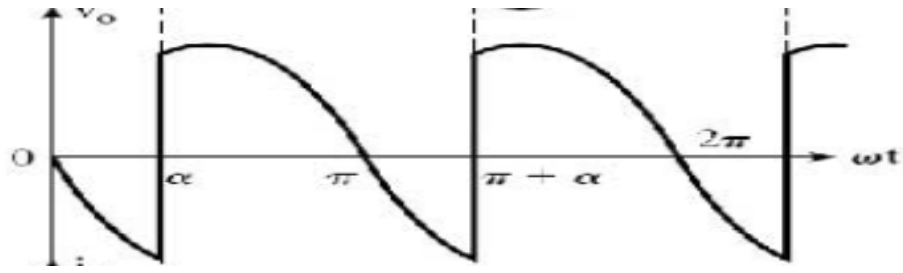
Figure 4. 12: 3-phase controlled rectifier output voltage waveform over a cycle.

As the peaks are symmetrical over the full cycle, therefore the average voltage value of the waveform in Figure 4.12 over a period of $\frac{2\pi}{m}$, is equal to the average voltage over the cycle period interval.

Thus,

$$V_{av} = \frac{m}{2\pi} \int_{\left(\alpha-\frac{\pi}{m}\right)}^{\left(\alpha+\frac{\pi}{m}\right)} V_m \, \cos \theta \, \, d\theta = \frac{V_m}{2\pi} \left[\sin \theta\right]_{\left(\alpha-\frac{\pi}{m}\right)}^{\left(\alpha+\frac{\pi}{m}\right)} \qquad \text{Equation 4.8}$$

$$= \frac{m \, V_m}{\pi} \sin \frac{\frac{\pi}{m}}{\pi m} \cos \alpha$$

$$= \frac{V_m}{\pi/m} \sin \frac{\frac{\pi}{m}}{\pi m} \cos \alpha$$

$$\therefore V_{av} = \frac{V_m}{\pi/m} \sin \frac{\frac{\pi}{m}}{\pi/m} \cos \alpha \qquad \text{Equation 4.9}$$

Where,

m = rectifier pulse number

V_m = AC source peak line voltage in Volts

$V_m = \sqrt{2}V_{LL \, rms}$; with $V_{LL \, rms}$ = AC source root mean square line-to-line voltage.

Therefore, for a 3-phase 6-pulse diode rectifier using Equation 4.9 with:

$m = 6$

$V_m = \sqrt{2}V_{LL \, rms}$

$$V_{av} = \frac{V_m}{\pi/6} \sin \frac{\frac{\pi}{6}}{\pi/6} \cos \alpha$$

$$= \frac{\sqrt{2}V_{LL \, rms}}{\pi/6} \sin \frac{\frac{\pi}{6}}{\pi/6} \cos \alpha \qquad \text{knowing that for diode rectifier α = 0°,}$$

$$= \frac{3\sqrt{2}V_{LL\,rms}}{\pi}$$

$$\cong 1.35\,V_{LL\,rms}$$

From the above calculations, during the rectification mode, the nanogrid bi-directional converter previously shown on Figure 4.10 will inject power into the microgrid at 400 V_{DC}. However, the system voltage requirement is 400 V_{DC}, therefore a controller system that drives PWM gate signals, through angle control will adjust the output voltage to the required amplitude. Figure 4.13 and Figure 4.14 shows converter simulations results for input and output voltage respectively.
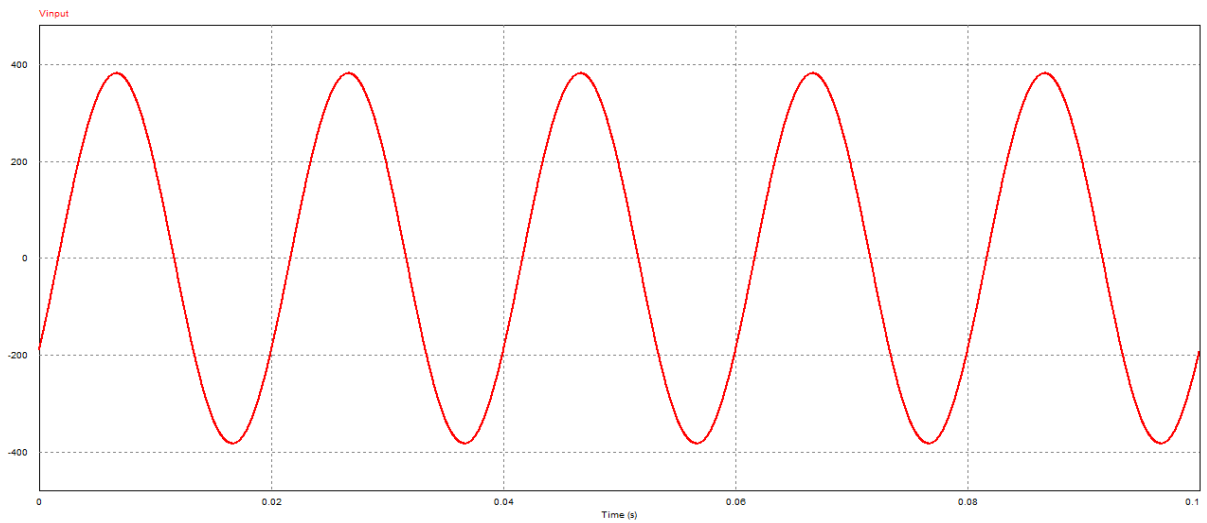
Figure 4.13: Nanogrid diesel generator voltage.
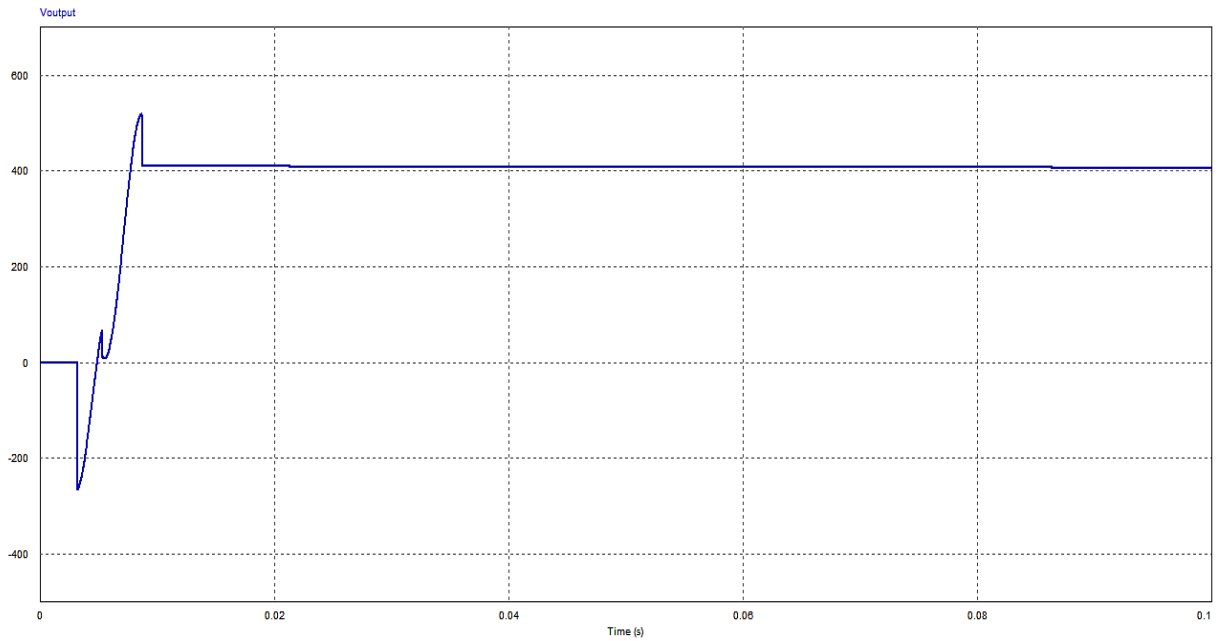
Figure 4. 14: Nanogrid converter in rectifier mode output voltage.

- **Inverter mode**

Figure 4.15 shows a nanogrid converter 3-phase inverter operation model as developed in PSIM. It consists of six IGBT switches, controlled by Pulse width modulation strategies, as well as RLC filters and DC source that emulate the DC microgrid. During inverter mode, power flows from the DC microgrid to the AC nanogrid through a coordinated IGBT switching following a sequence shown in Table 4.4. Only a pair of switches is activated at once and due to the switching process fluctuations occurs in the output voltage. Thus, the insertion of RLC filters to smooth the AC output voltage.
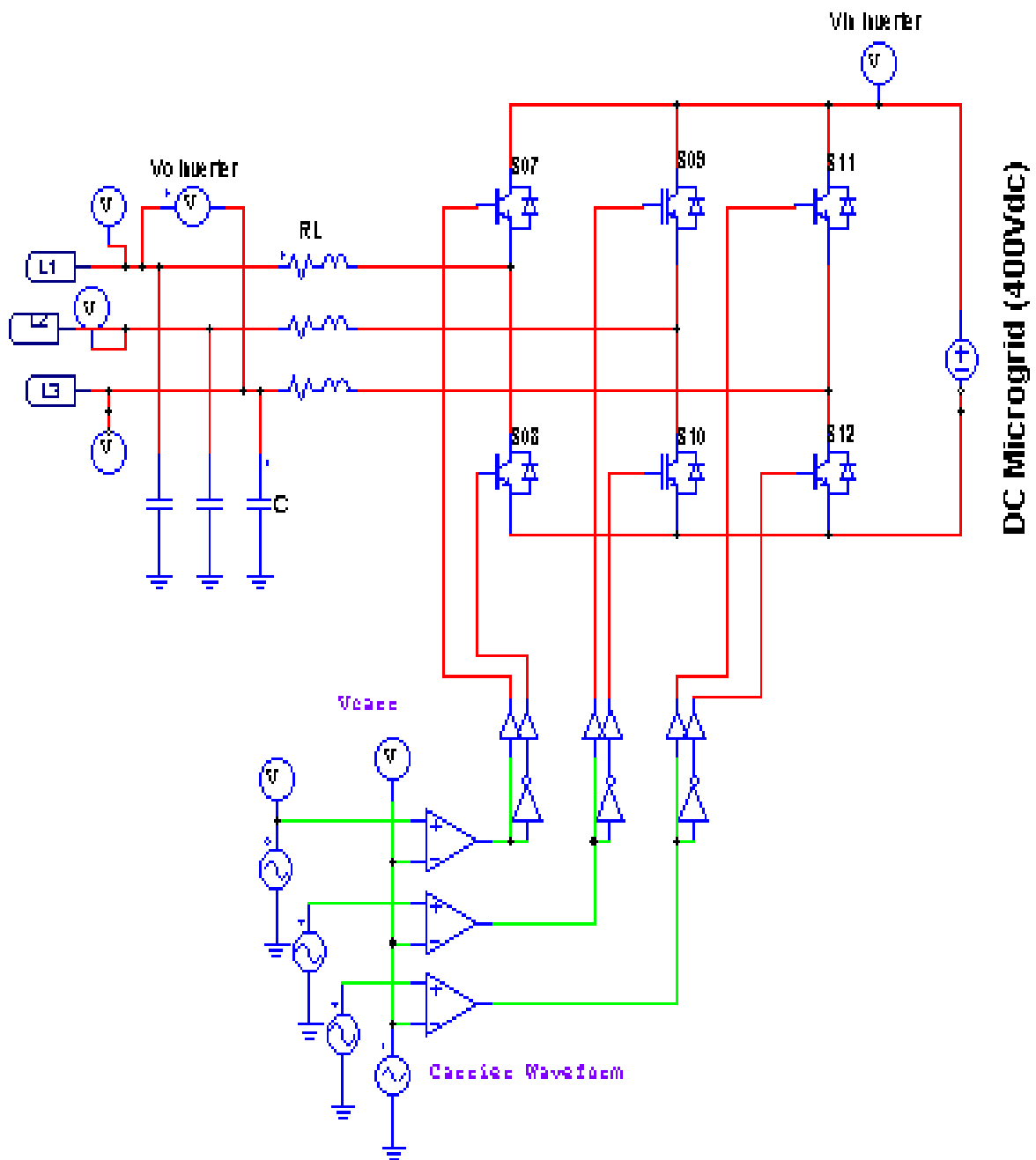
Figure 4. 15: Nanogrid converter, inverter operation model.

Table 4. 4: Inverter mode switching sequence.

Phases	S07	S08	S09	S10	S11	S12
V_A	On	Off	Off	On	Off	Off
V_B	Off	Off	On	Off	Off	On
V_C	Off	On	Off	Off	On	Off

Inverter operation model is simulated using parameters in Table 4.5, simulations results are shown in Figure 4.16, Figure 4.17 and Figure 4.18 for input voltage, output phase voltage and output line-to-line voltage respectively.

Table 4. 5: Nanogrid inverter operation model simulation parameters.

Parameters	Value
Input voltage	400 Vdc
Switching Frequency	15 kHZ
Resistance	1
Inductance	2 mH
Capacitance	800 μF
Simulation time	0.1 second
Reference frequency	50 HZ
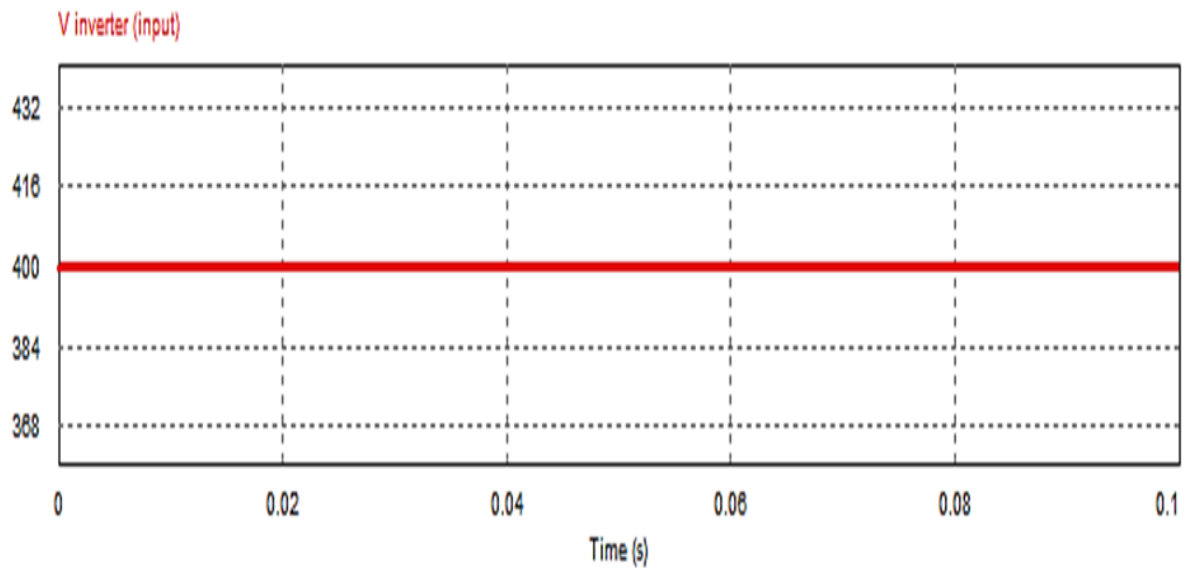
Figure 4. 16: Nanogrid converter, inverter mode input voltage.
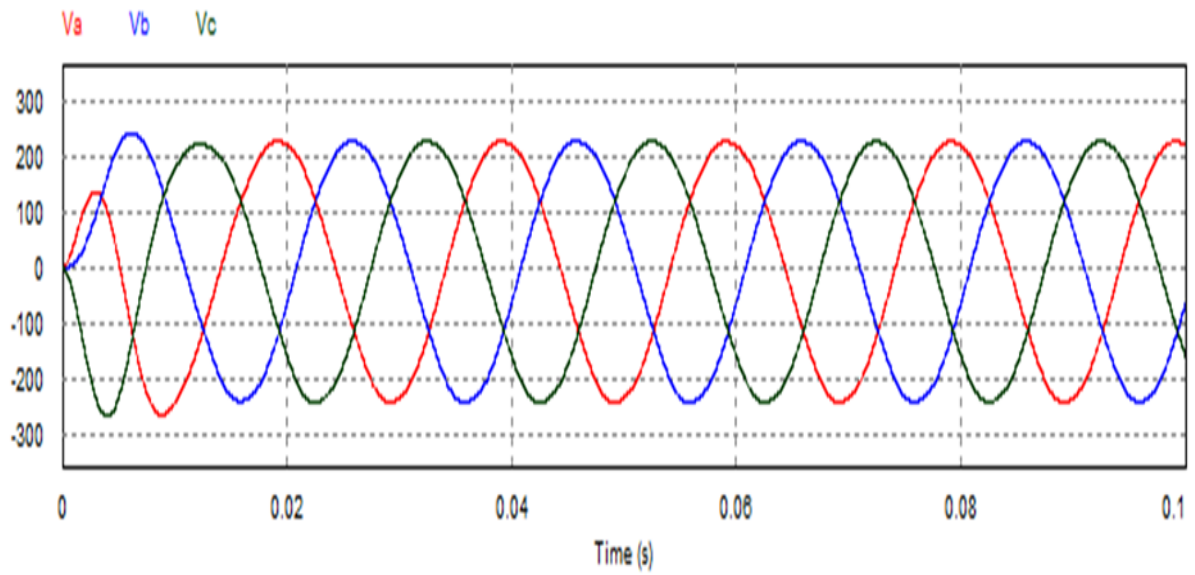
Figure 4. 17: Nanogrid converter, inverter mode output voltage per phase.
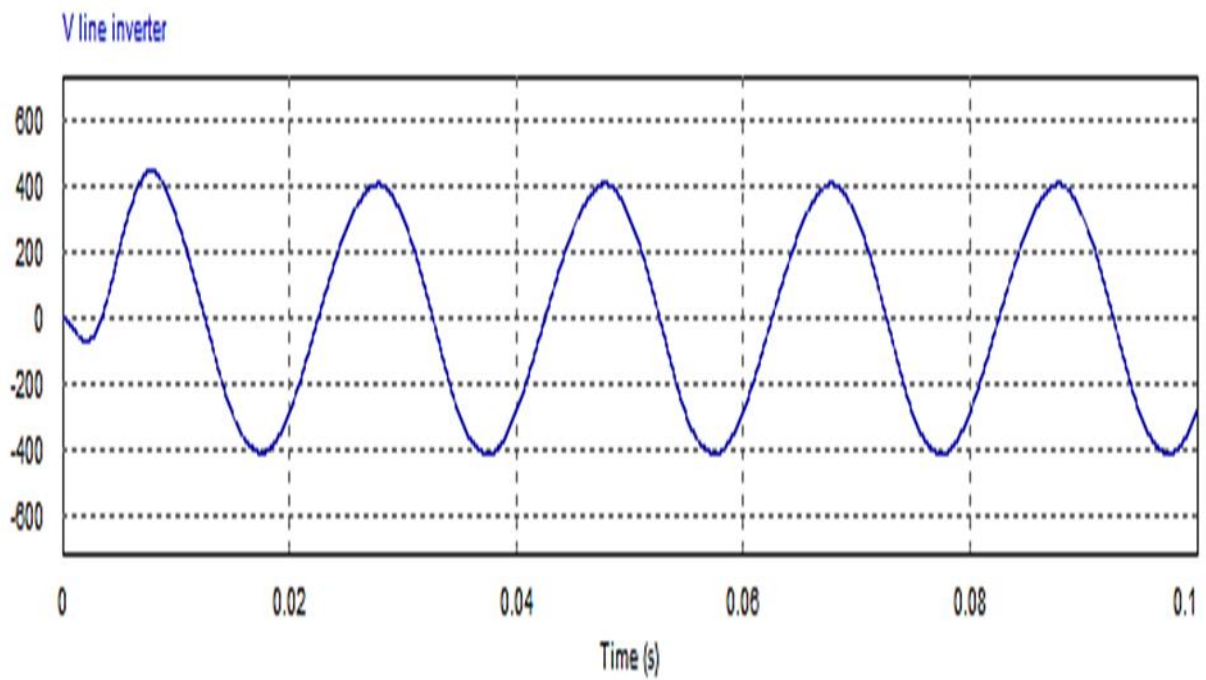
Figure 4. 18: Nanogrid converter, inverter mode output line voltage.

B. Nanogrid overall control scheme

Besides having specific control of each mode of the converter operation, an overall control is needed to supervise the interaction between both operation modes and the nanogrid power source as well as local loads. The overall control will also ensure a smooth transition between operating modes and prevent any simultaneous nanogrid/microgrid mutual feed in.

Figure 4.19 shows an overview of the control system and its interaction with the system components. As shown, the proposed controller will overlook on converter rectification and inversion, diesel generator interconnection or islanding of the nanogrid as well as filters switching in and out depending on the mode running.
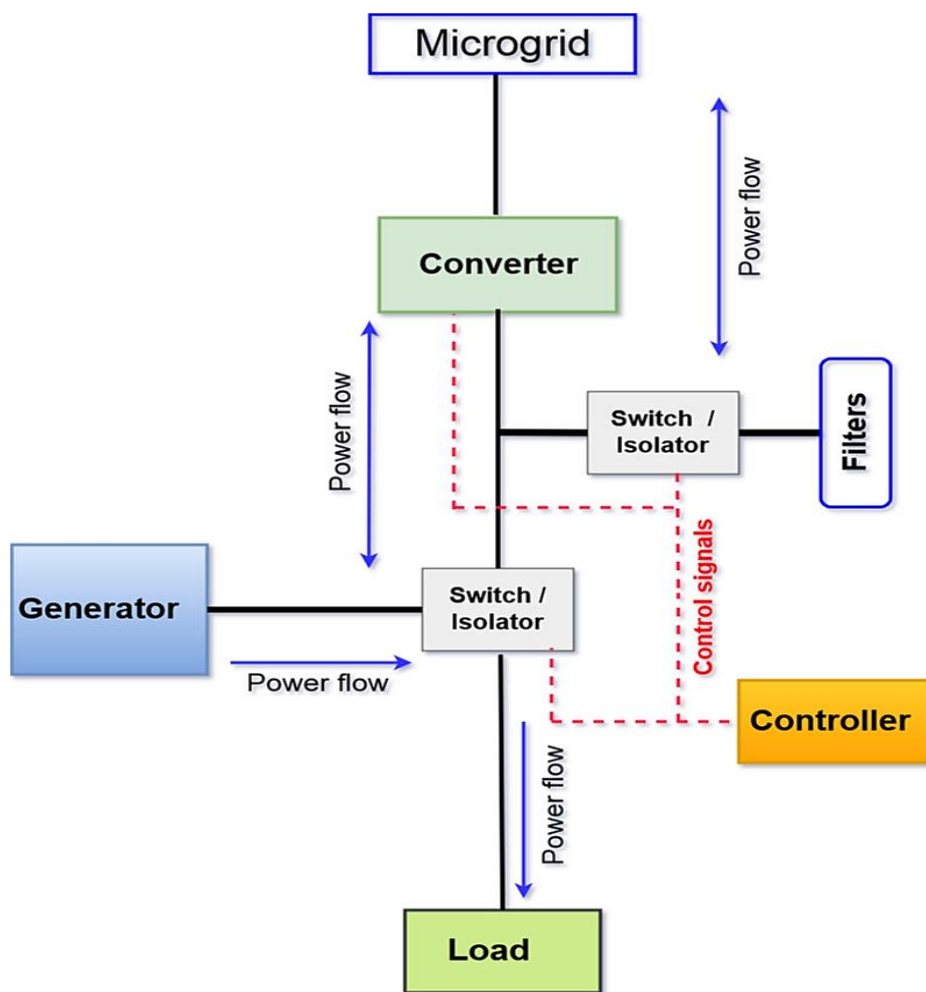
Figure 4. 19: Nanogrid control block diagram.

The controller, as the decision maker of the converter operation and other system components associated with the nanogrid, needs criteria to base on for switching in and out different operation modes and associated equipment.

Rectification mode will be activated upon successful fulfilment of following conditions:

1. The nanogrid supply (diesel generator) is running.
2. Nanogrid power consumption less than pre-set threshold, hence justification for power

Once all the above conditions are met the controller will switch on the converter to run into rectification mode, thus injecting power into the microgrid.

Inversion mode, it is activated for nanogrid power import from microgrid. Conditions for the converter to run into such modes are:

3. The nanogrid supply (Diesel generator) is not running.
4. Generator is isolated from nanogrid (load).

An additional mode can be added, the Islanding of the nanogrid, but this is considered as the initial mode before switching to any other mode.

Decision making by the controller is achieved using auxiliary equipment such as measurement, voltage and current detection, as well as protection devices. Therefore, a certain sequence and event coordination algorithm is needed. The controller algorithm overlooks the operations of the entire nanogrid network and connected equipment. It decides, from the information collected by auxiliary devices, the action to be performed by the converter and other associated equipment.

Figure 4.20 shows a flowchart diagram of the nanogrid control algorithm; island mode is set to be the initial mode; however, another setting allows the prosumers to choose the option of power exchange with the microgrid. As the generator starts, voltage generated (V_g) and frequency (F) are measured. They are compared to predefined values, in actual case 380 V and 50 Hz, for (V_g) and F respectively. Two scenarios can unfold:

1. The generated power meets predefined criteria.
2. Generated power does not meet predefined criteria.

 In the first scenario in case the generator output voltage (V_g) and frequency (F) do meet predefined values, which corresponds to low voltage AC networks standards as defined by IEEE, then the load switch is closed to allow power flow to the load. Continuous monitoring of the load power demand (P_L) as well as of the load voltage are done through measurement. A certain load power threshold ($P_{L\_threshold}$) defines the maximum load power consumption under which the nanogrid generator can export to the microgrid without compromising its local demand. If the nanogrid power consumption (P_L) is greater than the threshold ($P_{L\_threshold}$), no

power export is possible, and the controller continues the monitoring. In case nanogrid power consumption (P_L) is under the threshold ($P_{L\_threshold}$), then power exportation can take place. Therefore, the converter switch load is closed to allow power to flow towards the microgrid and filter switch is closed before starting the converter in rectifier mode and connecting the converter to the DC microgrid. A continuous monitoring of power exported (P_{Conv}) and voltage takes place to avoid overloading the minigrid generator which can affect power supply quality for both microgrid and nanogrid loads. If the power exported (P_{Conv}) is less than the threshold ($P_{LDC\_threshold\_max}$) or nanogrid power consumption (P_L) is still less than the threshold ($P_{L\_threshold}$), then power exportation to the microgrid will continue. On the other hand, in case the power exported (P_{Conv}) goes beyond the threshold ($P_{LDC\_threshold\_max}$) or in case of the nanogrid load demand (P_L) going beyond threshold ($P_{L\_threshold}$) for power export to take place, then the export process is terminated by switching off the converter, disconnecting filters, and islanding the nanogrid by opening the converter to load switch. Afterwards the controller will go back to the stage after the closure of the switch to the load, in island mode.

In scenario two, the output power is either not in line with predefined values or the generator is not working. In either case, the controller will look for importing power from the microgrid. However, a cross check of the prosumer choice is performed; whether grid interaction was opted for or nanogrid island mode. In the latter case, the controller will stop, while in the former case it will turn on the converter in inverter mode and switch on filters before starting the power import from the microgrid to the grid. Converter output power, voltage (V_{Conv}) and frequency (F) are compared to nanogrid predefined values which are 380Vac and 50Hz, in our particular case. If (V_{Conv}) and (F) do not match predefined values, then the controller will try again three times. If the values persist then the controller will end the process. On the other hand, if (V_{Conv}) and (F) do match predefined values, then the controller proceeds to close the converter to the load switch thus power from microgrid to enter the nanogrid. Prior to that, a cross check on the prosumer mode choice is performed. At this stage the prosumer might decide to stop the process. Thus, a continuous monitoring of these events along with other parameters is essential. If island mode or stop is not activated, meaning that the prosumer maintains grid interaction, then a loop monitoring up to the point after the closure of converter load switch is established to track any change. Additionally, if the prosumer chooses to stop the interaction with the microgrid, then the controller proceeds to turn off the converter. Lastly, filters are disconnected and the converter to load switch is opened before the controller stops.
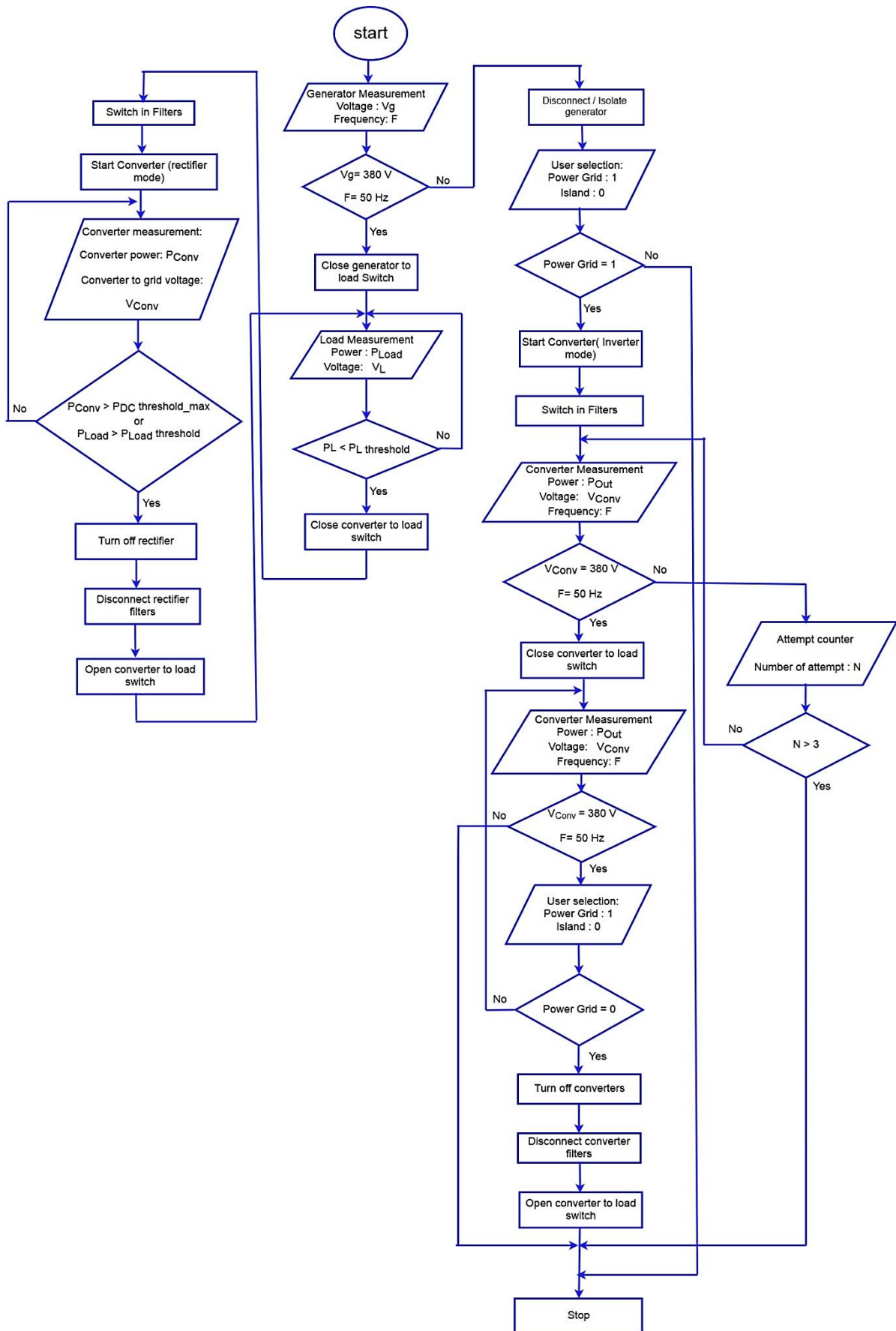
Figure 4. 20: Nanogrid control algorithm flowchart.

108

C. Microgrids interconnection converter design

From the nanogrid build-up into the DC microgrids, as developed in section 4.1, microgrids are interconnected for power sharing and to develop a network that will eventually connect to the grid. Microgrids are interconnected through intermediate low voltage DC networks operating at 3 kV with a DC-to-DC converter as interface.

As microgrids are developed using low voltage DC networks operating at 400 V, integration to a 3 kV operated network requires the use of a DC-DC converter with bi-directional capability. The converter will operate as a boost for power flowing from the microgrid to ILVDC networks, while buck mode runs when power flows from the network to the microgrid.

Figure 4.21 shows a circuit diagram of the proposed DC/DC buck boost bi-directional converter for microgrid integration to ILVDC network. Interleaved boost converter is used as it has improved efficiency, reduced current ripples as well as current stress on cells compared to a conventional converter (Thiyagarajan et al., 2014). It consists of six switches, three inductors, and two capacitors for input and output.

The switching is coordinated according to the number of phases or converter legs. Hence, during the boost mode, three lower switches are turned on. Switches are activated in sequence at different times, with a certain delay to reduced ripples. The master switch, S2, is the first to be activated, followed by the slave switches, S4 and S6. S4 is delayed being activated for a time equal to half the switching period of the master switch S2. Same for the third switch, S6, which is activated after a time equal to the half of the S4 switching period.
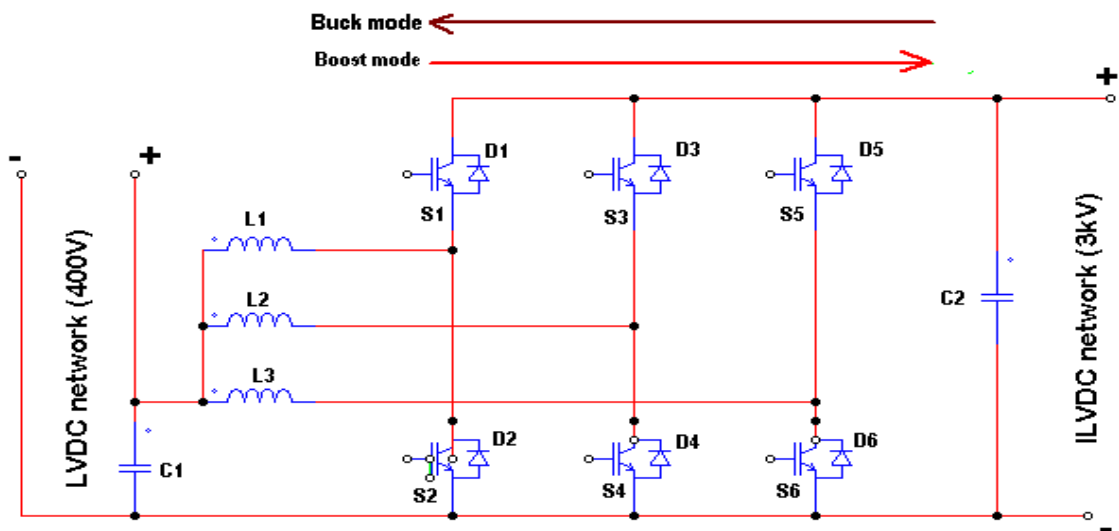
Figure 4. 21: Circuit diagram of an interleaved buck boost bi-directional converter.

The design of the interleaved buck boost bidirectional converter, on Figure 4.21, requires accurate sizing of the inductors and capacitors as well as the duty circle of the switching devices and the switching frequency. IGBT switches are used due to their ability with high voltage, high switching speed and mainly their low resistance.

Boost mode specifications are as follows for a 100 kW converter, power majored at 20%:

Input voltage (V_{IN}) = 400V , Power (P) = 120kW

Output voltage (V_O) = 3 kV

Knowing that for the boost converter, output voltage (V_O) is given by Equation 4.10:

$$\frac{V_O}{V_{IN}} = \frac{1}{1-D}$$
Equation 4.10

Where D is the duty circle

then,

$$\frac{3 \times 10^3}{400} = \frac{1}{1-D}$$

D= 0.87

Inductors sizing

As three phases are used, the total current equally shared by three inductors is given by Equation 4.11:

$$P = V \times I$$
Equation 4.11

Where,

P = Converter power (kW)

V = Converter input voltage (V)

I = Total converter current (A)

$$\therefore I = \frac{P}{V}$$

$$I = \frac{120 \times 10^3}{400}$$

$$I = \ 300 \ A$$

Therefore, current per phase (I_{PH}) is given by: $\frac{I}{N}$ with N: number of phase and I total current.

$$I_{PH} = 300 \div 3 = 100 \text{ A}$$

Each single phase of the three phases of the interleaved converter will sustain 100 A current and allowed ripple phase current (ΔI_{PH}) is 1%. Thus, the value of each inductor can be calculated using Equation 4.12 (Rahavi et al., 2012):

$$L = \frac{V_{IN}\ D\ T}{\Delta I_{PH}}$$
Equation 4.12

Where,

V_{IN} = Input voltage (volts)

D = Duty circle

T= Switching period (seconds) at switching frequency of 20 kHz

ΔI_{PH} = Ripple phase current (1 A)

$$L = L_1 = L_2 = L_3$$

$$L = \frac{400 \times 0.87}{2 \times 20 \times 10^3 \times 1}$$

$$= 8700 \text{ µH}$$

Capacitor sizing

The output capacitor is sized using the Equation 4.13. Converter full current is used for line loading calculation and output voltage ripple percentage set at 1%. Therefore output capacitor, C_O, is given by:

$$C_O = \frac{V_o \times D \times T}{R \times \Delta V_O}$$
Equation 4.13

Where,

D= Duty circle

T = Switching period (seconds) at switching frequency of 20 kHz

R= Load

ΔV_O = ripple voltage

Knowing that power can be expressed by,

$$\therefore Power (P) = \frac{V^2}{R}$$ Equation 4.14

Where,

V = Voltage (V)

R = Resistance

Then using Equation 4.14,

$$R = \frac{V^2}{P}$$

With

V = 3000 V

P= 120 x 10^3 W

Then,

$$R = \frac{3000^2}{120}$$

= 75 Ω

And ripple voltage (ΔV_O) at 1%:

$$\Delta V_O = 3000 \text{ V} \times 0.01$$

$$= 30 \ V$$

Therefore, using Equation 4.13, the output capacitor C_2 value is equal to:

$$C_2 = \frac{V_o \times D \times T}{R \times \Delta V_O}$$ Equation 4.13

$$= \frac{3000 \times 0.87 \times 1}{75 \times 30 \times 20 \times 10^3}$$

$$= 5800 \ \mu F$$

Determination of switching angle for boost operation

Gate pulse switching is essential for converter operation; hence the need for a well-coordinated switching operation. For an interleaved converter it has to be done in such way as to minimise output ripples and by the occasion reducing stress on switches as well as losses.

Therefore, for boost operation, switches S2, S4 and S6 are switched respectively. Each is activated for a duration equal to:

Ton = D Ts

Where,

D= Duty cycle

T_{ON} = Switch time-on

T_S = Switching period in seconds / electrical degree

Ton$= 0.87 \times \frac{1}{20 \times 10^3}$

      = 43.5 µSec

Table 4.6 shows the switching sequence of the switches, note that switch S4 is activated at T equals to the half of switch S2 ON time. The same is done for S6 which turns on at half of S4 ON. This procedure results in reduced ripples in output voltage.

Table 4. 6: Boost mode switching sequence.

Switch	Angles (degree)	Time (µSec)
S2	0	0
S4	156,6	21.84
S6	234,9	30.54

Figure 4.22 shows the interleaved bi-directional buck-booster converter model developed in PSIM. The model is simulated in boost mode operation, emulating the power transfer from the microgrid to the interconnected microgrid network operating in intermediate low voltage direct current range. Simulations are run for 1 ms and results are shown on Figure 4.23. The input voltage of 400 V from the LVDC network is stepped up to 3 kV by the converter.
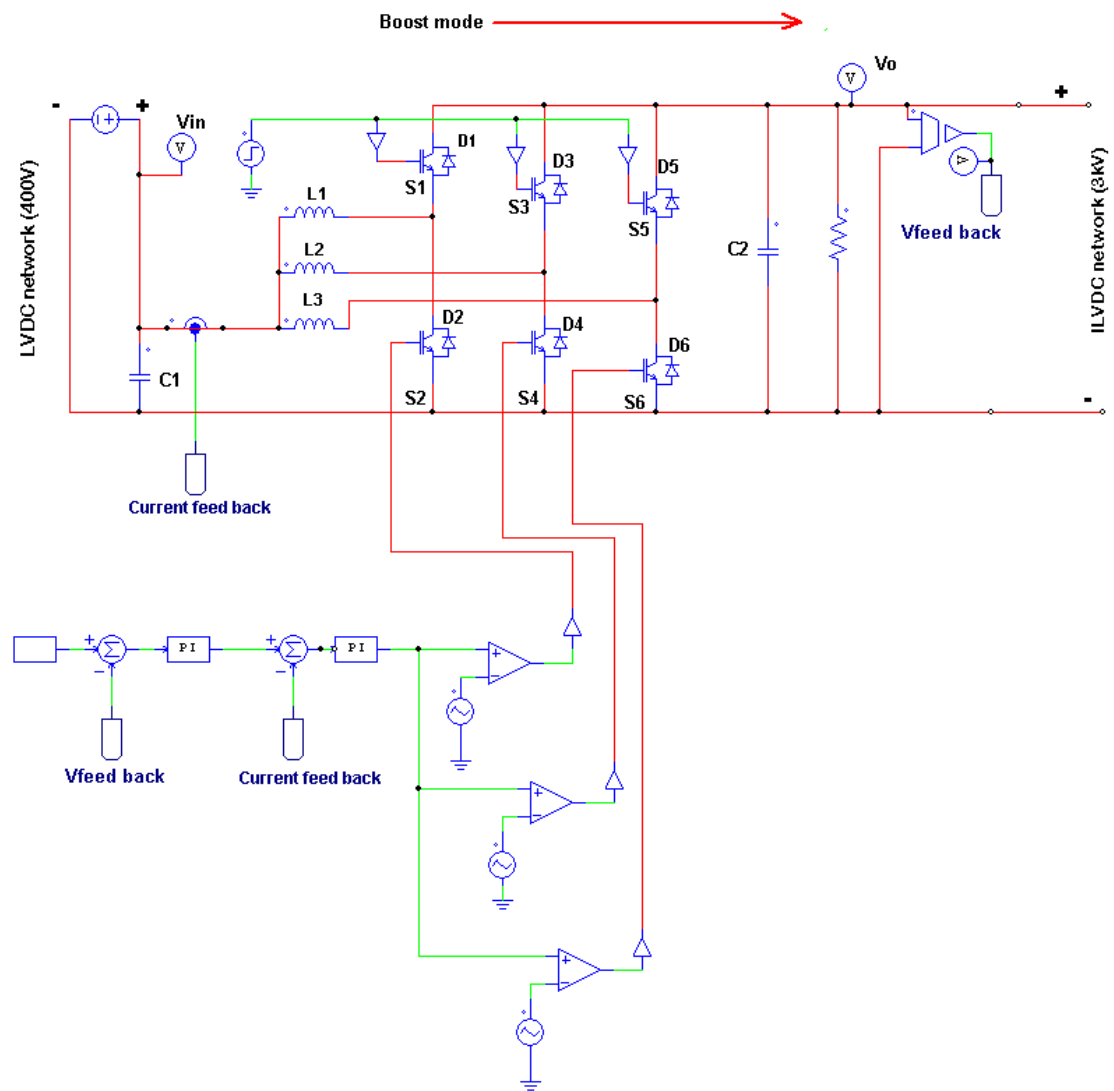
Figure 4. 22: Model of a bi-directional buck boost converter in boost operation mode.
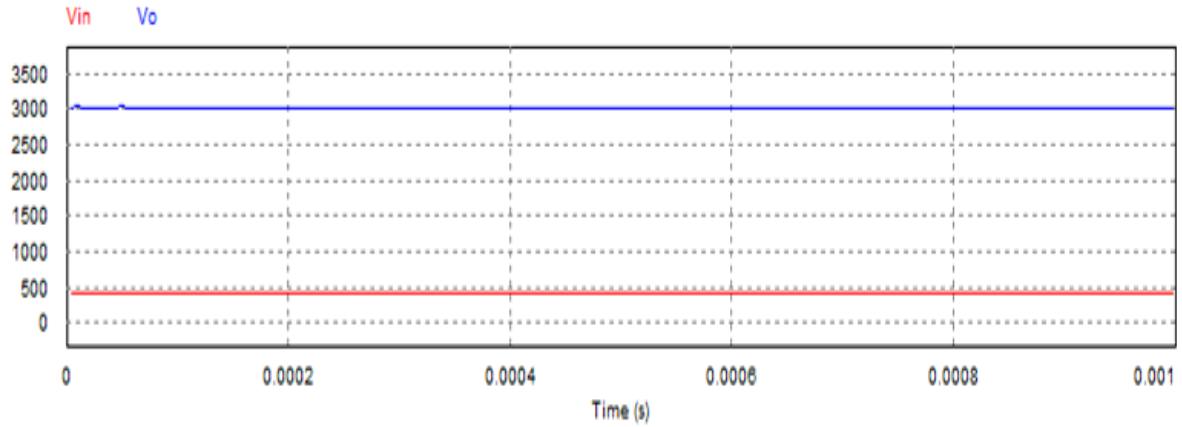
Figure 4. 23: Simulation results of a bi-directional buck boost converter in boost operation mode.

Determination of switching angle for buck operation

For buck mode, specifications are as follows:

Power (P) = 120 kW

Input voltage (V_{IN}) = 3 kV

Output voltage (V_O)= 400 V

The duty circle (D) is calculated from buck operation Equation 4.15:

$$V_O = D\ V_{IN}$$
<div align="right">Equation 4.15</div>

Therefore,

$$D = \frac{V_O}{V_{IN}}$$

$$= \frac{400\ V}{3 \times 10^3\ V}$$

$$= 0.13$$

Capacitor sizing for buck operation

Sizing of the output capacitor for buck operation (C1) is performed as for boost operation with a difference in parameters considered, as the power flows in the reverse direction. Considering the Intermediate Low Voltage Direct Current (ILVDC) network as a source and the LVDC microgrids networks as a load. Therefore, using Equation 4.16:

$$C_1 = \frac{V_O \times D \times T}{R \times \Delta V_O}$$
<div align="right">Equation 4.16</div>

115

Where,

V_O = Output voltage (400 V)

ΔV_O = Ripple output voltage (1%)

   = 4 V

T = Switching period

D = Duty circle (buck operation)

Then,

$C_1 = 44 \text{ mF}$

Figure 4.24 shows the converter buck operation model as developed in the PSIM environment. During this mode of operation, power is transferred from the ILVDC network to the microgrid interconnection low voltage direct current network. Switches S1, S3 and S6 are sequentially activated while the bottom switches are disabled. However, freewheeling diodes operate to provide a path for the returning current. Simulation results of converter buck operation are shown in Figure 4.25, where there is a successful step down of the converter input voltage (Vin) from 3 kV to 400 V (Vo).
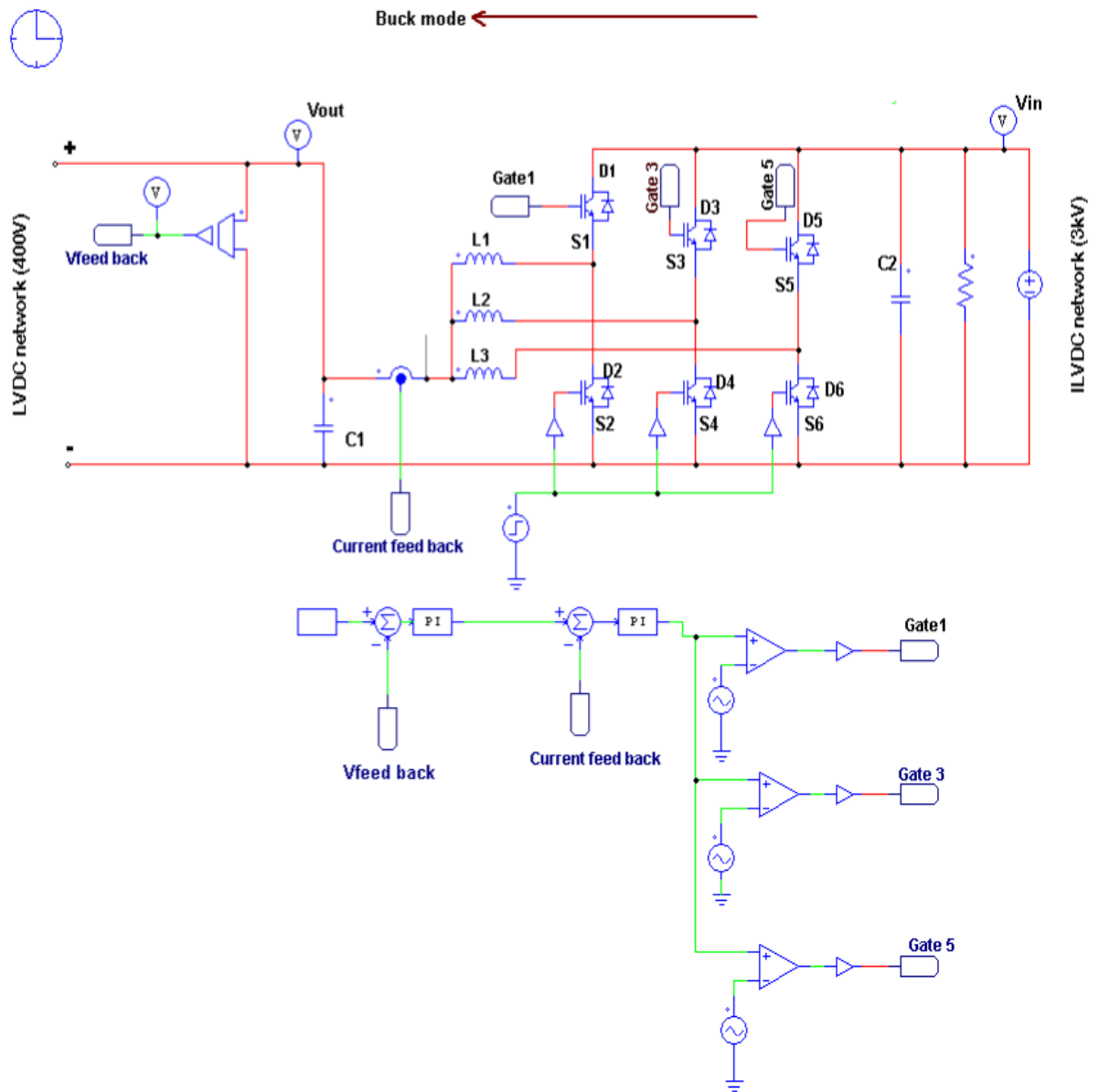
Figure 4. 24: Model of a bi-directional buck boost converter in buck operation mode.
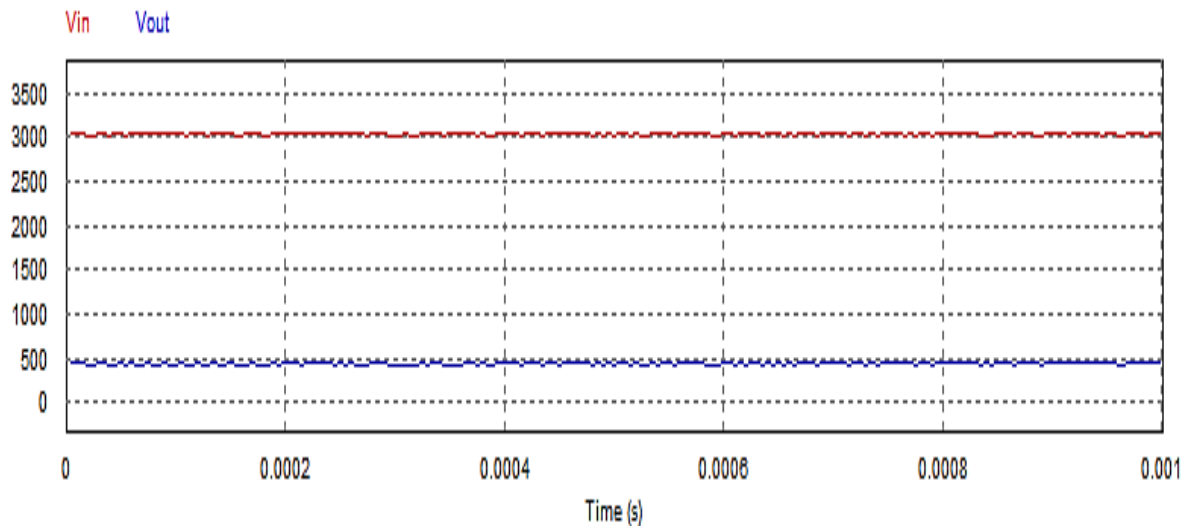
Figure 4. 25: Simulation results of a bi-directional buck boost converter in buck operation mode.

D. Microgrid control

Microgrid stands between the nanogrid and minigrid, acting as a bridge for power flow to or from within local interconnection of nanogrid clusters as laid out in section 4.2. The microgrid controller has two main roles:

- Manager clustered resources within microgrid.
- Overseeing power import and export of the microgrid.

Management of local resources is done through an assessment of available resources against the demand. This can be achieved through communication systems, as each nanogrid provides its status in terms of production and its own local demand. Through this channel, the nanogrid without production send a request for power import to the microgrid controller. The latter will in turn send a request for power sharing to activate nanogrid within the microgrid and supply the load. A continuous monitoring will ensure a halt of power supply in the event of load disconnection or in the case of not enough contribution vis a vis the demand.

In case there is not enough contribution from within the microgrid, or an increase of the demand beyond what is the norm, the controller will initiate the power import process. It consists of sending a request for power supply to other interconnected microgrids within the minigrid through ILVDC networks. Moreover, it prepares itself for power import by starting the converter into buck mode upon positive feedback from the nanogrid. Note that the microgrid is operating at 400 V_{DC} while the minigrid is at 3 kV_{DC}.

A continuous monitoring in conditions within the microgrid and outside for power import provides guides to connect or to disconnect load. The controller oversees power export

operations upon receiving a request from the minigrid controller for power support. The procedure is the same as with the request from within the microgrid with a slight difference in threshold value for power export. Figure 4.26 shows an algorithm flowchart for the microgrid controller.
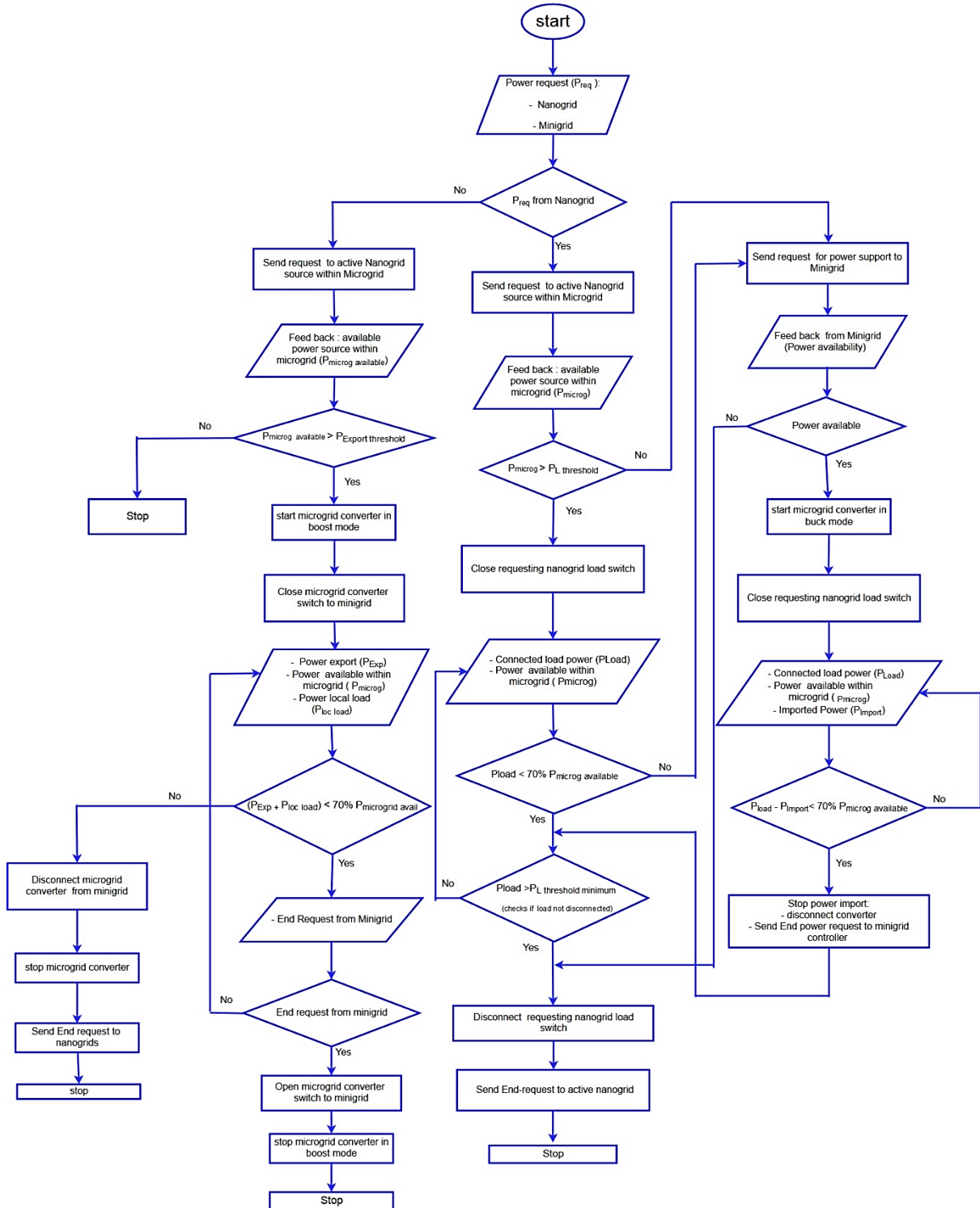
Figure 4. 26: Microgrid controller algorithm flowchart.

119

4.2.3 Minigrid development

Minigrid (<1 MW) is constructed upon the interconnection of various microgrids (< 100 kW), which its self is built upon a cluster of nanogrid (<1 kW). The minigrid operating at an intermediate low voltage DC and it serves two purposes:

1. Facilitating load shielding amongst interconnected microgrids.
2. Integrating sparse microgrids to the grid.

A. Voltage level selection

Microgrids to be interconnected, following dwelling type in African rural and per urban area, are generally 1-3 km apart. Hence, the use of intermediate low voltage direct current system operating at 3 kV under the guidance of IEC60038. The choice is made from a comparison of 1.5 kV, 3 kV and 6.6 kV voltage systems with emphasis on ACSR lines as well as the voltage drop in the lines. Referring to the datasheet in appendix 1, Table 4.7 shows conductors selection for above mentioned voltage levels. 1 MW is assumed to be the aggregated power from the microgrids interconnection and at least a line loading not exceeding 65% of conductor rating.

Table 4. 7: Conductor parameters for selected voltage levels.

Voltage level (kV)	Current (A)	Conductor current rating (A)	DC Ω /km
1.5	667	1123	0.0445
3	334	470	0.186
6.6	152	240	0.553

Figure 4.27 shows an estimation of voltage drops in ACSR lines for the three voltage levels. It is understood that the higher the voltage, the lesser the current flowing through the lines which in turn results in low voltage drop. 6.6 kV theoretically would have been one with the lowest voltage drop. However, as the conductor cross section area decreases to allow low current to flow, the resistance per kilometre increases accordingly.
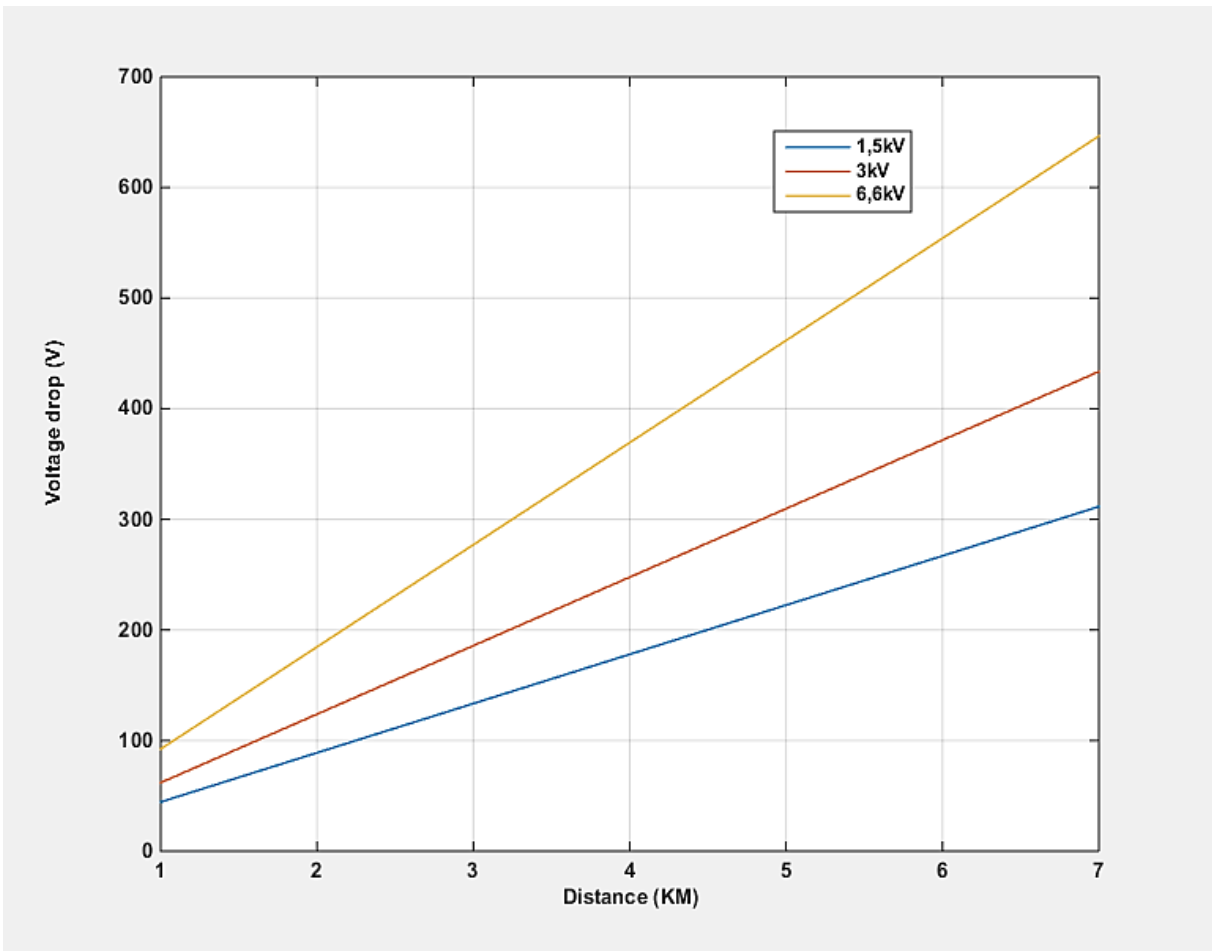
Figure 4. 27: Line voltage drop per distance comparison of selected voltage levels.

3 kV proved to be the right choice in this context, though a slight larger voltage drop compared to 1.5 kV, the mass per km of the latter would be heavier. Referring to the standard of ACSR in South Africa (appendix 1) from Aberdare, the conductor size for 3 kV will be lighter than for 1.5 kV for the same amount of power transferred. Thus, an optimal interconnection platform in terms of cost of installations versus losses. Therefore, 3 kV rated networks provide for interconnections of microgrids, allowing load sharing amongst them.

Moreover, 3 kV DC systems are currently in use in railways systems and are matured as technology as research continues to improve their safety and performance (Cinieri et al., 2007; Szeląg et al., 2015). Therefore, smooth adaptation of equipment and techniques used in railways system for minigrid development through microgrids interconnection is achievable.

B. Minigrid Converter

In addition to serving as a platform for microgrid interconnection, the 3 kV DC minigrid stands as the bridge in bottom-up grid extension based on swarm electrification concept with the nanogrid as a unit cell, in a coordinated framework as developed in Chapter 1 and Chapter 4 section 4.1.

A minigrid tied to the grid is accomplished through a bi-directional DC to AC converter. The latter provides a way for power input from the grid or power export towards the grid if needed for support. Figure 4.28 shows converter topologies as developed in the PSIM environment, operating in two modes, namely as a rectifier and inverter for power import and export respectively.
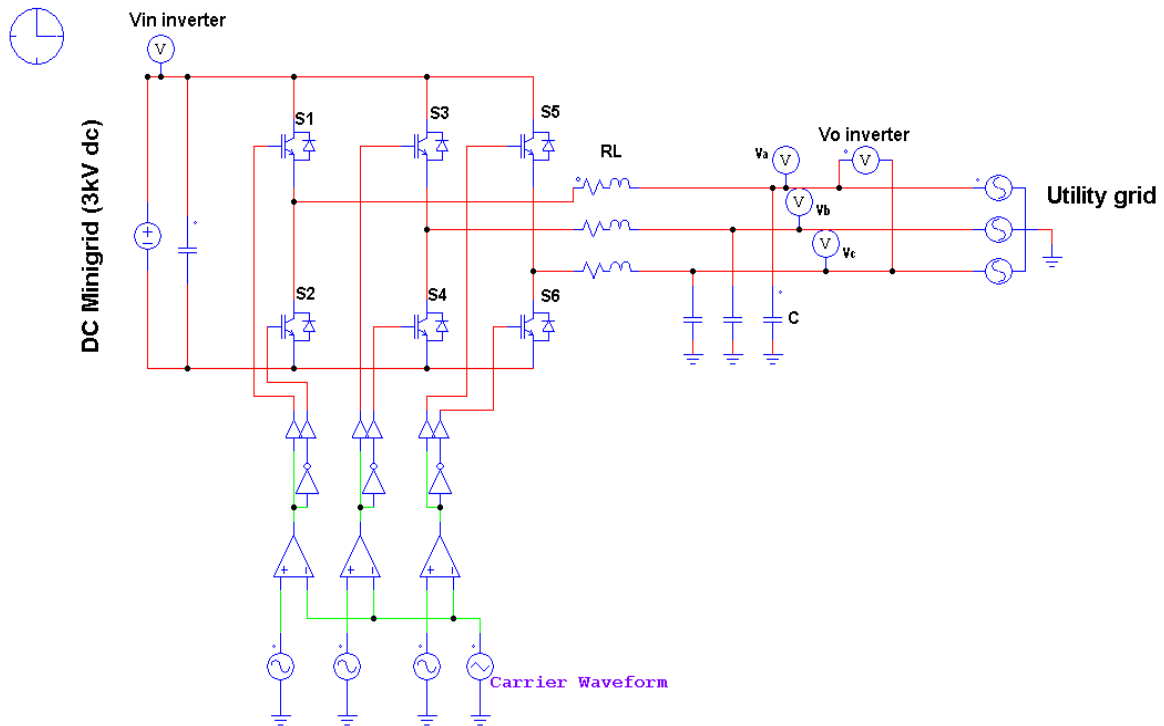
Figure 4. 28: Minigrid converter topology.

1. Inverter mode

During this mode the power is transferred from the minigrid to the primary distribution grid. The latter is considered to operate at 11 kV, therefore a transformer on the grid side is needed to step up the converter 3 kV output voltage to grid level or a buck boost on the minigrid side to level up the minigrid converter input voltage to the grid prior to conversion to AC. The last option would require a converter with high voltage rating switches, which would increase the cost of the converter. Therefore, in this work it is assumed that a transformer is interfaced between the converter and the grid to step up the former output voltage to the grid level 11 kV. Figure 4.29 shows the minigrid converter circuit operating in inverter mode; pulse width modulation control is used for switches control along with filters for smoothing out harmonics.
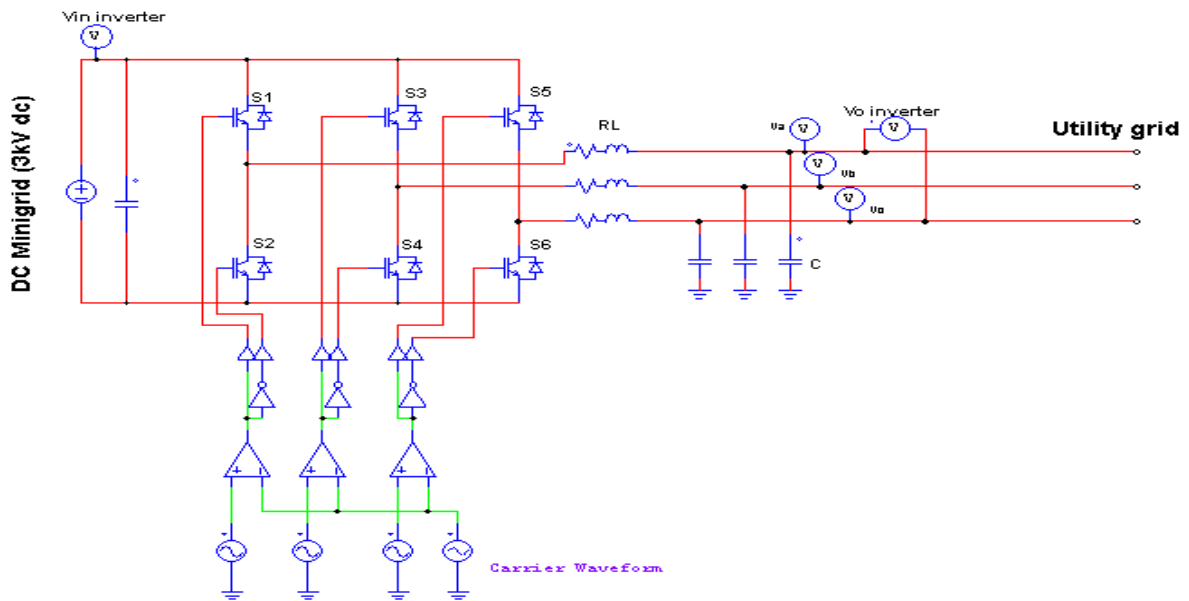
Figure 4. 29: Minigrid converter in inverter operation mode.

The model is simulated using parameters in Table 4.8 and results are shown in Figure 4.31 for inverter line-to-line output voltage, while Figure 4.32 shows three-phase output voltages injected in the utility grid. Figure 4.30 shows the converter input voltage, which is also the minigrid voltage of 3 kV. It is assumed that the 3 kV AC line-to-line voltage injected into the utility grid will be stepped up by a transformer to the level of grid primary distribution value.

Table 4. 8: Simulation parameters for minigrid converter in inverter operation mode.

Parameters	Value
Input voltage	3 kV dc
PWM Sinusoidal voltage source	1) 1.5 V, 50 HZ, 0º, 0 V , 0 sec 2) 1.5, 50 HZ , -120º ,0 V, 0 sec 3) 1.5, 50 HZ, -240º, 0 V , 0 sec
Carrier	2 V, 15 kHZ, 0.9, -1 V, 0 sec ,0º
IGBT	Ideal
3 R	2 Ω
3 L	1.5 mH
3 C	880 µF
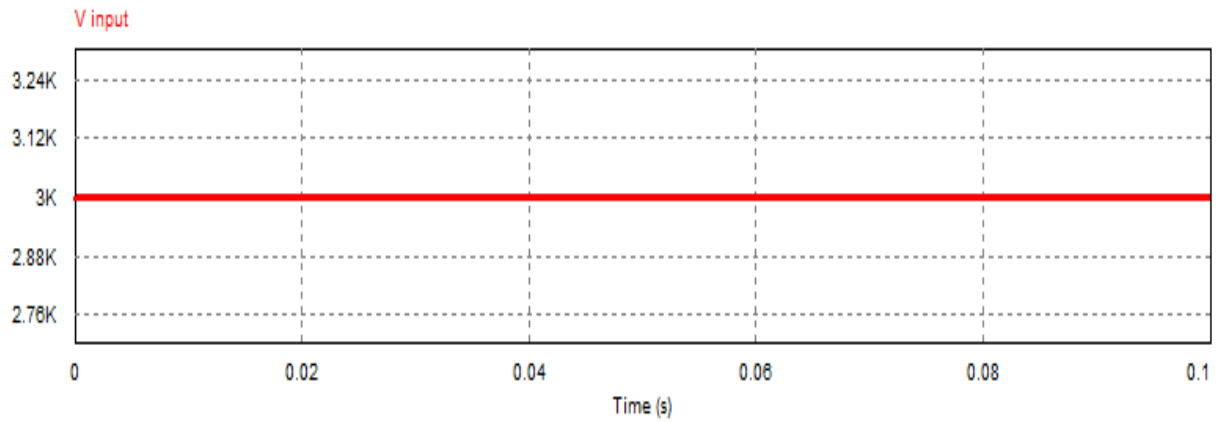
Figure 4. 30: Simulation result of minigrid converter in inverter operation mode, input voltage.
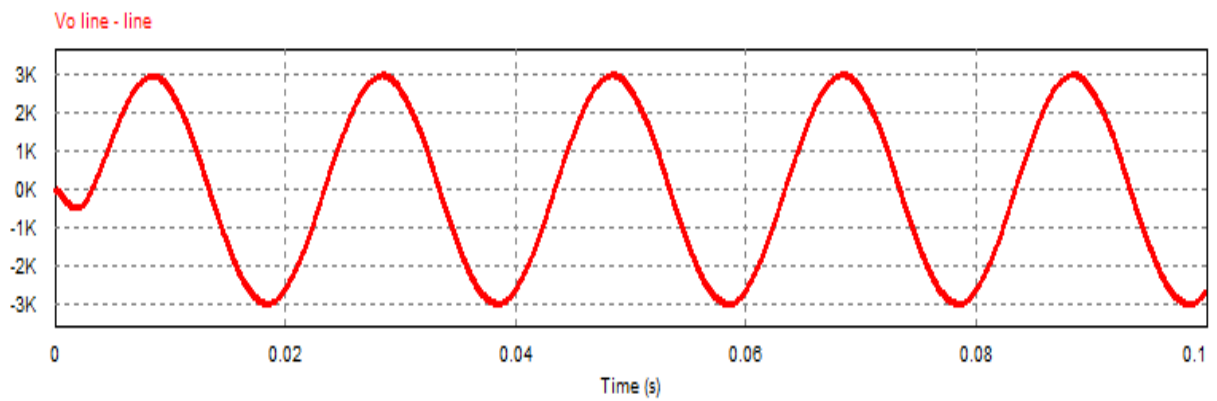
Figure 4. 31: Simulation result of minigrid converter in inverter operation mode, output line voltage.
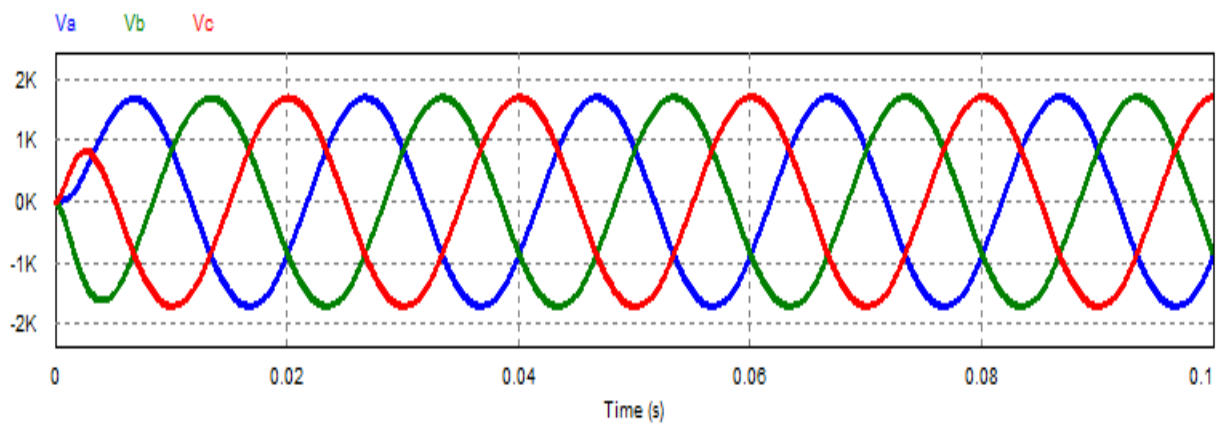
Figure 4. 32: Simulation result of minigrid converter in inverter operation mode, three phase output voltage.

124

2. Rectifier mode

In this mode of operation, the converter acts as an interface for power transfer from the utility primary distribution to the DC minigrid. Connected to the 3 kV AC utility grid, the converter will rectify the voltage to 3 kV DC and inject it into the minigrid. Figure 4.33 shows a model of the converter operating in rectifier mode as developed in PSIM. During rectification, operation switches are switched off and only their freewheeling diodes perform the task. LC filters are introduced for smoothing purposes on the DC side. Simulations are using parameters in Table 4.9 and results are shown in Figure 4.34 and Figure 4.35. The latter, being the rectifier output DC voltage while the former is the peak-to-peak input voltage.
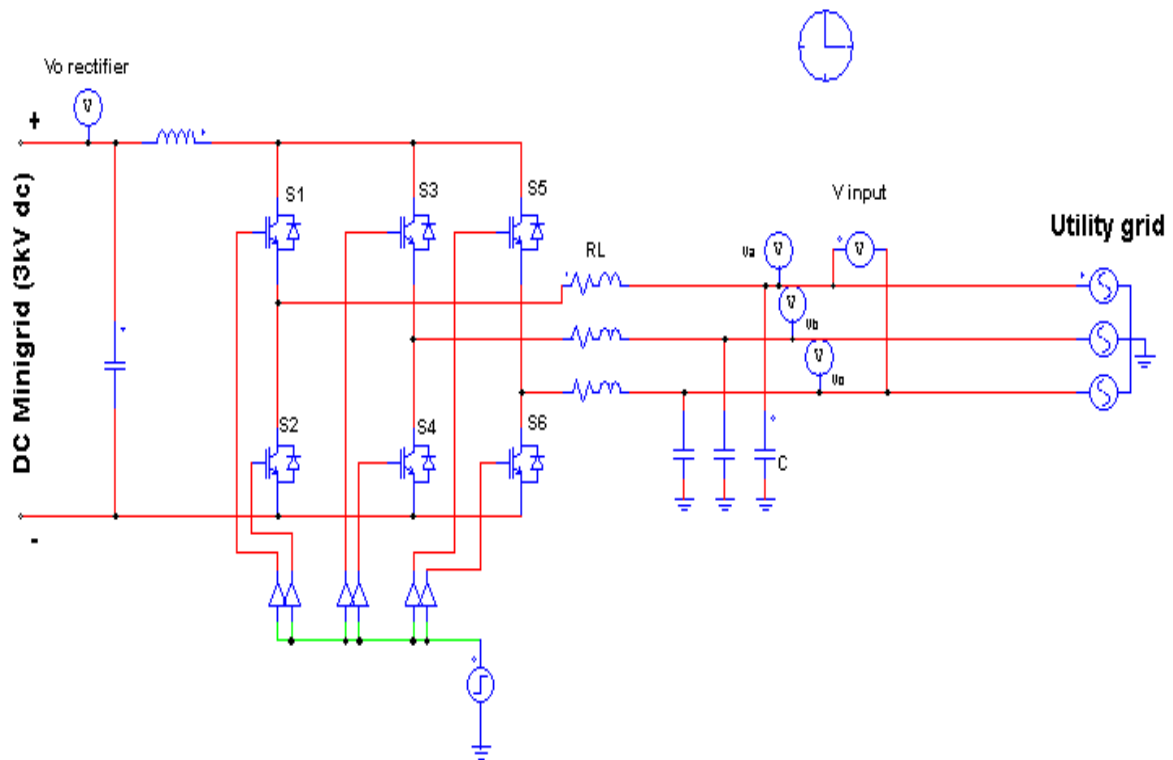
Figure 4. 33: Minigrid converter in rectifier operation mode.

Table 4. 9: Minigrid converter in rectifier operation mode simulation parameters.

Parameters	Value
Input voltage (rms): 1.4 * Vpeak	3 kV AC, 50 Hz , 3 phase
DC Filter	1) L = 1.5 mH 2) C = 880 µF
IGBT	Off
Simulation time	0.1 s
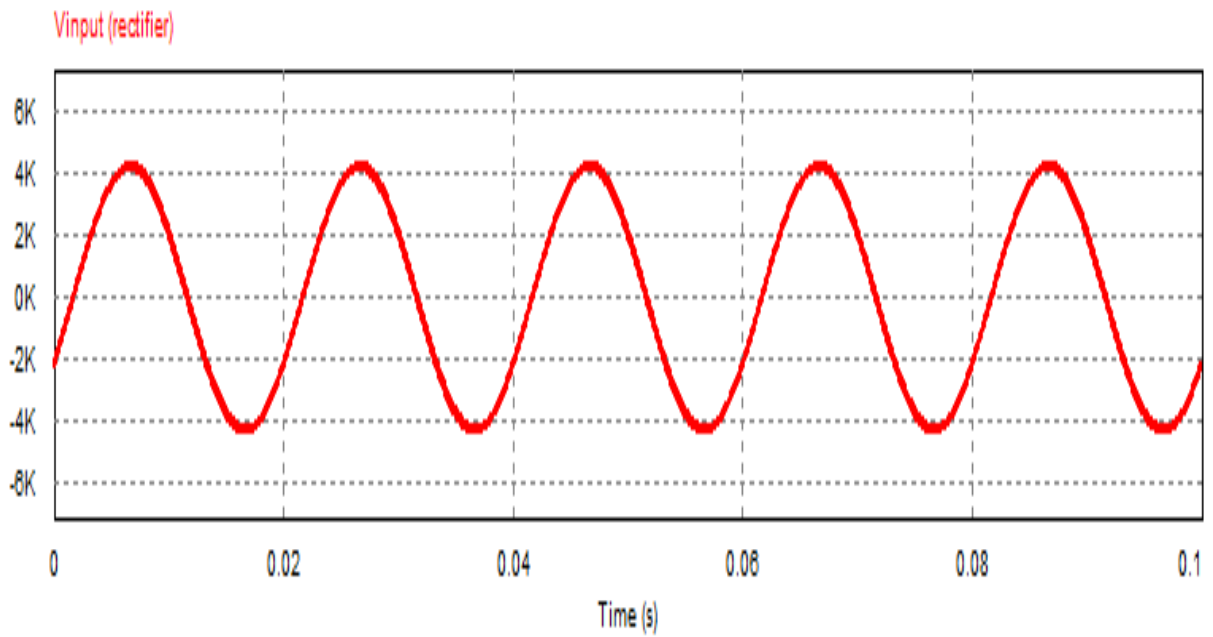
Figure 4. 34: Minigrid converter in rectifier operation mode peak input voltage.
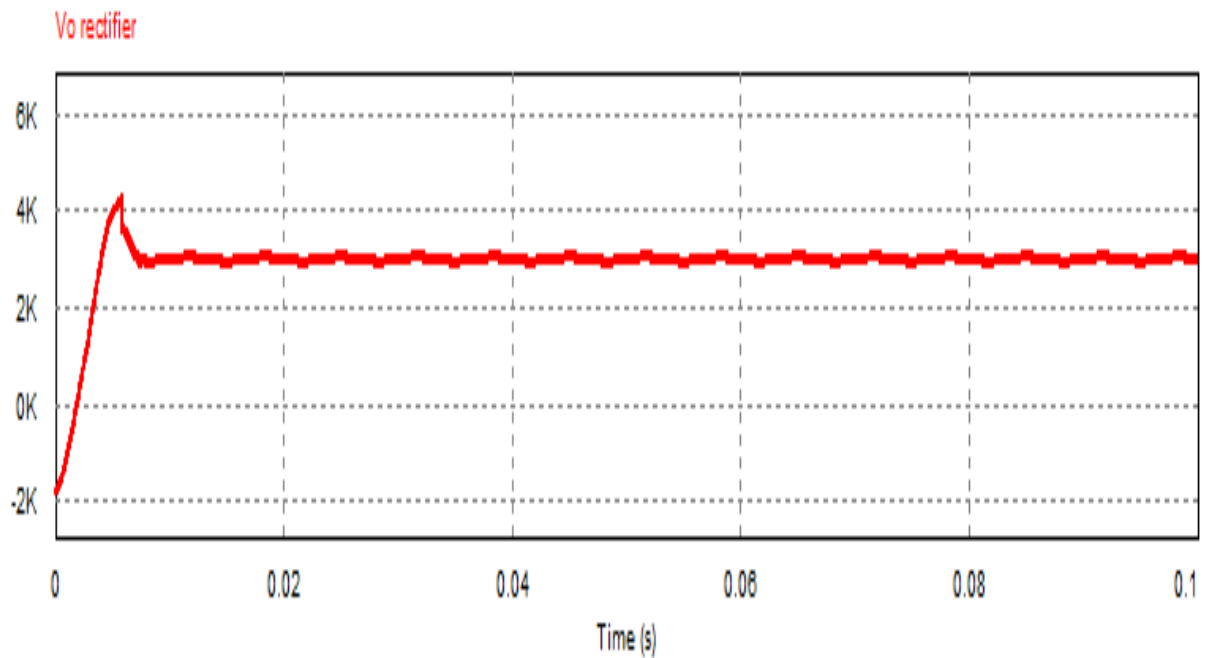
Figure 4. 35: Simulation results of minigrid converter in rectifier operation mode, DC output voltage.

126

C. Minigrid control

The control of the minigrid is part of a large decentralized control built up on nanogrid and microgrid controls. This means that the minigrid controller relies on both nanogrid and microgrid controllers to oversee or reach individual power sources and loads sparsely connected in its geographic network.

The minigrid is expected to exchange power with the utility grid. In reality, it is a link between microgrids themselves and the utility grid. Microgrids themselves are links between nanogrids, simply put, a link between all neighbouring single loads and all single power generator, as well as with the utility grid.

The power exchange between the grid and minigrid is done on request. If one microgrid is having imbalance between its own demand and the supply, it sends the request for assistance to the minigrid controller as discussed previously in section 4.2.2. Therefore, this involves communication systems at all levels of the network. A communication system is proposed as well in section 4.5. of this chapter.

Figure 4.36 shows the minigrid control algorithm flowchart. It describes all the steps and decision-making involved. First, the controller checks for any power request (P_{req}) either from the microgrids or the utility grid and two scenarios will unfold:

-In case the power request comes from the microgrid, the controller will forward the request to the active microgrids to check the availability to respond to the request depending on their own actual status. The feedback from those microgrids provides the total power they might provide without compromising their own load. From the feedback by microgrids, if available power (P_{micro_avail}) is above a certain threshold, a positive feedback is sent to the requesting microgrid and the command is sent to close its switches to the minigrid. Continuous measurements are taken for the total amount of power exported to the microgrid (P_{Exp_micro}) and the available power from microgrids (P_{micro_avail}). A certain minimum power threshold (P_{Exp_min}) is set for power exportation to the microgrid for safety reasons to avoid a situation where the requesting microgrid does no longer need the support from other microgrids but failed to send a cancelling request to notify the minigrid controller. Thus, if the power exported to a requesting microgrid (P_{Exp_micro}) is less than the minimum required (P_{Exp_min}) then the process is interrupted, and an end request is sent to all contributing microgrids to stop their contributions. Otherwise, the power from microgrids (P_{micro_avail}) is also monitored against the maximum threshold ($P_{threshold}$) which means the minimum reserve of power to avoid the overloading of microgrid generators and disturb supply/demand balance within the microgrid. Therefore, if power available from microgrids (P_{micro_avail}) is still greater than the minimum reserve threshold ($P_{threshold}$), then a final check for any end-request from the microgrid is performed and in case there is, an end export

request is sent to active microgrids. Otherwise, the sequence repeats itself from the 2nd feedback stage.

The minigrid controller will request support from the grid in case the power support from other microgrids (P_{micro_avail}) is less than the minimum power threshold. This happens either after the 1st or the 2nd feedback from active microgrids. After the controller decision to request support from the utility grid, the first step is to check grid power availability ($P_{Utility\_grid\ avail}$) by measurement. In case there is no power available, then a request-decline feedback is sent to the requesting microgrid and the import process will not proceed. On the other hand, if there is power on the grid, a positive feedback is sent to the requesting microgrid. The minigrid converter is then started in the rectifier operational mode followed by the closing of the switch to utility to allow power flow from the utility grid to the minigrid.

There is a continuous monitoring of the availability of grid power ($P_{Utility\_grid\ avail}$) along with the check for any end-request from the microgrid. If the power from the grid still available and there is no request from the microgrid to end power importation from the grid, then the controller will continue to monitor the feedback for any change in conditions. On the other hand, in case the power from the grid is not available, then the converter is stopped and disconnected from the minigrid. Afterwards, a decline-request is sent to the importing microgrid and the controller stops. So far, power import is discussed, either from other microgrids or the utility grid.

In case the request for power support comes from the grid, the controller forwards the request to active microgrids and from the feedback of the latter, total available power capacity (P_{micro_avail}) is assessed against a minimum power threshold ($P_{threshold\_gridexp}$) required for the export to take place. If the available microgrids power capacity (P_{micro_avail}) is less than the threshold ($P_{Utility\_grid\ avail}$), then the export is impossible to proceed. Therefore, a request to decline is sent to the grid controller by the minigrid controller which results in the latter stopping.

On the other hand, if the available power capacity from the microgrids (P_{micro_avail}) is greater than the threshold for power exportation ($P_{threshold\_gridexp}$); then minigrid converter is activated to operate in rectifier mode and the circuit breaker to the grid is closed. Thus, allowing power injection into the grid. A continuous monitoring of microgrids available power capacity (P_{micro_avail}) and of power exported (P_{Export}) proceeds. In case the power capacity from microgrids (P_{micro_avail}) goes below a certain power export threshold ($P_{threshold\_gridexp}$), then the process to halt power export starts. Otherwise, the total power exported (P_{Export}) is compared to the minimum power export threshold ($P_{Exportminimum\_gridexp}$), that is set to check if the utility demand still needs the support from the minigrid. If (P_{Export}) is less than ($P_{threshold\_gridexp}$), then the power export halt process starts. Otherwise, the monitoring of the feedback continues.

The halt process consists of stopping the converter, operating in inverter mode, and the sending of an end export request to all active microgrids followed by a disconnection of the minigrid from the grid. However, this is slightly different from the halt process at the first feedback where only a decline request is sent to the grid controller. Afterwards, the minigrid controller, as no further steps have been taken, just goes straight to stop.
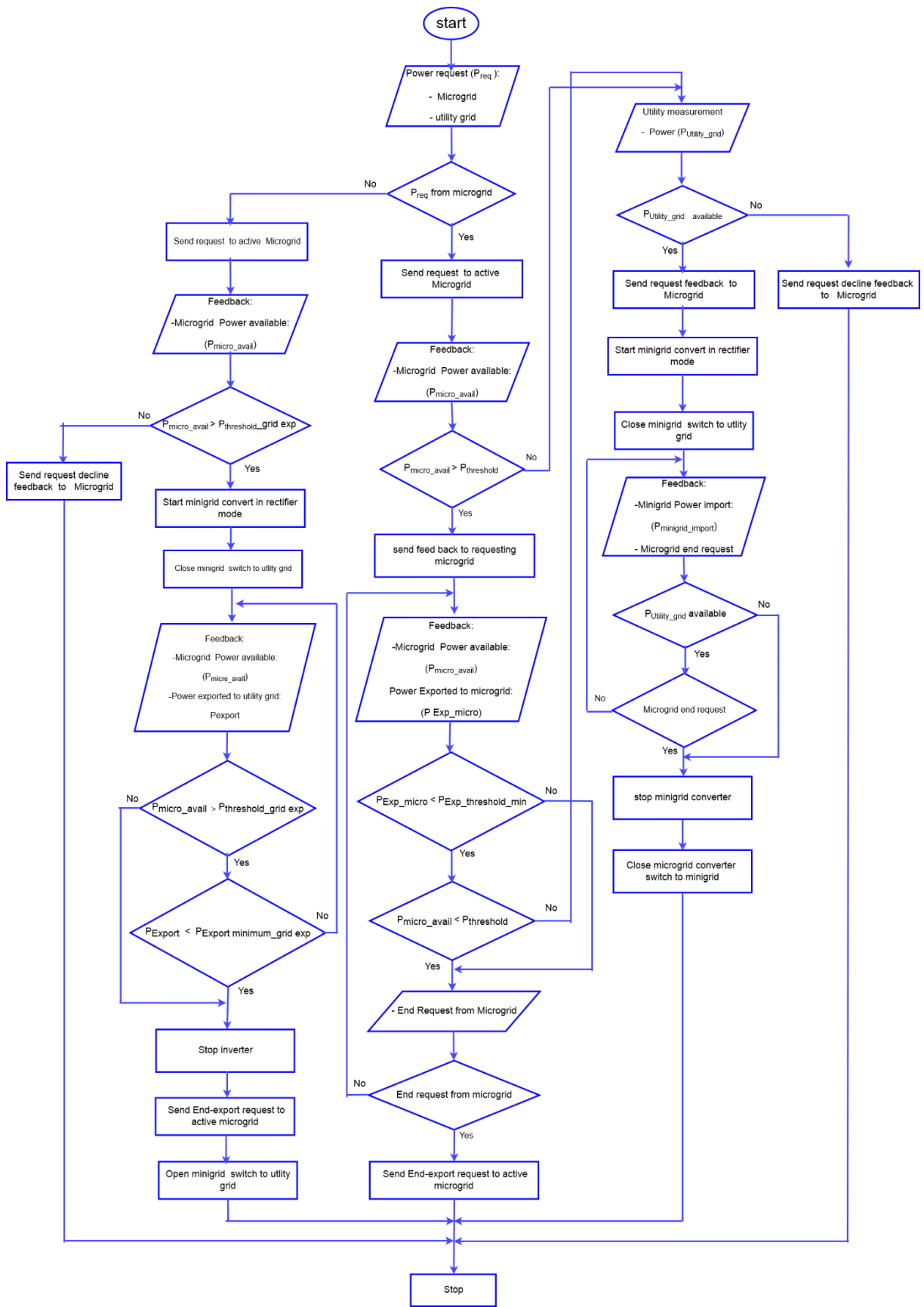
Figure 4. 36 :Minigrid controller algorithm flowchart.

4.3 Communication system for ILVDC distribution network for sparse electrified areas interconnection

4.3.1 Proposed system topology

Communication has a central role in the modern power system, from the control point of view, to protection and demand side management. For an intermediate low voltage direct current network, the communication system serves as a link between converters for control purposes at all levels from nanogrid to grid integration of the minigrid as put out in section 4.2. The interconnection of nanogrids, basic units for bottom up integration considered for this research, rely on communication system for power exchange.

Figure 4.37 shows the proposed communication system and topology: a packet-switched communication system transposed upon the intermediate low voltage direct current network. It uses the power line as a communication channel. Packet-switched systems are modern communication systems and have proven to be effective in data transfer as explained in Chapter 2 section 2.6. Power line communication is a proven matured technique in use and seem to be an economic method for wired data transfer.

As shown on Figure 4.37 communication networks are extended up to the nanogrid, which might open the opportunity for other applications such as IP telephony and cable TV, in addition to control, protection and metering. This is mostly a pathway to the internet of things and improved accuracy in energy management.

The extension of the communication networks to nanogrid level requires a safe and efficient power line communication coupling system. Therefore, a coupling system for the DC nanogrid is proposed in section 4.5.2
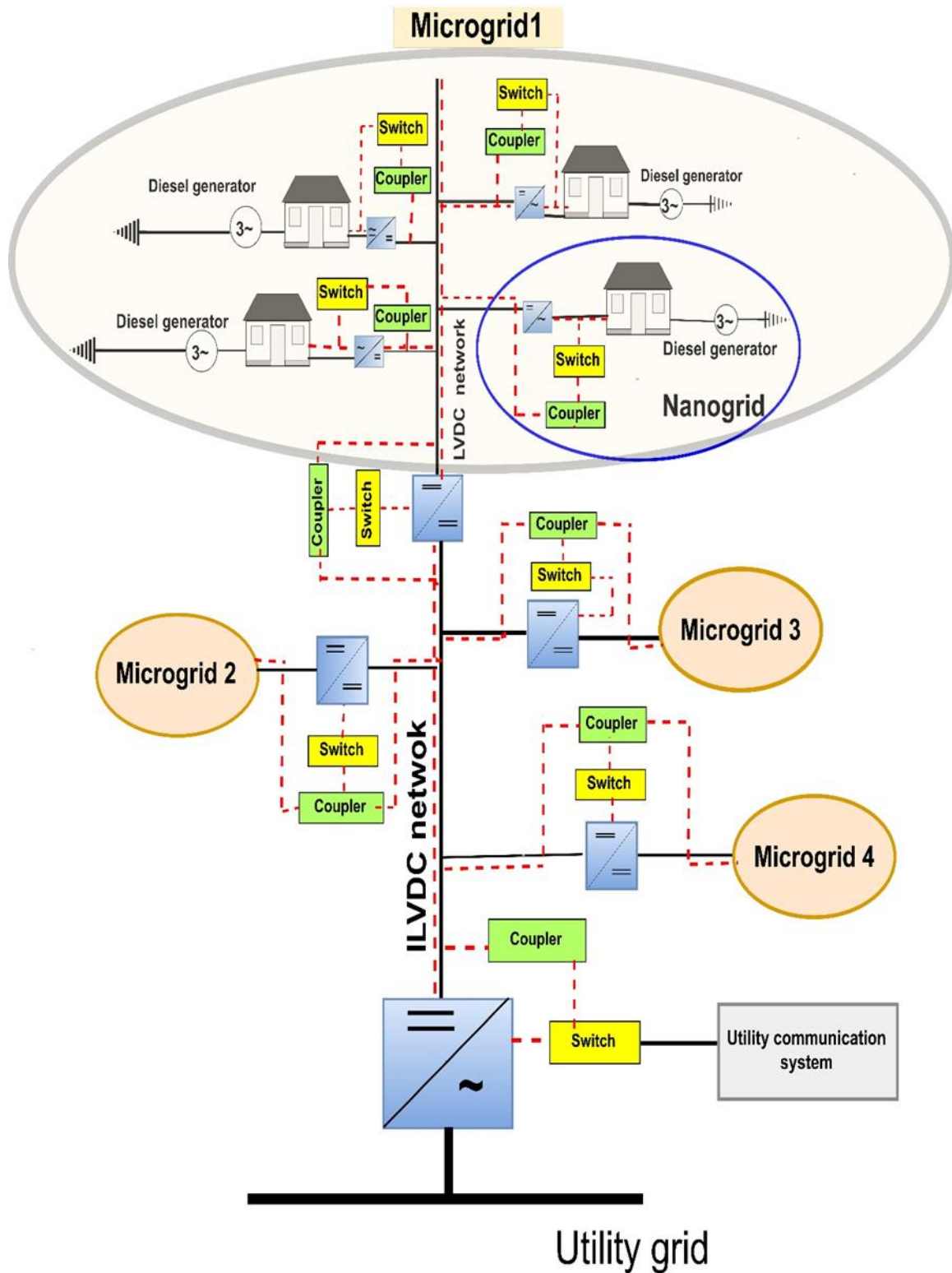
Figure 4. 37: Power line communication over ILVDC network topology

With the above proposed communication system and topology, an efficient link between the utility grid and nanogrid is established. Signal repeaters can be added on top of each microgrid switch to increase the communication signal strength as well as for data correction. Note that converters used have bi-directional communication capability, for instructions/status reception

and transmission. Moreover, each converter, coupler, and in turn nanogrid are IP identified through their respective switches. However, IP allocation and more advanced computer networking implementation are not discussed in this research.

4.3.2 Power line communication couplers for ILVDC networks

A. Introduction

Couplers play a primordial role in communication signal transmission over power line. They are used for communication signals injection or extraction into and from power lines. Various coupling methods are used on all levels of the power system and are discussed in Chapter 2, section 2.6.

Amongst the qualities sought for in a power line communication coupler is efficiency and safety. Efficiency is looked at in terms of maximum power transfer of communication signal at transmission and reception end. This means maximizing on lower insertion and return losses. While in terms of safety, a power line communication coupler must provide a complete galvanic isolation. It isolates undesirable currents to flow to transceiver circuit by blocking power line voltage to cross and only allowing through communication signals. This not only protects communication devices but also users from short circuits and electrocution.

B. Proposed power line communication coupler design

A power line communication system proposed for intermediate low voltage direct current comprises of couplers from the minigrid to nanogrid level. The latter level, also referred to as the last mile, being in the end-user's environment, requires more safety than for other levels. Available power line communication couplers on the market offer a certain degree of galvanic isolation against surges and short circuits to transceiver and users based on surge arrestor and transformer saturation for transformer coupled circuit. However, any short circuit within the transformer itself or surge failure would result in a damaged transceiver and eventually harmful DC voltage flowing to users.

Therefore, in this research we propose a broad band opto-capacitive power line coupler for DC nanogrid that would provide a complete galvanic isolation between end user transceiver and the power line. Broad band was selected as operational frequency range to provide a room for advanced metering and control as well as further applications such as telephony and cable TV services.

The proposed coupling method is shown in Figure 4.38, an opto-capacitive coupling. It consists of transmitting circuit injecting communication signal into the power line through a capacitive coupling and a reception side coupled to power line through a capacitor and an opto-coupler. A filtering stage in series with a buffer process the signal before sending it to opto-coupler

which provides a complete electrical isolation between the power line and the transceiver, as the received signal is replicated to the digital transceiver side without any actual electrical connection.
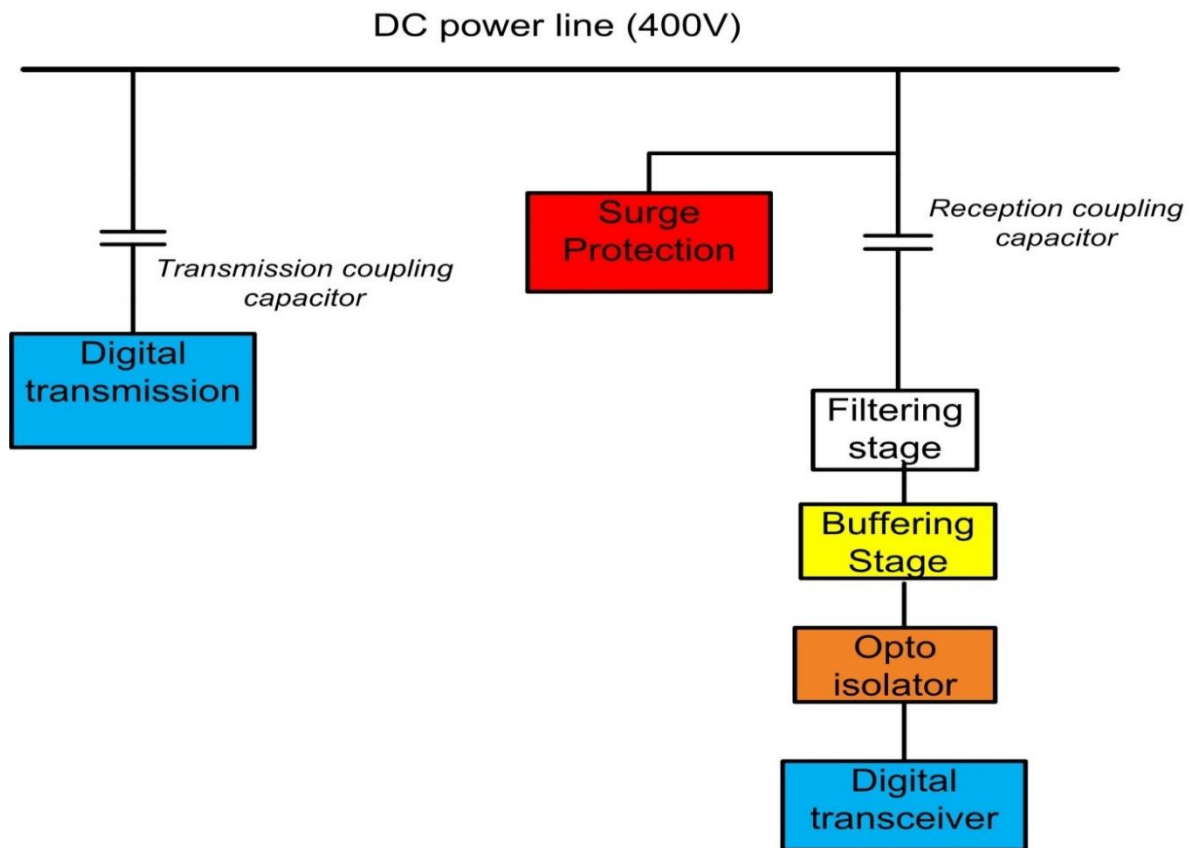
Figure 4. 38: Opto-capacitive coupler for PLC signal reception over a DC power line concept.

As mentioned above, the proposed coupler for power line communication signal reception consists of many stages:

- *Coupling capacitor*: the primary role of the mentioned capacitor is to block DC line voltage while allowing only communication signal currents to flow towards the filters. This communication signal is an amplitude modulated signal.

- *Filtering stage*: at this stage the received signal is a mix of carrier signals and communication signals needed for processing. The carrier is removed, and the remaining communication is forwarded to the buffer stage for further processing.

- *Buffer stage*: this stage links the filter stage to the opto-isolator/coupler. The filtered digital signal still has some noise that may cause errors in signal reading or processing by the transceiver. Therefore, the buffer defines the patterns of the signal by differentiating the noise from the real signal.

- *Opto-isolator stage*: Here, the digital communication signal received is recovered but there is an electrical connection from the line up to the opto-coupler. Applying the working principle of the latter, the input digital communication signal is reproduced into the optic-coupled circuit. Therefore, there is no direct electrical connection with the DC power line. An independent voltage source is used for communication signal duplication in the secondary circuit of the optical coupler.

In the event of a surge arrest failure or capacitor short circuit, the power line voltage can only cause damage up to the optical coupler, without affecting the transceiver or the users.

As the communication involved in intermediate low voltage direct current network developed in this research is a two-way communication, it is worth mentioning that the proposed method of coupling is also applicable for transmission with little modification but the same objective. Figure 4.39 shows an opto-capacitive coupler system for communication signal transmission over a DC power line.

Similar to the concept of an opto-capacitive coupler for PLC signal receiver shown Figure 4.38, an opto-coupler system for communication signal transmission over a DC power line consists of an opto-coupler, a surge arrestor, and coupling capacitor. These components serve the same role as for the signal reception. The signal to be transmitted is received from the source and is converted, in case it was not previously, into a digital signal. The latter is fed into an opto-coupler which replicates the signal on its output thus isolating electrically signal source to the rest of the process stages.

- *Signal source*: it might be an intelligent meter, intelligent electronic device in the network, converter with communication capability, telephony equipment, and internet switch/router. All the equipment connected to the network with communication capability are in accordance with IEEE 61850 standards.

- *Digital signal*: communication signals sent by the signal source in analogue form have to be converted to digital form in order to be sent to the opto-coupler.

- *Modulation*: telecommunication modulation consists in mixing a communication signal with a high frequency signal (carrier) to allow the transmission of the former over a channel with optimum power. Note that for this research amplitude modulation is considered.

-*Carrier*: a high frequency signal mostly sine wave, used for modulation for transmission of a communication signal.
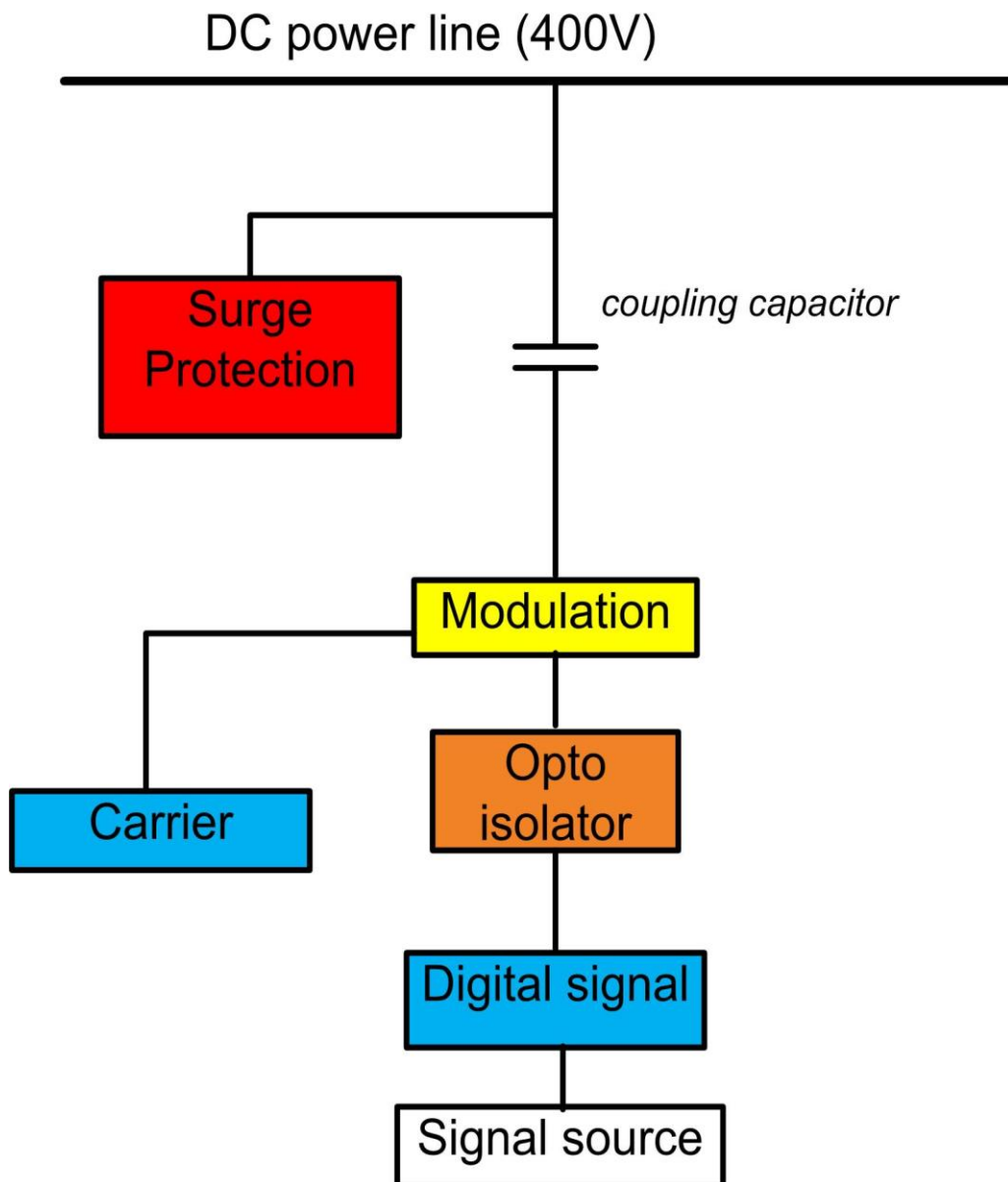
Figure 4. 39: Opto-capacitive coupler for PLC signal transmission over a DC power line concept.

C. Opto-capacitive coupler design

The coupler for PLC signal reception concept, proposed in the previous section, is modelled for physical or practical circuit design as shown in Figure 4.40. It consists of a transmission side, 400 V_{DC} line, coupling capacitor, band pass filter, op-amp as a buffer to the opto-isolator, and the opto-isolator. Amplitude Shift Keying (ASK) modulation technique is used for transmission. ASK is a digital modulation technique that consists in modulating the carrier with a digital communication signal to be transmitted. The carrier $f_C(t)$, a high frequency signal usually sine wave defined by Equation 4.17,is multiplied by the digital communication signal $f_D(t)$. The resultant modulated signal,$f_M(t)$, described by Equation 4.18 is transmitted over the selected medium, which is in the present case a power line. ASK modulation technique is

simple and transmitter requires less bandwidth in comparison with other digital modulation techniques.
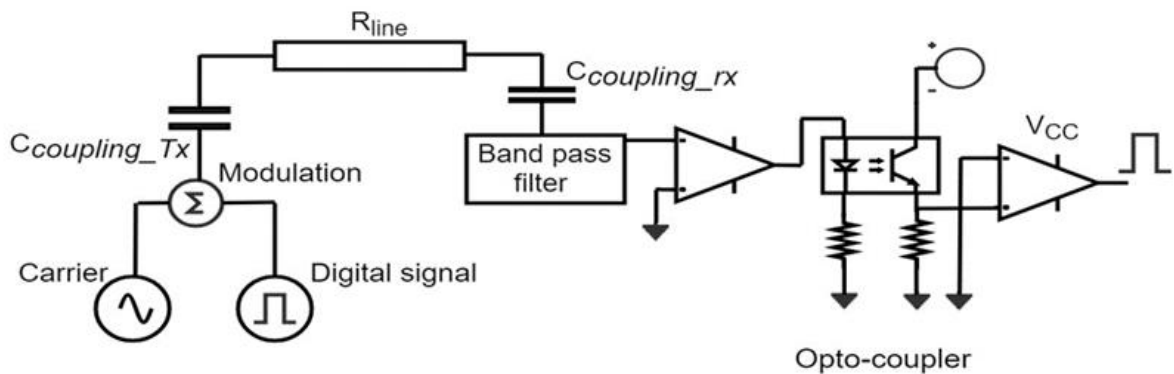
Figure 4. 40: Opto-capacitive coupling circuit diagram.

$$f_c = A_c \sin(2\pi f + \theta) \qquad\qquad\qquad\qquad \text{Equation 4.17}$$

$$f_M = f_D(t) \times A_c \sin(2\pi f + \theta) \qquad\qquad\qquad \text{Equation 4.18}$$

where,

A_c = amplitude of the carrier

f = Carrier frequency

θ = Carrier phase delay

The digital signal is emulated using a square voltage source. Figure 4.41 shows the square voltage signal parameters used for simulations such as peak-to-peak voltage amplitude (V_{pp}), duty circle (D), starting time, frequency, DC of set and phase delay. The digital signal parameters settings are shown in Table 4.10.
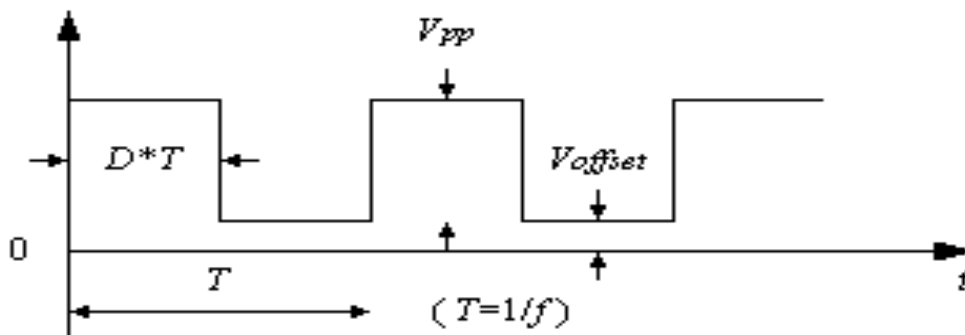
Figure 4. 41: Digital signal.

137

Table 4. 10: Digital signal parameters settings.

Parameter	Value	Units
Peak to peak voltage (Vpp)	10	V
Frequency (F)	2	MHz
Duty circle (D)	0.5	-
Phase delay	0	Degree
Start time	0	Sec
DC offset	0	V

The carrier signal (V_O) is provided by sinusoidal voltage source defined by Equation 4.19 and whose parameters are shown in Table 4.11.

$$V_O = V_m \times \sin(2\pi f t + \theta \times \frac{\pi}{180}) + V_{offset} \qquad \text{Equation 4.19}$$

Where,

V_m = Peak amplitude

f = Frequency$f$, in Hz

θ = Initial phase angle

t = Starting time, in sec. Before this time, the source is zero

V_{offset} = DC voltage offset

Table 4. 11: Carrier signal parameter settings.

Parameter	Value	Units
Peak amplitude (V_m)	10	V
Frequency (F)	30	MHz
Initial phase angle (θ)	0	Degree
Start time	0	Sec
DC offset	10	V

Coupling capacitors (C) are calculated based on the modulated signal frequency (f_0) using capacitor resonance Equation 4.20 for maximum power transfer of the modulated signal.

$$f_0 = \frac{1}{2\pi \times C \times R_{Line}}$$
<div align="right">Equation 4.20</div>

Where,

f_0= Resonance frequency (carrier frequency)

C = Coupling capacitor capacitance in Farad

R_{Line} = Line/channel impedance in ohms

Characterization and modelling of the Line impedance is calculated based on the assumption that the power line distance from the transmission point to the reception point is 2 km. A SANS1507/6 aerial service connection cable is considered for its insulated conductor type which decreases hazards in the event of fall or other high impedance faults. Technical information of this cable is shown in appendix 1.

Using a 20 mm² cable, with a phase conductor impedance of 2.34 Ω/km and resistance of 1. 9 Ω/km; the line is modelled using the transmission line equivalent circuit model shown in Fig.4. The model describes a power line long from point a to b, with respective instantaneous voltage and current represented by $v(a,t), v(b,t), i(a,t)$ and $i(b,t)$. Line per unit length resistance (Ω/m), inductance (H/m), capacitance (C/m) and conductance (Ω^{-1}/m) are represented by R, L, C and G respectively. The effect of those line parameters onto the signal propagation can be evaluated using Equation 4.21 of the transmission line in high frequency
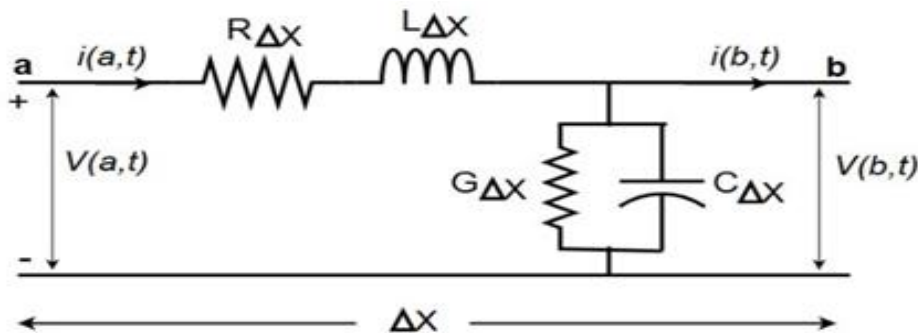
Figure 4. 42: Transmission line model

$$\begin{cases} -\frac{v(b,t)-v(a,t)}{\Delta x} = Ri(a,t) + L\frac{\partial i}{\partial t} \\ -\frac{i(b,t)-v(a,t)}{\Delta x} = Gv(a,t) + C\frac{\partial v}{\partial t} \end{cases}$$
<div align="right">Equation 4.21</div>

Considering $v(a,t) = Re[V(a,t)]$ and $i(a,t) = Re[I(a,t)]$ then Equation (4.21) can be written as follows:

$$-\frac{dV}{da} = (R + j\omega L)I(a)$$
$$-\frac{dI}{da} = (G + j\omega C)V(a)$$

Equation 4.22

$$\begin{cases} \frac{d^2V(a)}{da^2} = (R + j\omega L)(G + j\omega C)V(a) = \gamma^2 V(a) \\ \frac{d^2I(a)}{da^2} = (R + j\omega L)(G + j\omega C)I(a) = \gamma^2 I(a) \end{cases}$$

Equation 4.23

Where γ is the propagation coefficient which is given by Equation (4.24):

$$\gamma = \sqrt{(R + j\omega L)(G + j\omega C)} = \alpha + j\beta$$

Equation 4.24

With α the attenuation and β the coefficient, therefore the line impedance is given by Equation (4.26) knowing that

$$V_0 = V_0^+ e^{-\gamma a} + V_0^- e^{\gamma a} \text{ and } I_0 = I_0^+ e^{-\gamma a} + I_0^- e^{\gamma a}$$

Equation 4.25

Then characteristic impedance of the line Z_l in the range of interest (1.7- 30MHz) is calculated using Equation (4.26):

$$Z_l = \frac{V_0}{I_0} = \sqrt{\frac{(R + j\omega L)}{(G + j\omega C)}}$$

Equation 4.26

Where per unit parameters can be calculated as follows (Mulangu et al., 2012):

$$R = \frac{1}{\pi r}\sqrt{\frac{\pi f \mu}{\sigma}}$$

Equation 4.27

$$L = \frac{\mu}{\pi}cosh^{-1}\left(\frac{D}{2r}\right)$$

Equation 4.28

$$G = \frac{\pi\sigma}{cosh^{-1}\left(\frac{D}{2r}\right)}$$

Equation 4.29

$$C = \frac{\pi\varepsilon}{cosh^{-1}\left(\frac{D}{2r}\right)}$$

Equation 4.30

With μ the magnetic permeability = $4\pi \times 10^{-7}$ H/m, f the frequency = 30 MHz, σ the conductivity of line material, r the radius of the conductor and D the clearance between the line= 600mm, the impedance of a 2000m long line can be calculated using Equation 4.26. If a

20 mm² aluminium conductor is considered, σ =3.77 x 10⁷ /Ωm, ρ = 2.8264x10⁻² Ωmm²/m, permittivity ε = 8.85 x 10⁻¹² F/m and r = 2.5mm, then the line impedance Z_l is equal to 657.5 Ω. Note that the conductance G is assumed to be zero , due to the fact that an overhead line is considered and the fact that the free space is the separation between the lines (Anatory et al., 2007). Table 4.12 shows the parameters values for both signals as well as for the line impedance Z_{Line}

Table 4. 12: Transmission circuit parameters

Parameters	Carrier	Digital signal
Frequency (MHz)	30	2
Amplitude (V)	4	2.5
Phase delay (degree)	0	0
Line impedance (Ω)	657.5	

Asynchronous ASK demodulation technique is used for digital signal extraction. In series with the coupling capacitor, the ASK demodulator consists of a rectifier coupled to a second order band pass filter. The coupling capacitor is sized to provide least reactance at the resonance frequency which corresponds to the carrier frequency (f_C) of 30 MHz. Moreover, the coupling capacitor reactance is matched with the line impedance to have a minimum reflection of the communication signal. Therefore, the coupling capacitor value is calculated using the Equation (4.31):

$$f_0 = \frac{1}{2\pi \times C \times Z_{Line}}$$
<div align="right">Equation 4.31</div>

Where:

f_0 = resonance frequency (carrier frequency)

C = Coupling capacitor capacitance in Farad

Z_{Line} = Line impedance in ohms

$$C = \frac{1}{2\pi \times f_0 \times Z_{Line}}$$

$$= 8.1\ pF$$

The signal from the coupling capacitor is processed by a rectifier and a band pass filter for communication signal extraction. Passive 1ˢᵗ order low pass and high pass filters associated

in series are used for the implementation of a passive band pass filter with a transfer function $F(j\omega)$ as shown in Figure 43a. The frequency response of the band pass filter is given by the product of both filters' frequency responses and the loading, as per Equation (4.32).

a) Band pass filter transfer function

b) Band pass filter circuit diagram
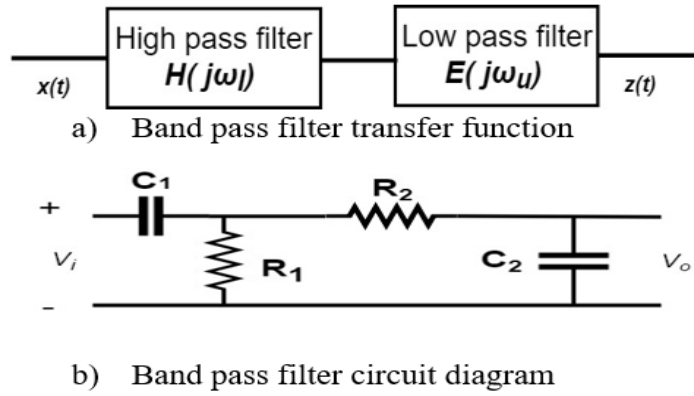
Figure 4. 43: Band pass filter.

$$F(\omega) = H(j\omega_l)\, G(j\omega_u)\, L(j\omega_0)$$ Equation 4.32

Assuming that the loading $L(\omega_0)$ is approximately equal to 1, then Equation (4.32) becomes:

$$F(\omega) = H(j\omega_l)\, G(j\omega_u)$$ Equation 4.33

Using RC filter shown in Figure 4.43b, then:

$$H(\omega) = \frac{R_1 C_1 j\omega_l}{1 + R_1 C_1 j\omega_l}$$ Equation 4.34

$$G(\omega) = \frac{R_2 C_2 j\omega_u}{1 + R_2 C_2 j\omega_u}$$ Equation 4.35

where

$\omega_l = 2\pi f_l$, f_l = lower cutting frequency

$\omega_u = 2\pi f_U$, f_u = upper cutting frequency   Equation 4.36

$$f_0 = \sqrt{f_l \, f_u} \quad , \quad f_0 = \text{fundamental frequency}$$

The frequency of the communication signal, 2 MHz, is taken as filter fundamental frequency f_0. Thus from Equation (4.20), lower and upper cutting off frequencies are 1.9 and 2.1 MHz respectively. Using Equation. (4.31) and considering the coupling capacitor as C_1 and R_2 as 28 Ω, knowing that:

$$f_l = \frac{1}{2\pi R_1 C_1} \quad \text{and} \quad f_u = \frac{1}{2\pi R_2 C_2} \qquad\qquad \text{Equation (4.37)}$$

Then, from Equation (4.31), the filter parameters are calculated as

$$R_1 = 10.34 \, k\Omega \; ; \quad R_2 = 28 \, \Omega \; ; \qquad C_2 = 2.7nF$$

D. Opto-capacitive coupler model validation

For validation of the opto-capacitive power line communication coupler proposed in the previous section, in Figure 4.40, a model is developed and simulated in the PowerSim (PSIM) environment. A simulation algorithm based on nodal analysis and trapezoidal rule for numerical analysis is used. PSIM Professional Version 9.0.3.400 is the version used for developing the opto-capacitive coupler for the power line communication circuit model in Figure 4.43.

Simulations are performed for a period of 2 µs using 0.5 ns as a time step and digital signal of 2 MHz and 2.5 V amplitude as the communication signal. The latter modulates a carrier signal of 30 MHz, 4 V. and the modulated signal is transmitted over the power line represented by a 657.5 Ω resistance through an 8.1 pF coupling capacitor. The set up in Figure 4.44 represents the model under normal operational conditions.
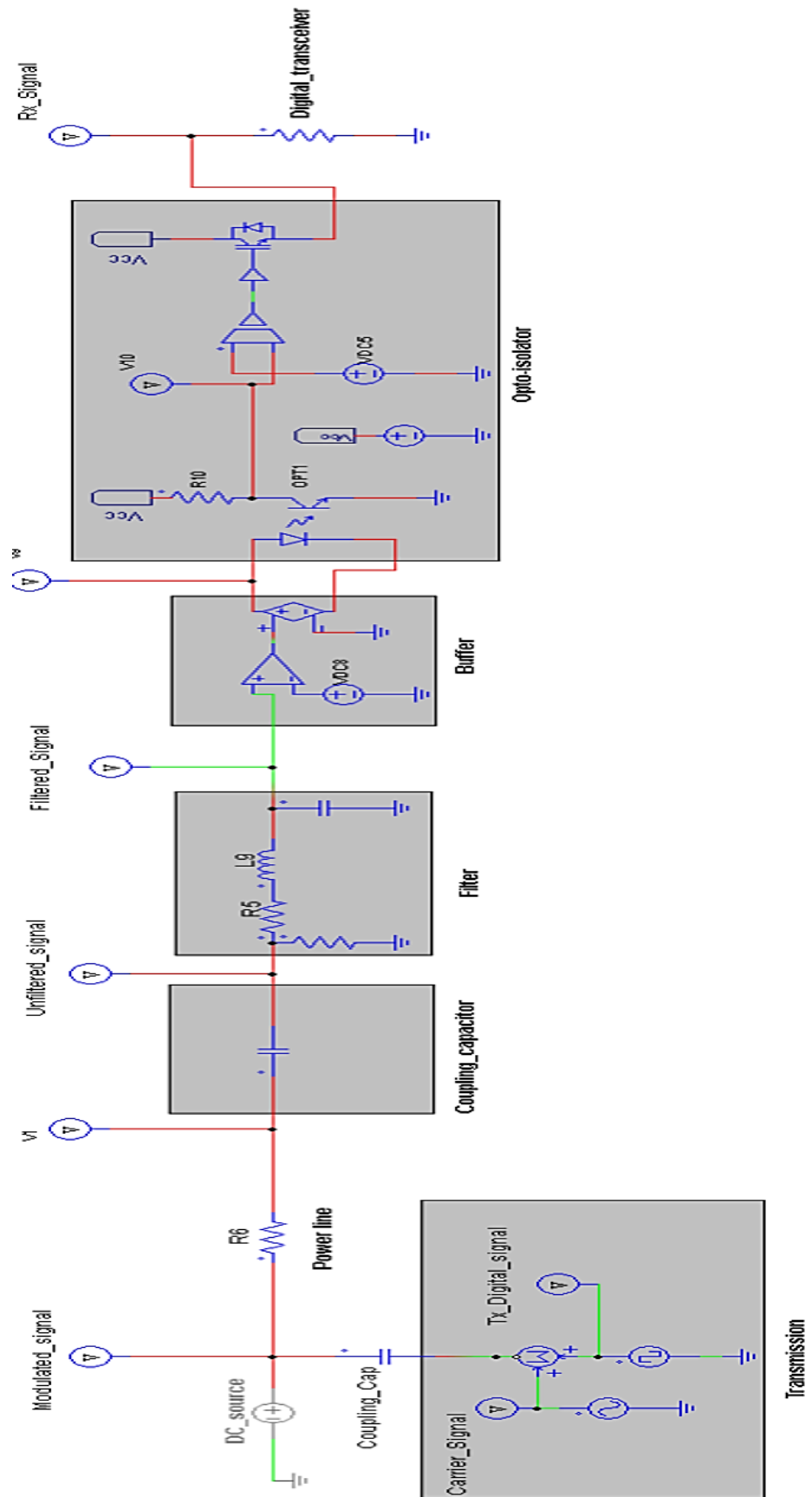
Figure 4. 44 :Opto-capacitive coupler for power line communication circuit model.

144

The transmitted signal is a resultant signal from the modulation of the carrier by the digital signal shown on Figure 4.45c. The carrier signal, with parameter specified in Table 4.11, is shown in Figure 4.45b. The ASK modulated signal shown in Figure 4.45a, is injected into the power line through coupling capacitor ($C_{coupling\_Tx}$). Its amplitude is the product of the carrier and the communication signal amplitudes. Therefore, the peak-to-peak voltage amplitude of the modulated signal injected into the power line is 10 V, which is in line with Comité Européen de Normalisation Électrotechnique CENELEC standards for power line communication. The injected signal travels along the line to the reception side.
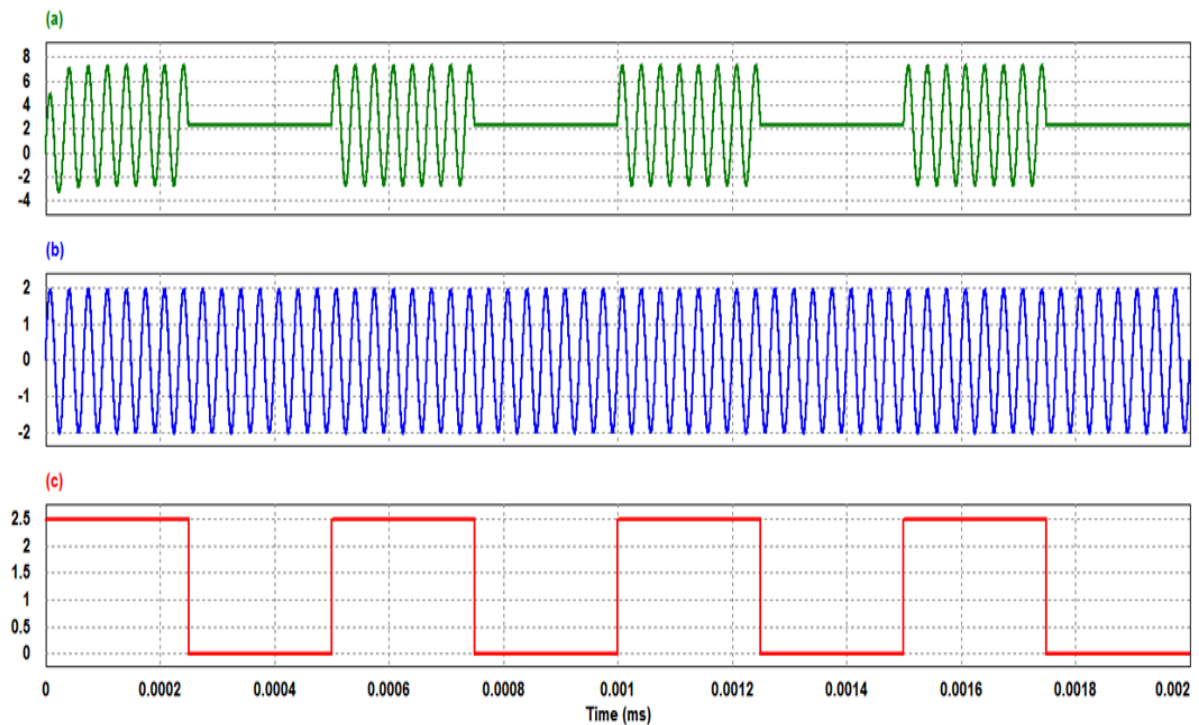
Figure 4. 45: Transmission side signals: a) modulated signal b) carrier and c) digital signal.

At the reception side, the coupling capacitor isolates the DC components of the transmitted signal and only the modulated transmitted is extracted. Figure 4.46a shows the recovered modulated signal which is fed into pass band filters for original signal recovery by filtering out the carrier. The pass band filter output signal is shown in Figure 4.46b. It is an attenuated digital signal affected by noise caused by the line impedance and filter losses. The filtered signal is fluctuating in amplitude and time, thus, cannot be directly used in opto-isolator. Hence, the use of a buffer stage prior to feeding the filtered signal into the opto-isolator. The output from the buffer is the input to the opto-isolator and is shown in Figure 4.46c. Up to this stage the amplitude recovered is 1.2V while the original digital signal is 5V. However, the signal amplitude is enough and consistent to be fed to the opto-isolator. It is worth noting that there is an electric connection from the power line down to the input of the opto isolator.

145
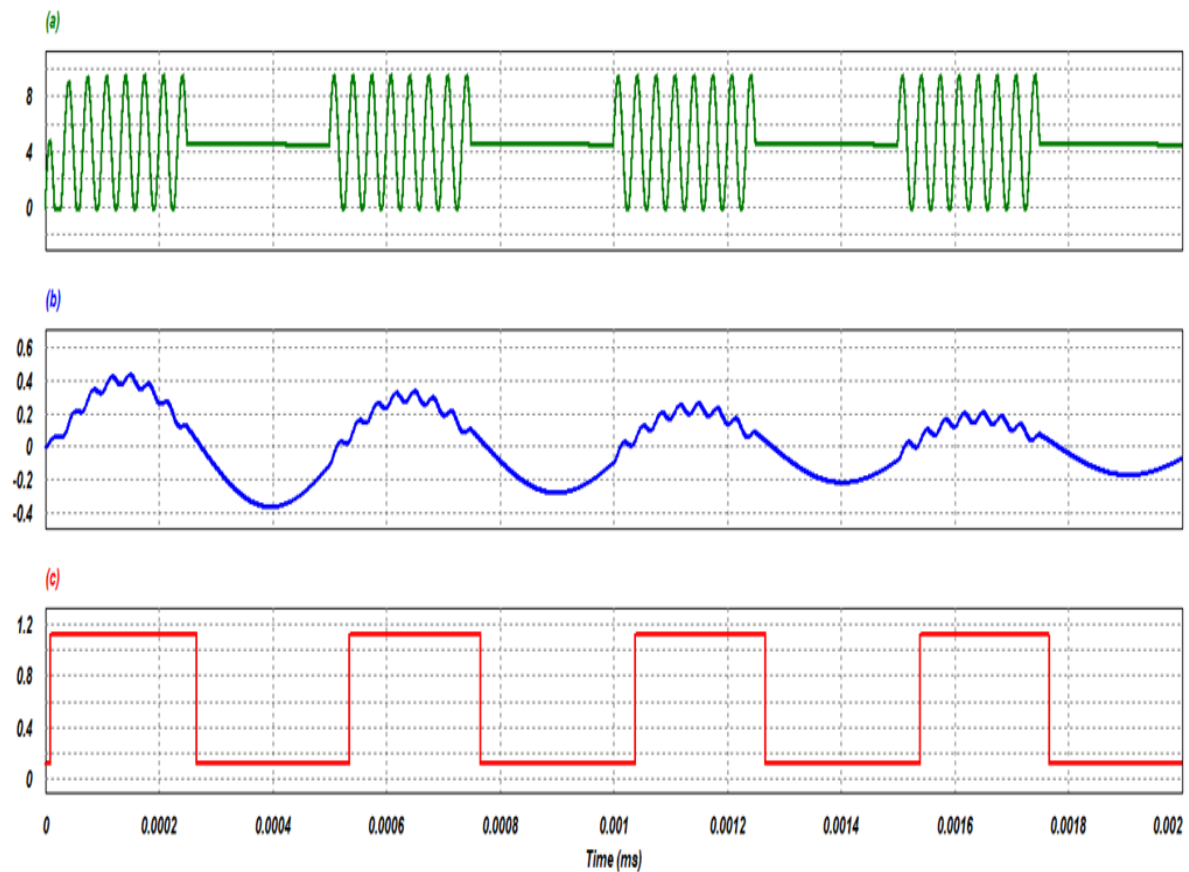
Figure 4. 46: reception side signals, (a) unfiltered signal ;(b) filtered signal; (c) Opto-isolator input signal.

The opto-isolator output amplitude depends on an independent voltage source Vcc. For the current simulation 10 V is used as Vcc, consequently the maximum output signal amplitude that can be obtained from the opto-isolator irrespective of the input signal amplitude. Figure 4.46b shows the opto-isolator output signal in comparison to the original transmitted digital signal shown in Figure 4.46a. From both graphs, a 180° phase between the original digital transmitted signal and opto-isolator output signal can be noticed. A phase shift would mean a change in bit sequence and consequently the wrong information would be received. Moreover, the nature of the phototransistor part of the opto-isolator makes its output signal to delay achieving its maximum amplitude. Hence, the need to use an operational amplifier phase shifter to recover the right sequence of the digital signal transmitted and for a faster level switching. Figure 4.46c shows a reconstructed digital signal which is fed to the transceiver and does match the original transmitted signal.

146

The amplitude of the recovered digital signal as shown in Figure 4.46c is 10 V, while the amplitude of the original transmitted digital signal shown in Figure 4.46a is 5 V. This highlights the ability of the circuit to adjust the received signal to the desired amplitude level by simply adjusting the Vcc. The delay in between the transmission and the replication of the signal is 0.02 μsec.
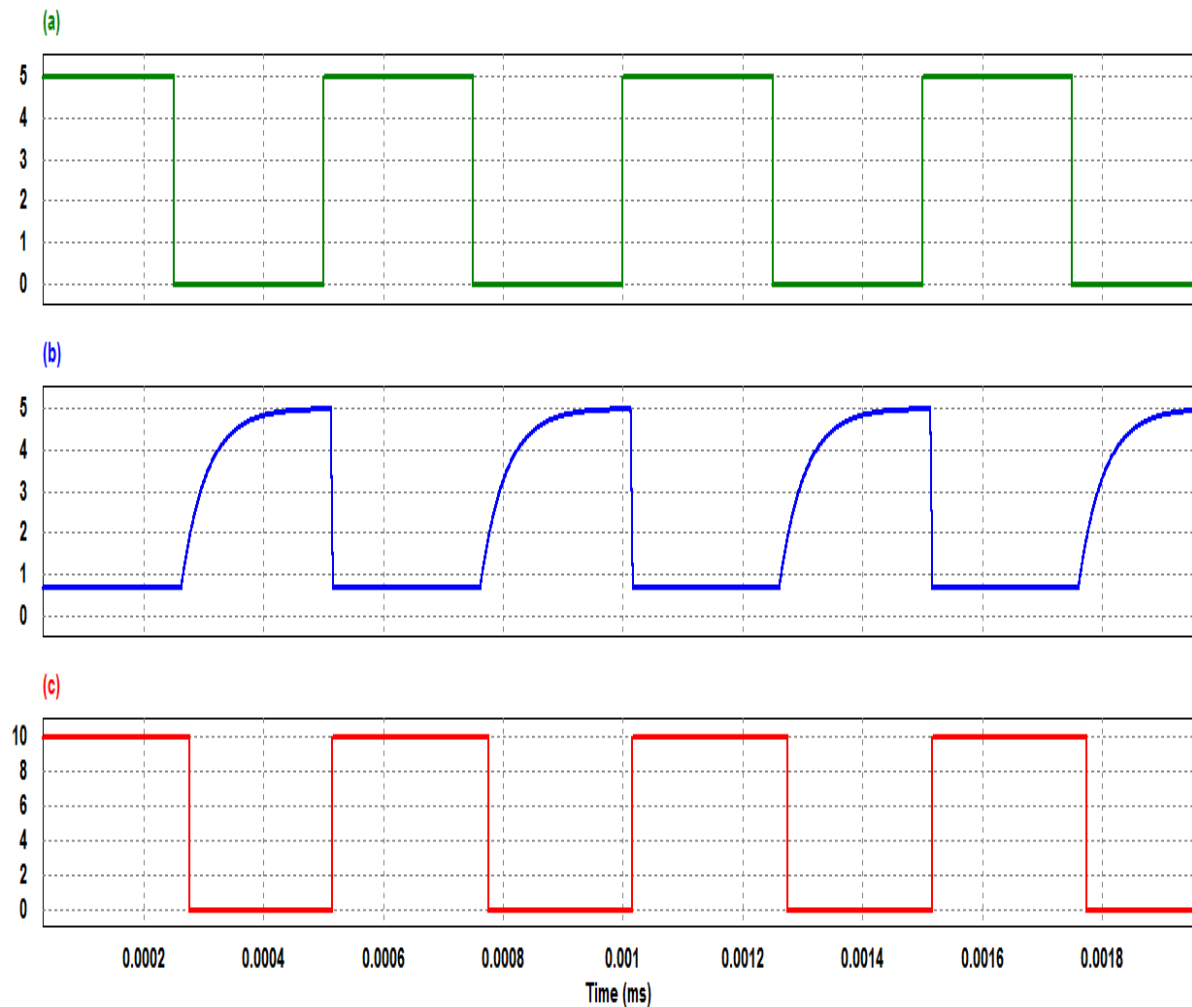
Figure 4. 47: Comparison of communication signal at different stage (a) transmitted digital signal (b) opto isolator output signal (c) transceiver received signal.

The opto-capacitive coupler enhances the safety for both equipment and users as it prevents accidental lines crossover of lines voltage signal to communication circuit and subsequently to the transceiver. The validation of this aspect is performed using the model in Figure 4.47 in which a hypothetical scenario of a surge arrestor failure resulting into surge wave crossing over into the coupling capacitor towards the transceiver. To assess the impact of the surge onto the system, analysis is done regarding the behaviour of the circuit during the fault. In general, a surge results from high impedance fault, lightning discharge on lines, and switching

147

transients. A surge is characterised by short overvoltage rise in range of microseconds and also by a high voltage gradient (Mirra et al., 1997; Piantini, 2008; Ishii et al., 2013).
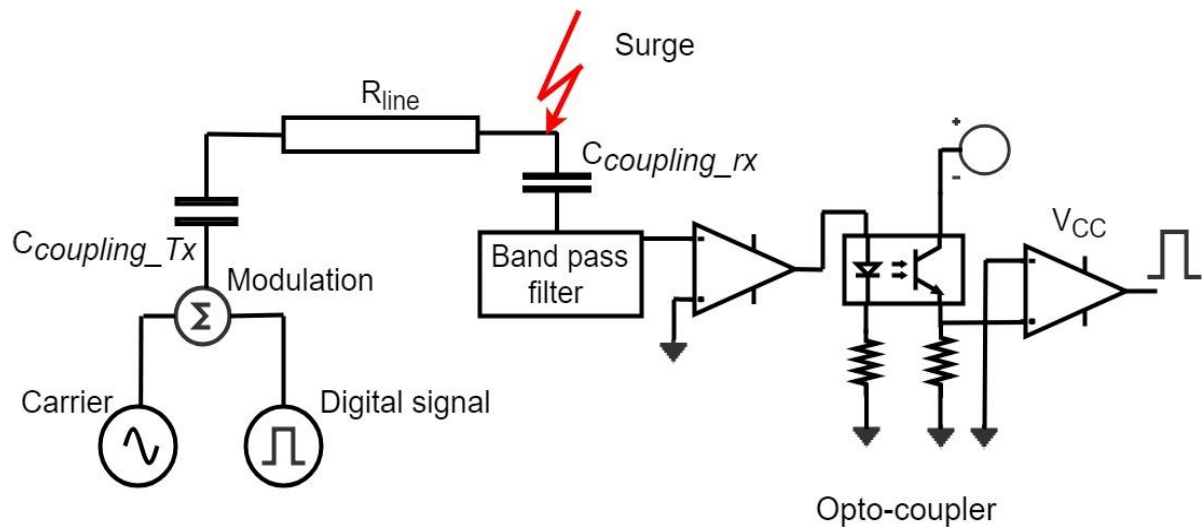
Figure 4. 48: Opto-capacitive coupling circuit diagram with lightning discharge on line.

The model in Figure 4.47 is simulated in PSIM with the introduction of a 1 kV surge occurring at 0.5 µsec for 0.02 µsec time interval and travelling through the coupling capacitor. The surge signal, shown in Figure 4.48a, affects the unfiltered communication signal received from the line as shown in Figure 4.48b. From the latter, an overshoot of 1 kV is observed onto the communication signal. The surge does affect the filtered signal as well, as shown in Figure 4.49a, where the communication signal is completely distorted with increased amplitude, and discharge time is delayed. Figure 4.49b shows a continuous high-level status in the output of the buffer circuit, which keeps the opto-isolator output in high-level throughout the surge period and the discharge of circuit components. Figure 4.49c shows the signal received by the transceiver during the fault. The signal has an amplitude that should show a normal communication signal, however, the signal is completely distorted which will be interpreted as a communication error. The damaging surge signal does not reach the transceiver and therefore the surge is seen as a communication error. Thus, providing a complete electrical isolation between the line and the communication equipment subsequently users.
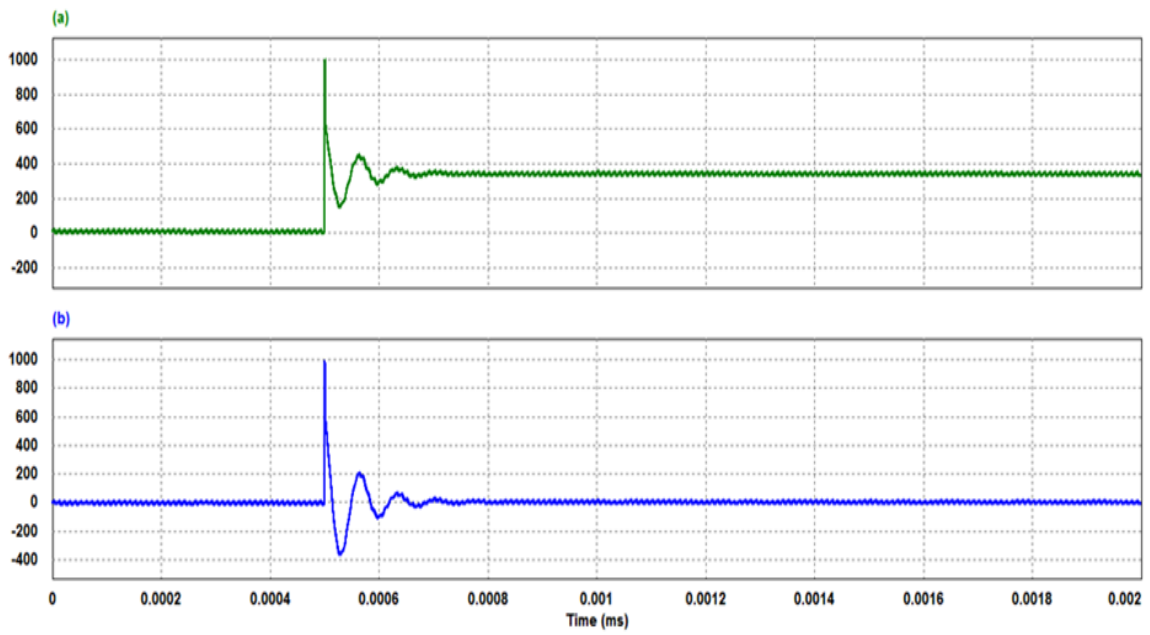
Figure 4. 49: Signal response at the coupling point, (a) surge signal; (b) unfiltered signal.
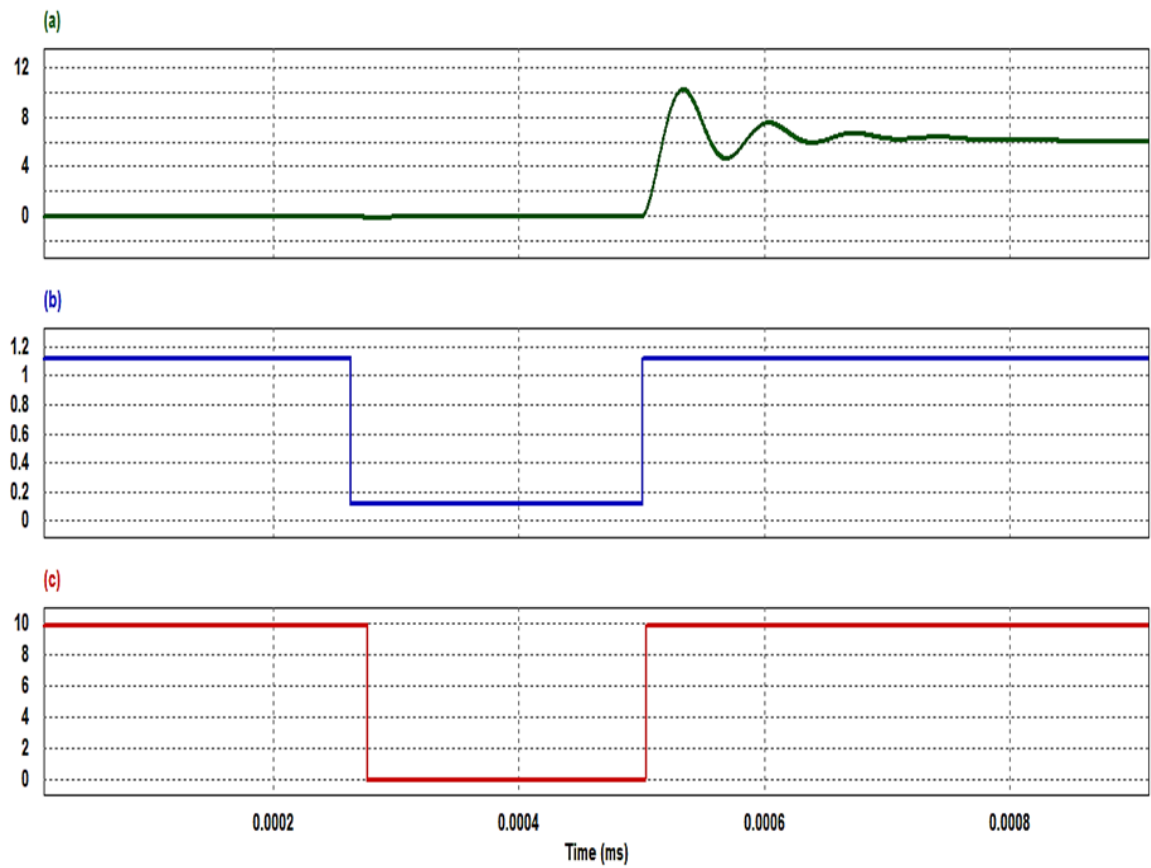
Figure 4. 50: Signal response at the reception side (a) filter output signal; (b) opto coupler input signal; (c) received signal at the transceiver.

4.4 Conclusion

In this chapter is proposed and designed an intermediate low voltage direct current distribution network for sparse electrified areas interconnection. The system is a bottom up network, starting from the nanogrids that interconnect to make a microgrid. The nanogrids considered are AC diesel generator which are interfaced to the DC microgrid via AC/DC converters. Each nanogrid is expected to supply its own local loads and export the surplus of its production to the microgrid bus for power sharing with other nanogrids. A voltage of 0.4 kV$_{DC}$ is used for microgrid formation, as from the literature 0.4 kV$_{DC}$ proved to be efficient in application for power supply to data centres.

Microgrids are themselves interconnected through intermediate voltage direct current network of 3 kV. The voltage is selected due to its wide use in railways system, thus making it much easier in regards of equipment and standards. The interconnection of microgrid allows load sharing through power exchange. As the microgrids are sparse, the interconnection implements the "Olympic ring" microgrid based grid extension discussed in chapter two.

Nanogrid converter is designed with modularized topology to allow easy and economic repair as only affected module should be replaced if needed. Proposed converters are modelled and simulated using PSIM. Results show that the design criteria set are met by the converters. Furthermore, the nanogrid overall control algorithm for operation is designed. The controller is based on continuous monitoring of power and the request from the microgrid.

Microgrid converter and overall control are developed to allow power exchange between microgrids should the need raise. Power line communication technology is used for communication between the converters and controllers, hence the opto capacitive coupler for DC nanogrid is designed in this chapter for a safe operation of controller over power lines. The concept is simulated in PSIM environment.

CHAPTER FIVE
SIMULATION AND ANALYSIS
5.1 Introduction

Intermediate low voltage direct current systems for interconnection of sparsely electrified areas, as proposed in chapter four, builds upon multiple neighbouring nanogrids that are interconnected to form a local 400 V_{DC} microgrid. Thereafter, sparse DC microgrids form a minigrid through a 3 kV intermediate low voltage DC network. The minigrid is connected to the utility through a converter.

In this chapter, the proposed ILVDC network system is simulated using DIgSILENT PowerFactory software version 15.1.7. For more than 30 years, DIgSILENT provides an environment for modelling, simulation, and analysis of power system networks: generation, transmission, distribution, and industrial network. Various studies have used it for analysis of distribution network (Schinke & Erlich, 2018; Marzal-Pomianowska et al., 2016; Heslop et al., 2014). Moreover, due to its standard library of electrical equipment and models make it a perfect tool for network studies. Hence, load flow study and short circuit analysis are performed for each microgrid as well as the minigrid. Simulation parameters used are obtained from chapter four and adjustments are made for clarity.

Three microgrids with 100 kW generation capacity each are considered for the formation of a minigrid operating at an intermediate low voltage direct current of 3 kV. The minigrid network interconnects all microgrids for power sharing among each other and for utility grid integration. The microgrids are identified as microgrid 1, 2, and 3 respectively. A similar identification method is used for nanogrids and local loads.

5.2 Microgrid 1

5.2.1 Description

The microgrid is modelled with a component from DigSilent library, therefore some of the parameters calculated in chapter four are ignored or adjusted. The model for microgrid 1 is shown in Figure 5.1. It consists of three nanogrid generators, nanogrid loads, and generals loads representing consumers connected to the microgrid. Converters are used to interface each nanogrid to the 0.4 kV DC microgrid bus bar and are also used as an interface for consumers connected to the microgrid.

A radial network topology is used due its low cost and proven efficiency in rural electrification as discussed in chapter two, section 2.3. Nanogrid local loads are supplied through their respective 400 V AC terminals, to which respective nanogrid generators are connected. The nanogrid generators are modelled as synchronous machines, which replicate the diesel electric power generator initially intended as presented in chapter four.
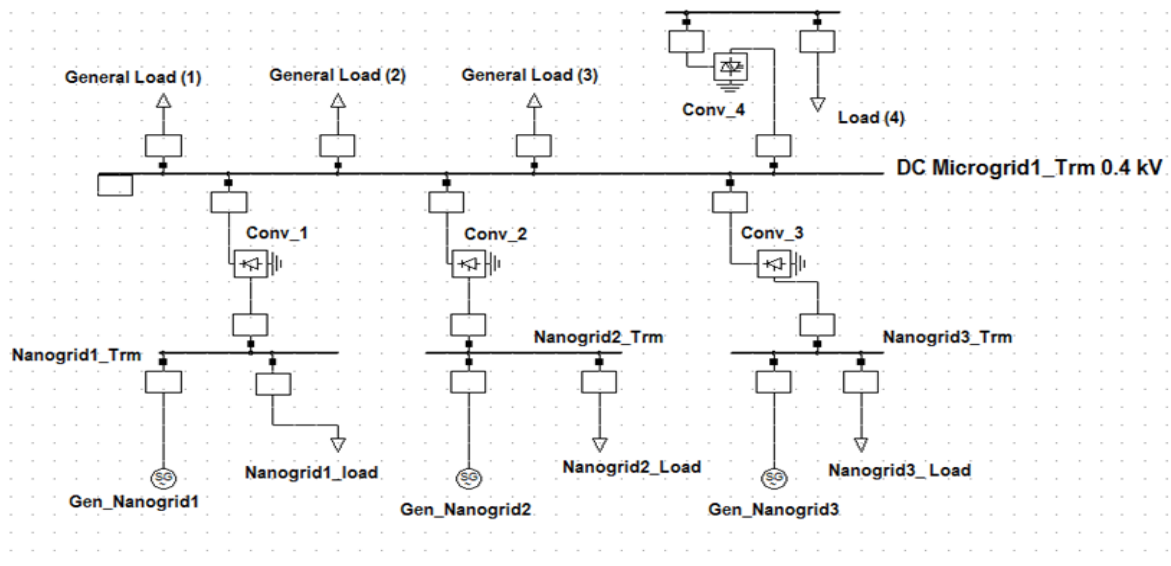
Figure 5. 1: Microgrid 1 model.

The total amount of dispatched power within the microgrid amounts to 100 kW. Note that the three nanogrids represent multiple small nanogrids within the microgrid as described in chapter four. However, for simplicity and clarity they are grouped to be represented by only three nanogrids and their local loads in addition to the general loads. Table 5.1 shows values of the load demand within the microgrids. The nanogrid generators are expected to supply power to the general loads without compromising on their own local loads while at the same time avoid overloading. Figure 5.2 shows a snapshot of the data of nanogrids synchronous generators within the microgrid 1. The dispatchable power from the nanogrids generator 1, 2 and 3 are 33 kW, 31.5 kW, and 35.5 kW respectively.

Table 5. 1: Microgrid 1 loads demand.

Load	Power (kW)
Nanogrid1_load	2.25
Nanogrid2_load	2
Nanogrid3_load	4
General_load 1	20
General_load 2	9
General_load 3	3
Low voltage Load	4.75
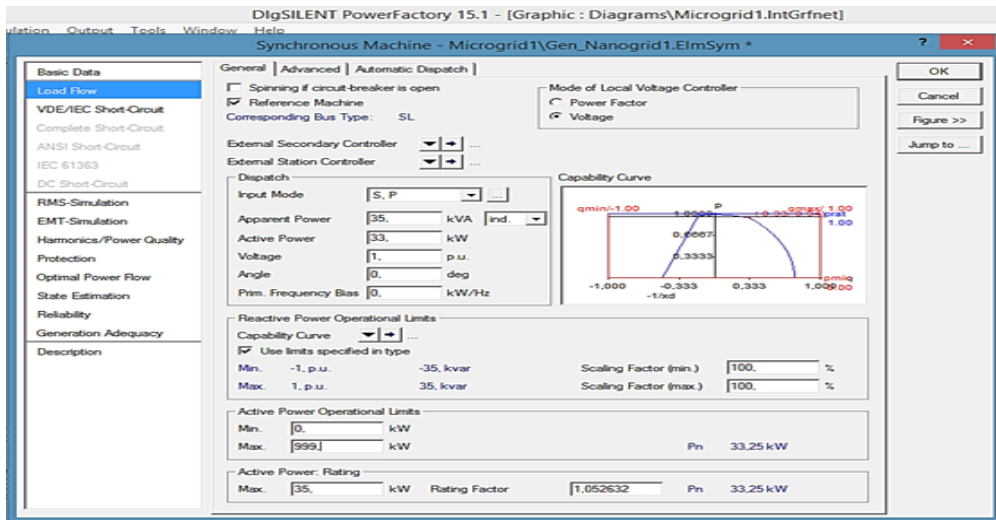
(a)
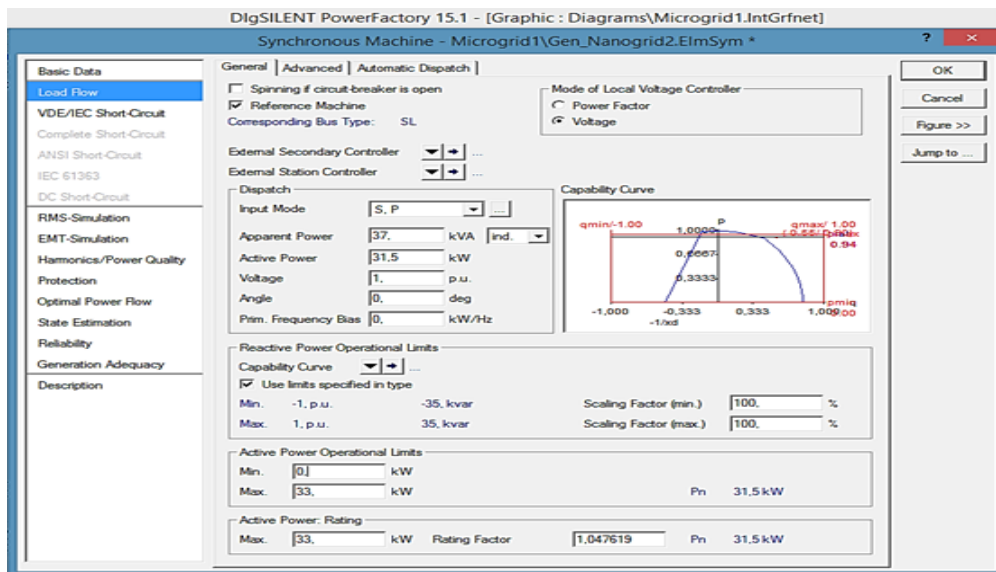
(b)
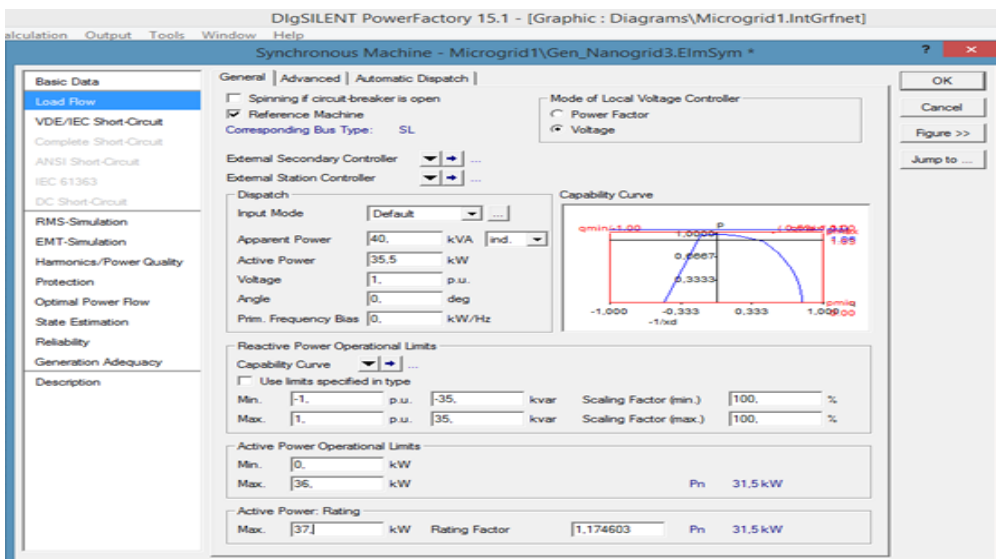
(c)

Figure 5. 2: Microgrid 1 generator data of nanogrids a) 1 b) 2 and c) 3.

Thyristor-based power electronics transformerless converters are used as an interface between the microgrid bus bar and the nanogrids terminals. The first nanogrid terminal (nanogrid1_Trm), second nanogrid terminal (nanogrid2_Trm), and the third nanogrid terminal (nanogrid3_Trm) are connected to the 0.4 kV DC microgrid bus through a 25 kW converter 1 (Conv_1), 30 kW converter 2 (Conv_2) and 25 kW converter 3 (Conv_3) respectively. It is assumed that any AC load part of general loads should be connected through the converter in inversion mode. However, for clarity and simplicity only the low voltage load (Load 4) is connected through a PWM converter for validation of the fact of power flow from the DC bus to AC loads connected to it. Figure 5.3 shows the converters specification used for simulation. Converter 1 and 3 have same the rated power of 25kW, but different firing angle control characteristics. The current is the controlled characteristic used for firing angle control of all the tree nanogrid converters.

(a)

(b)

(c)

(d)
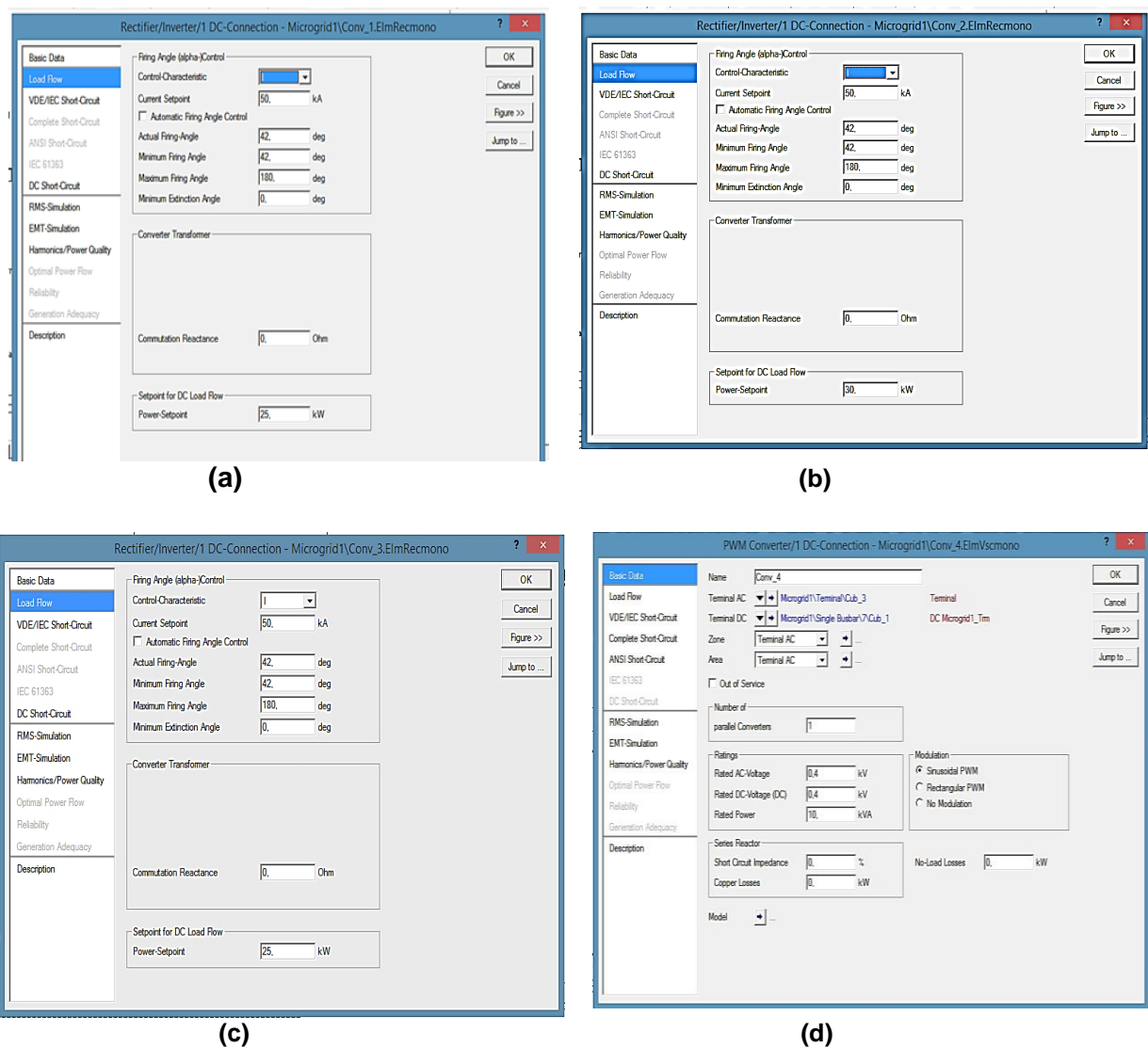
Figure 5. 3: Microgrid 1 converters settings a) conv_1, b) conv_2, c) conv_3 and d) conv_4.

5.2.2 Microgrid 1 load flow simulation results

Load flow analysis is performed on the microgrid 1 model described in section 5.2.1. The aim is to monitor and analyse the voltage at all buses and terminals if they are within required range. The loading of nanogrid generators is analysed in respect to connected loads. The load sharing amongst nanogrids is analysed as well.

Figure 5.4 shows the load flow voltage profile at the nanogrid terminals within microgrid 1. Here, all the nanogrids are generating 0.4 kV to supply their local and microgrid loads. From the nanogrids terminals, the local loads are supplied at the same voltage while microgrid loads (General loads) connected to the 0.4 kV DC bus bar are supplied through converters.
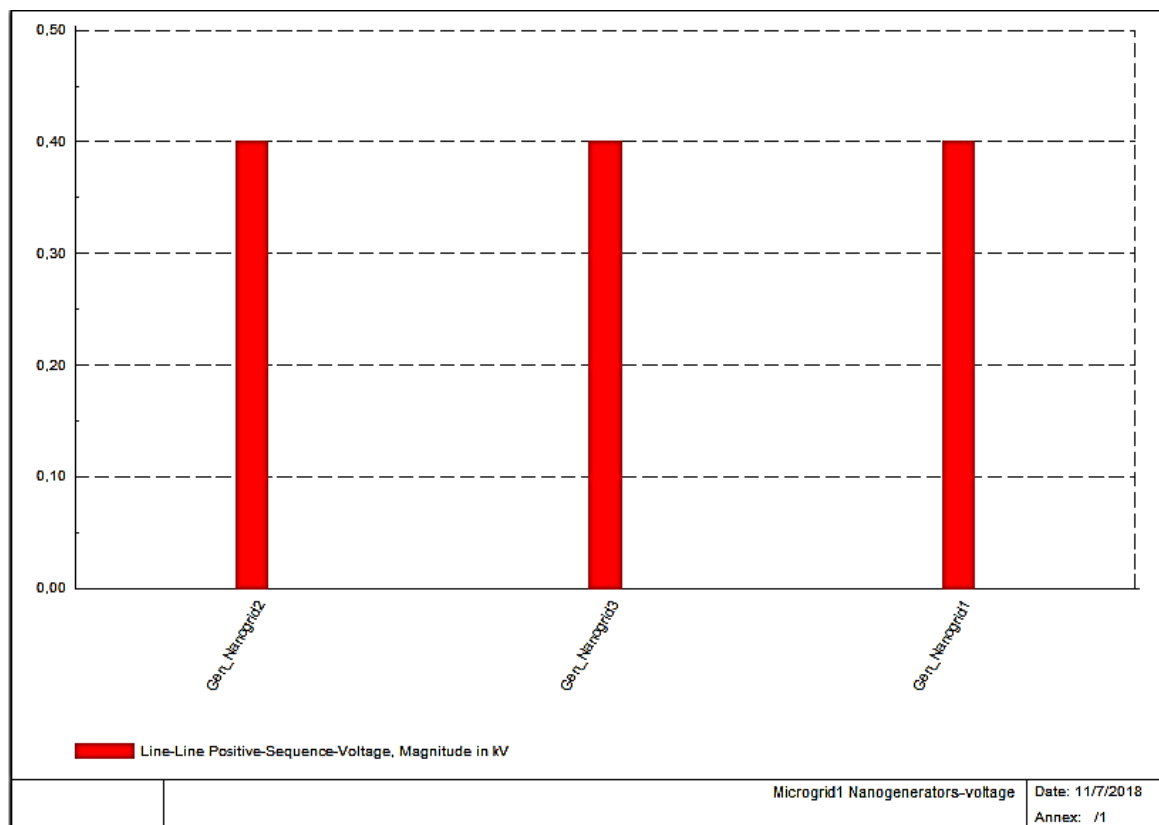
Figure 5. 4: Voltage profile of nanogrid generators within microgrid 1.

Power produced by each nanogrid generator is shown in Figure 5.5. The nanogrid 1 generator produces 16 kW, the nanogrid 2 generates 15.6 kW, and nanogrid 3 supplies 17.6 kW. The total power demand of local loads amount to 10.7 kW versus the 38.5 kW consumed by general loads connected to the DC microgrid. This amount of power demand by the general loads is more than the generating capacity of a single nanogrid generator. This is the reason for the interconnection of nanogrids to increase the capacity.
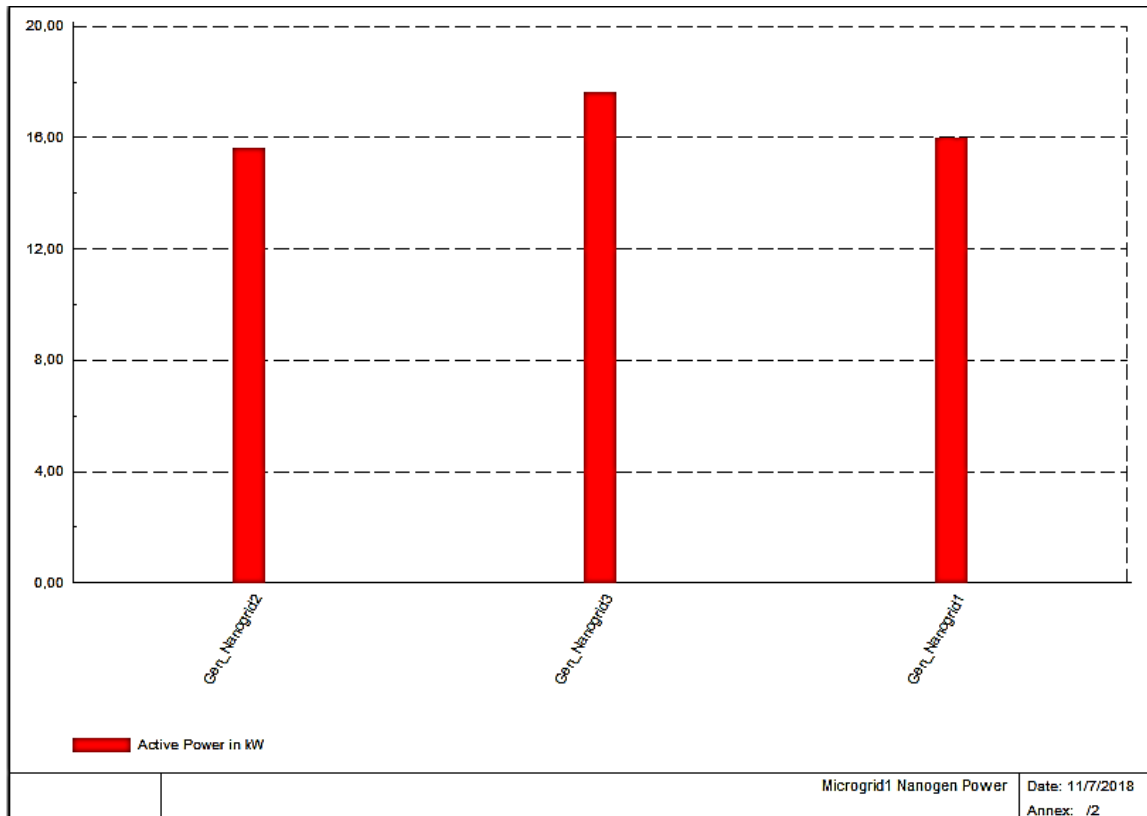
Figure 5. 5: Power generated by nanogrids within microgrid 1.

The interconnected nanogrid generators proved to be able to simultaneously sustain their local loads and general loads within the microgrids. Figure 5.6 shows the power demand profile of the loads within the microgrid. The general loads which represent the costumers connected on the microgrid take a lot of what is produced by the nanogrid generators without overloading them as shown on Figure 5.7. The nanogrid 3 generator is the most loaded, 63.8%, while nanogrid 2 and 1 are loaded at percentages of 57.6% and 58.1% respectively.

Despite having different loading percentages, the contribution in power supply of each nanogrid generator towards the general loads connected to the microgrid is the same, as shown on Figure 5.8. For a total demand of 38.5 kW exported to the microgrid through the nanogrid converters, each single nanogrid contributes 12.8 kW. The difference in the total power generated by the individual nanogrid rises from the local loads as the generators individually take care of their nanogrid loads. This is in line with the strategy of interconnecting electrified areas to increase the capacity to the level of being able to supply the other loads (the household without a generator) as elaborated in chapter four.

The loading of nanogrid generators is an essential characteristic for the control at nanogrid level as mentioned in the previous chapter in section of nanogrid overall control. The controller for the nanogrid consider the loading before allowing power export to the microgrid in turn to

the general loads. A certain limit on power exported is observed to avoid the overloading of the nanogrid generator. Hence, the monitoring of this parameter.
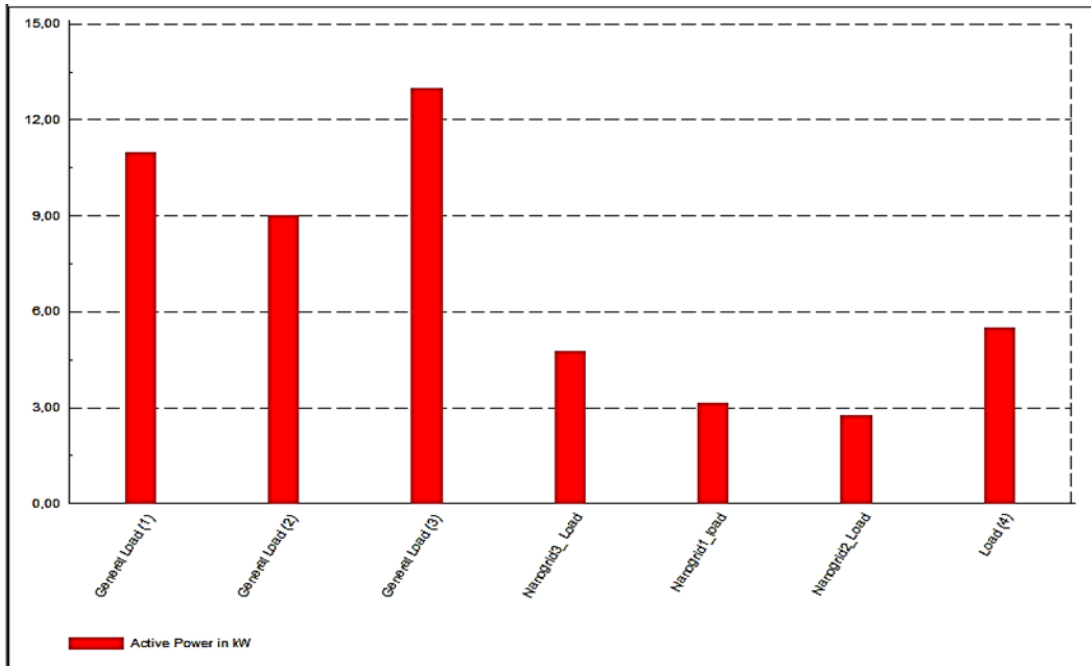
Figure 5. 6: Power demand profile of all loads within Microgrid 1.
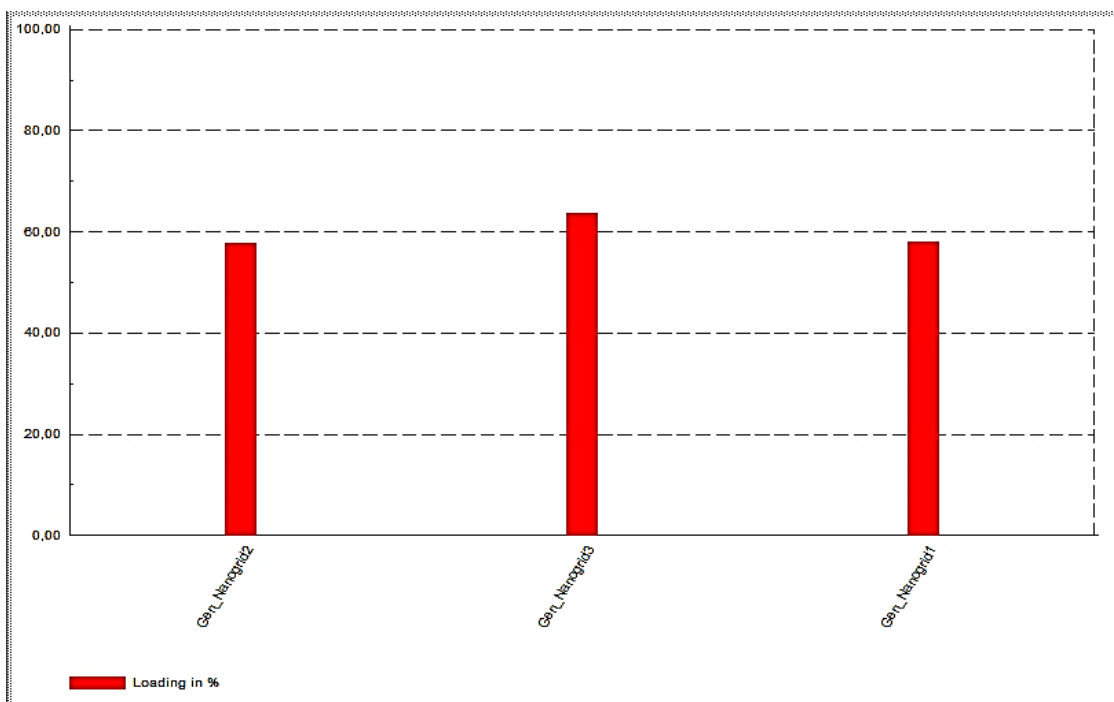
Figure 5. 7: Loading of nanogrid generators in Microgrid1.
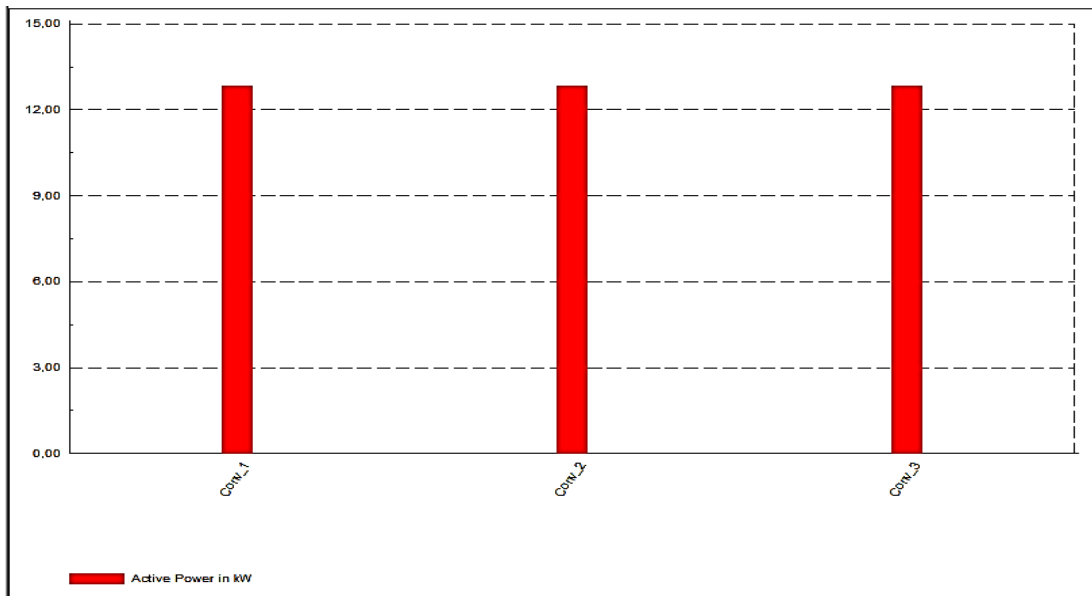
Figure 5. 8: Profile of power export through nanogrid converters within Microgrid 1.

5.3 Microgrid 2

5.3.1 Description

The Microgrid 2 as modelled in the DigSilent PowerFactory is shown Figure 5.9. It consists of four nanogrids with their respective generators, local loads, microgrid bus connected loads, and converters. Nanogrids are interconnected through a 0.4 kV DC bus to form the microgrid. Converters are used as an interface for the nanogrids integration to the DC microgrid. The total dispatched capacity within microgrid 2 is set to be more or less 100 kW.
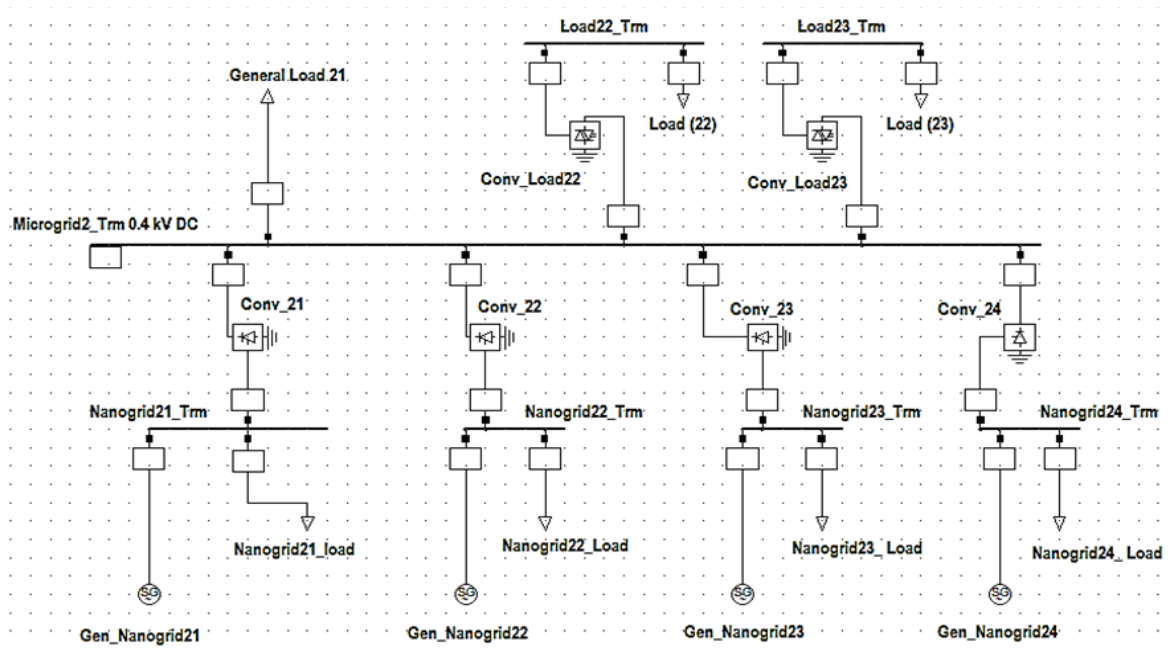
Figure 5. 9: Microgrid 2 model.

The four nanogrid generators used are synchronous generators named as Nanogrid21_Gen, Nanogrid22_Gen, Nanogrid23_Gen, and Nanogrid24_Gen. Their generation capacity is that of 35kW, 45kW, 10kW and 10kW, respectively. These values represent the distributed range of generating unities within the microgrid, which depict the disparity of generation capacities in dispersed electrified areas as discussed in chapter one and four. Figure 5.10 shows the simulation parameters of the four synchronous generators in microgrid 2.

Loads considered are local loads and the microgrid bus loads. The local ones are loads directly supplied by the nanogrids through their 0.4 kV AC terminal. These are Nanogrid21_load, Nanogrid22_load, Nanogrid23_load and the Nanogrid24_load. They represent, as explained in the previous chapter, the loads of household to which the nanogrid generator is attached. Microgrid loads General load21, load22 and load23; in the same context, represent the loads attached to the microgrid bus. These might be unelectrified households which would get power by the 0.4 kW DC microgrid bus. They are usually AC loads, hence the connection through a converter as illustrated by load (22) and load (23). The general load represents the power demand of a set of unelectrified households or small workshops, which would otherwise be complex to represent individually. Therefore, for clarity and simplicity, they are presented as the general load. Figure 5.11 and Figure 5.13 shows the loads parameters, where the power is 1.5 kW, 2 kW, 2.5 kW and 2 kW for Nanogrid21, Nanogrid22_load, Nanogrid23_load and Nanogrid23_Load respectively. General Load21, Load (22) and Load (23) power demands are 18 kW, 9.5 kW and 28.5 kW respectively.

Thyristor-based converters are used for the integration of nanogrids to microgrid 2. The same type converter operating in rectification mode, with specification on a, is used for all four nanogrids. The firing angle α of the thyristor used is 42, as calculated in chapter four in the designing of the converter operation in rectifier mode. On the other hand, Conv_load (22) and Conv_load (23) are sinusoidal PWM based inverters with the power handling capability of 10 kW and 30 kW. Their settings are shown on Figure 5.12.

All the converters within microgrid 2 have bidirectional capability. In the event of loss of any nanogrid generator, the nanogrid overall control strategy developed in chapter four should operate the converter in inverter mode to allow local loads to be supplied from the DC microgrid. Thus, achieving mutual support of nanogrids is part of the bottom-up grid extension in the concept of swarm electrification. A similar approach is used in microgrid 1 and 3 of the intermediate low voltage direct current network under study.
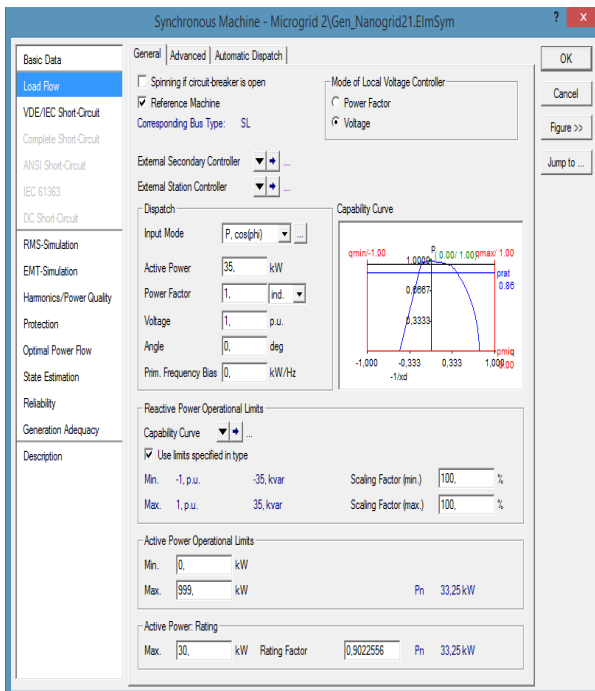
(a)
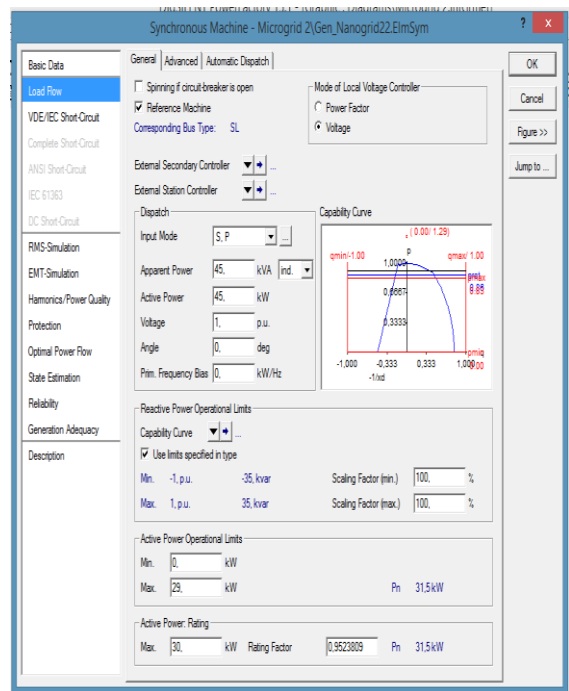
(b)
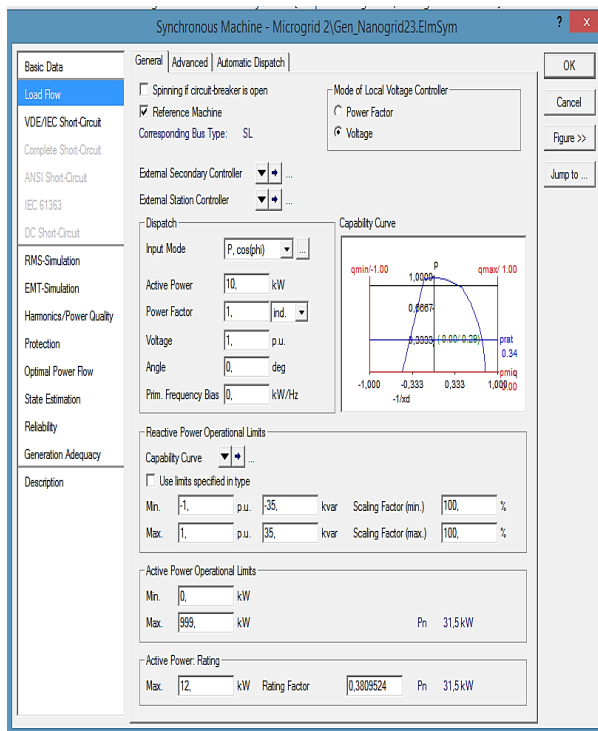
(c)
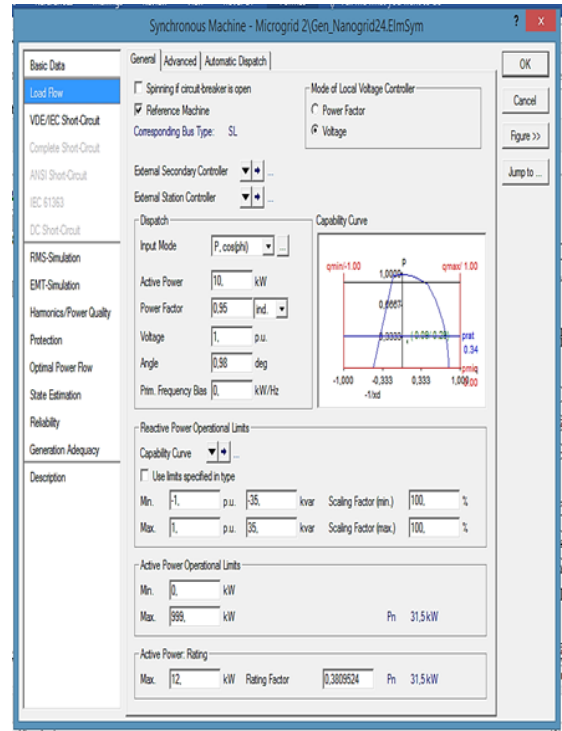
(d)

Figure 5. 10: Microgrid 2, generator data of nanogrids: a) 1, b) 2, c) 3 and d) 4.

160
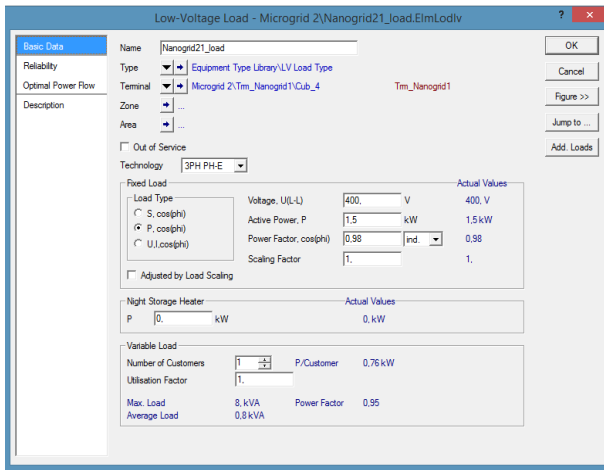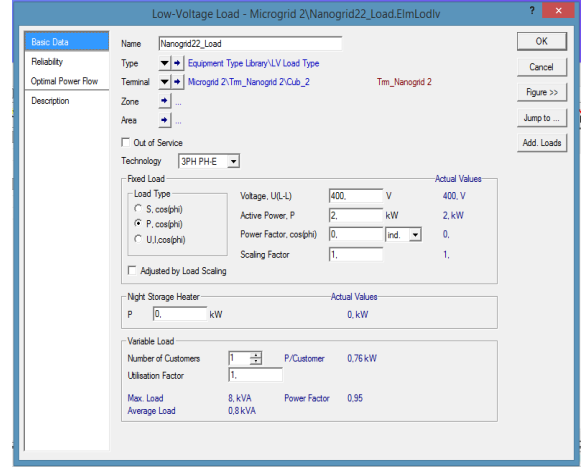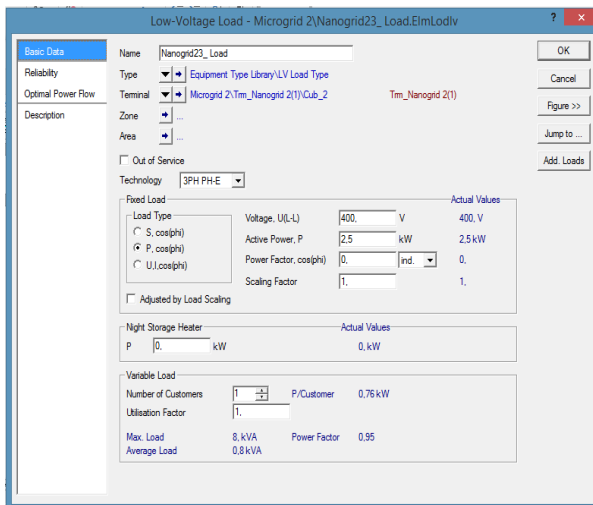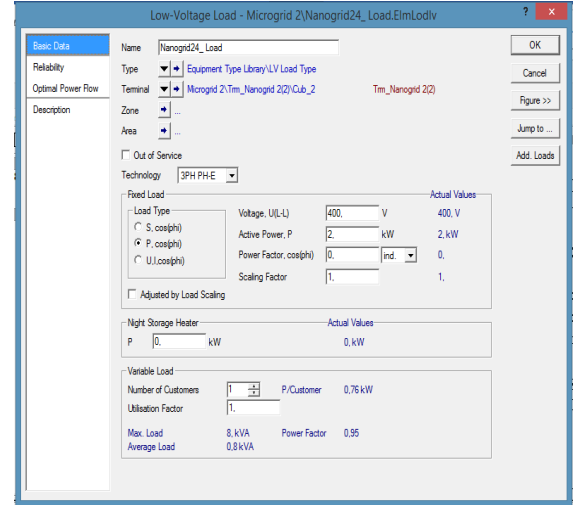
Figure 5.11: Local loads data of: a) Nanogrid21, b) Nanogrid22, c) Nanogrid23 and d) Nanogrid24
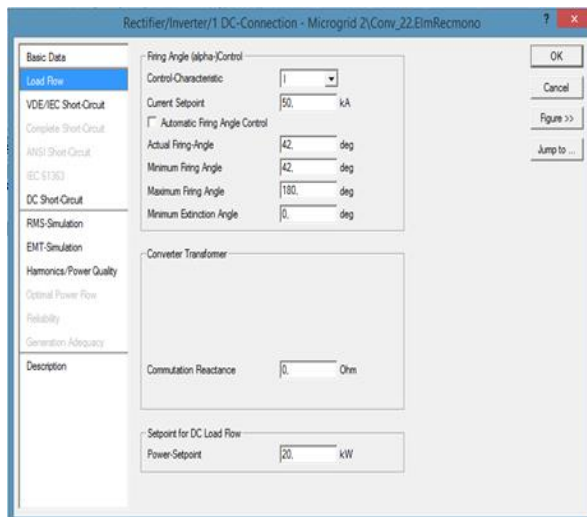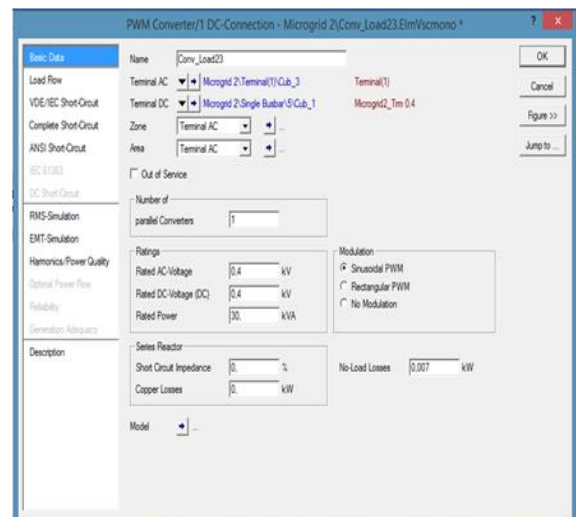
Figure 5. 12: Microgrid 2 converter settings for: a) Nanogrid and microgrid loads converters.
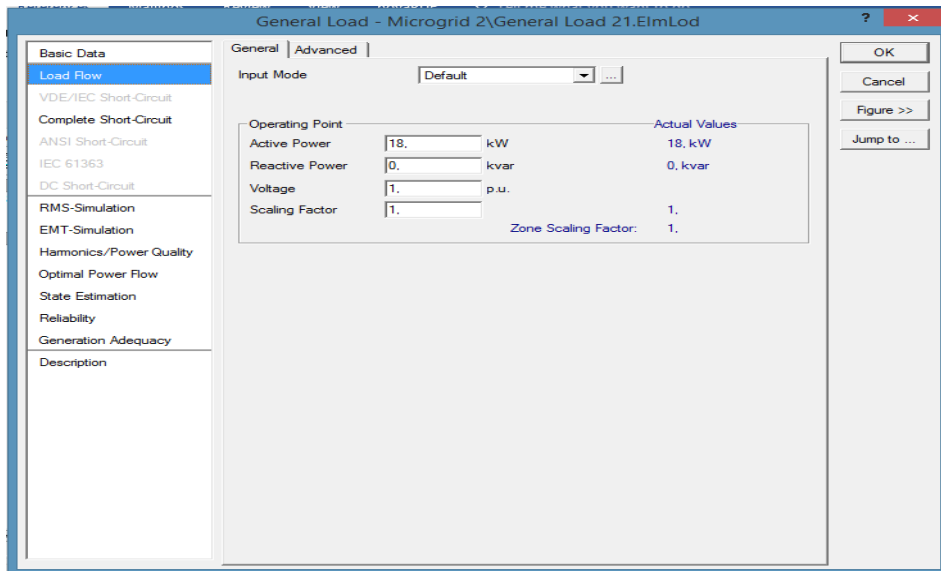
(a)
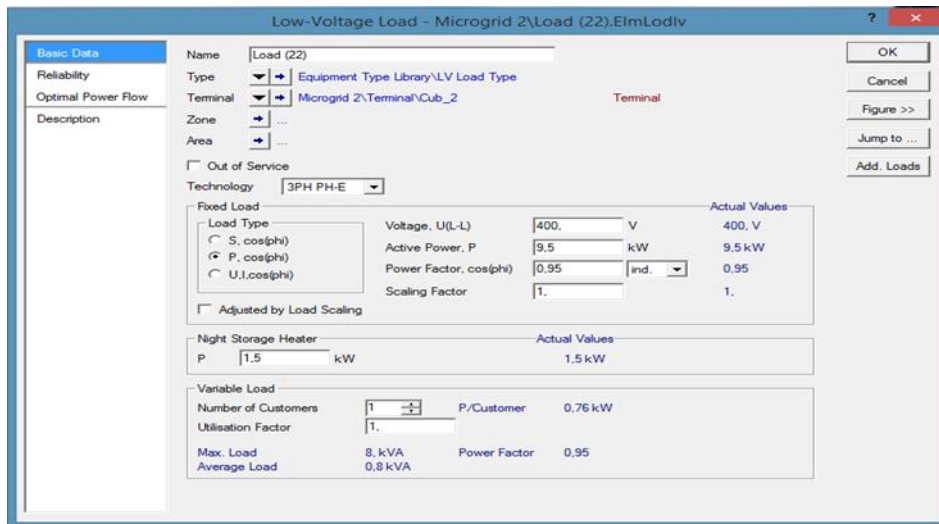
(b)
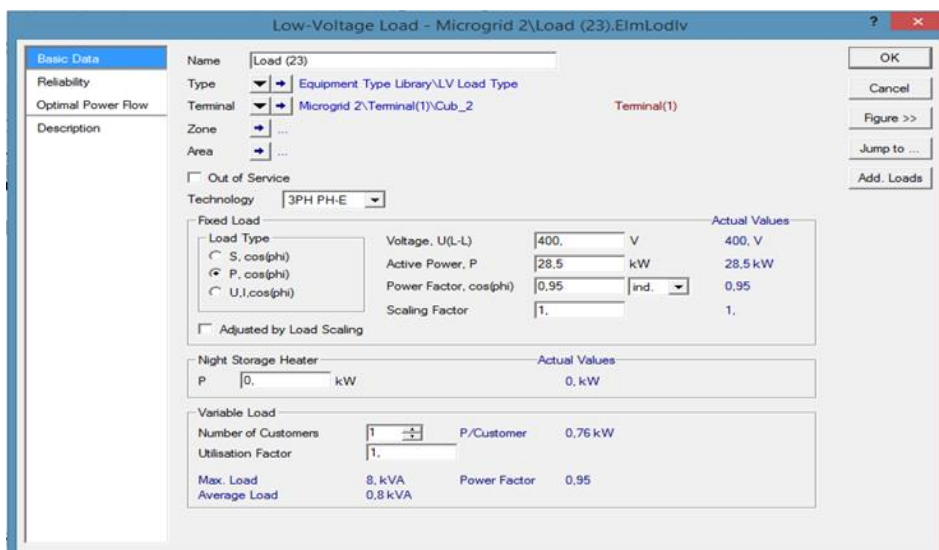
(c)

Figure 5. 13: Microgrid 2 bus load parameters: a) General load 21; b) Load 22 and c) Load 23.

5.3.2 Microgrid 2 load flow

The load flow simulation of Microgrid 2 model described in the previous section is performed using DigSilent PowerFactory 15.1.7. Analysis is done on the voltage profile and power flow in different branches and nodes of the network in order to see whether the microgrid behaves according to design criteria as developed in chapter four.

Simulation results of voltage profiles of all the nanogrids terminals in microgrid 2 are shown in Figure 5.14. As can be observed from the latter, each of the nanogrid generators within the microgrid 2 is generating 0.4 kV which directly supplies its respective local load, and indirectly the microgrid connected loads through converters Conv_21, Conv_22, Conv_23 and Conv_24.
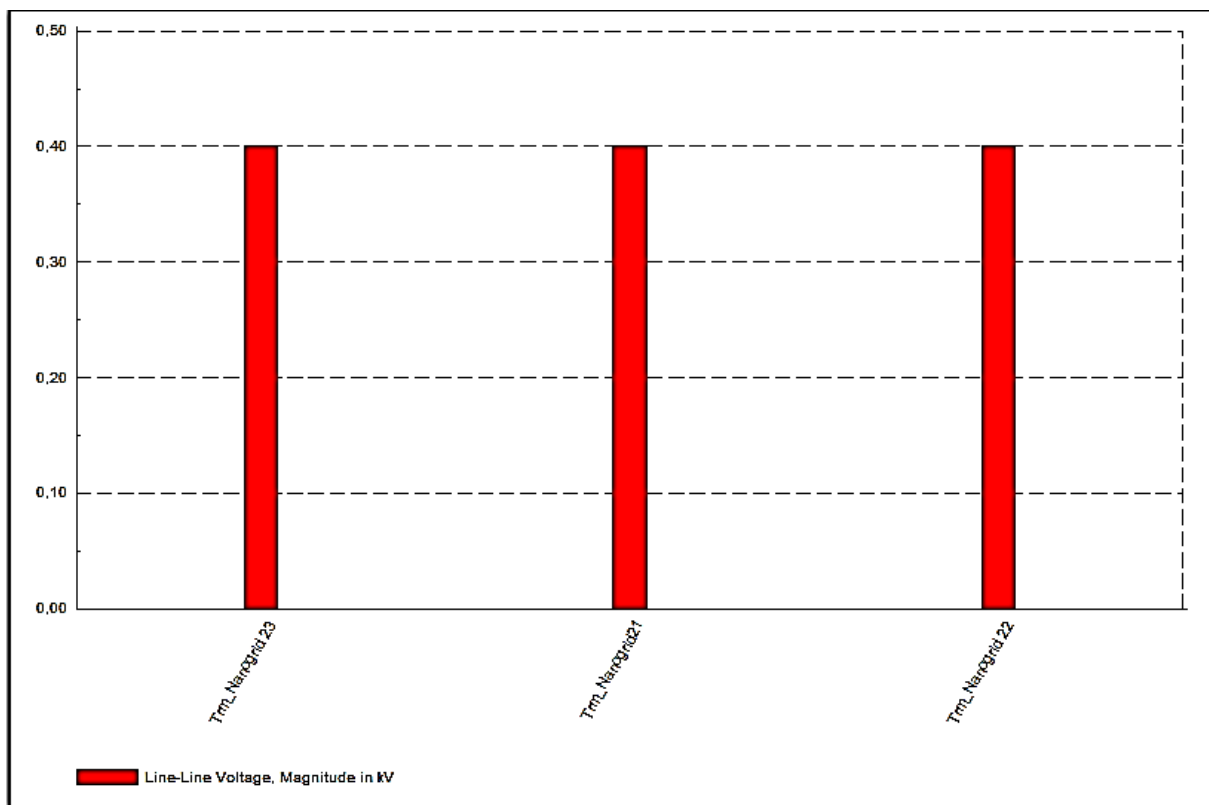
Figure 5. 14: Voltage profile of nanogrid generators within microgrid 2.

As mentioned, the nanogrids generators supply the microgrid connected loads through the 0.4kV DC microgrid bus. The microgrid loads power demand is shared equally among the nanogrid generators within the microgrid. Hence, the total power generated by each microgrid is the sum of its own local load power demand and the extra power demand to meet its allocated load sharing portion. Figure 5.15 shows the total power generated by each nanogrid generator. The nanogrid 21 (Gen_Nanogrid21) produces 17 kW, 17.5 kW for Nanogrid22 and Nanogrid24, while Nanogrid24 generator supplies 18 kW.
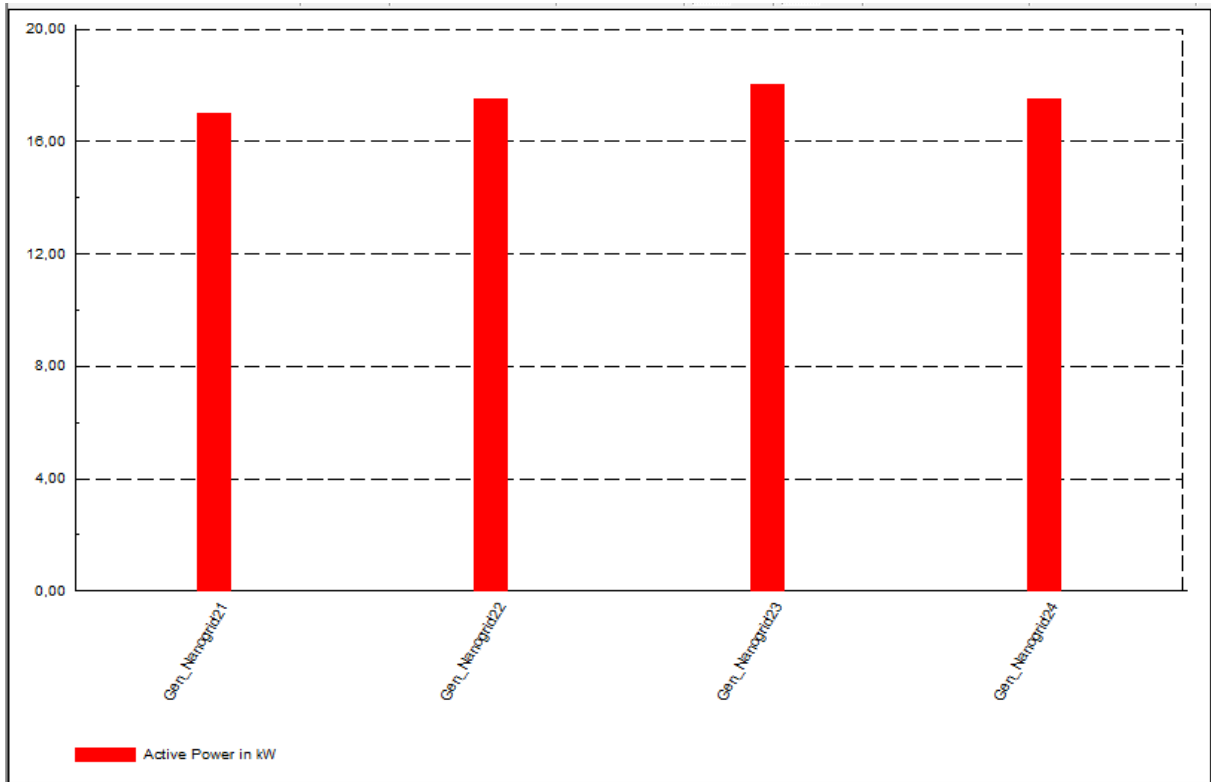
Figure 5. 15: Power profile of nanogrids within microgrid 2

The power produced by the nanogrid generators is distributed among the loads within the microgrid 2. Figure 5.16 shows the individual power demand of all the loads within the microgrid, the load sharing holds only for power supplied to loads connected to microgrid bus. Hence, the total power produced by any single nanogrid generator is a combination of local power demand and power exported via the converters. It can be seen from the power demand profile that a majority of power produced by the nanogrids is exported to the microgrid bus connected loads, namely the General_Load 21, Load (22) and (23). The total demand of these loads is equally supported by all the nanogrid generators as shown on the simulation results of power exported by each nanogrids through the converters Conv_21, Conv_22, Conv_23 and Conv_24. Each of the nanogrid generator contributes 14.8 kW towards the microgrid loads without compromising its local loads and while avoiding overloading. Figure 5.17 shows simulation results of the loading of each nanogrid generator, with a loading of 62.7 %, 72.9 %, 73% and 72.9% for Nanogrid21, Nanogrid22, Nanogrid23 and Nanogrid24 generators respectively.
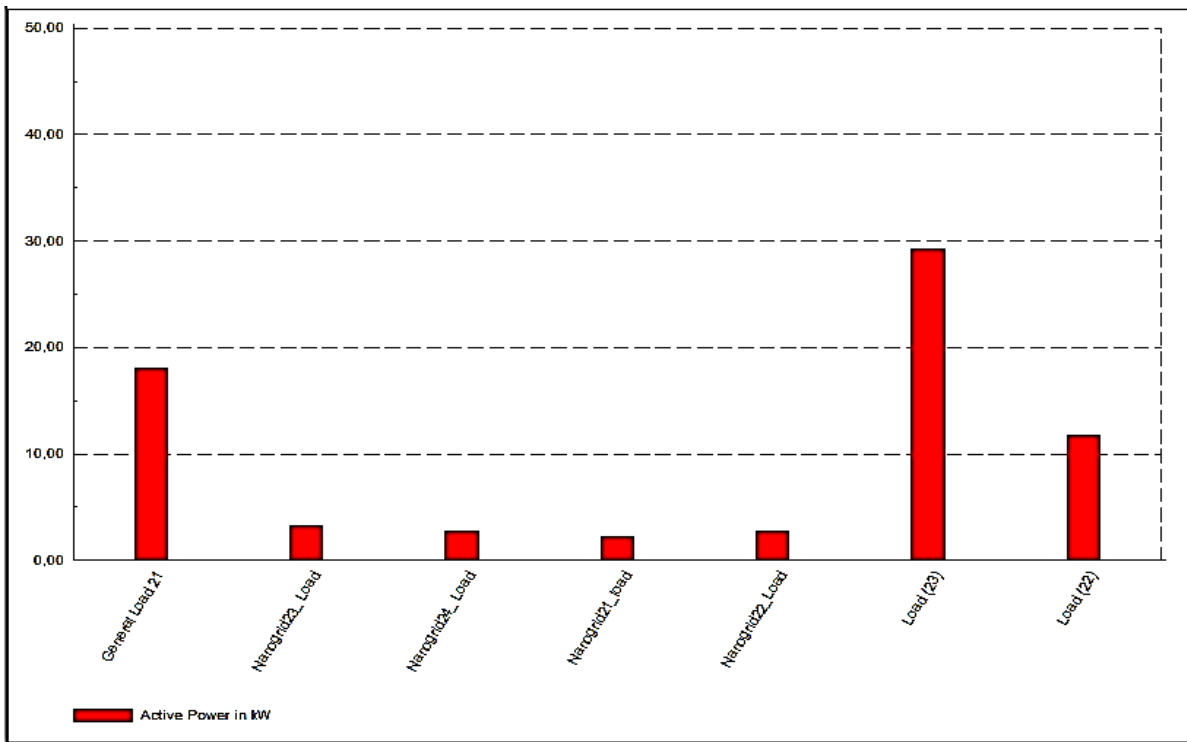
Figure 5. 16: Power demand profile of all loads within microgrid 2.
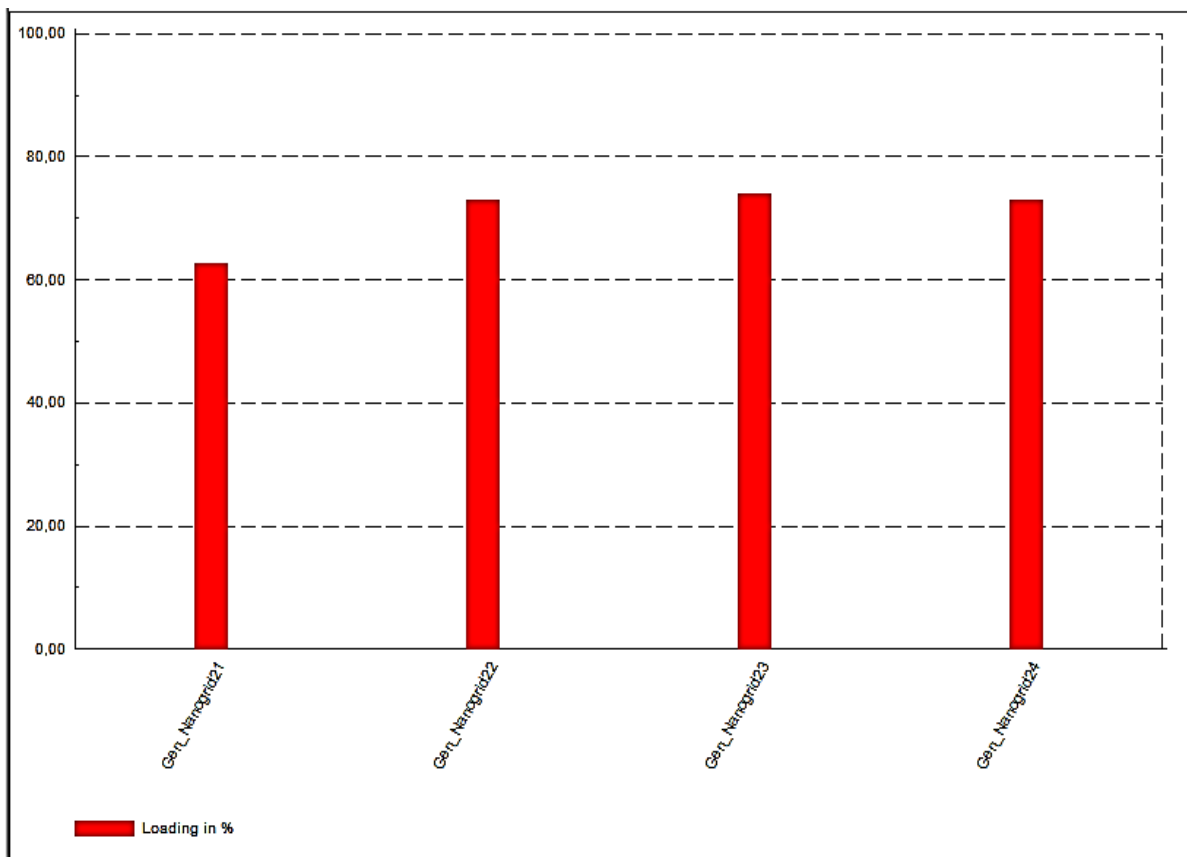
Figure 5. 17: Loading of nanogrid generators in microgrid 2.

The nanogrid overall controllers are responsible for monitoring and controlling the power exportation to the microgrid through the converter. They are tasked to initiate or terminate the

power exported as discussed in chapter four. The initiation of power export starts upon notification from the microgrid requesting the power export from the nanogrid to the microgrid, while the termination of the power export process is initiated by the controller as well. The condition that leads to termination of power export to the microgrid bus are either due to there being no more load connected to microgrid bus or an overloading of the generator. Hence the parameter is constantly monitored.

From the results discussed above, the objectives of power sharing between sparsely electrified and unelectrified areas is achieved in microgrid 2 without compromising on the stability criteria of nanogrid generators.

5.4 Microgrid 3

5.4.1 Description

Microgrid 4 is, shown on Figure 5.18, like others discussed in previous section of this chapter. It is also modelled in DigSilent PowerFactory environment and consist of three nanogrid generators namely, Gen_nanogrid31, Gen_Nanogrid32, Gen_Nanogrid33. Nanogrid generators are supplying the local loads (Nanogrid31_Load, Nanogrid32_Load, Nanogrid33_Load) and the microgrid connected loads (Load 31 and 32) at the same time. Power export from nanogrids to the microgrid is achieved through converters (Conv_31, Conv_32, Conv_33).
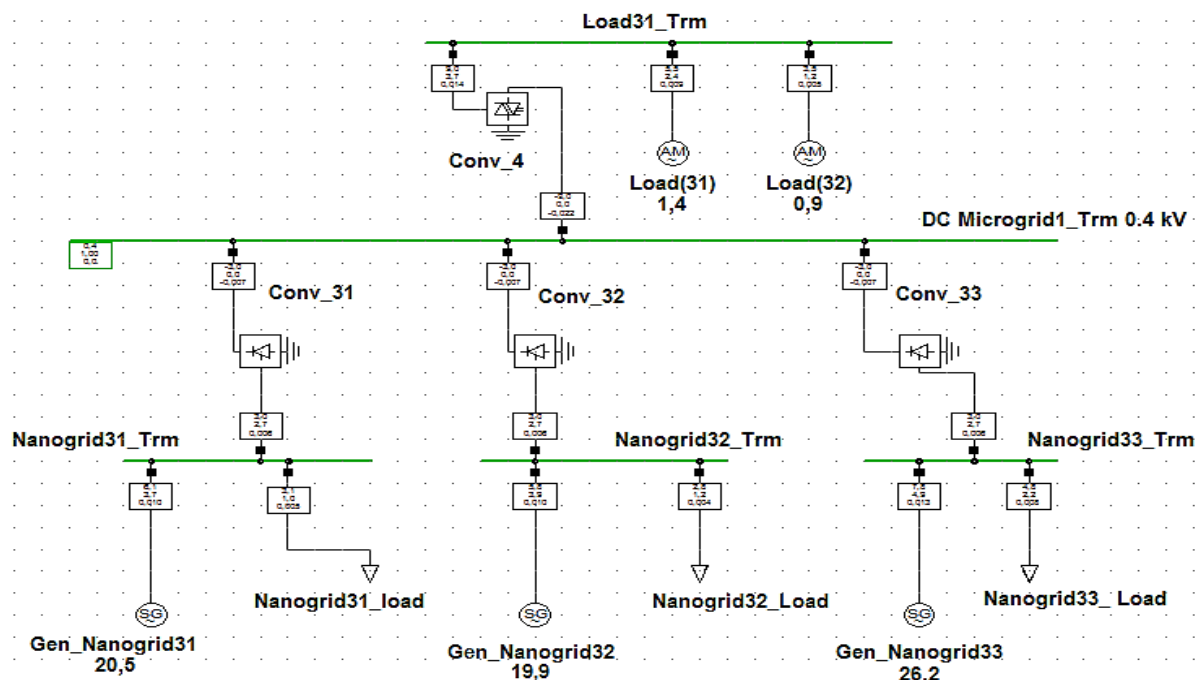
Figure 5. 18: Microgrid 3 model.

Synchronous machines are used to model the nanogrid diesel generators as developed in the previous chapter.

Figure 5.19 shows simulations parameters of all the nanogrids generators within microgrid 3. The total installed capacity of the microgrid is 100 kW with Gen_nanogrid31 producing 45 kW while Gen_nanogrid32 and Gen_nanogrid33 produce 35 kW and 15.5 kW, respectively. They are all 3-phase and generate a line voltage of 0.4 kV which is supplied directly to the nanogrid local loads connected to their respective terminals, namely Nanongrid31_Trmn, Nanogrid32_Trmn and Nanogrid33_Trmn. Simulations parameters of all the loads supplied from nanogrid terminals are show in Figure 5.21 and Figure 5.20 which presents the parameters for microgrid bus connected loads (31) and (32).

The microgrid connected load (31) and (32) are standard asynchronous motors of 5.5 kW and 3 kW, representing customers with commercial loads such as a milling machine in rural areas or electrical sewing machines. Only the steady state of those machine is considered for this study.
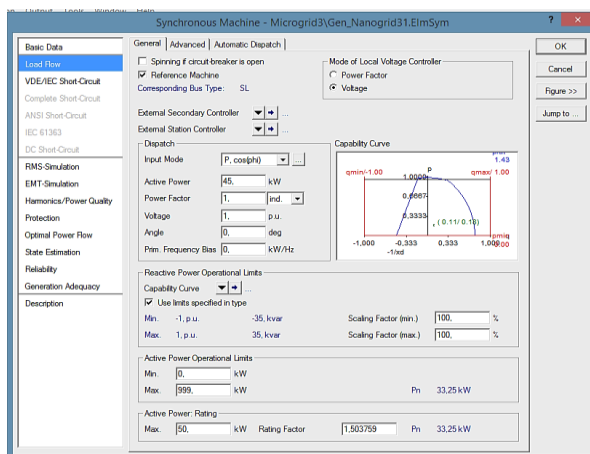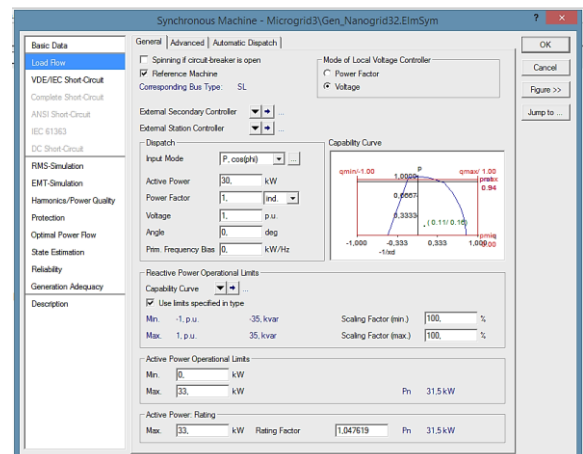
(a)   (b)
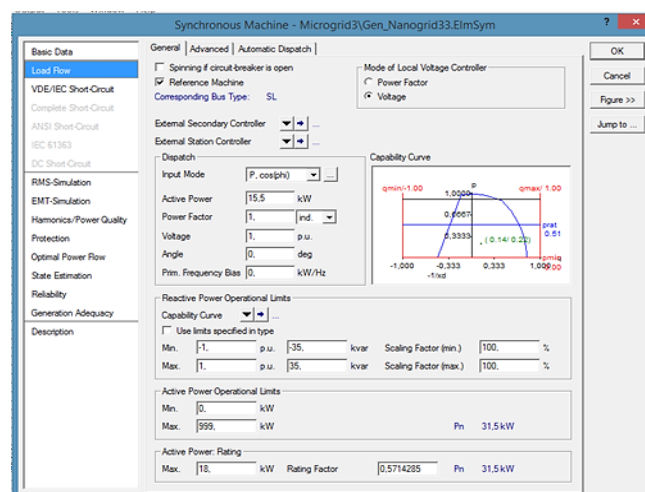
(c)

Figure 5. 19: Microgrid 3, data of nanogrids generators: a) 31, b) 32 and c) 33.
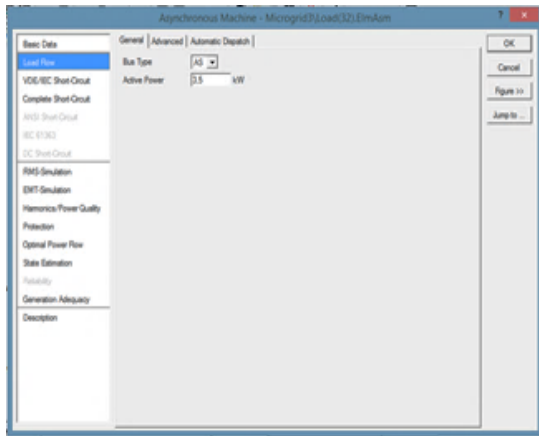
(a)
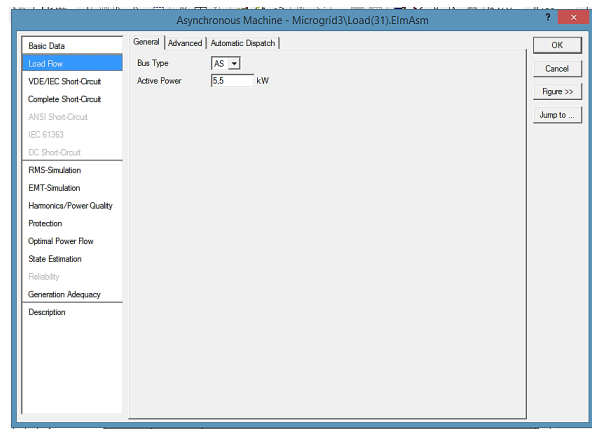
(b)

Figure 5. 20: Microgrid3 bus connected loads parameters: a) Load (31) and b) Load (32
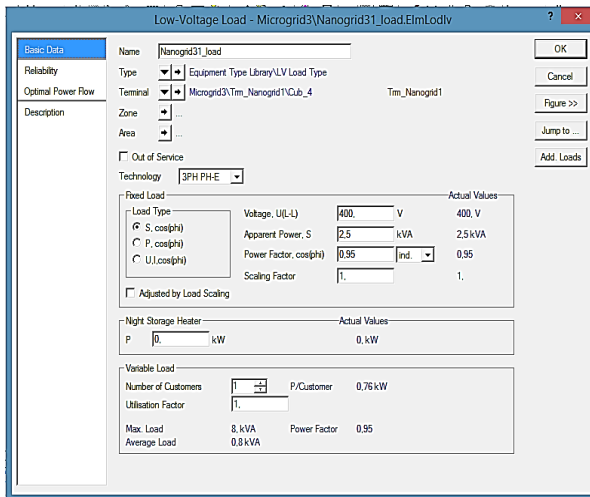
(a)
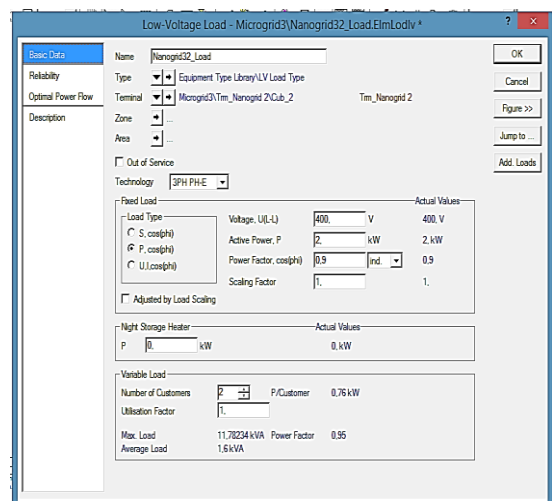
(b)
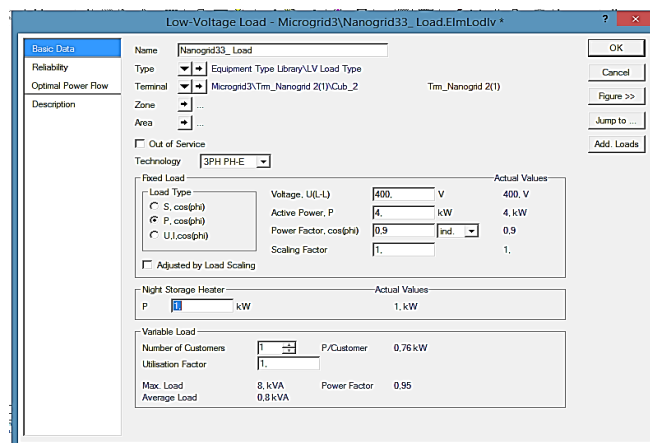
(c)

Figure 5. 21: Microgrid 3 local loads parameters for nanogrids: a) 31 b) 32 and c) 33.

Local loads are usually household equipment single-phase AC with low inductive component, as can be seen from Figure 5.21. The power factor is close to 1. These local loads are the priority for the nanogrid generators and this is ensured by the nanogrid overall controller that allows the power export to the microgrid on the condition that local loads are supplied, and generators are not overloaded.

The loads value in microgrid are as follows: 2.5 kW with power factor of 0.95 for Nanogrid 31, 2 kW with power factor of 0.95 for Nanogrid32 and 4 kW with 0.9 power factor for Nanogrid33. The latter does have a night storage heater of 1 kW.

Converters operating in rectification mode are used as an interface between nanogrids and the DC microgrid bus. For clarity and simplicity, the same type of converter is used, and its parameters are shown in Figure 5.22a. A 0.4 kV, 10 kVA PWM converter is used as interface for microgrid connected loads: Load (31) and (32). Figure 5.22b shows the PWM converter parameters used for simulations.

(a)   **(b)**
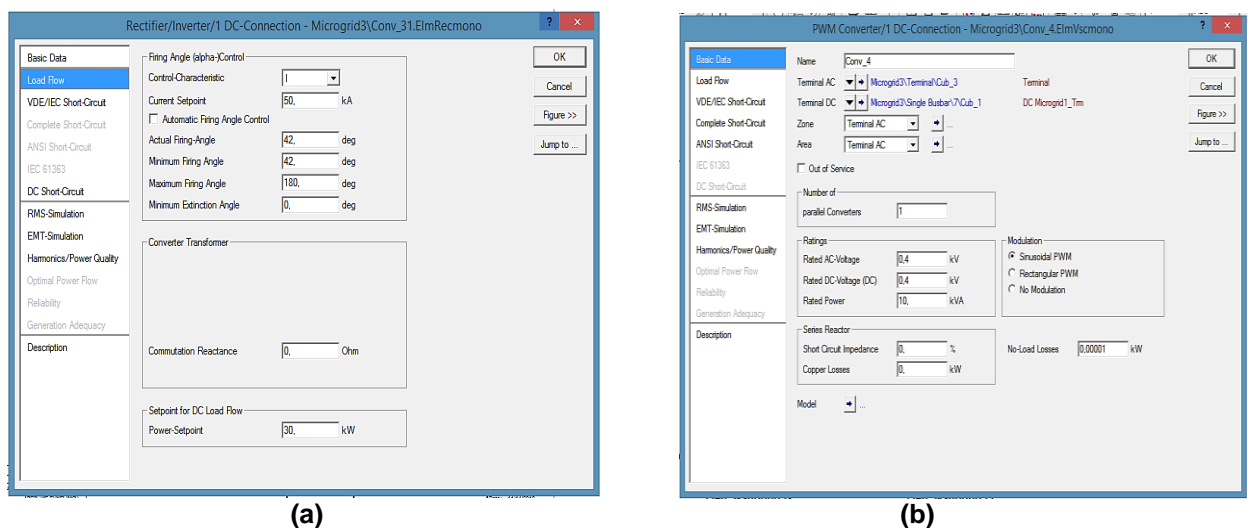
Figure 5.22: Microgrid 3 converters parameters for a) nanogrid and b) microgrid connected loads.

5.4.2 Microgrid 3 load flow simulation results

Load flow simulation is performed on the microgrid 3 model described in the section 5.4.1, and the DigSilent PowerFactory 15.1.7 environment is used for the simulation with the intention to assess the behaviour of the designed microgrid against the set criteria of power export and load sharing between the nanogrids as previously discussed.

Figure 5.23 shows the simulation results of the voltage profile at the terminal of the nanogrid generators within the microgrid 3.

They are generating 0.4 kV AC voltage which is the desired voltage to supply the nanogrids local loads and to supply through the nanogrids converters the 0.4 kV DC microgrid bus connected load (31) and (32).
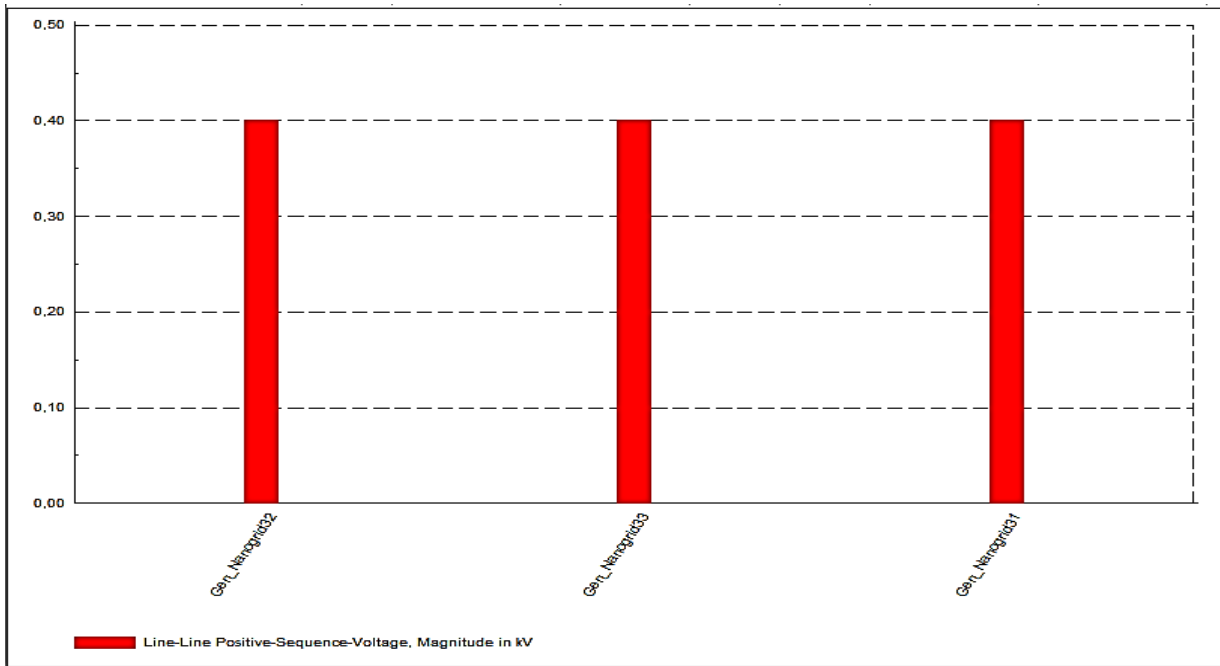
Figure 5. 23: Voltage profile of nanogrid generators within microgrid 3.

As mentioned, each nanogrid generator is required to provide power to its local load and loads connected to the microgrid through converters. The power profile of all nanogrids within the microgrid 3 is shown in Figure 5.24. Nanogrid31 generates 6.1 kW, while Nanogrid32 and Nanogrid33 generate 5.8 kW and 8.8 kW respectively.
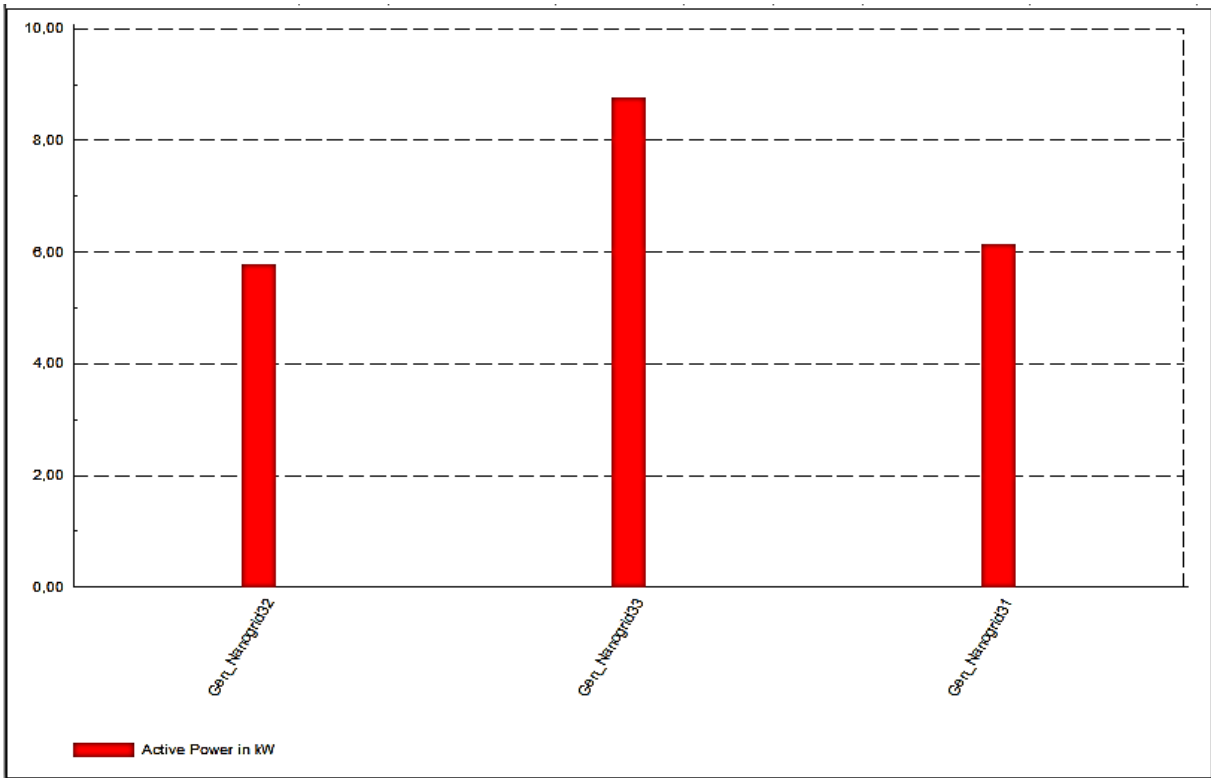
Figure 5. 24: Power profile of all nanogrids generators within microgrid 3.

Power produced is shared between local and microgrid loads through converters, namely Conv_31, Conv_32 and Conv_33. From Figure 5.25 taking into account the power demand profile of all loads, it is observed that the nanogrid generators are successful supplying power to all the loads.
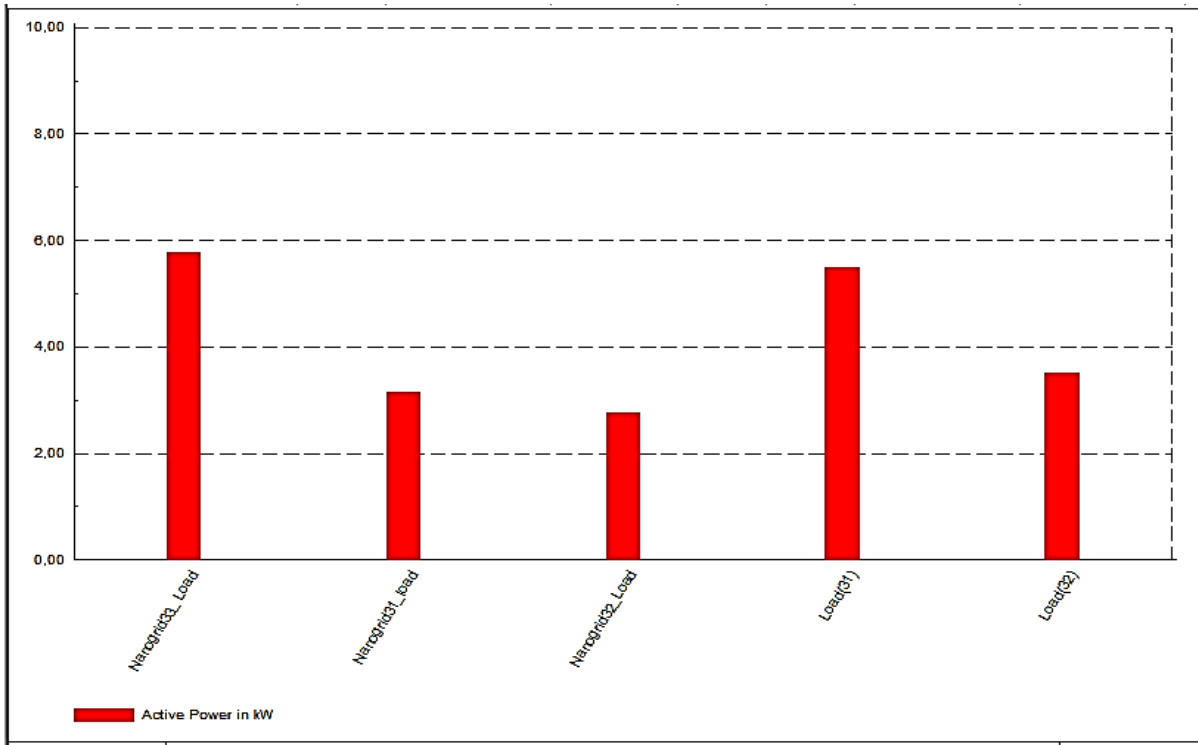
Figure 5. 25: Power demand profile of all loads within microgrid 3.

The power demand from microgrid connected loads is evenly divided among the nanogrid, which is well illustrated in Figure 5.25, where it is shown that the power export profile by each nanogrid through the converters Conv_31, Conv_32, and Conv_33. It is observed that each of the three nanogrids is exporting 3 kW to the microgrid to meet the total demand of 9 kW from load (31) and (32).

The process of power export between the nanogrid generator and the microgrid bus is achieved without overloading the generator as shown in Figure 5.26 of all nanogrid generators loading. The nanogrid31 generator is loading up to 20.5%, while nanogrid32 and nanogrid33 are loaded up to 19.9% and 28,7%, respectively. In microgrid 3, like for microgrids presented in previous sections, the loading of the nanogrid generator is a key parameter to monitor in order to successfully achieve the interconnection of nanogrids to form an operational microgrid. Each nanogrid overall controller would interrupt the power export and keep the local loads in case of critical loading of the generator according to the machine specifications.
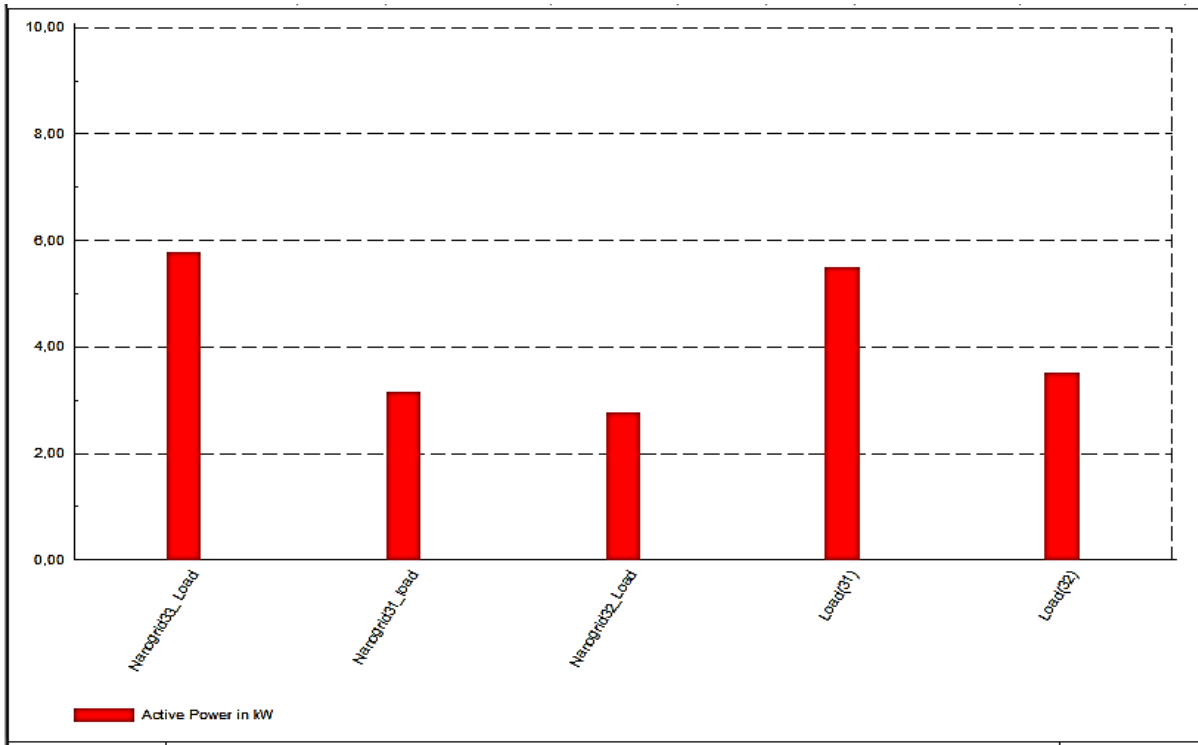
Figure 5. 25: Profile of power export through nanogrid converters within microgrid 3.
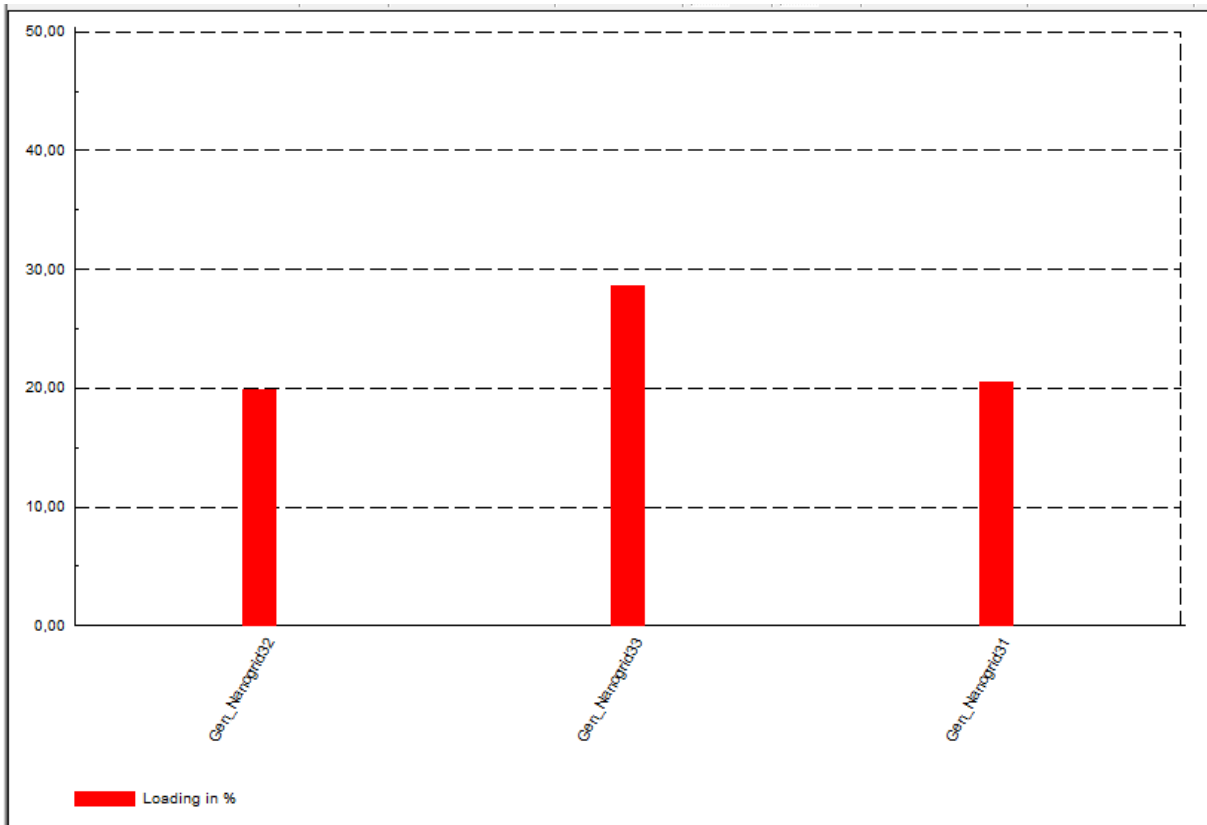
Figure 5. 26: Microgrid 3 nanogrids generators loading.

5.5 Intermediate low voltage direct current minigrid

The intermediate low voltage direct current (ILVDC) system as proposed in chapter four aims for the interconnection of sparsely electrified areas for power exchange and for an eventual utility grid connection. In this section, microgrids discussed in the previous section are considered as sparse electrified areas to be interconnected to form a minigrid.

Therefore, the minigrid consists of the three 0.4kV DC microgrids interconnected through a 3 kV DC network. A DC-DC converter is interfaced between each microgrid and the 3 kV DC bus; the converter has bi-directional capability associated to two operation modes, namely, boost and buck. It operates as boost for power export to the minigrid and as buck for the purpose of importing power to microgrids. The microgrid overall control, discussed in chapter four, regulates operations according to actual context in the microgrid. It decides which action is to be taken, and if any power exchange is needed between power import or export it decides which one to activate and consequently the converter mode of operation.

Power exchange can be between microgrids themselves or with the utility grid. The latter would provide support to microgrids in the event of insufficient generating capacity within the minigrid.

For the evaluation of the interconnection of microgrids and its impact on individual microgrid nanogrids and nanogrids loads involved, three scenarios are considered, and load flow simulations are performed on each. The three scenarios are:

1. All the three microgrid are interconnected for minigrid formation through an ILVDC network, with each microgrid considered as self-sufficient.
2. One microgrid requires power support from the two remaining microgrids.
3. All the microgrids require power support from the utility grid.

5.5.1 Scenario 1: ILVDC network interconnection for microgrids

5.5.1.1 Description

This scenario represents the interconnection of all microgrids in normal operating conditions with each microgrid demand versus supply equation balanced. Hence, there is no need for power exchange despite being interconnected. The objective is to see the voltage profile of the formed minigrid and the loading on its lines. Figure 5.27 shows the 3 kV ILVDC network which is linked to the utility 3 kV AC through an AC/DC converter, as modelled in DigSilent PowerFactory. Connected on the same bus is a distribution transformer serving utility connected customers which is represented by a general load of 2 MW.
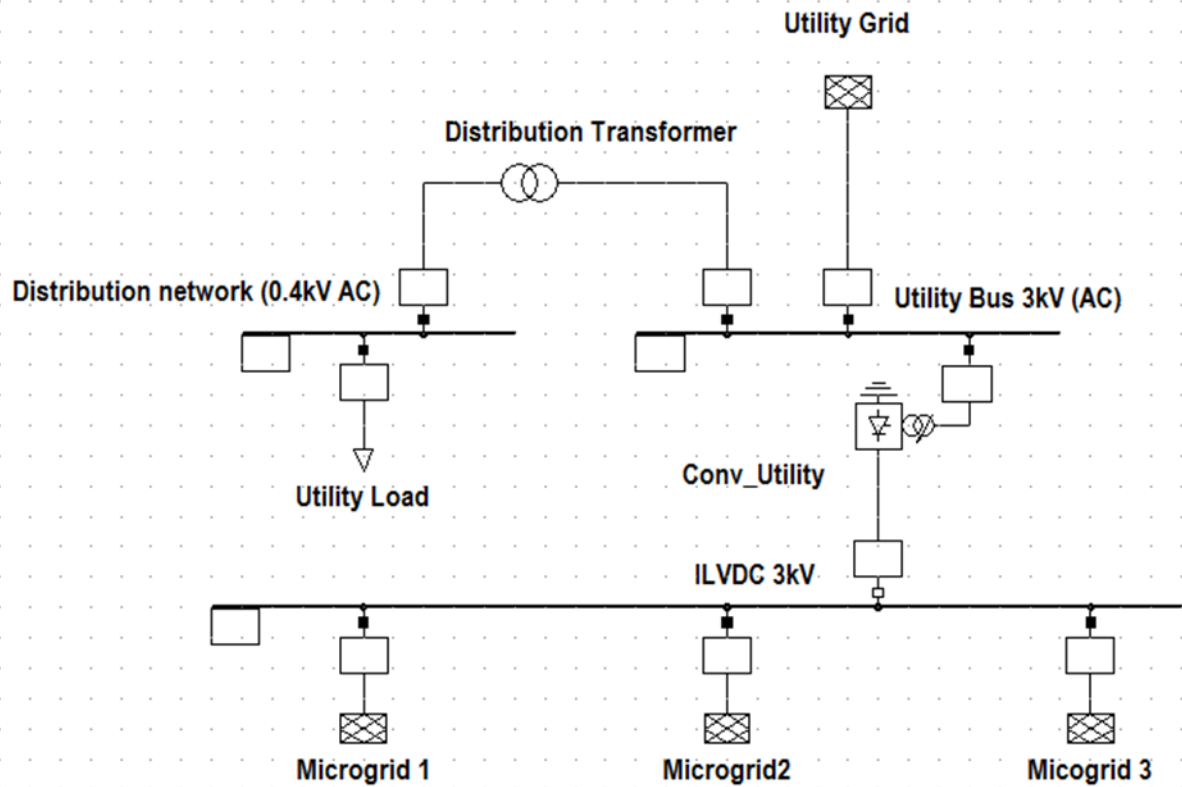
Figure 5. 27: ILVDC network interconnection with the utility grid.

For the first scenario, all microgrids are connected to the abovementioned ILVDC bus through feeders and distributors mostly over headlines. The efficiency and related losses due to the lines and other equipment in the network are not the focus of this study. Hence, they have not been specifically highlighted, and are instead implicitly embedded with the loads as losses are seen as a load from the generator perspective. Therefore, for this scenario, each microgrid is connected to the ILVDC network through a modular DC/DC converter as shown in Figure 5.28; for microgrid 1, 2, and 3 the converter used is bi-directional modular type. The reason for the use of the modular converter is to achieve the desired high voltage level using affordable low voltage rated components in addition to easy maintenance and replacement of a faulty component without replacing the whole converter.
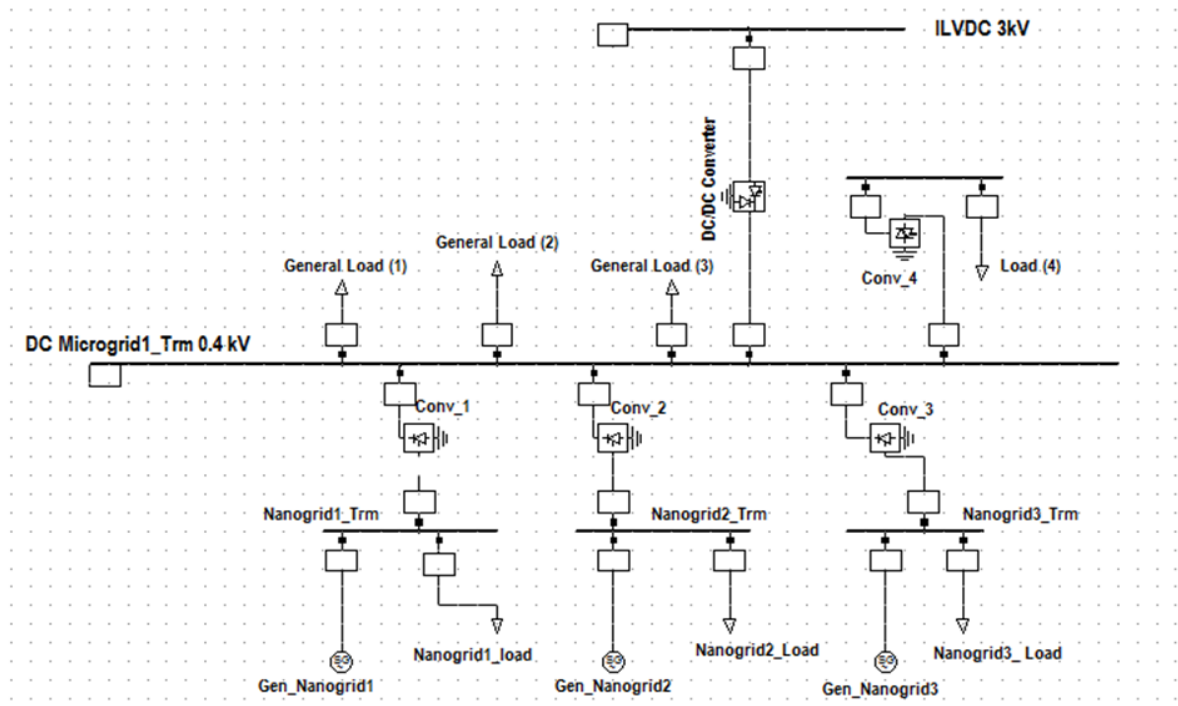
Figure 5. 28: Microgrid 1 interconnection to the ILVDC network.

A similar approach is used for microgrid 2 and 3 as shown in Figure 5.29 and Figure 5.30. A modular DC/DC converter boosts the 0.4 kV from the microgrid bus up to the ILVDC bus voltage level which is 3 kV. Converter harmonics are not considered in this case and an assumption is made that the converter harmonics complies within the range stated by the IEC 61000-3- 2 and IEEE 519 standards. The import of power to the microgrid buck converter is considered to have similar attributes with regards to the harmonic standards. Furthermore, in modelling the microgrid for buck operation modularity of the converter was not considered as the focus is on power flow and voltage profile at the bus.

Converter simulations settings of both converters are shown in Figure 5.31, for buck operation four 25 kA rated modules and a duty circle of 1.9 for the three, and 1.125 for the remaining, are used to boost the 0.4 kV to 3 kV, while for the buck operation the duty circle is set at 0.13.

176
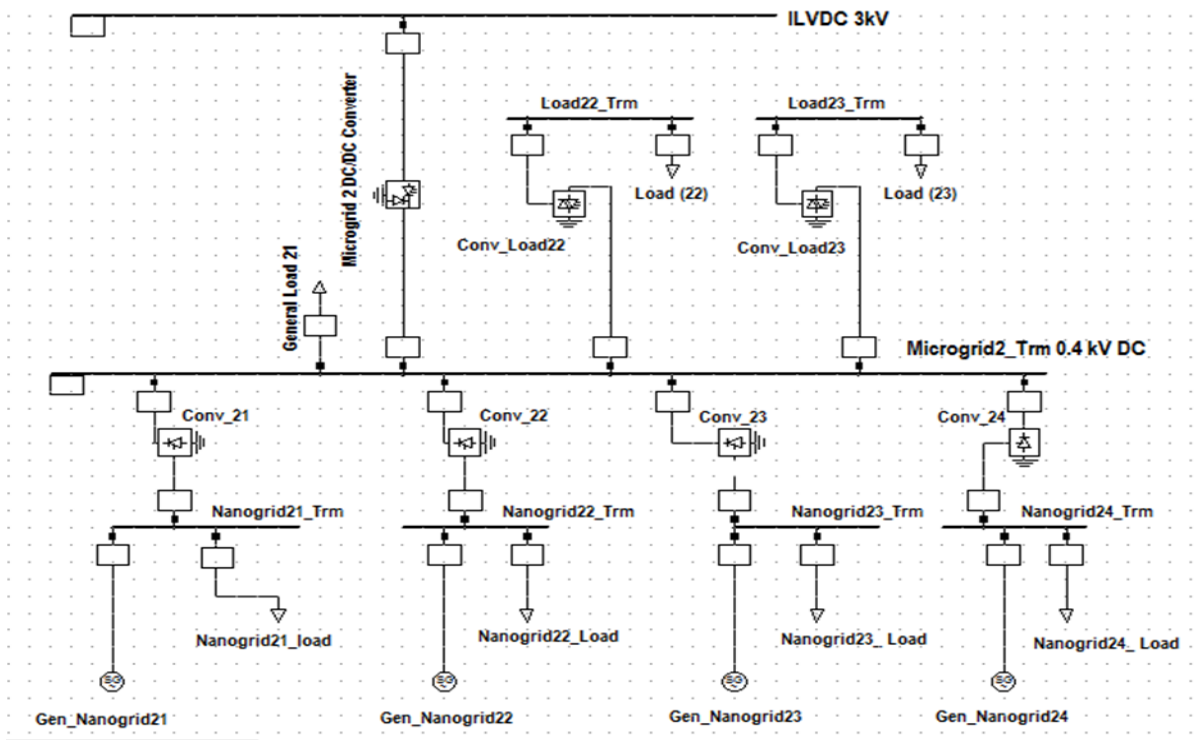
Figure 5. 29: Microgrid 2 interconnection to the ILVDC network.
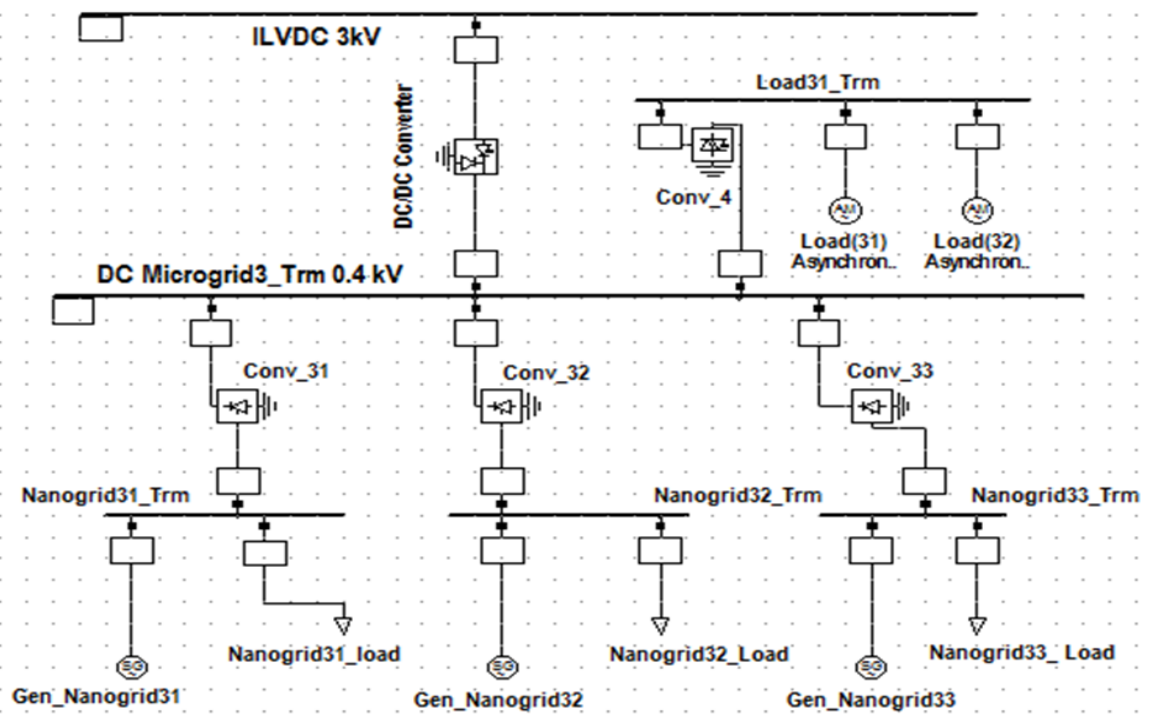
Figure 5. 30: Microgrid3 interconnection to the ILVDC network.

177

(a)   **(b)**
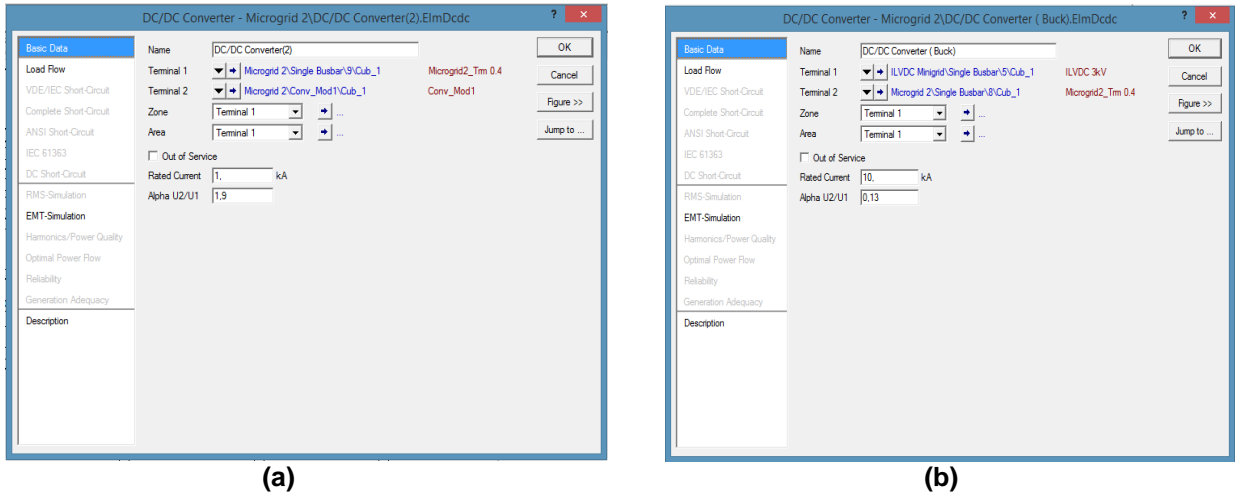
Figure 5. 31: Microgrid to ILVDC interface converter settings a) Boost mode and b) Buck mode.

5.5.1.2 Scenario 1 simulation results

A simulation of the network interconnection developed in DigSilent is conducted to analyse the behaviour of all components of the microgrids. The voltage profile at the ILVDC bus bar, power exchange, and the nanogrids generators loading are the subjects of analysis. As discussed in the previous section, this scenario consists of interconnecting microgrids for the formation of a minigrid. However, none of them require power imports and the utility grid is disconnected from the minigrid. A balanced positive sequence load flow is performed, with an automatic tap adjusting transformer for reactive control being considered, and active power control as dispatched by each microgrid. The distributed slack by generation is the option used for balancing and a maximum of 25 Newton Raphson iteration with automatic adaptation for convergence. A maximum acceptable load flow error for the model equation is 0.1%.

Load flow simulation results are shown in Figure 5.32 in which the voltage profile is at the ILVDC bus after the interconnection of three microgrids. The voltage at the interconnection bus is 3.1 kV, in the range of 1.05 as required, thus the interconnection for minigrid formation is successful. Looking at the loading of each microgrid generator, as shown in Figure 5.33, the interconnection does not affect the loading of the generators as in this scenario there is no power exchange.

The generators are supplying nanogrid local loads and microgrid connected loads. The loading remain is within the stability range, that is, less than 80% of its generation capacity. For scenario one, the proposed network achieves the objectives intended.
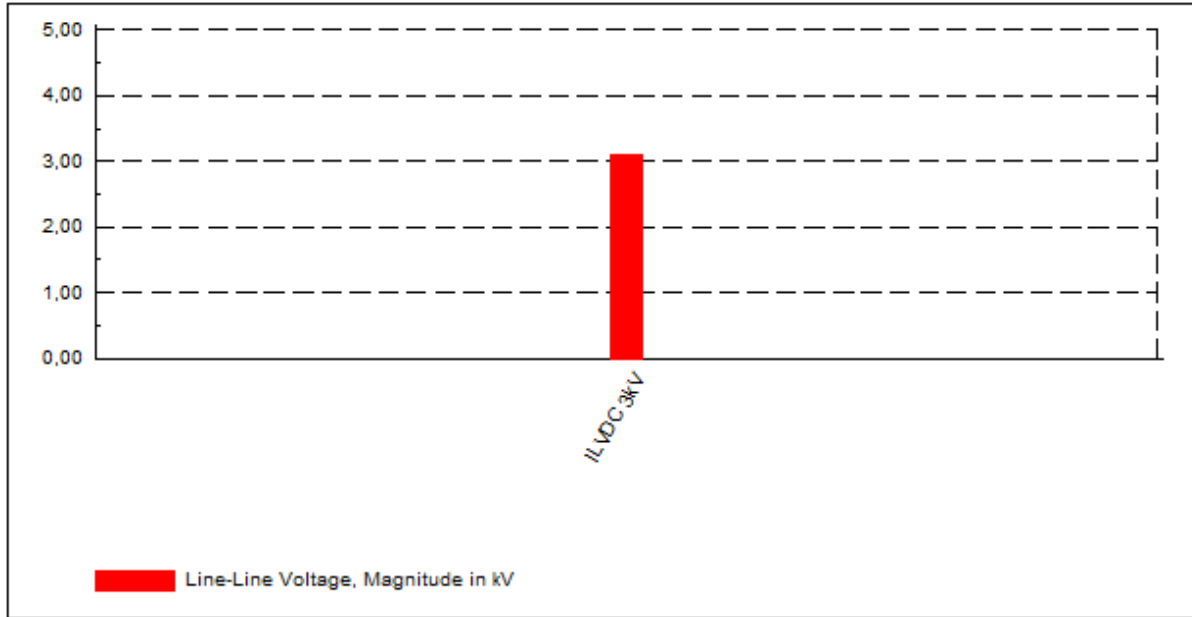
Figure 5. 32: Voltage profile at the ILVDC minigrid bus.
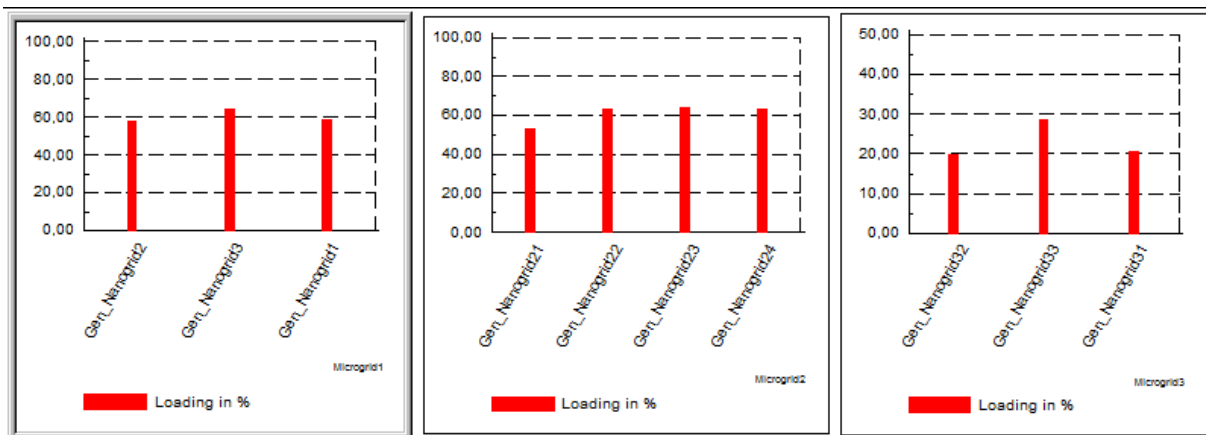
Figure 5. 33: Microgrids generators loading.

5.5.2 Scenario 2: Microgrids power exchange through the ILVDC network

5.5.2.1 Description

In this case, interconnected microgrids are exchanging power over the intermediate low voltage direct current (ILVDC) network. The exchange results from one microgrid requesting support from other microgrids. The scenario represents the normal operation of the network, which consist of power exchange from one microgrid with enough reserve due to low loading, to the other ones with slightly higher demand from their loads. Thus, support is requested from other microgrids through their interconnection.

Microgrid 2 shown in Figure 5.34 is considered as the subject of scenario two where due to the load demand is relatively high compared to microgrid 1 and microgrid 3. The total load demand connected on the microgrid 2 bus is 65.1 kW, while for microgrid 1 it is 37.5 kW and 9kW for microgrid 3. It is clear that microgrid 2 would need much support than microgrid 1and that microgrid 3 will be supporting both if need be.

Note that in terms of loads and machine specification all microgrids are in normal conditions as describe in scenario one in the previous section. They are expected to support each other to cover the power demand from the loads. The loading of generators and power exchange are characteristics of interest in this case.

It is worthwhile reminding that the microgrids are interconnected through 3 kV by a DC/DC converter with bi-directional capability. It operates as a boost converter for power export to the ILVDC grid and as a buck converter for power import. During the export, it boosts up the microgrids bus voltage from 0.4 kV up to 3 kV the ILVDC network bus voltage.

Simulations of this scenario as in the previous case are performed using DIgSILENT PowerFactory with the stability criteria generator loading set at 80%; Beyond this point the generator is considered to be overloaded. The voltage profile is set at 3 kV with permissible deviation of 1.05 per unit.
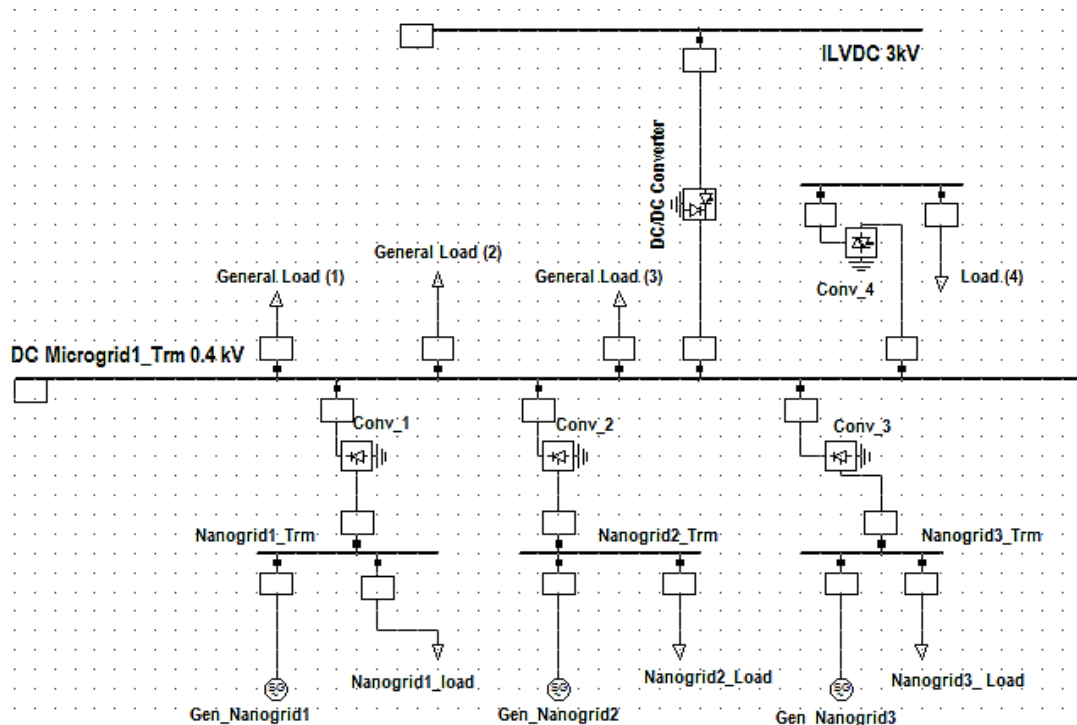
Figure 5. 34: Scenario 2- all microgrid 2 generators on.

180

5.5.2.2 Scenario 2 simulations results

A. Description

Two sets of load flow simulations are performed. The first is the normal interconnection of all microgrids and the second simulation considers the loss of two generators by microgrid 2. In both cases, the loading of generators and power flow in each microgrid are analysed to determine the operability of the proposed system for the interconnection and development of a grid from bottom-up.

B. Scenario2A: Normal interconnection of all microgrids

Figure 5.35 shows the terminals load flow report of microgrid 1. From the report we can see that the loading of the nanogrid generators are 36.35%, 40.15% and 35.81% for nanogrid 1, 2, and 3, respectively. All three nanogrids within the microgrids contribute equally to the microgrid formation through the converter by providing 11.15 kW.

```
μ-------------------------------------------------------------------------------------------------------------
| Grid: Microgrid1          System Stage: Microgrid1     | Study Case: Study Case           | Annex:        / 5 |
-------------------------------------------------------------------------------------------------------------
|          rated                        Active Reactive Power             |                                  |
|         Voltage      Bus-voltage      Power   Power  Factor Current Loading|          Additional Data       |
|         [kV]  [p.u.]   [kV]   [deg]   [kW]    [kvar]  [-]    [kA]    [%]  |                                  |
-------------------------------------------------------------------------------------------------------------
|Terminal                                                                 |                                  |
|         0,40   1,00   0,40   0,00                                        |                                  |
|  Cub_2  /Lodlv   Load (4)             5,51    1,81   0,95   0,01         |                                  |
|  Cub_3  /Vscmono Conv_4               5,51    1,81   0,95   0,01         |                                  |
|                                                                         |                                  |
|Trm_Nanogrid 2                                                           |                                  |
|         0,40   1,00   0,40   0,00                                        |                                  |
|  Cub_1  /Sym      Gen_Nanogrid2      13,91   11,27   0,78   0,03   35,81 |Typ:     SL                       |
|  Cub_2  /Lodlv    Nanogrid2_Load      2,76    1,22   0,91   0,00         |                                  |
|  Cub_3  /Recmono  Conv_2             11,15   10,05   0,74   0,02         |                                  |
|                                                                         |                                  |
|Trm_Nanogrid 2(1)                                                        |                                  |
|         0,40   1,00   0,40   0,00                                        |                                  |
|  Cub_1  /Sym      Gen_Nanogrid3      15,91   12,24   0,79   0,03   40,15 |Typ:     PV                       |
|  Cub_2  /Lodlv    Nanogrid3_ Load     4,76    2,19   0,91   0,01         |                                  |
|  Cub_3  /Recmono  Conv_3             11,15   10,05   0,74   0,02         |                                  |
|                                                                         |                                  |
|Trm_Nanogrid1                                                            |                                  |
|         0,40   1,00   0,40   0,00                                        |                                  |
|  Cub_4  /Lodlv    Nanogrid1_load      3,01    1,34   0,91   0,00         |                                  |
|  Cub_6  /Sym      Gen_Nanogrid1      14,16   11,39   0,78   0,03   36,35 |Typ:     SL                       |
|  Cub_7  /Recmono  Conv_1             11,15   10,05   0,74   0,02         |                                  |
|                                                                         |                                  |
-------------------------------------------------------------------------------------------------------------
```

Figure 5. 35: Microgrid1 all terminals power flow profile and loadings, Scenario 2A.

The total power contribution by the three nanogrids towards the microgrid 1 bus is 33.6 kW while the load demand attached to the bus, namely General loads 1 to 4, amounts to 37.5 kW. The power deficit between the microgrid supply and the load demand is provided by the other microgrid through the ILVDC network as shown in Figure 5.36 of the microgrid 1 bus power flow profile. 4.1 kW is imported from the ILVDC grid through the DC/DC converter, which is also observable in Figure 5.37 of the microgrid 3 bus power profile results.

```
----------------------------------------------------------------------------------------------------------
| Grid: Microgrid1          System Stage: Microgrid1     | Study Case: Study Case        | Annex:        / 4 |
----------------------------------------------------------------------------------------------------------
|          rated              Active Reactive Power                        |                                   |
|       Voltage     Bus-voltage    Power   Power   Factor Current Loading|        Additional Data            |
|       [kV] [p.u.]   [kV]   [deg]  [kW]  [kvar]   [-]   [kA]    [%]  |                                   |
----------------------------------------------------------------------------------------------------------
|Single Busbar                                                           |                                   |
| 3       0,40  0,00   0,00   0,00                                      |                                   |
| DC Microgr,40  1,00   0,40   0,00                                     |                                   |
|  Cub_1 /Lod      General Load (1)   20,00   0,00   1,00   0,05        |P10:   20,00 kW   Q10:   0,00 kvar |
|  Cub_1 /Lod      General Load (2)    9,00   0,00   1,00   0,02        |P10:    9,00 kW   Q10:   0,00 kvar |
|  Cub_1 /Lod      General Load (3)    3,00   0,00   1,00   0,01        |P10:    3,00 kW   Q10:   0,00 kvar |
|  Cub_1 /Dcdc     DC/DC Converter(1)  -4,05  0,00   1,00  -0,01   1,01 |                                   |
|  Cub_1 /Dcdc     DC/DC Converter(2)   0,00  0,00   1,00   0,00   0,00 |                                   |
|  Cub_1 /Recmono  Conv_1             -11,15  0,00   1,00  -0,03        |                                   |
|  Cub_1 /Recmono  Conv_2             -11,15  0,00   1,00  -0,03        |                                   |
|  Cub_1 /Recmono  Conv_3             -11,15  0,00   1,00  -0,03        |                                   |
|  Cub_1 /Vscmono  Conv_4              -5,51  0,00   1,00  -0,01        |                                   |
|                  Total            -------  -------                    |                                   |
|                  Load:              32,00   0,00                      |                                   |
|                                                                        |                                   |
|Conv_Mod1                                                               |                                   |
|        0,76  0,00   0,00   0,00                                        |                                   |
|  Cub_1 /Dcdc     DC/DC Converter(2)   0,00  0,00   1,00   0,00   0,00 |                                   |
|  Cub_2 /Dcdc     DC/DC Converter(3)   0,00  0,00   1,00   0,00   0,00 |                                   |
|                                                                        |                                   |
|Conv_Mod2                                                               |                                   |
|        1,44  0,00   0,00   0,00                                        |                                   |
|  Cub_1 /Dcdc     DC/DC Converter(3)   0,00  0,00   1,00   0,00   0,00 |                                   |
|  Cub_2 /Dcdc     DC/DC Converter(4)   0,00  0,00   1,00   0,00   0,00 |                                   |
|                                                                        |                                   |
|Conv_Mod3                                                               |                                   |
|        2,76  0,00   0,00   0,00                                        |                                   |
|  Cub_1 /Dcdc     DC/DC Converter(4)   0,00  0,00   1,00   0,00   0,00 |                                   |
|  Cub_2 /Dcdc     DC/DC Converter(5)   0,00  0,00   1,00   0,00   0,00 |                                   |
|                                                                        |                                   |
----------------------------------------------------------------------------------------------------------
```

Figure 5. 36: Microgrid 1 bus power flow profile, Scenario 2A.

An export of 24.5 kW from microgrid 3 through the DC/DC converter towards the ILVDC is observed. The exported power from the microgrid comes from the equal contributions of all nanogrids within microgrid 3. Each nanogrid, through its AC/DC converter, is exporting power towards the microgrid 3 bus with an average of -11.2 kW, which amounts to 33.6 kW in total. A small amount of that power, 9 kW, is consumed by the microgrid connected loads while the rest is transferred to the ILVDC network.

```
----------------------------------------------------------------------------------------------------------
| Grid: Microgrid3          System Stage: Microgrid3     | Study Case: Study Case        | Annex:        / 6 |
----------------------------------------------------------------------------------------------------------
|          rated              Active Reactive Power                        |                                   |
|       Voltage     Bus-voltage    Power   Power   Factor Current Loading|        Additional Data            |
|       [kV] [p.u.]   [kV]   [deg]  [kW]  [kvar]   [-]   [kA]    [%]  |                                   |
----------------------------------------------------------------------------------------------------------
|Single Busbar                                                           |                                   |
| 3       0,40  0,00   0,00   0,00                                      |                                   |
| DC Microgr,40  1,00   0,40   0,00                                     |                                   |
|  Cub_1 /Dcdc     DC/DC Converter      0,00  0,00   1,00   0,00   0,00 |                                   |
|  Cub_1 /Dcdc     DC/DC Converter(4)  24,46  0,00   1,00   0,06   6,09 |                                   |
|  Cub_1 /Recmono  Conv_31            -11,15  0,00   1,00  -0,03        |                                   |
|  Cub_1 /Recmono  Conv_32            -11,15  0,00   1,00  -0,03        |                                   |
|  Cub_1 /Recmono  Conv_33            -11,15  0,00   1,00  -0,03        |                                   |
|  Cub_1 /Vscmono  Conv_4              -9,00  0,00   1,00  -0,02        |                                   |
|                                                                        |                                   |
|Conv_Mod1                                                               |                                   |
|        0,76  0,00   0,00   0,00                                        |                                   |
|  Cub_1 /Dcdc     DC/DC Converter      0,00  0,00   1,00   0,00   0,00 |                                   |
|  Cub_2 /Dcdc     DC/DC Converter(1)   0,00  0,00   1,00   0,00   0,00 |                                   |
|                                                                        |                                   |
|Conv_Mod2                                                               |                                   |
|        1,44  0,00   0,00   0,00                                        |                                   |
|  Cub_1 /Dcdc     DC/DC Converter(1)   0,00  0,00   1,00   0,00   0,00 |                                   |
|  Cub_2 /Dcdc     DC/DC Converter(2)   0,00  0,00   1,00   0,00   0,00 |                                   |
|                                                                        |                                   |
|Terminal                                                                |                                   |
|        0,40  1,00   0,40   0,00                                        |                                   |
|  Cub_4 /Asm      Load(31)             5,50  2,45   0,91   0,01   1,40 |Slip:   3,26 %   xm:   4,00 p.u.  |
|  Cub_5 /Asm      Load(32)             3,50  1,22   0,94   0,01   0,86 |Slip:   1,92 %   xm:   4,00 p.u.  |
|  Cub_3 /Vscmono  Conv_4               9,00  3,66   0,93   0,01        |                                   |
|                  Total            -------  -------                    |                                   |
|                  Motor Load:         9,00   3,66                      |                                   |
----------------------------------------------------------------------------------------------------------
```

Figure 5. 37: Microgrid 3 bus power flow profile, Scenario 2A.

The power exported from the microgrid is generated by the three nanogrid generators: Gen_Nanogrid31, 32, and 33. Each generator contributes 11.15kW towards the microgrids bus in addition to the power delivered to the nanogrids loads as shown in Figure 5.38 of the power profile and loading at all terminals within microgrid 3. From the power profile and loading results, it can be seen that the power export and the supply to local loads do not overload the generators, as loadings of 36.16%, 35.42%, and 41.75% are observed for Nanogrid 31, 32 and 33 generators.

```
□------------------------------------------------------------------------------------------------
| Grid: Microgrid3         System Stage: Microgrid3      | Study Case: Study Case            | Annex:                 / 7 |
------------------------------------------------------------------------------------------------
|         rated              Active Reactive Power                    |                              |
|      Voltage     Bus-voltage        Power   Power   Factor Current Loading|          Additional Data          |
|      [kV]  [p.u.]   [kV]    [deg]   [kW]    [kvar]   [-]    [kA]    [%]  |                              |
------------------------------------------------------------------------------------------------
|Trm_Nanogrid 32                                                      |                              |
|        0,40   1,00   0,40    0,00                                    |                              |
|  Cub_1  /Sym     Gen_Nanogrid32    13,91   10,96   0,79    0,03   35,42 |Typ:    SL                  |
|  Cub_2  /Lodlv   Nanogrid32_Load    2,76    0,91   0,95    0,00       |                              |
|  Cub_3  /Recmono Conv_32           11,15   10,05   0,74    0,02       |                              |
|                                                                      |                              |
|Trm_Nanogrid33                                                       |                              |
|        0,40   1,00   0,40    0,00                                    |                              |
|  Cub_1  /Sym     Gen_Nanogrid33    16,91   12,24   0,81    0,03   41,75 |Typ:    SL                  |
|  Cub_2  /Lodlv   Nanogrid33_ Load   5,76    2,19   0,93    0,01       |                              |
|  Cub_3  /Recmono Conv_33           11,15   10,05   0,74    0,02       |                              |
|                                                                      |                              |
|Trm_Nanogrid31                                                       |                              |
|        0,40   1,00   0,40    0,00                                    |                              |
|  Cub_4  /Lodlv   Nanogrid31_load    3,14    1,03   0,95    0,00       |                              |
|  Cub_6  /Sym     Gen_Nanogrid31    14,29   11,08   0,79    0,03   36,16 |Typ:    SL                  |
|  Cub_7  /Recmono Conv_31           11,15   10,05   0,74    0,02       |                              |
|                                                                      |                              |
|Conv_Mod3                                                            |                              |
|        2,80   0,00   0,00    0,00                                    |                              |
|  Cub_1  /Dcdc   DC/DC Converter(2)  0,00    0,00   1,00    0,00   0,00 |                              |
|  Cub_2  /Dcdc   DC/DC Converter(3)  0,00    0,00   1,00    0,00   0,00 |                              |
|                                                                      |                              |
------------------------------------------------------------------------------------------------
```

Figure 5. 38:Microgrid3 all terminals power flow profile and loadings, Scenario2A.

From the above discussion in scenario two in the case with the normal interconnection of microgrids through the ILVDC network, microgrid 3 is exporting 24.5 kW towards the ILVDC bus. Knowing that microgrid 1 is importing 4.1 kW, consequently, the remaining 20,4 kW are taken by microgrid 2 as confirmed by the microgrid 2 bus power profile results shown in Figure 5.39. From the Figure 5.40 it is observed that 20.41 kW is imported from the ILVDC bus to the microgrid 2 bus through the DC/DC converter.

The average total load demand connected to the microgrid 2 bus is 65.1 kW. The nanogrid generators supply 44.8 kW in total and the deficit 20,4 kW is imported from microgrid 3. The loading and power profile of all terminals in microgrid 3 are shown in Figure 5.39. It can be seen that the loading of the nanogrids generators is 34,2%, 20.68%, 42.04% and 41.36% for Gen_Nanogrid 21, 22, 23 and 24 respectively. From the loading values obtained, it shows that power contribution of other microgrids towards microgrid2 demand plays a role in maintaining the low loading of the generators. This is clearer with the second set of the load flow simulation in the next section, where the unavailability of generators is considered.

```
----------------------------------------------------------------------------------------------------------------------------------
| Grid: Microgrid 2          System Stage: Microgrid 2     | Study Case: Study Case            | Annex:                    / 2  |
----------------------------------------------------------------------------------------------------------------------------------
|          rated             Active Reactive Power         |                                                                    |
|       Voltage    Bus-voltage    Power  Power  Factor Current Loading|                 Additional Data                          |
|       [kV]  [p.u.]   [kV]   [deg]  [kW]  [kvar]   [-]    [kA]    [%] |                                                          |
----------------------------------------------------------------------------------------------------------------------------------
|Single Busbar                                             |                                                                    |
| 3       0,40    0,00    0,00    0,00                     |                                                                    |
| Microgrid2,40   1,00    0,40    0,00                     |                                                                    |
|  Cub_1  /Lod       General Load 21    35,00   0,00  1,00   0,09   |P10:    35,00 kW   Q10:  11,50 kvar                       |
|  Cub_1  /Dcdc      DC/DC Converter (  -20,41  0,00  1,00  -0,05   5,08 |                                                     |
|  Cub_1  /Dcdc      DC/DC Converter(2)   0,00  0,00  1,00   0,00   0,00 |                                                     |
|  Cub_1  /Recmono   Conv_21            -11,15  0,00  1,00  -0,03   |                                                          |
|  Cub_1  /Recmono   Conv_22            -11,15  0,00  1,00  -0,03   |                                                          |
|  Cub_1  /Recmono   Conv_23            -11,15  0,00  1,00  -0,03   |                                                          |
|  Cub_1  /Recmono   Conv_24            -11,15  0,00  1,00  -0,03   |                                                          |
|  Cub_1  /Vscmono   Conv_Load22        -11,76  0,00  1,00  -0,03   |                                                          |
|  Cub_1  /Vscmono   Conv_Load23        -18,26  0,00  1,00  -0,05   |                                                          |
|                                                          |                                                                    |
|Conv_Mod1                                                 |                                                                    |
|         0,76    0,00    0,00    0,00                     |                                                                    |
|  Cub_1  /Dcdc      DC/DC Converter(2)   0,00  0,00  1,00   0,00   0,00 |                                                     |
|  Cub_2  /Dcdc      DC/DC Converter(3)   0,00  0,00  1,00   0,00   0,00 |                                                     |
|                                                          |                                                                    |
|Conv_Mod2                                                 |                                                                    |
|         1,44    0,00    0,00    0,00                     |                                                                    |
|  Cub_1  /Dcdc      DC/DC Converter(3)   0,00  0,00  1,00   0,00   0,00 |                                                     |
|  Cub_2  /Dcdc      DC/DC Converter(4)   0,00  0,00  1,00   0,00   0,00 |                                                     |
|                                                          |                                                                    |
|Conv_Mod3                                                 |                                                                    |
|         2,76    0,00    0,00    0,00                     |                                                                    |
|  Cub_1  /Dcdc      DC/DC Converter(4)   0,00  0,00  1,00   0,00   0,00 |                                                     |
|  Cub_2  /Dcdc      DC/DC Converter(5)   0,00  0,00  1,00   0,00   0,00 |                                                     |
|                                                          |                                                                    |
----------------------------------------------------------------------------------------------------------------------------------
```

Figure 5. 39: Microgrid 2 bus power flow profile 2A.

```
----------------------------------------------------------------------------------------------------------------------------------
| Grid: Microgrid 2          System Stage: Microgrid 2     | Study Case: Study Case            | Annex:                    / 3  |
----------------------------------------------------------------------------------------------------------------------------------
|          rated             Active Reactive Power         |                                                                    |
|       Voltage    Bus-voltage    Power  Power  Factor Current Loading|                 Additional Data                          |
|       [kV]  [p.u.]   [kV]   [deg]  [kW]  [kvar]   [-]    [kA]    [%] |                                                          |
----------------------------------------------------------------------------------------------------------------------------------
|Terminal                                                  |                                                                    |
|         0,40    1,00    0,40    0,00                     |                                                                    |
|  Cub_2  /Lodlv     Load (22)           11,76   3,37  0,96   0,02   |                                                          |
|  Cub_3  /Vscmono   Conv_Load22         11,76   3,37  0,96   0,02   |                                                          |
|                                                          |                                                                    |
|Terminal(1)                                               |                                                                    |
|         0,40    1,00    0,40    0,00                     |                                                                    |
|  Cub_2  /Lodlv     Load (23)           18,26   6,00  0,95   0,03   |                                                          |
|  Cub_3  /Vscmono   Conv_Load23         18,26   6,00  0,95   0,03   |                                                          |
|                                                          |                                                                    |
|Trm_Nanogrid 24                                           |                                                                    |
|         0,40    1,00    0,40    0,98                     |                                                                    |
|  Cub_1  /Sym       Gen_Nanogrid24      13,91  15,30  0,67   0,03   41,36 |Typ:    SL                                         |
|  Cub_2  /Lodlv     Nanogrid24_ Load     2,76   5,25  0,47   0,01   |                                                          |
|  Cub_3  /Recmono   Conv_24             11,15  10,05  0,74   0,02   |                                                          |
|                                                          |                                                                    |
|Trm_Nanogrid 22                                           |                                                                    |
|         0,40    1,00    0,40    0,00                     |                                                                    |
|  Cub_1  /Sym       Gen_Nanogrid22      13,91  15,30  0,67   0,03   20,68 |Typ:    SL                                         |
|  Cub_2  /Lodlv     Nanogrid22_Load      2,76   5,25  0,47   0,01   |                                                          |
|  Cub_3  /Recmono   Conv_22             11,15  10,05  0,74   0,02   |                                                          |
|                                                          |                                                                    |
|Trm_Nanogrid 23                                           |                                                                    |
|         0,40    1,00    0,40    0,00                     |                                                                    |
|  Cub_1  /Sym       Gen_Nanogrid23      14,41  15,30  0,69   0,03   42,04 |Typ:    SL                                         |
|  Cub_2  /Lodlv     Nanogrid23_ Load     3,26   5,25  0,53   0,01   |                                                          |
|  Cub_3  /Recmono   Conv_23             11,15  10,05  0,74   0,02   |                                                          |
|                                                          |                                                                    |
|Trm_Nanogrid21                                            |                                                                    |
|         0,40    1,00    0,40    0,00                     |                                                                    |
|  Cub_4  /Lodlv     Nanogrid21_load      2,26   0,55  0,97   0,00   |                                                          |
|  Cub_6  /Sym       Gen_Nanogrid21      13,41  10,60  0,78   0,02   34,20 |Typ:    SL                                         |
|  Cub_7  /Recmono   Conv_21             11,15  10,05  0,74   0,02   |                                                          |
----------------------------------------------------------------------------------------------------------------------------------
```

Figure 5. 40: Microgrid 2 all terminals power flow profile and loadings, Scenario 2A.

C. Scenario2B: Interconnection of all microgrids and loss of generators within microgrid 2

The interconnection of all the three microgrids through the intermediate low direct current network simulation results discussed in the previous section shows the interaction between the microgrids. Power exchange between microgrid 3 and microgrid 2 is more significant as 20.41 kW are exported from microgrid 3 to microgrid 2 in order to support it. It has been observed that power exchange does not heavily influence the loading onto microgrid 3 generators, as a small portion of power is supplied to support microgrid 2 generating units.

In this section, a scenario of microgrid 2 losing two out its four generators and the resulting impact on the interconnected microgrids is discussed. Figure 5.41 shows the microgrid 2 model upon which the minigrid contingency analysis is based. Gen_Nanogrid21 is considered completely out of service as shown by the open circuit breaker while Gen_Nanogrid22 is isolated from the microgrid 2 bus yet is still supplying its own local loads. The latter case represents the situation where the nanogrid owner decides to isolate her/himself from the microgrid 2 bus or in the case of a faulty converter.
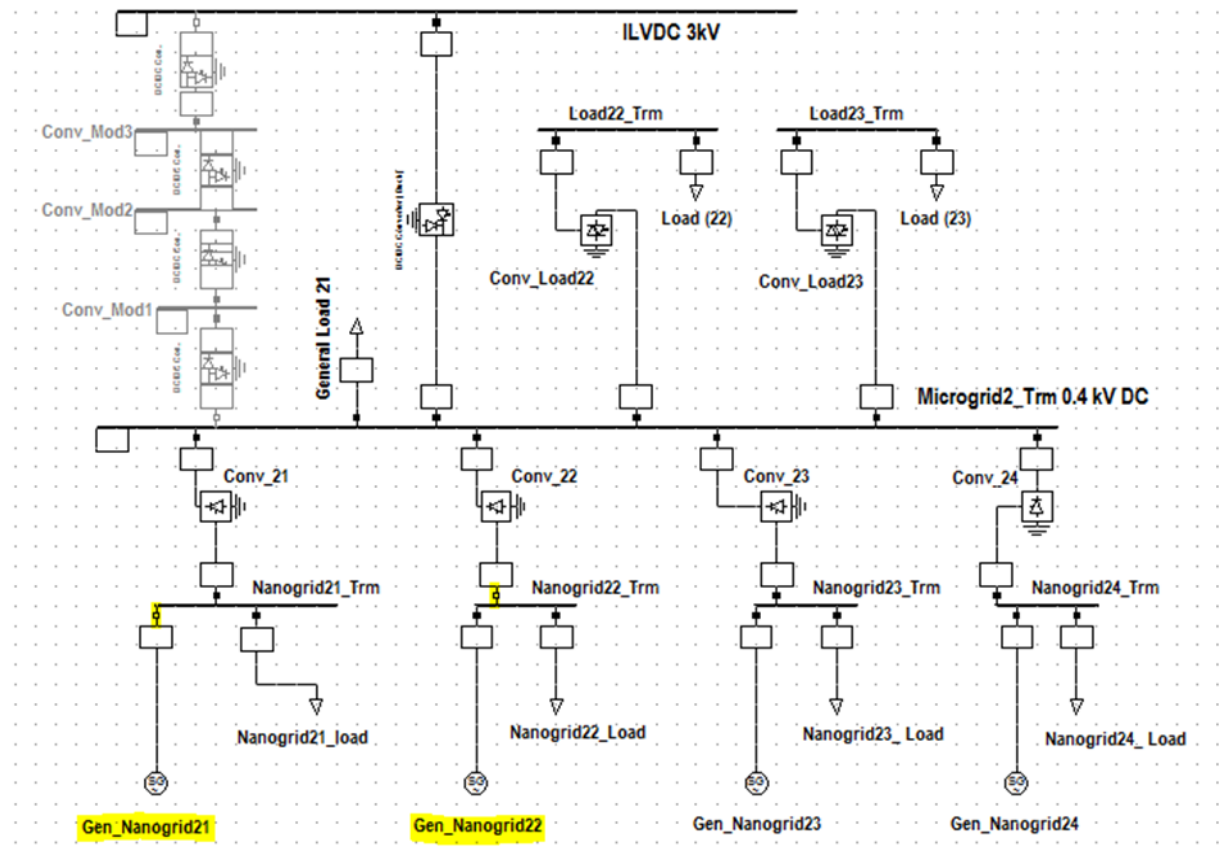
Figure 5. 41: Scenario 2 microgrid 2 with two generators off.

Two simulations of this scenario are performed, the first is performed with microgrid 2 in island mode operating with only two generators, Gen_Nanogrid23 and Gen_Nanogrid24. Gen_Nanogrid21 is switched off and isolated from the nanogrid21 terminal. This is to represent a condition where the generator is not running due to one reason or another, such as fuel shortage, faulty conditions, or being intentionally switched off by the owner. On the other hand, the Gen_Nanogrid22 is running but is isolated from microgrid 2 bus bar. This isolation might represent intentional isolation of the nanogrid by the owner or by the controller or might be due to a fault on the converter. The aim for this scenario simulation is to see with certainty the impact of losing half of the generation capacity on the rest of the nanogrid generators within the microgrid 2. The second simulation is performed with microgrid 2 in the same condition of two missing generators, however, is interconnected to the other microgrids. The aim is to analyse the contribution of microgrid 1 and 3 towards the stability of microgrid 2 upon the interconnection.

Figure 5.42 shows the islanded microgrid 2 terminals power profile and loading simulation results. The loss of Gen_Nanogrid21 and the isolation from the microgrid 2 bus of Gen_Nanogrid22 affects the remaining generators. The latter must take up the entire microgrid 2 demand, which drives the generators into overload condition with Gen_Nanogrid23 going up to 99.43% and 98.71% for Gen_Nanogrid24. This overloading drives both generators beyond their thermal stability which can result in insulation break up as well as the burn out of the machine if overload relay is not operated.

Grid: Microgrid 2				System Stage: Microgrid 2				Study Case: Study Case			Annex:	/ 3
	rated Voltage [kV]	[p.u.]	Bus-voltage [kV]	[deg]	Active Power [kW]	Reactive Power [kvar]	Power Factor [-]	Current [kA]	Loading [%]		Additional Data	
Terminal												
	0,40	1,00	0,40	0,00								
Cub_2 /Lodlv	Load (22)				11,76	3,37	0,96	0,02				
Cub_3 /Vscmono	Conv_Load22				11,76	3,37	0,96	0,02				
Terminal(1)												
	0,40	1,00	0,40	0,00								
Cub_2 /Lodlv	Load (23)				18,26	6,00	0,95	0,03				
Cub_3 /Vscmono	Conv_Load23				18,26	6,00	0,95	0,03				
Trm_Nanogrid 22												
	0,40	1,00	0,40	0,00								
Cub_1 /Sym	Gen_Nanogrid22				2,76	5,25	0,47	0,01	5,93	Typ:	SL	
Cub_2 /Lodlv	Nanogrid22_Load				2,76	5,25	0,47	0,01				
Cub_3 /Recmono	Conv_22				0,00	0,00	1,00	0,00				
Trm_Nanogrid 23												
	0,40	1,00	0,40	0,00								
Cub_1 /Sym	Gen_Nanogrid23				35,77	34,53	0,72	0,07	99,43	Typ:	SL	
Cub_2 /Lodlv	Nanogrid23_ Load				3,26	5,25	0,53	0,01				
Cub_3 /Recmono	Conv_23				32,51	29,28	0,74	0,06				
Trm_Nanogrid21												
	0,40	0,00	0,00	0,00								
Cub_4 /Lodlv	Nanogrid21_load				0,00	0,00	1,00	0,00				
Cub_6 /Sym	Gen_Nanogrid21				0,00	0,00	1,00	0,00	0,00	Typ:	SL	
Cub_7 /Recmono	Conv_21				0,00	0,00	1,00	0,00				
Trm_Nanogrid 24												
	0,40	1,00	0,40	0,98								
Cub_1 /Sym	Gen_Nanogrid24				35,27	34,53	0,71	0,07	98,71	Typ:	SL	
Cub_2 /Lodlv	Nanogrid24_ Load				2,76	5,25	0,47	0,01				
Cub_3 /Recmono	Conv_24				32,51	29,28	0,74	0,06				

Figure 5. 42: Scenario2B, Microgrid 2 terminals power load flow profile and loading (microgrid 2 in Island mode).

Meanwhile, the loading within microgrid 3 is 27.04% for Gen_Nanogrid31, 26.29% for Gen_Nanogrid32, and 32,67% for Gen_Nanogrid33 as shown in Figure 5.43 microgrid 3 all terminals power load flow profile and loading. As microgrid 3 is being interconnected with microgrid 1 through the ILVDC network, therefore microgrid 1 is getting power support of 14 kW from microgrid 3 through the DC/DC converter connected to the ILVDC network as shown Figure 5.44 where in microgrid 1 all terminals power flow and loading percentage is shown.

```
p-------------------------------------------------------------------------------------------------------
| Grid: Microgrid3        System Stage: Microgrid3    | Study Case: Study Case        | Annex:        / 7 |
-------------------------------------------------------------------------------------------------------
|        rated               Active Reactive Power            |                                         |
|        Voltage    Bus-voltage   Power  Power Factor Current Loading|        Additional Data           |
|        [kV]  [p.u.]  [kV]  [deg]  [kW]  [kvar]  [-]   [kA]   [%]  |                                    |
-------------------------------------------------------------------------------------------------------
|Conv_Mod3                                                    |                                         |
|        2,80   0,00   0,00   0,00                            |                                         |
|  Cub_1 /Dcdc    DC/DC Converter(2)  0,00  0,00  1,00  0,00  0,00 |                                    |
|  Cub_2 /Dcdc    DC/DC Converter(3)  0,00  0,00  1,00  0,00  0,00 |                                    |
|                                                             |                                         |
|Trm_Nanogrid31                                               |                                         |
|        0,40   1,00   0,40   0,00                            |                                         |
|  Cub_4 /Lodlv    Nanogrid31_load    3,14  1,03  0,95  0,00       |                                    |
|  Cub_6 /Sym      Gen_Nanogrid31    10,89  8,02  0,81  0,02  27,04 |Typ:    SL                          |
|  Cub_7 /Recmono  Conv_31            7,75  6,99  0,74  0,02       |                                    |
|                                                             |                                         |
|Trm_Nanogrid 32                                              |                                         |
|        0,40   1,00   0,40   0,00                            |                                         |
|  Cub_1 /Sym      Gen_Nanogrid32    10,51  7,90  0,80  0,02  26,29 |Typ:    SL                          |
|  Cub_2 /Lodlv    Nanogrid32_Load    2,76  0,91  0,95  0,00       |                                    |
|  Cub_3 /Recmono  Conv_32            7,75  6,99  0,74  0,02       |                                    |
|                                                             |                                         |
|Trm_Nanogrid33                                               |                                         |
|        0,40   1,00   0,40   0,00                            |                                         |
|  Cub_1 /Sym      Gen_Nanogrid33    13,51  9,18  0,83  0,02  32,67 |Typ:    SL                          |
|  Cub_2 /Lodlv    Nanogrid33_ Load   5,76  2,19  0,93  0,01       |                                    |
|  Cub_3 /Recmono  Conv_33            7,75  6,99  0,74  0,02       |                                    |
|                                                             |                                         |
-------------------------------------------------------------------------------------------------------
```

Figure 5. 43: Scenario2B, Microgrid 3 terminals power load flow profile and loading (Microgrid 2 in Island mode).

```
-------------------------------------------------------------------------------------------------------
| Grid: Microgrid1        System Stage: Microgrid1    | Study Case: Study Case        | Annex:        / 4 |
-------------------------------------------------------------------------------------------------------
|        rated               Active Reactive Power            |                                         |
|        Voltage    Bus-voltage   Power  Power Factor Current Loading|        Additional Data           |
|        [kV]  [p.u.]  [kV]  [deg]  [kW]  [kvar]  [-]   [kA]   [%]  |                                    |
-------------------------------------------------------------------------------------------------------
|Single Busbar                                                |                                         |
| 3        0,40   0,00   0,00   0,00                          |                                         |
| DC Microgr,40  1,00   0,40   0,00                           |                                         |
|  Cub_1 /Lod      General Load (1)   20,00  0,00  1,00  0,05      |P10:   20,00 kW   Q10:   0,00 kvar   |
|  Cub_1 /Lod      General Load (2)    9,00  0,00  1,00  0,02      |P10:    9,00 kW   Q10:   0,00 kvar   |
|  Cub_1 /Lod      General Load (3)    3,00  0,00  1,00  0,01      |P10:    3,00 kW   Q10:   0,00 kvar   |
|  Cub_1 /Dcdc     DC/DC Converter  -14,25  0,00  1,00 -0,04  3,55 |                                    |
|  Cub_1 /Recmono  Conv_1            -7,75  0,00  1,00 -0,02       |                                    |
|  Cub_1 /Recmono  Conv_2            -7,75  0,00  1,00 -0,02       |                                    |
|  Cub_1 /Recmono  Conv_3            -7,75  0,00  1,00 -0,02       |                                    |
|  Cub_1 /Vscmono  Conv_4            -5,51  0,00  1,00 -0,01       |                                    |
|                  Total            -------  -------               |                                    |
|                  Load:            32,00  0,00                    |                                    |
|                                                             |                                         |
|Terminal                                                     |                                         |
|        0,40   1,00   0,40   0,00                            |                                         |
|  Cub_2 /Lodlv    Load (4)           5,51  1,81  0,95  0,01       |                                    |
|  Cub_3 /Vscmono  Conv_4             5,51  1,81  0,95  0,01       |                                    |
|                                                             |                                         |
|Trm_Nanogrid 2                                               |                                         |
|        0,40   1,00   0,40   0,00                            |                                         |
|  Cub_1 /Sym      Gen_Nanogrid2     10,51  8,21  0,79  0,02  26,67 |Typ:    SL                          |
|  Cub_2 /Lodlv    Nanogrid2_Load     2,76  1,22  0,91  0,00       |                                    |
|  Cub_3 /Recmono  Conv_2             7,75  6,99  0,74  0,02       |                                    |
|                                                             |                                         |
|Trm_Nanogrid 2(1)                                            |                                         |
|        0,40   1,00   0,40   0,00                            |                                         |
|  Cub_1 /Sym      Gen_Nanogrid3     12,51  9,18  0,81  0,02  31,03 |Typ:    PV                          |
|  Cub_2 /Lodlv    Nanogrid3_ Load    4,76  2,19  0,91  0,01       |                                    |
|  Cub_3 /Recmono  Conv_3             7,75  6,99  0,74  0,02       |                                    |
|                                                             |                                         |
-------------------------------------------------------------------------------------------------------
```

Figure 5. 44: Scenario2B, Microgrid 1 terminals power load flow profile and loading (Microgrid 2 in island mode).

187

As mentioned, short of two generators and in island mode from the ILVDC network and with other microgrids; microgrid 2 remaining generators are overloaded up to 99.43% and 98.71% for Gen_Nanogrid23 and Gen_Nanogrid24, respectively. To avoid that overloading and the damage associated with it regarding the generators, an interconnection of microgrid 2 with other microgrids needs to be done for load sharing. shows simulation results of the microgrid 2 power profile at all terminals after interconnection with other microgrids through the ILVDC networks. The loading of Gen_Nanogrid23 and Gen_Nanogrid24 drops dramatically to 49.52% and 48.83%, respectively. This change is due to the power import from the other microgrid through the ILVDC network bus, as shown in Figure 5.46, representing microgrid 2 all converters terminals power load flow. 37.14 kW are imported through the microgrid 2 DC/DC converter. This power is supplied to the General load (21) demand of 35 kW and the rest to the other loads connected onto the microgrid 2 bus.

```
□-----------------------------------------------------------------------------------------------------
| Grid: Microgrid 2          System Stage: Microgrid 2     | Study Case: Study Case       | Annex:            / 3 |
-----------------------------------------------------------------------------------------------------
|           rated               Active Reactive Power                |                                     |
|        Voltage      Bus-voltage   Power   Power  Factor Current Loading|          Additional Data        |
|        [kV]  [p.u.]   [kV]   [deg]  [kW]   [kvar]  [-]    [kA]   [%]  |                                     |
-----------------------------------------------------------------------------------------------------
|Trm_Nanogrid 23                                                     |                                     |
|         0,40   1,00   0,40   0,00                                  |                                     |
|   Cub_1 /Sym      Gen_Nanogrid23    17,20   17,81  0,69   0,04  49,52 |Typ:     SL                        |
|   Cub_2 /Lodlv    Nanogrid23_ Load   3,26    5,25  0,53   0,01        |                                     |
|   Cub_3 /Recmono  Conv_23          13,94   12,56  0,74   0,03        |                                     |
|                                                                    |                                     |
|Trm_Nanogrid21                                                      |                                     |
|         0,40   0,00   0,00   0,00                                  |                                     |
|   Cub_4 /Lodlv    Nanogrid21_load   0,00    0,00  1,00   0,00        |                                     |
|   Cub_6 /Sym      Gen_Nanogrid21    0,00    0,00  1,00   0,00   0,00 |Typ:     SL                        |
|   Cub_7 /Recmono  Conv_21          0,00    0,00  1,00   0,00        |                                     |
|                                                                    |                                     |
|Trm_Nanogrid 24                                                     |                                     |
|         0,40   1,00   0,40   0,98                                  |                                     |
|   Cub_1 /Sym      Gen_Nanogrid24    16,70   17,81  0,68   0,04  48,83 |Typ:     SL                        |
|   Cub_2 /Lodlv    Nanogrid24_ Load   2,76    5,25  0,47   0,01        |                                     |
|   Cub_3 /Recmono  Conv_24          13,94   12,56  0,74   0,03        |                                     |
|                                                                    |                                     |
-----------------------------------------------------------------------------------------------------
```

Figure 5. 45: Scenario2B, microgrid2 all converters terminals power load flow and loading.

```
-----------------------------------------------------------------------------------------------------
| Grid: Microgrid 2          System Stage: Microgrid 2     | Study Case: Study Case       | Annex:            / 2 |
-----------------------------------------------------------------------------------------------------
|           rated               Active Reactive Power                |                                     |
|        Voltage      Bus-voltage   Power   Power  Factor Current Loading|          Additional Data        |
|        [kV]  [p.u.]   [kV]   [deg]  [kW]   [kvar]  [-]    [kA]   [%]  |                                     |
-----------------------------------------------------------------------------------------------------
|Single Busbar                                                       |                                     |
| 3        0,40   0,00   0,00   0,00                                 |                                     |
| Microgrid2,40  1,00   0,40   0,00                                  |                                     |
|   Cub_1 /Lod      General Load 21    35,00   0,00  1,00   0,09       |P10:    35,00 kW   Q10:  11,50 kvar |
|   Cub_1 /Dcdc     Microgrid 2 DC/DC -37,14   0,00  1,00  -0,09  9,25 |                                     |
|   Cub_1 /Recmono  Conv_21           0,00    0,00  1,00   0,00        |                                     |
|   Cub_1 /Recmono  Conv_22           0,00    0,00  1,00   0,00        |                                     |
|   Cub_1 /Recmono  Conv_23          -13,94   0,00  1,00  -0,03        |                                     |
|   Cub_1 /Recmono  Conv_24          -13,94   0,00  1,00  -0,03        |                                     |
|   Cub_1 /Vscmono  Conv_Load22      -11,76   0,00  1,00  -0,03        |                                     |
|   Cub_1 /Vscmono  Conv_Load23      -18,26   0,00  1,00  -0,05        |                                     |
|                                                                    |                                     |
|Terminal                                                            |                                     |
|         0,40   1,00   0,40   0,00                                  |                                     |
|   Cub_2 /Lodlv    Load (22)         11,76    3,37  0,96   0,02       |                                     |
|   Cub_3 /Vscmono  Conv_Load22       11,76    3,37  0,96   0,02       |                                     |
|                                                                    |                                     |
|Terminal(1)                                                         |                                     |
|         0,40   1,00   0,40   0,00                                  |                                     |
|   Cub_2 /Lodlv    Load (23)         18,26    6,00  0,95   0,03       |                                     |
|   Cub_3 /Vscmono  Conv_Load23       18,26    6,00  0,95   0,03       |                                     |
|                                                                    |                                     |
|Trm_Nanogrid 22                                                     |                                     |
|         0,40   1,00   0,40   0,00                                  |                                     |
|   Cub_1 /Sym      Gen_Nanogrid22     2,76    5,25  0,47   0,01  5,93 |Typ:     SL                        |
|   Cub_2 /Lodlv    Nanogrid22_Load    2,76    5,25  0,47   0,01       |                                     |
|   Cub_3 /Recmono  Conv_22           0,00    0,00  1,00   0,00        |                                     |
|                                                                    |                                     |
-----------------------------------------------------------------------------------------------------
```

Figure 5. 46:Scenario2B, Microgrid 2 terminals power load flow profile and loading after interconnection with ILVDC bus.

Part of the power imported by the microgrid is provided by the microgrid 3, which was also supplying the microgrid 1 as seen in the previous scenario with microgrid 2 in island mode. Microgrid 3 was supplying 14 kW to the microgrid 3 with a loading of 27.04% for Gen_Nanogrid31, 26.29% for Gen_Nanogrid32, and 32,67% for Gen_Nanogrid33. The connection of microgrid 2 has an impact on microgrid 3 as the latter in addition to its own loads must supply microgrid 2. Hence, an increase in the microgrid 3 generators loading is observed in simulation results shown in Figure 5.47 of the microgrid 3 all terminal power flow profile and loading, where a loading of 43.64% for Gen_Nanogrid31, 42.91% for Gen_Nanogrid32 and 49.22% for Gen_Nanogrid33 is observed. This shows the load sharing between microgrid 2 and microgrid 3, which contributes in reducing the stress onto the machines in microgrid 2.

```
□----------------------------------------------------------------------------------------------
| Grid: Microgrid3          System Stage: Microgrid3    | Study Case: Study Case          | Annex:            / 7 |
----------------------------------------------------------------------------------------------
|           rated                        Active Reactive Power                 |                              |
|        Voltage    Bus-voltage          Power   Power  Factor Current Loading|       Additional Data        |
|        [kV]  [p.u.]   [kV]    [deg]    [kW]    [kvar]  [-]    [kA]    [%]  |                              |
----------------------------------------------------------------------------------------------
|Conv_Mod3                                                                     |                              |
|        2,80   0,00   0,00    0,00                                          |                              |
|  Cub_1 /Dcdc      DC/DC Converter(2)   0,00    0,00   1,00   0,00   0,00 |                              |
|  Cub_2 /Dcdc      DC/DC Converter(3)   0,00    0,00   1,00   0,00   0,00 |                              |
|                                                                              |                              |
|Trm_Nanogrid31                                                               |                              |
|        0,40   1,00   0,40    0,00                                          |                              |
|  Cub_4 /Lodlv     Nanogrid31_load      3,14    1,03   0,95   0,00          |                              |
|  Cub_6 /Sym       Gen_Nanogrid31      17,08   13,59   0,78   0,03  43,65 |Typ:    SL                    |
|  Cub_7 /Recmono   Conv_31             13,94   12,56   0,74   0,03          |                              |
|                                                                              |                              |
|Trm_Nanogrid 32                                                              |                              |
|        0,40   1,00   0,40    0,00                                          |                              |
|  Cub_1 /Sym       Gen_Nanogrid32      16,70   13,47   0,78   0,03  42,91 |Typ:    SL                    |
|  Cub_2 /Lodlv     Nanogrid32_Load      2,76    0,91   0,95   0,00          |                              |
|  Cub_3 /Recmono   Conv_32             13,94   12,56   0,74   0,03          |                              |
|                                                                              |                              |
|Trm_Nanogrid33                                                               |                              |
|        0,40   1,00   0,40    0,00                                          |                              |
|  Cub_1 /Sym       Gen_Nanogrid33      19,70   14,75   0,80   0,04  49,22 |Typ:    SL                    |
|  Cub_2 /Lodlv     Nanogrid33_ Load     5,76    2,19   0,93   0,01          |                              |
|  Cub_3 /Recmono   Conv_33             13,94   12,56   0,74   0,03          |                              |
|                                                                              |                              |
----------------------------------------------------------------------------------------------
```

Figure 5. 47: Scenario2B, microgrid 3 all terminals power flow and loading profile.

The total power exported by the microgrid 3 amounts up to 32 kW out of the 37.14 kW imported by the microgrid 2. Each nanogrid within microgrid 3 contributes 13.4 kW towards the microgrid 3 bus and 9 kW is supplied to the load (31) as shown in Figure 5.48 and Figure 5.49.

Microgrid 1 contributes the rest of the power needed by microgrid 2, thus 4.31 kW is exported through the DC/DC converter of the microgrid 1 bus as shown in Figure 5.50. Each nanogrid within microgrid 1 is contributing 13.9 kW, thus making a total of 41.7 kW to supply a load demand of 37.5 kW connected to the microgrid 1 bus. There is a complete difference in the behaviour of microgrid1 in this scenario 2B, with microgrid 2 connected, compared to the scenario 2B with microgrid 2 in island mode. Power export is observed in the latter scenario while for the former scenario in island mode a power import of 14 kW was observed. This affects the loading of the nanogrids within the microgrid which goes up to 43.8% for Gen_Nanogrid31, 43.3% for Gen_Nanogrid32, and 47.6% for Gen_Nanogrid33.

```
| Grid: Microgrid3          System Stage: Microgrid3    | Study Case: Study Case           | Annex:              / 6  |
--------------------------------------------------------------------------------------------------------------------------
|        rated              Active Reactive Power                              |                                        |
|      Voltage     Bus-voltage    Power  Power  Factor Current Loading|                Additional Data                  |
|      [kV] [p.u.]   [kV]  [deg]  [kW]   [kvar]  [-]    [kA]    [%]  |                                                  |
--------------------------------------------------------------------------------------------------------------------------
|Single Busbar                                                        |                                                |
|  3        0,40    0,00   0,00   0,00                                |                                                |
|  DC Microgr,40    1,00   0,40   0,00                                |                                                |
|   Cub_1 /Dcdc     DC/DC Converter    0,00   0,00  1,00  0,00   0,00 |                                                |
|   Cub_1 /Dcdc     DC/DC Converter(4) 32,83  0,00  1,00  0,08   8,18 |                                                |
|   Cub_1 /Recmono  Conv_31           -13,94  0,00  1,00 -0,03       |                                                |
|   Cub_1 /Recmono  Conv_32           -13,94  0,00  1,00 -0,03       |                                                |
|   Cub_1 /Recmono  Conv_33           -13,94  0,00  1,00 -0,03       |                                                |
|   Cub_1 /Vscmono  Conv_4            -9,00   0,00  1,00 -0,02       |                                                |
|                                                                     |                                                |
|Conv_Mod1                                                            |                                                |
|           0,76    0,00   0,00   0,00                                |                                                |
|   Cub_1 /Dcdc     DC/DC Converter    0,00   0,00  1,00  0,00   0,00 |                                                |
|   Cub_2 /Dcdc     DC/DC Converter(1) 0,00   0,00  1,00  0,00   0,00 |                                                |
|                                                                     |                                                |
|Conv_Mod2                                                            |                                                |
|           1,44    0,00   0,00   0,00                                |                                                |
|   Cub_1 /Dcdc     DC/DC Converter(1) 0,00   0,00  1,00  0,00   0,00 |                                                |
|   Cub_2 /Dcdc     DC/DC Converter(2) 0,00   0,00  1,00  0,00   0,00 |                                                |
|                                                                     |                                                |
|Terminal                                                             |                                                |
|           0,40    1,00   0,40   0,00                                |                                                |
|   Cub_4 /Asm      Load(31)          5,50   2,45  0,91  0,01   1,40 |Slip:    3,26 %    xm:   4,00 p.u.              |
|   Cub_5 /Asm      Load(32)          3,50   1,22  0,94  0,01   0,86 |Slip:    1,92 %    xm:   4,00 p.u.              |
|   Cub_3 /Vscmono  Conv_4            9,00   3,66  0,93  0,01       |                                                |
|                   Total            -------  -------                 |                                                |
|                   Motor Load:      9,00   3,66                      |                                                |
|                                                                     |                                                |
--------------------------------------------------------------------------------------------------------------------------
```

Figure 5. 48: Scenario2B, microgrid 3 all converters terminals power load flow and loading profile.

```
--------------------------------------------------------------------------------------------------------------------------
| Grid: Microgrid1          System Stage: Microgrid1    | Study Case: Study Case           | Annex:              / 4  |
--------------------------------------------------------------------------------------------------------------------------
|        rated              Active Reactive Power                              |                                        |
|      Voltage     Bus-voltage    Power  Power  Factor Current Loading|                Additional Data                  |
|      [kV] [p.u.]   [kV]  [deg]  [kW]   [kvar]  [-]    [kA]    [%]  |                                                  |
--------------------------------------------------------------------------------------------------------------------------
|Single Busbar                                                        |                                                |
|  3        0,40    0,00   0,00   0,00                                |                                                |
|  DC Microgr,40    1,00   0,40   0,00                                |                                                |
|   Cub_1 /Lod      General Load (1)  20,00  0,00  1,00  0,05       |P10:   20,00 kW   Q10:   0,00 kvar              |
|   Cub_1 /Lod      General Load (2)  9,00   0,00  1,00  0,02       |P10:    9,00 kW   Q10:   0,00 kvar              |
|   Cub_1 /Lod      General Load (3)  3,00   0,00  1,00  0,01       |P10:    3,00 kW   Q10:   0,00 kvar              |
|   Cub_1 /Dcdc     DC/DC Converter   4,31   0,00  1,00  0,01   1,07 |                                                |
|   Cub_1 /Recmono  Conv_1           -13,94  0,00  1,00 -0,03       |                                                |
|   Cub_1 /Recmono  Conv_2           -13,94  0,00  1,00 -0,03       |                                                |
|   Cub_1 /Recmono  Conv_3           -13,94  0,00  1,00 -0,03       |                                                |
|   Cub_1 /Vscmono  Conv_4           -5,51   0,00  1,00 -0,01       |                                                |
|                   Total            -------  -------                 |                                                |
|                   Load:            32,00  0,00                      |                                                |
|                                                                     |                                                |
|Terminal                                                             |                                                |
|           0,40    1,00   0,40   0,00                                |                                                |
|   Cub_2 /Lodlv    Load (4)          5,51   1,81  0,95  0,01       |                                                |
|   Cub_3 /Vscmono  Conv_4            5,51   1,81  0,95  0,01       |                                                |
|                                                                     |                                                |
|Trm_Nanogrid 2                                                       |                                                |
|           0,40    1,00   0,40   0,00                                |                                                |
|   Cub_1 /Sym      Gen_Nanogrid2     16,70  13,78  0,77  0,03  43,30 |Typ:    SL                                     |
|   Cub_2 /Lodlv    Nanogrid2_Load    2,76   1,22  0,91  0,00       |                                                |
|   Cub_3 /Recmono  Conv_2            13,94  12,56  0,74  0,03       |                                                |
|                                                                     |                                                |
|Trm_Nanogrid 2(1)                                                    |                                                |
|           0,40    1,00   0,40   0,00                                |                                                |
|   Cub_1 /Sym      Gen_Nanogrid3     18,70  14,75  0,79  0,03  47,63 |Typ:    PV                                     |
|   Cub_2 /Lodlv    Nanogrid3_ Load   4,76   2,19  0,91  0,01       |                                                |
|   Cub_3 /Recmono  Conv_3            13,94  12,56  0,74  0,03       |                                                |
--------------------------------------------------------------------------------------------------------------------------
| Grid: Microgrid1          System Stage: Microgrid1    | Study Case: Study Case           | Annex:              / 5  |
--------------------------------------------------------------------------------------------------------------------------
|        rated              Active Reactive Power                              |                                        |
|      Voltage     Bus-voltage    Power  Power  Factor Current Loading|                Additional Data                  |
|      [kV] [p.u.]   [kV]  [deg]  [kW]   [kvar]  [-]    [kA]    [%]  |                                                  |
--------------------------------------------------------------------------------------------------------------------------
|Trm_Nanogrid1                                                        |                                                |
|           0,40    1,00   0,40   0,00                                |                                                |
|   Cub_4 /Lodlv    Nanogrid1_load    3,01   1,34  0,91  0,00       |                                                |
|   Cub_6 /Sym      Gen_Nanogrid1     16,95  13,90  0,77  0,03  43,84 |Typ:    SL                                     |
|   Cub_7 /Recmono  Conv_1            13,94  12,56  0,74  0,03       |                                                |
|                                                                     |                                                |
--------------------------------------------------------------------------------------------------------------------------
```

Figure 5. 49: Scenario2B, microgrid 1 all converters terminals power load flow and loading profile.

190

5.6 Conclusion

In this chapter are performed load flow simulations and analysis of the intermediate low voltage direct current systems for interconnection of sparse electrified areas developed in chapter 4. The model of the designed network is developed and simulated in DigSilent PowerFactory.

Three microgrids are considered as sparsed electrified areas and each made up of nanogrids diesel generators modelled as synchronous generators in this study. Load flow simulations are performed on each microgrid for performance evaluation in terms of generator loading and voltage profile.

For power exchange load flow simulation was performed on interconnected microgrids, with two scenarios: the first scenario considered the situation where each microgrid is self-sufficient in terms of power generated and consumed by local and microgrid bus connected loads. The second scenario considered a situation where one of the three microgrids needs power support from the rest. This scenario was taken into two stages, where for the first stage the microgrid2 was in island mode and had two of its generators not running. The second stage consisted in interconnecting the same microgrid 2 to the rest of microgrids through the ILVDC network.

Load flow results of scenario showed a successful interconnection of microgrid through ILVDC network systems, with 3 kV$_{DC}$ voltage profile observed at ILVDC bus.

For the scenario 2, the stage one load flow results showed an 90% overloading of the only two working nanogrid. This demonstrated the vulnerability of a microgrid in island mode, thus the need of interconnection. In stage two of the scenario 2, load flow analysis results showed a significance drop in the microgrid2 generators loading and at the same time a moderate increase in the loading of the generators of other microgrids. This demonstrates the effectiveness of the interconnection as the power import from the rest of microgrid interconnected to microgrid2 through the intermediate low voltage DC network was contributing to balance the supply – demand equation in microgrid2 despite the loss of 50% of its generation capacity.

CHAPTER SIX
CONCLUSION AND RECOMMENDATION

6.1 Introduction

The purpose of this research was to develop an Intermediate Low Voltage Direct Current (ILVDC) interconnection system for sparse electrified areas. The system is part of the bottom-up grid extension strategy for increasing the electrification rate in sub-Saharan region considering the dispersed locations of settlements and off-grid solutions used locally such as diesel generator sets.

6.2 Outcomes of the thesis

This thesis aimed to develop an interconnection system of sparse electrified areas based on Intermediate Low Voltage Direct Current (ILVDC) for power exchange on request. This interconnection is between neighboring areas, with the nanogrid being the basic entity for a microgrid formation.

In chapter one, are mainly discussed the background of the research, its significance, objectives, contribution and methodology used.

Specific objectives included:

1. Reviewing the existing theories and practice of power system distribution network, the operation and extension for both DC and AC systems.

2. The development of strategies for interconnection of off-grid generation sources based on DC network with eventual utility grid connection.

3. Design converter and control strategies of nanogrid for microgrid formation

4. Design converter and control strategies of microgrid for Minigrid formation

5. Design converter and control strategies for minigrid interconnection with the utility grid.

6. Propose a communication system for an Intermediate Low Voltage Direct Current network.

7. The development of an Intermediate Low Voltage Direct Current distribution grid and perform a load flow analysis.

The aim and objectives are achieved and described throughout the chapters:

In line with the first objective, chapter two reviews the power system structure with focus on distribution networks operation principles and applications. An overview of network key components such as lines, poles and transformers are presented to understand the current practices and new trends. Actual and new trends of different types of protection and associated communication systems used in distribution networks are also discussed. Network planning and extension theories, practices and challenges are reviewed. It is understood that poor planning, settlement structure and financial burden are the barrier for electricity network extension. Microgrids as one of the solutions prone by reviewed articles are discussed.

Under the same objective, chapter three reviews the concepts of low voltage direct current, with an overview on DC systems. Applications and challenges associated with interruption DC faults currents. However, literature shows advancement in the field of DC protection using solid state breakers. In same chapter, Low voltage DC system standards, components, control and protection as well as the cable are discussed in depth. From the literature, a discordance in voltage classification between low and voltage is observed with standard overlapping. Therefore, for this research, IEC 60083 voltage range from 2 to 3.9 kV_{DC} usually in application for traction system is defined as Intermediate Low Voltage Direct Current range and 3 kV is used throughout the thesis. Furthermore, from the literature, there is potential for application of low voltage direct current network in Africa for swarm electrification.

Chapter four focused on objectives from 2 to 6, with the Intermediate Low Voltage Direct Current network proposed. The network made up from nanogrids considered as the basic entities for the formation of a microgrid. A typical nanogrid consists of an isolated generation unit and local loads attached to it. For the formation of DC microgrid, nanogrids are integrated through AC/DC converters. The latter are bidirectional to allow power exchange in both directions. They are designed and simulated using PSIM and an overall nanogrid control strategy is developed. Similarly, a DC/DC converter is designed to integrate the microgrid to the ILVDC network. It is a bidirectional converter with two mode operations namely the boost for power export from the microgrid to the ILVDC network and buck operation for power import from the other microgrids through the ILVDC interconnection system. Microgrid overall control is developed and as for nanogrids overall control it relies on the communication system.

Power line communication system is proposed due to its effectiveness and low cost as power lines are used a transmission channel. An Opto-capacitive coupler for nanogrid application is designed and simulated in PSIM.

In chapter five are achieved the objective 7, the load flow analysis of the proposed ILVDC interconnection system. The latter is modelled and simulated in DigSilent PowerFactory

environment. Load flow is performed for each of the three microgrids involved in interconnection separately and a scenario of power shortage in microgrid 2 is created for power exchange between microgrids analysis. Results show a successful power exchange within the microgrid and between the microgrids.

6.3 Recommendation

The Intermediate Low Voltage Direct Current (ILVDC) systems for interconnection of sparse electrified are successfully designed and tested through computer simulations. It is feasible; however, its implementation starts from the bottom with nanogrids owners. They will be the ones to initiate the process and make the funds available for the process at least for the microgrid creation. Investors can take over from the microgrid stage for funding and operation of the network. Through those interconnections in "Olympic ring", a lot of people will have access to electricity at low cost.

Business models should be developed to encourage nanogrids owners to join and for microgrid operations and maintenance fund generations.

6.4 Future work

Further research on Intermediate Low Voltage Direct Current interconnection system should look on:

- Protection system for nanogrids when connected to microgrids as the interconnection may cause an increase of fault levels, thus, there is a need for deep study.
- Protection coordination of interconnected microgrids.
- Integration of other resources such renewable energy and their intermittence effect on dispatching in the network
- Optimised economic dispatch of microgrids generating unit
- Business model for optimum operation of the Intermediate Low Voltage Direct Current-based network for bottom-up grid extension

References

A, R., Benes, F. & Filho, F.A.R. 2016. Current transformers saturation and its implications in protective differential schemes detection and operation decision using wavelet transform and Artificial Neural Networks. In *Development in Power System Protection 2016 (DPSP), 13th International Conference on*. Edinburgh: IET: 1–6. http://ieeexplore.ieee.org/document/7795083/.

Abdelmoumene, A. & Bentarzi, H. 2014. A review on protective relays' developments and trends. *Journal of Energy in Southern Africa*, 25(2): 91–95.

Adam, G.P., Ahmed, K.H., Finney, S.J. & Williams, B.W. 2011. Modular multilevel converter for medium-voltage applications. In *2011 IEEE International Electric Machines and Drives Conference, IEMDC 2011*.

Adam, G.P., Alajmi, B., Ahmed, K.H., Finney, S.J. & Williams, B.W. 2011. New flying capacitor multilevel converter. In *Proceedings - ISIE 2011: 2011 IEEE International Symposium on Industrial Electronics*. 335–339.

Afamefuna, D., Chung, I.Y., Hur, D., Kim, J.Y. & Cho, J. 2014. A techno-economic feasibility analysis on LVDC distribution system for rural electrification in South Korea. *Journal of Electrical Engineering and Technology*.

Agarwal, H.K. & Barua, P. 2010. Insulated and Covered Conductors Systems for Low and Medium voltage Over head distribution line. *Design*: 1–8. https://supremeco.files.wordpress.com/2010/02/distribution-lines.pdf.

Aghajani, A., Golozar, M.A., Saatchi, A., Raeissi, K., Urgen, M. & Shabani, S. 2013. Stray Alternating Current and Environmental Effects on Concrete Power Poles. *Materials Performance*, 52(8): 30–34. http://www.scopus.com/inward/record.url?eid=2-s2.0-84882942186&partnerID=tZOtx3y1%5Cn%3CGo to ISI%3E://WOS:000322863000008.

Aibangbee, J.O. & Onohaebi, S.O. 2015. Microprocessor-Based Protective Relays Applications in Nigeria Power System Protections. *International Journal of Engineering Trends and Technology (IJETT)*, 26(2): 88–94. http://www.ijettjournal.org/2015/volume-26/number-2/IJETT-V26P216.pdf.

Alexander, P., Apple, J., Elneweihi, A., Haas, R. & Swift, G.W. 2006. *Power System Protection*. http://ieeexplore.ieee.org/xpl/bkabstractplus.jsp?bkn=5264125.

Almaguer, H.A.D., Coelho, R.A., Coelho, V.L., Nosaki, P.L. & Piantini, A. 2013. A feasibility

study on the use of concrete pole bases as a grounding topology for distribution systems. In *2013 International Symposium on Lightning Protection, SIPDA 2013*. 209–213.

Amirnaser, Y. & Reza Iravani. 2010. *Voltage-Sourced Converters in Power Systems: Modeling, Control, and Applications*. New Jersey: John Wiley & Sons, Inc.

Amoiralis, E.I., Tsili, M.A., Kladas, A.G. & Souflaris, A.T. 2012. Distribution transformer cooling system improvement by innovative tank panel geometries. *IEEE Transactions on Dielectrics and Electrical Insulation*, 19(3): 1021–1028.

Andrade, F.J.A., Marques, C.A.G., Oliveira, T.R., Campos, F.P. V, De Oliveira, E.J. & Ribeiro, M. V. 2013. Preliminary analysis of additive noise on outdoor and low voltage electric power grid in Brazil. In *ISPLC 2013 - 2013 IEEE 17th International Symposium on Power Line Communications and Its Applications, Proceedings*. 109–113.

ANSI. 1999. American national standard requirements for power-line carrier coupling capacitors and coupling capacitor voltage transformers. : 42–42.

Anthony, T. 2004. Rio Grande Electric Monitors Remote Energy Assets via Satellite. *Utility Automation & Engineering T&D Magazine*. https://www.elp.com/articles/powergrid_international/print/volume-9/issue-4/features/rio-grande-electric-monitors-remote-energy-assets-via-satellite.html.

Arifianto, I. & Cahyono, B. 2009. Power transformer cooling system optimization. In *Proceedings of the IEEE International Conference on Properties and Applications of Dielectric Materials*. 57–59.

Ault, G.W. & McDonald, J.R. 2000. Planning for Distributed Generation within Distribution Networks in Restructured Electricity Markets. *IEEE Power Engineering Review*, 20(2): 52–54.

Aung, M.T. & Milanović, J. V. 2006. The influence of transformer winding connections on the propagation of voltage sags. *IEEE Transactions on Power Delivery*, 21(1): 262–269.

Avila, N., Carvallo, J.P., Shaw, B. & Kammen, D.M. 2017. *The energy challenge in sub-Saharan Africa : A guide for advocates and policy makers Part 1 : Generating energy for sustainable and equitable development*.

Awad, A.E. 2006. Basics of Fiber Optics. *Fiber Optics Technician's Manual*.

Awadallah, M., Xu, T., Venkatesh, B. & Singh, B. 2015. On the Effects of Solar Panels on Distribution Transformers. *IEEE Transactions on Power Delivery*, PP(99): 1–1. http://ieeexplore.ieee.org/lpdocs/epic03/wrapper.htm?arnumber=7127048.

Awofeso, N. 2011. Generator diesel exhaust: A major hazard to health and the environment in Nigeria. *American Journal of Respiratory and Critical Care Medicine*.

Azimoh, C.L., Klintenberg, P., Mbohwa, C. & Wallin, F. 2017. Replicability and scalability of mini-grid solution to rural electrification programs in sub-Saharan Africa. *Renewable Energy*, 106: 222–231. https://linkinghub.elsevier.com/retrieve/pii/S0960148117300174 25 September 2018.

Bahrman, M.P. & Johnson, B.K. 2007. The ABCs of HVDC transmission technologies. *IEEE Power and Energy Magazine*.

Bak, K.E.L., Baitc, A., Bes, A., Abbe, C., Aoki, A.S.I. & Brazil, L. 2012. SURVE EY ON ME ETHODS A AND TOOL LS FOR PL LANNING OF ' ACTI IVE ' N NETWOR. , (158).

Bakshi, U.. & Bakshi.M.V. 2009. *Protection-and-Switchgear*. https://books.google.co.za/books?id=EW72SVS47EC&source=gbs_book_other_version s.

Baran, M. & Mahajan, N.R. 2006. PEBB based DC system protection: Opportunities and challenges. In *Proceedings of the IEEE Power Engineering Society Transmission and Distribution Conference*. 705–707.

Barghi Latran, M. & Teke, A. 2015. Investigation of multilevel multifunctional grid connected inverter topologies and control strategies used in photovoltaic systems. *Renewable and Sustainable Energy Reviews*, 42: 361–376.

Barnes, M. & Beddard, A. 2012. Voltage source converter HVDC links - The state of the art and issues going forward. In *Energy Procedia*. 108–122.

Baruti, G. 2017. Overcurrent protection. *Razdelilna in industrijska omrežja*: 1–20. http://lrf.fe.uni-lj.si/e_rio/Seminarji1617/PretokovnaZascita.pdf.

Bathurst, G., Hwang, G. & Tejwani, L. 2015. MVDC - The New Technology for Distribution Networks. *11th IET International Conference on AC and DC Power Transmission*, (Dc): 1–5.

Bayliss, C. & Hardy, B. 2007. *Transmission and Distribution Electrical Engineering*. 3rd ed. Oxford: Elsevier Ltd.

Bayliss, C.R. & Hardy, B.J. 2012. Chapter 6 -Current and Voltage Transformers. *Transmission and Distribution Electrical Engineering*: 157–170. http://www.sciencedirect.com/science/article/pii/B9780080969121000058.

Bayliss, C.R. & Hardy, B.J. 2007. Power Transformers. *Transmission and Distribution Electrical Engineering*: 499–564. http://www.sciencedirect.com/science/article/pii/B9780750666732500185.

Becker, D.J. & Sonnenberg, B.J. 2011. DC microgrids in buildings and data centers. In *INTELEC, International Telecommunications Energy Conference (Proceedings)*.

Bhattacharyya, S.C. 2014. Business Issues for Mini-Grid-Based Electrification in Developing Countries. In Bhattacharyya, Subhes C. & D. Palit, eds. *Mini-Grids for Rural Electrification of Developing Countries*. New York: Springer: 145–164.

Bhattacharyya, S.C. & Palit, D. 2016. Mini-grid based off-grid electrification to enhance electricity access in developing countries: What policies may be required? *Energy Policy*.

Binkofski, J. 2005. Influence of properties of magentic materials. In *International Symposium on Power Line Communications and Its Applications, 2005.* Vancouver: IEEE: 281–284.

Bíscaro, A.A.P., Pereira, R.A.F., Kezunovic, M. & Mantovani, J.R.S. 2016. Integrated Fault Location and Power-Quality Analysis in Electric Power Distribution Systems. *IEEE Transactions on Power Delivery*, 31(2).

Blair, H.T. 2016. *Energy Production Systems Engineering*. I. P. Editorial, ed. New Jersey: John Wiley & Sons, Inc.

Boddie, C.A. 1927. Telephone Communication over Power Lines by High Frequency Currents. *Proceedings of the Institute of Radio Engineers*, 15(7): 559–640.

Bollen, M.H. 2000. Understanding Power Quality Problems: Voltage Sags and Interruptions. *IEEE Press, New York*. http://books.google.ps/books/about/Understanding_Power_Quality_Problems.html?id=Je0eAQAAIAAJ&pgis=1%5Cnhttp://scholar.google.com/scholar?hl=en&btnG=Search&q=intitle:UNDERSTANDING+POWER+QUALITY+PROBLEMS+Voltage+Sags+and+Interruptions+Math#1%5Cnhttp://schol.

BOOTH, C. & BELL, K. 2013. Protection of transmission and distribution (T&D) networks. In Z. Melhem, ed. *Electricity transmission, distribution and storage systems*. Woodhead Publishing Limited,: 76–107.

Bose, B.K. 2009. Power electronics and motor drives recent progress and perspective. *IEEE Transactions on Industrial Electronics*, 56(2): 581–588.

Bouford, J.D. 2008. Spacer cable reduces tree caused customer interruptions. In *Transmission and Distribution Exposition Conference: 2008 IEEE PES Powering Toward the Future, PIMS 2008*.

Brenna, A., Beretta, S., Bolzoni, F., Pedeferri, M.P. & Ormellese, M. 2017. Effects of AC-interference on chloride-induced corrosion of reinforced concrete. *Construction and Building Materials*, 137: 76–84.

Callavik, M., Blomberg, A., Häfner, J. & Jacobson, B. 2013. Break-through!: ABB's hybrid HVDC breaker, an innovation breakthrough enabling reliable HVDC grids. *ABB Review*, (2): 7–13.

Cataliotti, A., Di Cara, D., Fiorelli, R. & Tinè, G. 2012. Power-line communication in medium-voltage system: Simulation model and onfield experimental tests. *IEEE Transactions on Power Delivery*, 27(1): 62–69.

Cecati, C., Mokryani, G., Piccolo, A. & Siano, P. 2010. An overview on the Smart Grid concept. In *IECON Proceedings (Industrial Electronics Conference)*. 3322–3327.

Celina, M. & George, G.A. 1995. Characterisation and degradation studies of peroxide and silane crosslinked polyethylene. *Polymer Degradation and Stability*, 48(2): 297–312.

Chaudhuri, N., Chaudhuri, B., Majumder, R. & Yazdani, A. 2014. *Multiterminal direct-current grids:Modelling, Analysis, and Control*. Wiley/IEEE.

Chen, Z., Blaabjerg, F. & Iov, F. 2005. A study of synchronous machine model implementations in Matlab/Simulink simulations for new and renewable energy systems. In *2005 International Conference on Electrical Machines and Systems*. https://www.academia.edu/13014096/A_study_of_synchronous_machine_model_implementations_in_Matlab_Simulink_simulations_for_new_and_renewable_energy_systems?auto=download.

Chiandone, M., Sulligoi, G., Milano, F., Piccoli, G. & Mania, P. 2014. Back-to-back MVDC link for distribution system active connection: A network study. In *3rd International Conference on Renewable Energy Research and Applications, ICRERA 2014*. 1001–1006.

Chuang, C.-L., Wang, Y.-C., Lee, C.-H., Liu, M.-Y., Hsiao, Y.-T. & Jiang, J.-A. 2010. An Adaptive Routing Algorithm Over Packet Switching Networks for Operation Monitoring of Power Transmission Systems. *IEEE Transactions on Power Delivery*.

Cigre. 2017. IEC 61850 Communication Model. In S. Carlos & M. Mehrdad, eds. *Utility Communication Networks and Services: Specification, Deployment and Operation*. Paris: Springer: 7.

Cinieri, E., Fumi, A., Salvatori, V. & Spalvieri, C. 2007. A new high-speed digital relay protection of the 3-kVdc electric railway lines. *IEEE Transactions on Power Delivery*, 22(4): 2262–2270.

Clapp, A.L., Dagenhart, J.B., Landinger, C.C., McAuliffe, J.W. & Thue, W.A. 1997. Design and application of aerial systems using insulated and covered wire and cable. *IEEE Transactions on Power Delivery*, 12(2): 1006–1011.

Colak, I., Kabalci, E. & Bayindir, R. 2011. Review of multilevel voltage source inverter topologies and control schemes. *Energy Conversion and Management*, 52(2): 1114–1128.

Coltman, J.W. 2002. The transformer [historical overview]. *Industry Applications Magazine, IEEE,* 8(1): 8–15.

Cossi, A.M., da Silva, L.G.W., Lázaro, R.A.R. & Mantovani, J.R.S. 2012. Primary power distribution systems planning taking into account reliability, operation and expansion costs. *IET Generation, Transmission & Distribution*, 6(3): 274. http://digital-library.theiet.org/content/journals/10.1049/iet-gtd.2010.0666.

Costa, L.G.S., Picorone, A.A.M., Ribeiro, M.V., Da Costa, V.L.R. & De Queiroz, A.C.M. 2015. Projeto e caracterização de acopladores para power line communications. In *XXXIII Simpósio Brasileiro de Telecomunicações,*. 1–5. https://www.researchgate.net/publication/282778959_Projeto_e_Caracterizacao_de_Ac opladores_para_Power_Line_Communications.

Cuzner, R.M. & Venkataramanan, G. 2008. The status of DC micro-grid protection. In *Conference Record - IAS Annual Meeting (IEEE Industry Applications Society)*.

Daleep, Singh Sekhon ; Harmandar, K. & Malhotra, J. 2016. Upgrading a 20 Gbps DWDM system to 160 Gbps system using add/drop multiplexers and couplers. In *2016 International Conference on Computational Techniques in Information and Communication Technologies (ICCTICT)*. New Dehli: IEEE: 463–469.

Das, A. & Balakrishnan, V. 2012. Sustainable energy future via grid interactive operation of spv system at isolated remote island. *Renewable and Sustainable Energy Reviews*.

Das, D., Ganguly, S. & Sahoo, N.. 2013. Recent advances on power distribution system planning : a state-of-the-art survey. *Energy Syst*: 165–193.

Deegan, C. 2008. Environmental costing in capital investment decisions: Electricity distributors and the choice of power poles. *Australian Accounting Review*, 18(1): 2–15.

Dudley, G. & Mulkey, D. 2004. Transformer Locations. In J. H. Harlow, ed. *ELECTRIC POWER TRANSFORMER ENGINEERING*. Florida: CRC Press LLC. http://www.google.com/patents?hl=en&lr=&vid=USPATD324371&id=APgpAAAAEBAJ&oi=fnd&dq=ELECTRIC+TRANSFORMER&printsec=abstract%5Cnhttp://www.google.com/patents?hl=en&lr=&vid=USPATD324371&id=APgpAAAAEBAJ&oi=fnd&dq=Electric+transformer&printsec=abstract.

Dulău, L.I., Abrudean, M. & Bică, D. 2014. Effects of Distributed Generation on Electric Power Systems. *Procedia Technology*.

E.C.W. de Jong & P.T.M Vaessen. 2007. Briefing Paper: DC power distribution for server farms. *KEMA Consulting*.

Eberhard, A. 2000. *Competition and Regulation in the Electricity Supply Industry in South Africa*. Cape Town. https://www.gsb.uct.ac.za/files/Electricity_competion_in_SA-Eberhardt.pdf.

El-Hawary, M.E. 2002. *Electric Energy Systems. An Overview*. THE ELECTR. L. Grigsby, ed. New York: CRC Press.

Elsayed, A.T., Mohamed, A.A. & Mohammed, O.A. 2015. DC microgrids and distribution systems: An overview. *Electric Power Systems Research*, 119: 407–417. http://ac.els-cdn.com/S0378779614003885/1-s2.0-S0378779614003885-main.pdf?_tid=b598aeb6-7200-11e7-81d6-00000aacb35d&acdnat=1501073483_55f5cb97fb4a58de9f08a13d12ece081.

Emhemed, A. & Burt, G. 2013. the Effectiveness of Using Iec61660 for Characterising Short-Circuit. In *Electricity Distribution (CIRED 2013), 22nd International Conference and Exhibition on*. Stockholm: 3–6.

Emhemed, A.A.S. & Burt, G.M. 2014. An advanced protection scheme for enabling an LVDC last mile distribution network. *IEEE Transactions on Smart Grid*, 5(5): 2602–2609.

Emhemed, A.A.S., Fong, K., Fletcher, S. & Burt, G.M. 2017. Validation of fast and selective protection scheme for an LVDC distribution network. *IEEE Transactions on Power Delivery*, 32(3): 1432–1440.

Emleh, A., Beer, A. de, Ferreira, H. & Vinck, A.H. 2013. Interference detection on powerline communications channel when in-building wiring system acts as an antenna,. In *International Symposium Electronic in Marine,2013*. Zadar , Croatia: IEEE: 141–144.

ESKOM. 2015. *Fact sheet:Selecting the right type of generator*. http://www.eskom.co.za/AboutElectricity/FactsFigures/Documents/SelectingTypeGenerator.pdf.

Essiambre, R.J. & Tkach, R.W. 2012. Capacity trends and limits of optical communication networks. In *Proceedings of the IEEE*.

Etumi, A.A.A. & Anayi, F.J. 2016. The application of correlation technique in detecting internal and external faults in three-phase transformer and saturation of current transformer. *IEEE Transactions on Power Delivery*, 31(5): 2131–2139.

Faiz, J. & Heydarabadi, R. 2014. Diagnosing power transformers faults. *Russian Electrical Engineering*, 85(12): 785–793. http://link.springer.com/10.3103/S1068371214120207.

Ferreira, H.C., Lampe, L., Newbury, J. & Swart, T.G. 2010. *Power Line Communications: Theory and Applications for Narrowband and Broadband Communications over Power Lines*. H. C. Ferreira, L. Lampe, J. Newbury, & T. G. Swart, eds. Wiley.

Fletcher, S.D. a., Norman, P.J., Galloway, S.J. & Burt, G.M. 2011. Analysis of the effectiveness of non-unit protection methods within DC microgrids. *IET Conference on Renewable Power Generation (RPG 2011)*: 111–111. http://digital-library.theiet.org/content/conferences/10.1049/cp.2011.0142.

Fouad, F.H. & Detwiler, R.J. 2012. High-strength materials for spun concrete poles. *Pci Journal*: 27–32.

Fox-Rogers, L. & Murphy, E. 2014. Informal strategies of power in the local planning system. *Planning Theory*, 13(3): 244–268. http://plt.sagepub.com/cgi/doi/10.1177/1473095213492512.

Fox, G.H. 2010. Power System Selectivity : The Basics of Protective Coordination. *Neta World*: 1–9. http://www.netaworld.org/sites/default/files/public/neta-journals/NWwtr09_Fox.pdf.

Freeman, R.L. 2006. *Radio System Design for Telecommunications: Third Edition*.

Fregosi, D., Ravula, S., Brhlik, D., Saussele, J., Frank, S., Bonnema, E., Scheib, J. & Wilson, E. 2015. A comparative study of DC and AC microgrids in commercial buildings across different climates and operating profiles. In *2015 IEEE 1st International Conference on Direct Current Microgrids, ICDCM 2015*.

Fu-min, Z., Li, M., Nian, L. & Jin-shan, C. 2012. Assessment for Distribution Network Planning Schemes of Urban Electric Power System. *Energy Procedia*, 14: 1067–1074. http://linkinghub.elsevier.com/retrieve/pii/S1876610211044766.

Gabba, A.P. & Hill, J.D. 2001. Make automatic power source transfers a success for your plant. *IEEE Transactions on Industry Applications*, 37(2): 423–433. http://ieeexplore.ieee.org/document/913705/.

Gaidajis, G., Angelakoglou, K. & Aktsoglou, D. 2010. E-waste : Environmental Problems and Current Management. *Journal of Engineering Science and Technology Review*, 3(1): 193–199. https://www.researchgate.net/publication/49607064_E-waste_Environmental_Problems_and_Current_Management.

Galli, S., Scaglione, A. & Wang, Z. 2011. For the Grid and Through the Grid: The Role of Power Line Communications in the Smart Grid. *Proceedings of the IEEE*, 99(6): 998–1027. arrier transmission on power lines;power system control;power system planning;smart power grids;PLC;engineering modeling;fading models;network control;network planning;power distribution network;power line communications;sensor networking;smart grid contr.

Ganesan, S. 2006. Selection of current transformers and wire sizing in substations. *2006 59th Annual Conference for Protective Relay Engineers*, 2006: 124–133.

Ganguly, S., Sahoo, N.C. & Das, D. 2013. Recent advances on power distribution system planning: A state-of-the-art survey. *Energy Systems*, 4(2): 165–193.

Gawande, S.P., Pardeshi, S.M., Kadwane, S.G., Ramteke, M.R., Daigavane, M.B., Debre, P.D. & Bagde, B.Y. 2017. Capacitor Voltage Balancing Techniques for Three Level Capacitor Clamped Multilevel Inverter under Load Compensation. In *IEEE International Conference on Power Electronics, Drives and Energy Systems, PEDES 2016*.

Gayathri Devi, K.S., Arun, S. & Sreeja, C. 2014. Comparative study on different five level inverter topologies. *International Journal of Electrical Power and Energy Systems*.

Geno, P. 2011. A Review about Vector Group Connections In Transformers. *International Journal of Advancements in Technology*, 2(2): 215–221. https://www.omicsonline.org/open-access/a-review-about-vector-group-connections-in-transformers-0976-4860-2-215-221.pdf.

Gentzoglanis, A. 2013. Regulation of the electricity industry in Africa. *African Journal of Economic and Management Studies*, 4(1): 34–57. http://search.proquest.com/docview/1355520229?accountid=27292.

Georgilakis, P.S., Member, S. & Hatziargyriou, N.D. 2013. in Power Distribution Networks : Models , Methods , and Future Research. *IEEE Transactions on Power Systems*, 28(3): 3420–3428.

Gers, J.M. & Holmes, E.J. 2004. *Protection of Electricity Distribution Networks*.

Geun-Joon, L. 2011. Superconductivity Application in Power System. In Adir Moysés Luiz, ed. *Applications of High-Tc Superconductivity*.

Gironaa, M.M., Peraltab, M.S., Lazopoulou, M., Ackomd, E.K., Vallveb, X. & Szabóa, S. 2018. Electrification of Sub-Saharan Africa through PV/hybrid mini-grids: Reducing the gap between current business models and on-site experience. *Renewable and Sustainable Energy Reviews*, 91: 1148–1161. https://doi.org/10.1016/j.rser.2018.04.018.

Grabovickic, R., Labuschagne, C., Fischer, N. & Glynn, O. 2012. Protection of transformer-ended feeders using multifunction relays. In *Proceedings of the IEEE Power Engineering Society Transmission and Distribution Conference*.

Grami, A. 2016. Wireless Communications. In *Introduction to Digital Communications*.

Grassi, A.. & Pignari, S. 2012. Coupling/decoupling circuits for powerline communications in differential DC power buses. In *IEEE International Symposium on Power Line Communications and Its Applications*. IEEE: 392–397.

Grassi, F., Pignari, S.A. & Wolf, J. 2011. Channel characterization and EMC assessment of a PLC system for spacecraft DC differential power buses. *IEEE Transactions on Electromagnetic Compatibility*, 53(3): 664–675.

Grimm, M., Hartwig, R. & Lay, J. 2013. Electricity Access and the Performance of Micro and Small Enterprises: Evidence from West Africa. *The European Journal of Development Research*, 25(5): 815–829. http://link.springer.com/10.1057/ejdr.2013.16.

Grond, M.O.W., Morren, J. & Slootweg, J.G. 2013. Integrating smart grid solutions into distribution network planning. In *2013 IEEE Grenoble Conference PowerTech, POWERTECH 2013*.

Grond, M.O.W., Morren, J. & Slootweg, J.G. 2012. Survey of Power System Planning Models and Optimization Techniques. In *IEEE Young Researchers Symposium in Electrical Power Engineering*. 1–6.

das Guerra Fernandes Guerra, F. & Santos Mota, W. 2007. Current transformer model. *IEEE Transactions on Power Delivery*, 22(1): 187–194.

Gungor, V.C., Sahin, D., Kocak, T., Ergut, S., Buccella, C., Cecati, C. & Hancke, G.P. 2013. A Survey on smart grid potential applications and communication requirements. *IEEE Transactions on Industrial Informatics*.

Güngör, V.C., Sahin, D., Kocak, T., Ergüt, S., Buccella, C., Cecati, C. & Hancke, G.P. 2011. Smart grid technologies: Communication technologies and standards. *IEEE Transactions on Industrial Informatics*.

Gupta, K.K., Ranjan, A., Bhatnagar, P., Sahu, L.K. & Jain, S. 2016. Multilevel inverter topologies with reduced device count: A review. *IEEE Transactions on Power Electronics*, 31(1): 135–151.

Haema, J. & Phadungthin, R. 2013. Development of condition evaluation for power transformer maintenance. In *International Conference on Power Engineering, Energy and Electrical Drives*. 620–623.

Hakala, T., Lahdeaho, T. & Jarventausta, P. 2015a. Low-Voltage DC Distribution-Utilization Potential in a Large Distribution Network Company. *IEEE Transactions on Power Delivery*.

Hakala, T., Lahdeaho, T. & Jarventausta, P. 2015b. Low Voltage DC Distribution - Utilization Potential in a Large Distribution Network Company. *IEEE Transactions on Power Delivery*, 30(4): 1694–1701. http://ieeexplore.ieee.org/lpdocs/epic03/wrapper.htm?arnumber=7027220.

Hamidi, V., Smith, K.S. & Wilson, R.C. 2010. Smart Grid technology review within the Transmission and Distribution sector. *Innovative Smart Grid Technologies Conference Europe (ISGT Europe), 2010 IEEE PES*: 1–8.

Hamilton, H. & Schulz, N.N. 2007. DC protection on the electric ship. In *IEEE Electric Ship Technologies Symposium, ESTS 2007*. 294–300.

Harness, R., Gombobaatar, S. & Yosef, R. 2008. Mongolian distribution power lines and raptor electrocutions. In *Papers Presented at the Annual Conference - Rural Electric Power Conference*.

Harness, R.E. 1998. Steel Distribution Poles-Environmental Implications. In *1998 Rural Electric Power Conference April 26-28, 1998.* D1 1-5.

Haron, A.R., Mohamed, A. & Shareef, H. 2012. A review on protection schemes and coordination techniques in microgrid system. *Journal of Applied Sciences*, 12(2): 101–112.

Harvey, L. 2016. *Introduction to Power Utility Communications*. Artech house.

Heathcote, M.J. 2007. 4 - Transformer construction. *J & P Transformer Book (Thirteenth Editon)*: 105–318. http://www.sciencedirect.com/science/article/pii/B9780750681643500065.

Hemmati, R., Hooshmand, R.-A. & Taheri, N. 2015. Distribution network expansion planning and DG placement in the presence of uncertainties. *International Journal of Electrical Power & Energy Systems*, 73: 665–673. http://linkinghub.elsevier.com/retrieve/pii/S014206151500229X.

Heslop, S., Macgill, I., Fletcher, J. & Lewis, S. 2014. Method for determining a PV generation limit on low voltage feeders for evenly distributed PV and Load. In *Energy Procedia*. 207–216.

Hewitson, L.G., Brown, M. & Balakrishnan, R. 2015. Relays. In *Practical Power System Protection*. Newnes: 96–132. http://www.sciencedirect.com/science/article/pii/B9780750663977500093.

Hollberg, P. 2015. *Swarm grids. Innovation in rural electrification,*. KTH School of Industrial Engineering and Management. https://www.divaportal.org/smash/get/diva2:850116/FULLTEXT01.pdf.

Hossain, E., Kabalci, E., Bayindir, R. & Perez, R. 2014. A Comprehensive Study on Distributed network Technology. *International Journal of Renewable Energy Research*, 4(4): 1094–1107.

Htay, M. & Win, K.S. 2008. Design and Construction of Automatic Voltage Regulator for Diesel Engine Type Stand-alone Synchronous Generator. *World Academy of Science, Energy and Technology*, (18): 652–658.

Hu, Y. & Li, V.O.K. 2001. Satellite-based internet: A tutorial. *IEEE Communications Magazine*, 39: 154–162.

Huang, Y. 2003. Power Transformers. *Power*, 18(3): 843–848. http://www.ncbi.nlm.nih.gov/pubmed/21954093.

Huurdeman, A. a. 2003. *the Worldwide History of*.

Ibe, O.C. 2018. *Fundamentals of Data Communication Networks*. JohnWiley & Sons, Inc.

IEA. 2016. World Energy Outlook 2016. *International Energy Agency: Paris, France*: 28. https://www.eia.gov/forecasts/aeo/data/browser/#/?id=8-AEO2016&cases=ref2016~ref_no_cpp&sourcekey=0.

IEA. 2017. *World Energy Outlook 2017*. https://www.iea.org/weo2017/.

IEA & World Bank. 2015. *Progress Toward Sustainable Energy 2015: Global Tracking Framework Report*. http://www.worldbank.org/content/dam/Worldbank/Event/Energy and Extractives/Progress Toward Sustainable Energy - Global Tracking Framework 2015 - Key Findings.pdf.

IEC 60364-1. 2005. Part 1: Fundamental Principles, Assessment of General Characteristics, Definitions,. In *Low-Voltage Electrical Installations*. Geneva, Switzerland: International Electrotechnical Commission.

IEEE. 2010. IEEE 1709 Recommended Practice for 1 kV to 35 kV Medium-Voltage DC Power Systems on Ships. *Power*, (November). https://ieeexplore-ieee-org.libproxy.cput.ac.za/stamp/stamp.jsp?tp=&arnumber=5623440.

IEEE. 2000. IEEE Std C37.91-2000. In *IEEE Guide for Protective Relay Applications to Power Transformers*.

IET standard. 2015. *Code of Practice for Low and Extra Low Voltage Direct Current Power Distribution in Buildings*. IET.

Ilves, K., Norrga, S., Harnefors, L. & Nee, H.P. 2012. Analysis of arm current harmonics in modular multilevel converters with main-circuit filters. In *International Multi-Conference on Systems, Signals and Devices, SSD 2012 - Summary Proceedings*.

IRENA. 2012. Prospects for the African power sector. *Scenarios and strategies for Africa Project.*

Ishii, T., Oguchi, S., Sakamoto, Y. & Okabe, S. 2013. A field study of lightning overvoltages in low-voltage distribution lines. *Electrical Engineering in Japan (English translation of Denki Gakkai Ronbunshi)*, 183(2): 12–21.

Issa, F., Devaux, O., Marthe, E. & Rachidi, F. 2004. Influence of power switching on power line communications in medium voltage networks. In *2004 IEEE International Conference on Communications (IEEE Cat. No.04CH37577)*. Paris: IEEE: 114–117.

Iyer, S., Dunford, W.G. & Ordonez, M. 2015. DC distribution systems for homes. In *IEEE Power and Energy Society General Meeting.*

Jahromi, M.G., Mirzaeva, G., Mitchell, S.D. & Gay, D. 2015. Advanced fault tolerance strategy for DC microgrids in mining excavators. In *IEEE International Symposium on Industrial Electronics*. 1502–1507.

Jamasb, T. 2006. Between the state and market: Electricity sector reform in developing countries. *Utilities Policy*, 14(1): 14–30.

Jan, S.T., Afzal, R. & Khan, A.Z. 2015. Transformer Failures, Causes & Impact. *International Conference Data Mining, Civil and Mechanical Engineering (ICDMCME'2015) Feb. 1-2, 2015 Bali (Indonesia)*: 49–52. http://iieng.org/siteadmin/upload/8693E0215039.pdf.

Jia, H., Zhou, T., Zhang, L., Ding, J., Fu, X. & Yang, L. 2017. Optical switch compatible with wavelength division multiplexing and mode division multiplexing for photonic networks-on-chip. *Optics Express*, 25(17): 20698–20707. https://www.osapublishing.org/oe/fulltext.cfm?uri=oe-25-17-20698&id=370720.

Jonsson, E., Aanensen, N.S. & Runde, M. 2014. Current interruption in air for a medium-voltage load break switch. *IEEE Transactions on Power Delivery*, 29(2): 870–875.

Jordaan, S., Van Rensburg, P.A.J., Beer, A. de & Ferreira, H. 2013. Long-wire half wave dipole antenna integrated into power cabling.

Jordaan, S., Van Rensburg, P.A.J., De Beer, A.S., Ferreira, H.C. & Vinck, A.J.H. 2015. A preliminary investigation of the UHF properties of LV cable for WiFi over power line communications. In *2015 IEEE International Symposium on Power Line Communications and Its Applications, ISPLC 2015*. IEEE: 35–40.

Kaipia, T., Karppanen, J., Mattsson, A., Lana, A., Pinomaa, A. & Peltoniemi, P. 2017. LVDC rules – technical specifications for public LVDC distribution network. *CIRED - Open Access Proceedings Journal*, 2017(1): 293–296. http://digital-library.theiet.org/content/journals/10.1049/oap-cired.2017.0519.

Kaipia, T., Karppanen, J., Nuutinen, P., Pinomaa, A., Mattsson, A., Peltoniemi, P., Silventoinen, P., Partanen, J., Hakala, T., Lahdeaho, T., Luukkanen, M., Trinh, D., Virtanen, P. & Kasteenpohja, T. 2016. LVDC rules - towards industrial-scale application of low-voltage direct current in public power distribution. *CIRED Workshop 2016*: 117 (4 .)-117 (4 .). http://digital-library.theiet.org/content/conferences/10.1049/cp.2016.0717.

Kaipia, T., Salonen, P., Lassila, J. & Partanen, J. 2006. Possibilities of the low voltage DC distribution systems. *Nordac, Nordic Distribution and Asset Management Conference*.

Kalair, A., Abas, N. & Khan, N. 2016. Comparative study of HVAC and HVDC transmission systems. *Renewable and Sustainable Energy Reviews*.

Kale, K. & Patra, S.K. 2015. Characterization of broadband power line channel. In *Global Conference on Communication Technologies, GCCT 2015*.

Kalivas, G. 2009. *Digital Radio System Design*.

Kang, Y.C., Lee, B.E. & Kang, S.H. 2007. Transformer protection relay based on the induced voltages. *International Journal of Electrical Power and Energy Systems*, 29(4): 281–289.

Kasztenny, B., Thompson, M. & Fischer, N. 2010. Fundamentals of short-circuit protection for transformers. In *2010 63rd Annual Conference for Protective Relay Engineers*.

Kefalas, T.D. & Kladas, A.G. 2012. Development of distribution transformers assembled of composite wound cores. In *IEEE Transactions on Magnetics*. 775–778.

Khazaei, J., Idowu, P., Asrari, A., Shafaye, A.B. & Piyasinghe, L. 2018. Review of HVDC control in weak AC grids. *Electric Power Systems Research*, 162: 194–206.

Khomfoi, S. & Tolbert, L.M. 2011a. 17 – Multilevel Power Converters. In *Power Electronics Handbook*. 455–486.

Khomfoi, S. & Tolbert, L.M. 2011b. Multilevel power converters. In *Power Electronics Handbook*. 455–486.

Kikkert, C.J. 2011. Power transformer modelling and MV PLC coupling networks. In *2011 IEEE PES Innovative Smart Grid Technologies, ISGT Asia 2011 Conference: Smarter Grid for Sustainable and Affordable Energy Future*. 1–6.

Kirchhoff, H., Kebir, N., Neumann, K., Heller, P.W. & Strunz, K. 2016. Developing mutual success factors and their application to swarm electrification: microgrids with 100 % renewable energies in the Global South and Germany. *Journal of Cleaner Production*, 129: 190–200.

Kolluri, S. V., Ramamurthy, J.R., Wong, S.M., Peterson, M., Yu, P. & Chander, M.R. 2015. Relay-based undervoltage load shedding scheme for Entergy's Western Region. In *IEEE Power and Energy Society General Meeting*.

Kosonen, A., Ahola, J. & Pinomaa, A. 2010. Analysis of channel characteristics for motor cable communication with inductive signal coupling. In *IEEE ISPLC 2010 - International Symposium on Power Line Communications and its Applications*. 72–77.

Kumar, D., Zare, F. & Ghosh, A. 2017. DC Microgrid Technology: System Architectures, AC Grid Interfaces, Grounding Schemes, Power Quality, Communication Networks, Applications, and Standardizations Aspects. *IEEE Access*, 5: 12230–12256.

Kumar, M.S. & Revankar, S.T. 2017. Development scheme and key technology of an electric vehicle: An overview. *Renewable and Sustainable Energy Reviews*.

Lai, L.L., Chan, S.W., Lee, P.K. & Lai, C.S. 2011. Challenges to implementing distributed generation in area electric power system. In *Conference Proceedings - IEEE International Conference on Systems, Man and Cybernetics*. 797–801.

Lamedica, R., Pompili, M., Cauzillo, B.A., Sangiovanni, S., Calcara, L. & Ruvio, A. 2016. Instrument Voltage Transformer time-response to fast impulse. In *Harmonics and Quality of Power (ICHQP), 2016 17th International Conference on*. Belo Horizonte, Brazil: IEEE: 400–405. http://ieeexplore.ieee.org/document/7783305/.

Lana, A., Nuutinen, P., Karppanen, J., Peltoniemi, P., Kaipia, T. & Partanen, J. 2015. Control of directly connected energy storage in LVDC distribution network. *11th IET International Conference on AC and DC Power Transmission*.

Landinger, C.C., McAuliffe, J.W., Clapp, A.L., Dagenhart, J.B. & Thue, W.A. 1997. Safety considerations of aerial systems using insulated and covered wire and cable. *IEEE Transactions on Power Delivery*, 12(2): 1012–1014.

Laslo, S. 2012. Current Transformer. *Bonneville Power Administration*, 1. https://www.eiseverywhere.com/file_uploads/389f38b2dffd8bcc3c58da78777e4d71_Current_Transformers.pdf.

Lassila, J., Kaipia, T., Partanen, J. & Lohjala, J. 2007. New investment strategies in the modern electricity distribution business - Reliability in the long-term planning. In *2007 IEEE Power Engineering Society General Meeting, PES*.

Lehtinen, H. 2016. A Trick up the Sleeve Protection Improves Pole Performance. *Electric light and power*. http://www.elp.com/articles/powergrid_international/print/volume-21/issue-5/features/case-study-a-trick-up-the-sleeve-protection-improves-pole-performance.html 29 August 2017.

Li, H., Zhang, J. & Bhuyan, G. 2006. Reliability assessment of electrical overhead distribution wood poles. In *2006 9th International Conference on Probabilistic Methods Applied to Power Systems, PMAPS*.

Li, L., Yong, J., Zeng, L. & Wang, X. 2013. Investigation on the system grounding types for low voltage direct current systems. In *2013 IEEE Electrical Power and Energy Conference, EPEC 2013*.

Lobato, G.I.C., Silva, S.M., Amaral, F. V. & Filho, B.J.C. 2015. Powerline Communication (PLC) through power converter's DC bus: Applicability assessment. In *2015 IEEE 13th Brazilian Power Electronics Conference and 1st Southern Power Electronics Conference, COBEP/SPEC 2016*. 1–5.

Long, C., Wu, J., Thomas, L. & Jenkins, N. 2016. Optimal operation of soft open points in medium voltage electrical distribution networks with distributed generation. *Applied Energy*, 184: 427–437.

Lotero, R.C. & Contreras, J. 2011. Distribution system planning with reliability. *IEEE Transactions on Power Delivery*, 26(4): 2552–2562.

Lotlikar, S. 2017. Survey and Analysis of Literature in " E-waste Management ". *International Journal of Mechanical Engineering and Information Technology*, 05(01): 1835–1842. http://igmpublication.org/ijmeit issue/v5-i1/1 ijmeit.pdf.

Luis Guilherme, da S.C., Carlos M. de Queiroz, A., Bamidele, A., Da Costa, V.L.R. & Ribeiro, M. V. 2017. Coupling for Power Line Communication: A Survey. *Journal of communication and information systems*, 32(1): 8–22.

Lumbreras, S. & Ramos, A. 2016. The new challenges to transmission expansion planning. Survey of recent practice and literature review. *Electric Power Systems Research*, 134: 19–29.

LUNO. 2017. High Voltage Isolator Switch. *Lvneng Electricity Technology Co.,Ltd.* http://www.luno-transformer.com/35-high_voltage_isolator_switch.html.

Mackay, L., Blij, N.H. va. der, Ramirez-Elizondo, L. & Bauer, P. 2017. Toward the Universal DC Distribution System. *Electric Power Components and Systems*.

Magier, T., Tenzer, M. & Koch, H. 2018. Direct Current Gas-Insulated Transmission Lines. *IEEE Transactions on Power Delivery*.

Mahmoud, A.A. & Systems, P. 1983. Bibliography of Power Distribution System Planning. *IEEE Transactions on Power Apparatus and Systems*, PAS-102(6): 1778–1787. http://ieeexplore.ieee.org/xpl/freeabs_all.jsp?arnumber=4112142%5Cnhttp://ieeexplore.ieee.org/lpdocs/epic03/wrapper.htm?arnumber=4112142.

Manandhar, U., Ukil, A. & Jonathan, T.K.K. 2016. Efficiency comparison of DC and AC microgrid. In *Proceedings of the 2015 IEEE Innovative Smart Grid Technologies - Asia, ISGT ASIA 2015*.

Maqsood, A. & Corzine, K.A. 2017. Integration of Z-Source Breakers into Zonal DC Ship Power System Microgrids. In *IEEE Journal of Emerging and Selected Topics in Power Electronics*.

Martins, V.F. & Borges, C.L.T. 2011. Active distribution network integrated planning incorporating distributed generation and load response uncertainties. *IEEE Transactions on Power Systems*, 26(4): 2164–2172.

Marzal-Pomianowska, A., Diaz de Cerio Mendaza, I., Heiselberg, P. & Bak-Jensen, B. 2016. Application of High-Resolution Domestic Electricity Load Profiles in Network Modelling. A Case Study of Low Voltage Grid in Denmark. In *CLIMA 2016 - proceedings of the 12th REHVA World Congress*.

Mccalley, J., Oluwaseyi, O., Krishnan, V., Dai, R., Singh, C. & Kai, J. 2015. *System Protection Schemes : Limitations , Risks , and Management*. Iowa.

Mehta, R., Sidharth, Bhandari Shubham, B., Mehta, T., Kartik, K. & Atiqur, R. 2016. Studying the Open System Interconnection Model and Proposing the Concept of Layer Zero. *Indian Journal of Science and Technology*, 9(21): 1–4.

Meier, A. Von. 2006. Loads. In *ELECTRIC POWER SYSTEMS:A CONCEPTUAL INTRODUCTION*. Geneva: A Wiley-Interscience publication: 127–140. http://www.iec.ch/about/brochures/pdf/energy/iec_lvdc_the_better_way_en_lr.pdf.

Mendes, W.R., Samesima, M.I. & Moura, F.A.M. 2008. Influence of power transformer winding connections on the propagation of voltage sags through electric system. In *2008 5th International Conference on the European Electricity Market, EEM*.

Meng, H., Chen, S., Guan, Y.L., Law, C.L., So, P.L., Gunawan, E. & Lie, T.T. 2004. Modeling of Transfer Characteristics for the Broadband Power Line Communication Channel. *IEEE Transactions on Power Delivery*.

Mesas, J.J., Monjo, L.L., Sainz, L. & Pedra, J. 2015. Study of MVDC system benchmark networks. *Proceedings - 2015 International Symposium on Smart Electric Distribution Systems and Technologies, EDST 2015*: 235–240.

Mirra, C., Porrino, A., Ardito, A. & Nucci, C.A. 1997. Lightning overvoltages in low voltage networks. In *IEE Conference Publication*. 2.19.1-2.19.6.

Mittal, N., Singh, B., Singh, S.P., Dixit, R. & Kumar, D. 2012. Multilevel inverters: A literature survey on topologies and control strategies. In *ICPCES 2012 - 2012 2nd International Conference on Power, Control and Embedded Systems*.

Miyazaki, T., Okabe, S., Mori, K., Aiba, K., Hirai, T., Yoshinaga, J. & Sekioka, S. 2006. A study on a lightning-surge analysis composite model of a reinforced concrete pole and a grounding electrode in power distribution lines. *IEEJ Transactions on Power and Energy*, 126(7): 669–678. http://www.scopus.com/inward/record.url?eid=2-s2.0-33745775888&partnerID=40&md5=512f75efbbc16c7550cd7203fbb0a96e.

Mohtashami, S., Pudjianto, D. & Strbac, G. 2016. Strategic Distribution Network Planning With Smart Grid Technologies. *IEEE Transactions on Smart Grid*, PP(99): 1. http://ieeexplore.ieee.org/xpl/articleDetails.jsp?arnumber=7436811&queryText=Pudjianto&sortType=desc_p_Publication_Year.

Monadi, M., Koch-Ciobotaru, C., Luna, A., Candela, J.I. & Rodriguez, P. 2015. Implementation of the differential protection for MVDC distribution systems using real-time simulation and hardware-in-the-loop. *2015 IEEE Energy Conversion Congress and Exposition (ECCE)*: 3380–3385. http://ieeexplore.ieee.org/lpdocs/epic03/wrapper.htm?arnumber=7310137.

Moreno, A.F. & Mojica-Nava, E. 2014. LVDC microgrid perspective for a high efficiency distribution system. In *2014 IEEE PES Transmission and Distribution Conference and Exposition, PES T and D-LA 2014 - Conference Proceedings*.

Mork, B.., Ishchenko, D., Wang, X., Yerrabelli, A.., Quest, R. & Kinne, C.. 2005. Power Line Carrier Communications System Modeling. In *International Conference on Power system Transients (IPST'05)*. 1–6.

Mozina, C.J. 2006. Advances in multifunction digital transformer relays. In *Proceedings of the IEEE Power Engineering Society Transmission and Distribution Conference*. 858–862.

Najgebauer, M., Chwastek, K. & Szczygłowski, J. 2011. Energy efficient distribution transformers. *Przeglad Elektrotechniczny*, 87(2): 111–114.

Nami, A., Liang, J., Dijkhuizen, F. & Demetriades, G.D. 2015. Modular multilevel converters for HVDC applications: Review on converter cells and functionalities. *IEEE Transactions on Power Electronics*, 30(1): 18–36.

Newswire, P.R. 2014. Global Insulated Wire and Cable Market. *LON-Reportbuyer*. http://bd.univalle.edu.co/login?url=http://search.ebscohost.com/login.aspx?direct=true&db=bwh&AN=201410161602PR.NEWS.USPR.BR39874&lang=es&site=eds-live.

Nguyen, T.V., Petit, P., Maufay, F., Aillerie, M. & Charles, J.P. 2013. Powerline communication (PLC) on HVDC bus in a renewable energy system. In *Energy Procedia*.

Nilsson, D. & Sannino, A. 2004. Efficiency analysis of low-and medium-voltage DC distribution systems. *Power Engineering Society General …*: 1–7. http://ieeexplore.ieee.org/xpls/abs_all.jsp?arnumber=1373299.

Nutkani, I.U., Peng, W., Loh, P.C. & Blaabjerg, F. 2014. Cost-based droop scheme for DC microgrid. In *2014 IEEE Energy Conversion Congress and Exposition, ECCE 2014*.

Nuutinen, P., Lana, A. & Hakala, T. 2017. Lvdc Rules – Technical Specifications for Public Lvdc Distribution Network. *Cired 2017*, (June): 12–15. http://cired.net/publications/cired2017/pdfs/CIRED2017_0519_final.pdf.

Okoye, C.O. & Oranekwu-Okoye, B.C. 2018. Economic feasibility of solar PV system for rural electrification in Sub-Sahara Africa. *Renewable and Sustainable Energy Reviews*.

Olivares-Galván, J.C., de León, F., Georgilakis, P.S. & Escarela-Pérez, R. 2010. Selection of copper against aluminium windings for distribution transformers. *IET Electric Power Applications*, 4(6): 474. http://digital-library.theiet.org/content/journals/10.1049/iet-epa.2009.0297.

Oliveira;, T.R., Pereira;, C.A.G.M.M.S., Netto;, S.L. & Moises V. Ribeiro. 2013. The characterization of hybrid PLC-wireless channels: A preliminary analysis. In *17th International Symposium on Power Line Communications and Its Applications*. IEEE: 98–102.

Oliveira, T.R., Andrade, F., Picorone, A., Haniph, L., Netto, S.L. & Ribeiro, M. V. 2016. Characterization of hybrid communication channel in indoor scenario. *Journal of Communication and Information System.*, 31(1): 224–335.

Oni, O.E., Davidson, I.E. & Mbangula, K.N.I. 2016. A review of LCC-HVDC and VSC-HVDC technologies and applications. In *EEEIC 2016 - International Conference on Environment and Electrical Engineering*.

Onyeji, I., Bazilian, M. & Nussbaumer, P. 2012. Contextualizing electricity access in sub-Saharan Africa. *Energy for Sustainable Development*, 16(4): 520–527.

Othieno, H. & Awange, J. 2016. *Energy Resources in Africa*.

Ouroua, A., Beno, J. & Hebner, R. 2009. Analysis of fault events in MVDC architecture. In *IEEE Electric Ship Technologies Symposium, ESTS 2009*. 380–387.

Ouyang, W., Cheng, H., Zhang, X. & Yao, L. 2010. Distribution network planning method considering distributed generation for peak cutting. *Energy Conversion and Management*, 51(12): 2394–2401.

Panos, E., Densing, M. & Volkart, K. 2016. Access to electricity in the World Energy Council's global energy scenarios: An outlook for developing regions until 2030. *Energy Strategy Reviews*, 9: 28–49.

Papadopoulos, T.A., Kaloudas, C.G., Chrysochos, A.I. & Papagiannis, G.K. 2013. Application of narrowband Power-Line communication in medium-voltage smart distribution grids. *IEEE Transactions on Power Delivery*, 28(2): 981–988.

Parshall, L., Pillai, D., Mohan, S., Sanoh, A. & Modi, V. 2009. National electricity planning in settings with low pre-existing grid coverage: Development of a spatial model and case study of Kenya. *Energy Policy*, 37(6): 2395–2410.

Patrick, D.R. & Fardo, S.W. 2009. *Electrical Distribution Systems.* 2nd ed. Lilburn: Fairmont press,Inc.

Peake, O. 2009. The History of High Voltage Direct Current Transmission. In *3rd Australasian Engineering Heritage Conference 2009*.

Pei, X., Cwikowski, O., Vilchis-Rodriguez, D.S., Barnes, M., Smith, A.C. & Shuttleworth, R. 2016. A review of technologies for MVDC circuit breakers. In *IECON Proceedings (Industrial Electronics Conference)*. 3799–3805.

Peltoniemi, P. & Partanen, J. 2015. Prospects of Development of LVDC Electricity Distribution System Energy Efficiency. *CIRED 23rd International Conference on Electricity Distribution*.

Peng, F.Z., Qian, W. & Cao, D. 2010. Recent advances in multilevel converter/inverter topologies and applications. In *2010 International Power Electronics Conference - ECCE Asia -, IPEC 2010*. 492–501.

Pepukaye, B. & Shepherd, D. 2016. Emergence of a commercial market for mini-grids in Africa. *ESI-Africa's power journal*. https://www.esi-africa.com/emergence-commercial-market-mini-grids-africa/.

Piantini, A. 2008. Lightning Protection of Overhead Power Distribution Lines. *29 th International Conference on Lightning Protection*, (June): 1–29.

Piccolo, A. & Siano, P. 2009. Evaluating the Impact of Network Investment Deferral on Distributed Generation Expansion. *Power Systems, IEEE Transactions on*, 24(3): 1559–1567.

Picorone, A.Â.M., Amado, L.R. & Ribeiro, M.V. 2010. Linear and periodically time-varying PLC channels estimation in the presence of impulsive noise. In *IEEE ISPLC 2010 - International Symposium on Power Line Communications and its Applications*. 255–260.

Pighi, R. & Raheli, R. 2005. On multicarrier signal transmission for highvoltage power lines. In *IEEE International Symposium on Power Line Communications and Its Applications,*. IEEE: 32–36.

Pinomaa, A., Ahola, J., Kosonen, A. & Nuutinen, P. 2014. Applicability of narrowband power line communication in an LVDC distribution network. In *IEEE ISPLC 2014 - 18th IEEE International Symposium on Power Line Communications and Its Applications*.

Pinomaa, A., Ahola, J., Kosonen, A. & Nuutinen, P. 2015a. HomePlug green PHY for the LVDC PLC concept: Applicability study. In *2015 IEEE International Symposium on Power Line Communications and Its Applications, ISPLC 2015*. 205–210.

Pinomaa, A., Ahola, J., Kosonen, A. & Nuutinen, P. 2015b. Power line communication network for a customer-end AC grid in an LVDC distribution system. In *2014 IEEE International Conference on Smart Grid Communications, SmartGridComm 2014*.

pinterest.com. 2015. Steel distribution pole. https://za.pinterest.com/pin/365706432211730739/ 31 August 2017.

Prather, P.R. & Messmer, T. a. 2010. Raptor and Corvid Response to Power Distribution Line Perch Deterrents in Utah. *Journal of Wildlife Management*, 74(4): 796–800. http://www.bioone.org/doi/abs/10.2193/2009-204.

Pratt, A., Kumar, P. & Aldridge, T. V. 2007. Evaluation of 400V DC distribution in telco and data centers to improve energy efficiency. In *INTELEC, International Telecommunications Energy Conference (Proceedings)*.

Prudhvi Raj, R. 2013. Transformer Core Fault Detection and Control. *Advance in Electronic and Electric Engineering.*, 3(4): 485–490. https://www.ripublication.com/aeee/63_pp 485-490.pdf.

Pryor, B.M. 2003. 34 - Switchgear. In *Electrical Engineer's Reference Book (Sixteenth Edition)*. 1–36. http://www.sciencedirect.com/science/article/pii/B9780750646376500344.

Qawasmi, A., Soltau, N., De Doncker, R.W., Heidemann, M., Nikolic, G. & Schnettler, A. 2017. A comparison of circuit breaker technologies for medium voltage direct current distribution networks. In *2016 IEEE PES Transmission and Distribution Conference and Exposition-Latin America, PES T and D-LA 2016*.

Qu, Z., Zhang, G. & Xie, J. 2017. LEO Satellite Constellation for Internet of Things. *IEEE Access*, 5: 18391–18401.

Rahavi, J.S.A., Kanagapriya, T. & Seyezhai, R. 2012. Design and analysis of Interleaved Boost Converter for renewable energy source. *International Conference on Computing, Electronics and Electrical Technologies (ICCEET), 2012 .*: 447–451. http://ieeexplore.ieee.org/lpdocs/epic03/wrapper.htm?arnumber=6203850.

Rahnavard, A., Yavartalab, A., Samadi, M., Zekavati, A. & Jafari, M.A. 2013. Development of seismic capacity curve (S.C.C.) for power distribution concrete poles. *22nd International Conference and Exhibition on Electricity Distribution (CIRED 2013)*, 33(2): 0406–0406. http://digital-library.theiet.org/content/conferences/10.1049/cp.2013.0714.

Rajaram, R., Sathish Kumar, K. & Rajasekar, N. 2015. Power system reconfiguration in a radial distribution network for reducing losses and to improve voltage profile using modified plant growth simulation algorithm with Distributed Generation (DG). *Energy Reports*, 1: 116–122.

Rebizant, W., Szafran, J. & Wiszniewski, A. 2013. *Digital Signal Processing in Power System Protection and Control.* Springer.

Reed, G.F., Grainger, B.M., Sparacino, A.R., Taylor, E.J., Korytowski, M.J. & Mao, Z. 2012. Medium Voltage DC Technology Developments , Applications , and Trends University of Pittsburgh United States High Voltage DC Transmission : Solution for Transferring Bulk Power. *Cigre*: 1–7.

Research and Markets. 2017. *Africa Diesel Genset Market (2017-2023): Forecast by KVA Ratings, Verticals, Countries, Import Statistics and Competitive Landscape.* https://www.researchandmarkets.com/research/j3qvzs/africa_diesel.

Richardson, D.J. 2016. New optical fibres for high-capacity optical communications. *Philosophical transactions of royal society: Mathematical, Physical and Engineering Science*, 374(2062).

Rodriguez-Diaz, E., Vasquez, J.C. & Guerrero, J.M. 2016. Intelligent DC Homes in Future Sustainable Energy Systems: When efficiency and intelligence work together. *IEEE Consumer Electronics Magazine*.

Rodríguez, J., Lai, J.S. & Peng, F.Z. 2002. Multilevel inverters: A survey of topologies, controls, and applications. *IEEE Transactions on Industrial Electronics*, 49(4): 724–738.

Rongsheng, L. 2017. Progress of long-distance DC electrical power transmission. In *1st International Conference on Electrical Materials and Power Equipment (ICEMPE)*. Xi'an: IEEE. https://ieeexplore-ieee-org.libproxy.cput.ac.za/document/7982153.

Rudervall, R., Charpentier, J.P. & Sharma, R. 2000. High Voltage Direct Current (HVDC) Transmission Systems Technology Review Paper. *Energy Week*, (Ccc): 1–17.

Rusov, V. & Zhivodernikov, S. 2007. Transformer condition monitoring. In *Proceedings of 2008 International Conference on Condition Monitoring and Diagnosis, CMD 2008*. 1012–1014.

Saboori, H., Hemmati, R. & Jirdehi, M.A. 2015. Reliability improvement in radial electrical distribution network by optimal planning of energy storage systems. *Energy*, 93: 2299–2312.

Sahito, A.A., Jumani, M.J., Mahar, M.A. & Shah, S.S.. 2015. Reinforcement Proposal towards Loss Reduction in Distribution Network. *SINDHUNIVERSITYRESEARCH JOURNAL (SCIENCE SERIES)*, 47(2): 469–472. https://www.researchgate.net/profile/Anwar_Sahito/publication/282859486_Reinforceme nt_Proposal_towards_Loss_Reduction_in_Distribution_Network/links/561faf0a08aed8d d1940269e/Reinforcement-Proposal-towards-Loss-Reduction-in-Distribution-Network.pdf.

Salman, A.M. & Li, Y. 2015. Age-dependent fragility and life-cycle cost analysis of wood and steel power distribution poles subjected to hurricanes. *Structure and Infrastructure Engineering*, 12(8): 890–903. http://www.scopus.com/inward/record.url?eid=2-s2.0-84937120744&partnerID=tZOtx3y1.

Salomonsson, D., S??der, L. & Sannino, A. 2009. Protection of low-voltage DC microgrids. *IEEE Transactions on Power Delivery*, 24(3): 1045–1053.

Salonen, P., Kaipia, T., Nuutinen, P., Peltoniemi, P. & Partanen, J. 2008. An LVDC Distribution System Concept. *NORPIE, Nordic Workshop on Power and Industrial Electroncis*: 7. https://aaltodoc.aalto.fi/handle/123456789/809%5Cnhttp://lib.tkk.fi/Conf/2008/urn011603 .pdf.

La Salvia, J.A. 2006. Technological components for an anti-theft system in overhead networks. In *Proceedings of the IEEE Power Engineering Society Transmission and Distribution Conference*. 1307–1314.

De Sanctis, M., Cianca, E., Araniti, G., Bisio, I. & Prasad, R. 2016. Satellite communications supporting internet of remote things. *IEEE Internet of Things Journal*.

Sannino, A., Postiglione, G. & Bollen, M.H.J. 2003. Feasibility of a DC network for commercial facilities. *IEEE Transactions on Industry Applications*.

Sarmento, M. & Lacoursiere, B. 2006. A state of the art overview: Composite utility poles for distribution and transmission applications. In *2006 IEEE PES Transmission and Distribution Conference and Exposition: Latin America, TDC'06*.

Sayer, W.C. 1986. APPLICATION OF WOODEN POLES FOR DISTRIBUTION LINES. In *IEE Proceedings C - Generation, Transmission and Distribution*. IET: 425–429. http://ieeexplore.ieee.org/stamp/stamp.jsp?tp=&arnumber=4646928&isnumber=4646908.

Schinke, A. & Erlich, I. 2018. Enhanced Voltage and Frequency Stability for Power Systems with High Penetration of Distributed Photovoltaic Generation. *IFAC-PapersOnLine*, 51(28): 31–36. https://reader.elsevier.com/reader/sd/pii/S2405896318333913?token=5D0B94685A5EC3743FEEBC48B8DB157371545C4A31E532F658F3D9D8FE9588E1ABFF8BBBECE9E6D36BCF1A07A81B7DAB.

Schwartz, M. 2009. Carrier-wave telephony over power lines: early history. *IEEE Communications Magazine*, 47(1): 14–18. https://ieeexplore.ieee.org/document/4752669/?part=1%7Csec1.

SEECO. 2016. Substation Switches - Overview. http://www.seecoswitch.com/substation_overview.php 10 October 2017.

Sekioka, S. 2008. Lightning surge analysis model of reinforced concret pole and grounding lead conductor in distribution line. *IEEJ Transactions on Electrical and Electronic Engineering*, 3(4): 432–440.

Sharaf, H.M., Zeineldin, H.H., Ibrahim, D.K. & Zahab, E.E.D.A. El. 2015. Protection coordination of directional overcurrent relays considering fault current direction. In *IEEE PES Innovative Smart Grid Technologies Conference Europe*.

Shen, C., Jiang, D., Lv, W. & Wang, Y. 2012. An overview of the application of DC zonal distribution system in shipboard integrated power system. In *Proceedings - 2012 3rd International Conference on Digital Manufacturing and Automation, ICDMA 2012*.

Shen, H., Kang, P., Bian, K., Chen, G., Wang, S. & Rao, Q. 2014. Experimental study on grounding characteristics of reinforced concrete poles for 10 kV distribution lines. *Dianwang Jishu/Power System Technology*, 38(6).

Shivakumar, A., Normark, B. & Welsch, M. 2015. Household DC networks : State of the art and future prospects. *Insight_E Rapid Response Energy Brief*.

Shri, harsha J., Shilpa, G.N., Ramesh, E., Dayananda, L.N. & Nataraja, C. 2012. Voltage Source Converter Based HVDC Transmission. *International Journal of Engineering Science and Innovative Technology (IJESIT)*, 1(1): 97–106. https://www.researchgate.net/profile/Ramesh_E_Ramesh_E/publication/316989638_Voltage_Source_Converter_Based_HVDC_Transmission/links/591c23600f7e9b7727da0455/Voltage-Source-Converter-Based-HVDC-Transmission.pdf.

Sinclair, A., Finney, D., Martin, D. & Sharma, P. 2014. Distance Protection in Distribution Systems : How It Assists With Integrating Distributed Resources Distance Protection in Distribution Systems : How It Assists With Integrating Distributed Resources. *IEEE TRANSACTIONS ON I NDUSTRY APPLICATIONS,*, 50(3): 2186–2196. http://ieeexplore.ieee.org/stamp/stamp.jsp?arnumber=6654320.

Singh, R.P. 2007. *Digital Power System Protection*. P. Learning, ed. Prentice-Hall of India Pvt.Ltd.

Sleva, A.F. 2009. Protective Relay Functions. In *Protective Relay Principles*. Boca Raton, Florida: Taylor & Francis Group, LLC: 79–91.

Smith, K.A., Galloway, S.J., Emhemed, A. & Burt, G.M. 2016. Feasibility of Direct Current Street Lighting & Integrated Electric Vehicle Charging Points. In *6th Hybrid and Electric Vehicles Conference (HEVC 2016)*.

Sood, V.K. 2011. HVDC transmission. In *Power Electronics Handbook*.

Stagge, H. 2014. Medium-Voltage DC Grids for Future Distribution Systems. In *China International Conference on Electricity Distribution 2014*. http://www.csee.org.cn/data/zt_ciced2014/doc/RT5_1.pdf.

Stieneker, M. 2016. Medium-voltage DC distribution grids in urban areas. *Proceedings of IEEE International Symposium on Power Electronics for Distributed Generation Systems PEDG*: 1–7. http://ieeexplore.ieee.org/document/7527045/.

Sultana, U., Khairuddin, A.B., Aman, M.M., Mokhtar, A.S. & Zareen, N. 2016. A review of optimum DG placement based on minimization of power losses and voltage stability enhancement of distribution system. *Renewable and Sustainable Energy Reviews*, 63: 363–378.

Sun, Z. 2006. *Satellite Networking: Principles and Protocols*.

Surajit, C., Madhuchhanda, M. & Samarjit, S. 2011. Sag, Swell, Interruption, Undervoltage and Overvoltage. *Power Systems*, 62: 39–42.

Swana, Z.W., Van Rensburg, P.A.J. & Ferreira, H.C. 2015. Is resistive coupling feasible for the reception of power-line communications data? In *2015 IEEE International Symposium on Power Line Communications and Its Applications, ISPLC 2015*. Austin, TX, USA: IEEE: 47–52.

Szeląg, A., Maciołek, T. & Patoka, M. 2015. Effectiveness of filters in 3 kV DC railway traction substations supplied by distorted voltage–measurements and diagnostics. *ACTA IMEKO*, 4(2): 72-79. https://acta.imeko.org/index.php/acta-imeko/article/viewFile/IMEKO-ACTA-04 (2015)-02-13/379.

Tabari, M. & Yazdani, A. 2014. Stability of a dc distribution system for power system integration of plug-in hybrid electric vehicles. *IEEE Transactions on Smart Grid*.

Tagliapietra, S. 2017. Electrifying Africa: how to make Europe's contribution count. *Policy Contributions*.

Temprana, E., Myslivets, E., Kuo, B.P.P., Liu, L., Ataie, V., Alic, N. & Radic, S. 2015. Overcoming Kerr-induced capacity limit in optical fiber transmission. *Science*.

Temraz, H. & Quintana, V. 1993. Distribution system expansion planning models: an overview. *Electric power systems research*, 26: 1993. http://www.sciencedirect.com/science/article/pii/037877969390069Q.

Thangavelan, M., Parabavathi, K. & Ramesh, L. 2016. Review on Power Transformer Internal Fault Diagnosis. *Jornal of Electrical Engineering*. www.jee.ro.

Thimons, M. 2014. Steel utility poles versus wood. *Steel Times International*, 38(3): 37–38. http://search.ebscohost.com/login.aspx?direct=true&db=bth&AN=96045213&site=ehost-live.

Thiyagarajan, A., Praveen Kumar, S.G. & Nandini, A. 2014. Analysis and Comparison of Conventional and Interleaved DC/DC Boost Converter. In *Second International Conference on Current Trends In Engineering and Technology - ICCTET 2014*. Coimbatore: 198–205. http://ieeexplore.ieee.org/lpdocs/epic03/wrapper.htm?arnumber=6966287.

Thomas, H., Marian, A., Chervyakov, A., Stückrad, S., Salmieri, D. & Rubbia, C. 2016. Superconducting transmission lines - Sustainable electric energy transfer with higher public acceptance? *Renewable and Sustainable Energy Reviews*.

Tiku, D. 2014. Dc power transmission: Mercury-arc to thyristor HVdc valves [History]. *IEEE Power and Energy Magazine*.

Trotter, P.A., McManus, M.C. & Maconachie, R. 2017. Electricity planning and implementation in sub-Saharan Africa: A systematic review. *Renewable and Sustainable Energy Reviews*, 74: 1189–1209.

Tschudi, B.W., My, T. & Fortenbery, B. 2008. *DC Power for Improved Data Center Efficiency*. http://www.chip2grid.com/docs/DCDemoFinalReport.pdf.

ukpowernetworks. 2012. Aerial Bundled Conductor (ABC) Low Voltage Mains and Services. : 1–98. https://library.ukpowernetworks.co.uk/library/en/g81/Miscellaneous/Other/OHL+Design+Manual+-+Section+1+-+Aerial+Bundled+Conductor+%28ABC%29+Low+Voltage+Mains+and+Services.pdf.

Usman, A. & Shami, S.H. 2013. Evolution of communication technologies for smart grid applications. *Renewable and Sustainable Energy Reviews*.

V.K. Mehta and R. Mehta. 2011. *Principles of Power System*.

V.K. Mehta and R. Mehta. 2008. Protection against overvoltages. In *Principles of power system*. S. Chand: 552–569.

Wade, E.R. & Asada, H.H. 2006. Design of a broadcasting modem for a DC PLC scheme. *IEEE/ASME Transactions on Mechatronics*, 11(5): 533–540.

Wahlberg, M. & Rönnberg, S. 2011. Currents in Power Line Wood Poles. In *CIRED*. 1–4. http://pure.ltu.se/portal/en/publications/currents-in-power-line-wood-poles%2846fb4103-b4ef-4bc9-a1e9-0a5d3bb8a741%29.html.

Walter, A.E. 2003. Introduction and general philosophy. In *Protective Relaying: Theory and Applications*. New York: Marcel Dekker Inc Ltd: 432.

Wang, D.T.-C., Ochoa, L.F., Harrison, G.P., Dent, C.J. & Wallace, a R. 2008. Evaluating investment deferral by incorporating distributed generation in distribution network planning. *16h Power Systems Computation Conf.*: 7.

Wang, W., Xu, Y. & Khanna, M. 2011. A survey on the communication architectures in smart grid. *Computer Networks , Elsevier*, 55: 3604–3629. http://citeseerx.ist.psu.edu/viewdoc/download?doi=10.1.1.713.303&rep=rep1&type=pdf.

Wen, J., Qin, H., Wang, S. & Zhou, B. 2012. Basic connections and strategies of isolated phase-shifting transformers for multipulse rectifiers: A review. In *cccc2012 Asia-Pacific Symposium on Electromagnetic Compatibility, APEMC 2012 - Proceedings*. 105–108.

Whaite, S., Grainger, B. & Kwasinski, A. 2015. Power quality in DC power distribution systems and microgrids. *Energies*, 8(5): 4378–4399.

Winkler, H., Simões, A.F., Rovere, E.L. la, Alam, M., Rahman, A. & Mwakasonda, S. 2011. Access and Affordability of Electricity in Developing Countries. *World Development*, 39(6): 1037–1050.

Wolde-Rufael, Y. 2006. Electricity consumption and economic growth: A time series experience for 17 African countries. *Energy Policy*, 34(10): 1106–1114.

Xiao-Ping Zhang. 2010. Fundamental of electric power systems. In *Restructured Electric Power Systems: Analysis of Electricity Markets with Equilibrium Models*. 1–50.

Xiaodong, L., Jackson, W. & Laughy, R. 2007. Transformer winding connections for practical industrial applications. *Record of Conference Papers - Annual Petroleum and Chemical Industry Conference*: 1–9. http://ieeexplore.ieee.org/document/4365778/.

Yang, J., Fletcher, J.E. & O'Reilly, J. 2010. Multiterminal DC wind farm collection grid internal fault analysis and protection design. *IEEE Transactions on Power Delivery*, 25(4): 2308–2318.

Yong, J., Xu, X., Zeng, L. & Li, L. 2013. A review of low voltage DC power distribution system. *Zhongguo Dianji Gongcheng Xuebao/Proceedings of the Chinese Society of Electrical Engineering*.

You, S., Bindner, H.W., Hu, J. & Douglass, P.J. 2014. An overview of trends in distribution network planning: A movement towards smart planning. In *2014 IEEE PES T&D Conference and Exposition*. 1–5. http://ieeexplore.ieee.org/lpdocs/epic03/wrapper.htm?arnumber=6863446.

Zadeh, H.K. & Manjrekar, M. 2012. A novel IEC 61850-based distribution line/cable protection scheme design. In *2012 IEEE PES Innovative Smart Grid Technologies, ISGT 2012*.

Zhang, F., Liu, K., Chen, X., Huang, J., Luo, R., Liu, G., Li, Y. & Zhou, K. 2016. Error analysis of capacitor voltage transformer in the operation environment. In *ICHVE 2016 - 2016 IEEE International Conference on High Voltage Engineering and Application*.

Zhang, X.P. 2010. *Fundamentals of Electric Power Systems*.

Ziegler, G. 2004. Protection and Substation Automation: state of the art and dvelopment trends. *Electra*, (206): 14–23.

Aluminium Conductor Steel Reinforced - ACSR (South African Standard Sizes)

Code name	Equival. copper area	Stranding and wire diameter	Diameter over steel	Overall diameter (Std.)	Aluminium area	Steel area	Total area	Mass kg/km			Ultimate tensile strength	Coefficient of linear expansion	Initial modulus of elasticity	Final modulus of elasticity	DC resistance at 20°C	Current rating	Standard drum length
	mm²	mm	mm	mm	mm²	mm²	mm²	Aluminium	Steel	Total	Newton	/C° x 10⁻⁶	MPa	MPa	Ω/km	A	m
+ 21/3,5	12,8	6/1/2,11	2,11	6,33	20,9	3,5	24,5	58	27	85	7710	19,31	54600	80400	1,395	130	3000
+ 26/4,4	16,0	6/1/2,36	2,36	7,16	26,3	4,4	30,6	72	34	106	9610	19,31	52700	80400	1,116	150	3000
+ 37/6,1	22,4	6/1/2,79	2,79	8,45	36,7	6,1	42,8	100	48	148	13150	19,31	50700	80400	0,798	190	2500
+ 42/7,1	25,8	6/1/3,00	3,00	9,09	42,4	7,1	49,5	117	55	172	15200	19,31	50200	80400	0,680	210	1500
+ 53/8,8	32,3	6/1/3,35	3,35	10,15	52,9	8,8	61,7	145	69	214	18400	19,31	49500	80400	0,553	240	1500
+ 63/11	38,5	6/1/3,66	3,66	11,09	63,1	10,5	73,7	173	83	255	22500	19,31	49100	80400	0,463	260	1500
105/17	64,0	6/1/4,72	4,72	14,30	105	17,5	122	288	137	425	36540	19,31	48500	80400	0,278	360	1500
105/14	64,0	6/4,75 +7/1,57	4,71	14,29	105	12,7	118	292	102	394	32640	19,92	48800	76400	0,278	360	2000
158/37	96,4	30/7/2,59	7,77	18,31	158	36,9	195	436	290	726	69250	18,43	55700	83400	0,186	470	2000
264/62	161	30/7/3,35	10,05	23,69	264	61,7	326	729	485	1214	111400	18,43	53600	83400	0,111	650	2000
429/56	262	54/7/3,18	9,54	28,91	429	55,6	484	1185	436	1621	131900	19,91	47300	73200	0,0687	860	1500
662/84	404	54/3,95 +19/2,37	11,85	35,94	662	83,8	746	1826	663	2489	205500	19,96	46900	72300	0,0445	1123	1000